ISSN: 2067-3809

Universitatea Politehnica Timișoara

ACTA TECHNICA CORVINIENSIS – Bulletin of Engineering

Tome XIII [2020]
Fascicule 2
[April–June]

Editura POLITEHNICA

ACTA TECHNICA CORVINIENSIS
Bulletin of Engineering

Edited by:

UNIVERSITY POLITEHNICA TIMISOARA

with kindly supported by:

THE GENERAL ASSOCIATION OF ROMANIAN ENGINEERS (AGIR)
– branch of HUNEDOARA

Editor / Technical preparation / Cover design:

Assoc. Prof. Eng. KISS Imre, PhD.
UNIVERSITY POLITEHNICA TIMISOARA,
FACULTY OF ENGINEERING HUNEDOARA

Commenced publication year:
2008

ACTA TECHNICA CORVINIENSIS
Bulletin of Engineering

ASSOCIATE EDITORS and REGIONAL COLLABORATORS

The Editor and editorial board members do not receive any remuneration. These positions are voluntary. The members of the Editorial Board may serve as scientific reviewers.

We are very pleased to inform that our journal **ACTA TECHNICA CORVINIENSIS – Bulletin of Engineering** is going to complete its ten years of publication successfully. In a very short period it has acquired global presence and scholars from all over the world have taken it with great enthusiasm. We are extremely grateful and heartily acknowledge the kind of support and encouragement from you.

ACTA TECHNICA CORVINIENSIS – Bulletin of Engineering seeking qualified researchers as members of the editorial team. Like our other journals, **ACTA TECHNICA CORVINIENSIS – Bulletin of Engineering** will serve as a great resource for researchers and students across the globe. We ask you to support this initiative by joining our editorial team. If you are interested in serving as a member of the editorial team, kindly send us your resume to redactie@fih.upt.ro.

ACTA TECHNICA CORVINIENSIS – Bulletin of Engineering
ISSN: 2067-3809

INTERNATIONAL SCIENTIFIC COMMITTEE MEMBERS and SCIENTIFIC REVIEWERS

MANAGER & CHAIRMAN

ROMANIA 

Imre KISS, University Politehnica TIMISOARA, Faculty of Engineering HUNEDOARA, Department of Engineering & Management, General Association of Romanian Engineers (AGIR) – branch HUNEDOARA

INTERNATIONAL SCIENTIFIC COMMITTEE MEMBERS & SCIENTIFIC REVIEWERS from:

ROMANIA 

Viorel–Aurel ŞERBAN, University Politehnica TIMIŞOARA – TIMIŞOARA
Teodor HEPUŢ, University Politehnica TIMIŞOARA – HUNEDOARA
Mircea BEJAN, Tehnical University of CLUJ-NAPOCA – CLUJ-NAPOCA
Liviu MIHON, University Politehnica TIMIŞOARA – TIMIŞOARA
Ilare BORDEAŞU, University Politehnica TIMIŞOARA – TIMIŞOARA
Liviu MARŞAVIA, University Politehnica TIMIŞOARA – TIMIŞOARA
Ioan VIDA-SIMITI, Technical University of CLUJ-NAPOCA – CLUJ-NAPOCA
Csaba GYENGE, Technical University of CLUJ-NAPOCA – CLUJ-NAPOCA
Sava IANICI, "Eftimie Murgu" University of REŞIŢA – REŞIŢA
Ioan SZÁVA, "Transilvania" University of BRASOV – BRASOV
Sorin VLASE, "Transilvania" University of BRASOV – BRASOV
Horatiu TEODORESCU DRĂGHICESCU, "Transilvania" University of BRASOV – BRASOV
Maria Luminiţa SCUTARU,"Transilvania" University of BRASOV – BRASOV
Iulian RIPOŞAN, University Politehnica BUCUREŞTI – BUCUREŞTI
Ioan DZITAC, Agora University of ORADEA – ORADEA
Carmen ALIC, University Politehnica TIMIŞOARA – HUNEDOARA

SLOVAKIA 

Štefan NIZNIK, Technical University of KOŠICE – KOŠICE
Karol VELIŠEK, Slovak University of Technology BRATISLAVA – TRNAVA
Juraj ŠPALEK, University of ŽILINA – ŽILINA
Ervin LUMNITZER, Technical University of KOŠICE – KOŠICE
Miroslav BADIDA, Technical University of KOŠICE – KOŠICE
Milan DADO, University of ŽILINA – ŽILINA
Ľubomir ŠOOŠ, Slovak University of Technology in BRATISLAVA – BRATISLAVA
Miroslav VEREŠ, Slovak University of Technology in BRATISLAVA – BRATISLAVA
Milan SAGA, University of ŽILINA – ŽILINA
Imrich KISS, Institute of Economic & Environmental Security – KOŠICE
Vladimir MODRAK, Technical University of KOSICE – PRESOV
Michal HAVRILA, Technical University of KOSICE – PRESOV

CROATIA 

Drazan KOZAK, Josip Juraj Strossmayer University of OSIJEK – SLAVONKI BROD
Predrag COSIC, University of ZAGREB – ZAGREB
Milan KLJAJIN, Josip Juraj Strossmayer University of OSIJEK – SLAVONKI BROD
Miroslav CAR, University of ZAGREB – ZAGREB
Antun STOIĆ, Josip Juraj Strossmayer University of OSIJEK – SLAVONKI BROD
Ivo ALFIREVIĆ, University of ZAGREB – ZAGREB

HUNGARY 

Imre DEKÁNY, University of SZEGED – SZEGED
Béla ILLÉS, University of MISKOLC – MISKOLC
Imre RUDAS, Óbuda University of BUDAPEST – BUDAPEST
Tamás KISS, University of SZEGED – SZEGED
Cecilia HODÚR, University of SZEGED – SZEGED
Arpád FERENCZ, Pallasz Athéné University – KECSKEMÉT
Imre TIMÁR, University of Pannonia – VESZPRÉM
Kristóf KOVÁCS, University of Pannonia – VESZPRÉM
Károly JÁRMAI, University of MISKOLC – MISKOLC
Gyula MESTER, University of SZEGED – SZEGED
Ádám DÖBRÖCZÖNI, University of MISKOLC – MISKOLC
György SZEIDL, University of MISKOLC – MISKOLC
Miklós TISZA, University of MISKOLC – MISKOLC
Attila BARCZI, Szent István University – GÖDÖLLŐ
István BIRÓ, University of SZEGED – SZEGED
József GÁL, University of SZEGED – SZEGED
Ferenc FARKAS, University of SZEGED – SZEGED
Géza HUSI, University of DEBRECEN – DEBRECEN
Ferenc SZIGETI, College of NYÍREGYHÁZA – NYÍREGYHÁZA

The Scientific Committee members and Reviewers do not receive any remuneration. These positions are voluntary. We are extremely grateful and heartily acknowledge the kind of support and encouragement from all contributors and all collaborators!

ACTA TECHNICA CORVINIENSIS – Bulletin of Engineering is dedicated to publishing material of the highest engineering interest, and to this end we have assembled a distinguished Editorial Board and Scientific Committee of academics, professors and researchers.

ACTA TECHNICA CORVINIENSIS – Bulletin of Engineering publishes invited review papers covering the full spectrum of engineering. The reviews, both experimental and theoretical, provide general background information as well as a critical assessment on topics in a state of flux. We are primarily interested in those contributions which bring new insights, and papers will be selected on the basis of the importance of the new knowledge they provide.

ACTA TECHNICA CORVINIENSIS – Bulletin of Engineering encourages the submission of comments on papers published particularly in our journal. The journal publishes articles focused on topics of current interest within the scope of the journal and coordinated by invited guest editors. Interested authors are invited to contact one of the Editors for further details.

ACTA TECHNICA CORVINIENSIS – Bulletin of Engineering accept for publication unpublished manuscripts on the understanding that the same manuscript is not under simultaneous consideration of other journals. Publication of a part of the data as the abstract of conference proceedings is exempted.

Manuscripts submitted (original articles, technical notes, brief communications and case studies) will be subject to peer review by the members of the Editorial Board or by qualified outside reviewers. Only papers of high scientific quality will be accepted for publication. Manuscripts are accepted for review only when they report unpublished work that is not being considered for publication elsewhere.

The evaluated paper may be recommended for:

- **Acceptance without any changes** – in that case the authors will be asked to send the paper electronically in the required .doc format according to authors' instructions;
- **Acceptance with minor changes** – if the authors follow the conditions imposed by referees the paper will be sent in the required .doc format;
- **Acceptance with major changes** – if the authors follow completely the conditions imposed by referees the paper will be sent in the required .doc format;
- **Rejection** – in that case the reasons for rejection will be transmitted to authors along with some suggestions for future improvements (if that will be considered necessary).

The manuscript accepted for publication will be published in the next issue of **ACTA TECHNICA CORVINIENSIS – Bulletin of Engineering** after the acceptance date.

All the authors and the corresponding author in particular take the responsibility to ensure that the text of the article does not contain portions copied from any other published material which amounts to plagiarism. We also request the authors to familiarize themselves with the good publication ethics principles before finalizing their manuscripts

ACTA TECHNICA CORVINIENSIS – Bulletin of Engineering
ISSN: 2067-3809

TABLE of CONTENTS

***	MANUSCRIPT PREPARATION – GENERAL GUIDELINES	11
1.	**Jean JOY, Shruti KANGA, Suraj Kumar SINGH** – UNITED KINGDOM / INDIA 3D GIS – RETROSPECTIVE FLOOD VISUALISATION	13
2.	**Muhammad Asif RABBANI** – CYPRUS SOLAR POWER SYSTEMS AND DC TO AC INVERTERS	19
3.	**Elena GRESOVA, Jozef SVETLIK** – SLOVAKIA COMPREHENSIVE USAGE OF DECISION TREES: THE COST–SENSITIVE MODELING	29
4.	**Osama Mohammed Elmardi Suleiman KHAYAL** – SUDAN RELATION BETWEEN HUMAN FACTORS AND ERGONOMICS	33
5.	**Asmita Mayuresh MARATHE, Anagha PATHAK** – INDIA EVALUATION OF SNAKING ISSUES IN 250KWe POWER PLANT BASED ON DIRECT STEAM GENERATION USING PARABOLIC TROUGH COLLECTOR	41
6.	**S. HEMAJOTHI, S. ABIRAMI, S. AISHWARYA** – INDIA A NOVEL COLOUR TEXTURE BASED FACE SPOOFING DETECTION USING MACHINE LEARNING	47
7.	**Rasheed Uthman OWOLABI, Mohammed Awwalu USMAN, C.E. WISDOM** – NIGERIA TRANS–ESTERIFICATION OF CASTOR OIL USING HETEROGENEOUS BIO–CATALYST OBTAINED FROM BOVINE BONE	53
8.	**Mustefa JIBRIL, Tesfabirhan SHOGA** – ETHIOPIA QUARTER CAR ACTIVE SUSPENSION SYSTEM DESIGN USING OPTIMAL AND ROBUST CONTROL METHOD	59
9.	**S. KANNAPPAN, S. Aruna MASTANI** – INDIA A SURVEY ON MULTI–OPERAND ADDER	65
10.	**Suresh Kumar GOVINDARAJAN, Abhishek KUMAR** – INDIA DARCY BASED PERMEABILITY IN A PETROLEUM RESERVOIR BEFORE AND AFTER WATER–FLOODING: WHAT DOES IT DEPEND ON?	69
11.	**Adewale George ADENIYI, Joshua O. IGHALO, Samson Akorede ADEOYE, Damilola Edwards ABDULAZEEZ** – NIGERIA NUMERICAL INVESTIGATION OF THE EFFECTS OF TEMPERATURE AND BIOMASS DENSITY ON THE PRODUCTS EVOLUTION FROM WOOD PYROLYSIS	73
12.	**Muhanned AL–RAWI, Muaayed AL–RAWI** – YEMEN / IRAQ SYSTEM DESIGN OF CELL PHONE DETECTOR	79
13.	**Amar KALYANE, R.J. PATIL** – INDIA EXPERIMENTAL INVESTIGATION OF BLACK COTTON SOIL BY LIME AND FLY–ASH STABILIZATION	83
14.	**S. PRAVEEN KUMAR, K. NARASIMHA RAO, Y. KRISHNA MOHAN** – INDIA STUDY AND ANALYSIS OF THE OFFSET MHO CHARACTERISTICS FOR THE LOSS OF EXCITATION PROTECTION OF AN ALTERNATOR	89

15. **Andrei Mihai BACIU, Imre KISS** – ROMANIA
REVIEW ON THE POST–CONSUMER PLASTIC WASTE RECYCLING PRACTICES AND USE THEIR PRODUCTS INTO SEVERAL INDUSTRIAL APPLICATIONS 95

16. **Adewale George ADENIYI, Joshua O. IGHALO** – NIGERIA
COMPUTER–AIDED MODELLING OF THE PYROLYSIS OF RUBBER SAW DUST (Hevea Brasiliensis) USING ASPEN PLUS 105

17. **G.K. GIRISHA, S.L. PINJARE** – INDIA
IMPLEMENTATION OF NOVEL ALGORITHM FOR AUDITORY COMPENSATION IN HEARING AIDS USING STFT 109

18. **Mustefa JIBRIL, Tesfabirhan SHOGA** – ETHIOPIA
COMPARISON OF H∞ AND μ–SYNTHESIS CONTROL DESIGN FOR QUARTER CAR ACTIVE SUSPENSION SYSTEM USING SIMULINK 113

19. **Ghanendra KUMAR, Chakresh KUMAR** – INDIA
PERFORMANCE ANALYSIS OF CROSSTALK INDUCED OPTICAL COMMUNICATION SYSTEM 123

20. **Iqbal SINGH, Salil BHARANY** – INDIA
COMPARATIVE STUDIES OF VARIOUS TECHNIQUES FOR IMAGE COMPRESSION ALGORITHM 127

21. **Vasile George CIOATĂ, Vasile ALEXA, Bogdan Dorel CIOROAGĂ** – ROMANIA
PARAMETRIC DESIGN OF LINEAR HYDRAULIC MOTORS 135

22. **Olaolu George FADUGBA** – NIGERIA
APPLICATION OF MULTIVARIATE DATA ANALYSIS IN THE INTERPRETATION OF GEOTECHNICAL INDEX PARAMETERS – A CASE STUDY OF THE FEDERAL UNIVERSITY OF TECHNOLOGY AKURE, ONDO STATE 139

23. **Deepak NANDAL, Om Prakash SANGWAN, Nandal VIKAS** – INDIA
A COMPARATIVE STUDY OF POPULATION BASED META–HEURISTIC TECHNIQUES FOR VARIOUS APPLICATIONS IN SOFTWARE TESTING 143

24. **Cristian PANDELESCU, Elisa–Florina PLOPEANU, Nicolae CONSTANTIN, Elena Mădălina VLAD** – ROMANIA
ANALYSIS OF THE CURRENT SITUATION CONCERNING THE DURATION OF USE AND THE MAIN DEFECTIONS OF THE PUMPING AGGREGATES 147

25. **Shweta K. BORSE** – INDIA
A REVIEW: PREDICTING AIR QUALITY USING DIFFERENT TECHNIQUE 153

The ACTA TECHNICA CORVINIENSIS – Bulletin of Engineering, Tome XIII [2020], Fascicule 2 [April–June] includes original papers submitted to the Editorial Board, directly by authors or by the regional collaborators of the Journal.

ACTA TECHNICA CORVINIENSIS – Bulletin of Engineering
ISSN: 2067–3809

Faculty of Engineering Hunedoara,
5, Revolutiei, 331128, Hunedoara, ROMANIA
http://acta.fih.upt.ro

MANUSCRIPT PREPARATION – GENERAL GUIDELINES

Manuscripts submitted for consideration to ACTA TECHNICA CORVINIENSIS – Bulletin of Engineering must conform to the following requirements that will facilitate preparation of the article for publication. These instructions are written in a form that satisfies all of the formatting requirements for the author manuscript. Please use them as a template in preparing your manuscript. Authors must take special care to follow these instructions concerning margins.

INVITATION

We are looking forward to a fruitful collaboration and we welcome you to publish in our ACTA TECHNICA CORVINIENSIS – Bulletin of Engineering. You are invited to contribute review or research papers as well as opinion in the fields of science and technology including engineering. We accept contributions (full papers) in the fields of applied sciences and technology including all branches of engineering and management. ACTA TECHNICA CORVINIENSIS – Bulletin of Engineering publishes invited review papers covering the full spectrum of engineering and management. The reviews, both experimental and theoretical, provide general background information as well as a critical assessment on topics in a state of flux. We are primarily interested in those contributions which bring new insights, and papers will be selected on the basis of the importance of the new knowledge they provide.

Submission of a paper implies that the work described has not been published previously (except in the form of an abstract or as part of a published lecture or academic thesis) that it is not under consideration for publication elsewhere. It is not accepted to submit materials which in any way violate copyrights of third persons or law rights. An author is fully responsible ethically and legally for breaking given conditions or misleading the Editor or the Publisher.

ACTA TECHNICA CORVINIENSIS – Bulletin of Engineering is an international and interdisciplinary journal which reports on scientific and technical contributions. Every year, in four online issues (fascicules 1–4), ACTA TECHNICA CORVINIENSIS – Bulletin of Engineering [e-ISSN: 2067-3809] publishes a series of reviews covering the most exciting and developing areas of engineering. Each issue contains papers reviewed by international researchers who are experts in their fields. The result is a journal that gives the scientists and engineers the opportunity to keep informed of all the current developments in their own, and related, areas of research, ensuring the new ideas across an increasingly the interdisciplinary field. Topical reviews in materials science and engineering, each including:

— surveys of work accomplished to date
— current trends in research and applications
— future prospects.

As an open-access journal ACTA TECHNICA CORVINIENSIS – Bulletin of Engineering will serve the whole engineering research community, offering a stimulating combination of the following:

— Research Papers – concise, high impact original research articles,
— Scientific Papers – concise, high impact original theoretical articles,
— Perspectives – commissioned commentaries highlighting the impact and wider implications of research appearing in the journal.

ACTA TECHNICA CORVINIENSIS – Bulletin of Engineering encourages the submission of comments on papers published particularly in our journal. The journal publishes articles focused on topics of current interest within the scope of the journal and coordinated by invited guest editors. Interested authors are invited to contact one of the Editors for further details.

BASIC MANUSCRIPT REQUIREMENTS

The basic instructions and manuscript requirements are simple:

— Manuscript shall be formatted for an A4 size page.
— The all margins of page (top, bottom, left, and right) shall be 20 mm.
— The text shall have both the left and right margins justified.
— Single-spaced text, tables, and references, written with 11 or 12-point Georgia or Times New Roman typeface.
— No Line numbering on any pages and no page numbers.
— Manuscript length must not exceed 15 pages (including text and references).
— Number of the figures and tables combined must not exceed 20.
— Manuscripts that exceed these guidelines will be subject to reductions in length.

The original of the technical paper will be sent through e-mail as attached document (*.doc, Windows 95 or higher). Manuscripts should be submitted to e-mail: redactie@fih.upt.ro, with mention "for ACTA TECHNICA CORVINIENSIS".

STRUCTURE

The manuscript should be organized in the following order: Title of the paper, Authors' names and affiliation, Abstract, Key Words, Introduction, Body of the paper (in sequential headings), Discussion & Results, Conclusion or Concluding Remarks, Acknowledgements (where applicable), References, and Appendices (where applicable).

THE TITLE

The title is centered on the page and is CAPITALIZED AND SET IN BOLDFACE (font size 14 pt). It should adequately describe the content of the paper. An abbreviated title of less than 60 characters (including spaces) should also be suggested. Maximum length of title: 20 words.

AUTHOR'S NAME AND AFFILIATION

The author's name(s) follows the title and is also centered on the page (font size 11 pt). A blank line is required between the title and the author's name(s). Last names should be spelled out in full and succeeded by author's initials. The author's affiliation (in font size 11 pt) is provided below. Phone and fax numbers do not appear.

ABSTRACT

State the paper's purpose, methods or procedures presentation, new results, and conclusions are presented. A nonmathematical abstract, not exceeding 200 words, is required for all papers. It should be an abbreviated, accurate presentation of the contents of the paper. It should contain sufficient information to enable readers to decide whether they should obtain and read the entire paper. Do not cite references in the abstract.

KEY WORDS

The author should provide a list of three to five key words that clearly describe the subject matter of the paper.

TEXT LAYOUT

The manuscript must be typed single spacing. Use extra line spacing between equations, illustrations, figures and tables. The body of the text should be prepared using Georgia or Times New Roman. The font size used for preparation of the manuscript must be 11 or 12 points. The first paragraph following a heading should not be indented. The following paragraphs must be indented 10 mm. Note that there is no line spacing between paragraphs unless a subheading is used. Symbols for physical quantities in the text should be written in italics. Conclude the text with a summary or conclusion section. Spell out all initials, acronyms, or abbreviations (not units of measure) at first use. Put the initials or abbreviation in parentheses after the spelled-out version. The manuscript must be writing in the third person ("the author concludes... ").

FIGURES AND TABLES

Figures (diagrams and photographs) should be numbered consecutively using Arabic numbers. They should be placed in the text soon after the point where they are referenced. Figures should be centered in a column and should have a figure caption placed underneath. Captions should be centered in the column, in the format "Figure 1" and are in upper and lower case letters.

When referring to a figure in the body of the text, the abbreviation "Figure" is used Illustrations must be submitted in digital format, with a good resolution. Table captions appear centered above the table in upper and lower case letters.

When referring to a table in the text, "Table" with the proper number is used. Captions should be centered in the column, in the format "Table 1" and are in upper and lower case letters. Tables are numbered consecutively and independently of any figures. All figures and tables must be incorporated into the text.

EQUATIONS & MATHEMATICAL EXPRESSIONS

Place equations on separate lines, centered, and numbered in parentheses at the right margin. Equation numbers should appear in parentheses and be numbered consecutively. All equation numbers must appear on the right-hand side of the equation and should be referred to within the text.

CONCLUSIONS

A conclusion section must be included and should indicate clearly the advantages, limitations and possible applications of the paper. Discuss about future work.

Acknowledgements

An acknowledgement section may be presented after the conclusion, if desired. Individuals or units other than authors who were of direct help in the work could be acknowledged by a brief statement following the text. The acknowledgment should give essential credits, but its length should be kept to a minimum; word count should be <100 words.

References

References should be listed together at the end of the paper in alphabetical order by author's surname. List of references indent 10 mm from the second line of each references. Personal communications and unpublished data are not acceptable references.

- *Journal Papers:* Surname 1, Initials; Surname 2, Initials and Surname 3, Initials: Title, Journal Name, volume (number), pages, year.
- *Books:* Surname 1, Initials and Surname 2, Initials: Title, Edition (if existent), Place of publication, Publisher, year.
- *Proceedings Papers:* Surname 1, Initials; Surname 2, Initials and Surname 3, Initials: Paper title, Proceedings title, pages, year.

ACTA TECHNICA CORVINIENSIS – Bulletin of Engineering
ISSN: 2067-3809

[1.]Jean JOY, [2.]Shruti KANGA, [3.]Suraj Kumar SINGH

3D GIS – RETROSPECTIVE FLOOD VISUALISATION

[1.]Teesside University, Middlesbrough, UNITED KINGDOM
[2.]Centre for Climate Change and Water Research, Suresh Gyan Vihar University, Jaipur, INDIA
[3.]Centre for Sustainable Development, Suresh Gyan Vihar University, Jaipur, INDIA

Abstract: This paper discusses the possibilities of 3D GIS to analyse the Kerala Flood 2018. The study area is Meloor Panchayath, Thrissur District, Kerala, where huge destruction happened and the flood level was up to double storied buildings. 3D models can communicate effectively and it can be used to study the flood inundated area and can measure the destruction caused. The ArcScene 3D capabilities are tested and it came out to be not that effective. Therefore multiple software was used for creating an aesthetically appealing 3D model. This 3D model was used to analyse the temporal flood level and was used to create an animation video.
Keywords: 3D GIS, Flood, modeling, disaster

INTRODUCTION

Flooding occurs because of weather condition which creates a large volume of surface runoff flow that goes over the holding capacity of artificial drainages. This kind of high-intensity rainfall in a very short time can cause the problem of exceeding the limit of the infiltration capacity of soil and interception capacity of vegetation. This creates a huge surface runoff towards downslope due to gravity [1].

GIS collects data from different sources like GPS, soil samples, weather conditions, remote sensing, stream gages and also censuses. Once flooded area will be flooded again so checking the history of flood occurred areas helps us to identify flood risk areas. Using the acquired data, an analysis is done based on GIS to estimate the amount of influence and impact of each factor. GIS helps in the various process such as locating, planning, mitigation actions, aiding in response, and helps in recovery management [2]. Flood-prone areas can be founded by overlaying different layers of space hence more mitigation can be provided at the time and take necessary response. GIS is also used to display flood-related data in 2D and 3D to understand it in a better way. GIS generates maps that are used to inform the public and the government about flood events, evacuation routes, etc. [3] These records can be disseminated using internet technologies, developing interactive maps with the query option provided and updated in actual time, linked to the extra available information.

In 3D hazards like a flood can be visualized in realism. A 3D visualization project on flood was presented by [4] with the help of relevant images and overflowing water to show the land surface where the flood occurred. Köninger and Bartel 1998 states that the unavoidable part in the management of land is 3D GIS. Through 3D GIS a virtual city is made which is the natural add-on to the planning of City. In this technology, we give similar shape and depth to the objects as we see them in reality to increase the chances of understanding the environment [5].

The 3D model is a mathematical representation of 3D space. 3D models represent an important source of information in crisis situations. Some of the possibilities are visualizations and simulations of various disasters, planning evacuation, training rescue teams for emergency situations, etc. Also, 3D models record the shape and configuration of the city and they can be used to assess the extent of the damage, guiding helpers and rebuild the damaged area after a severe disasters [6]

3D visualization can be used for the presentation of hazards, vulnerabilities, and risks. It can help and improve efficiency in the decision-making process because it reduces the amount of cognitive effort. 3D modeling depends very much on the type of disaster to be presented and a group of users. The user is related to elements of risk because various users are interested in different elements of risk. The type of objects that will be modeled for a disaster situation, their representation and resolution/level of Detail are crucial in 3D modeling [7, 8].

There are many 3D modeling software but 3D modeling software with GIS capabilities is less [9]. So this study is about the way to create an aesthetically beautiful, realistic looking 3D space with floodwater inundated. Every feature in the model like building, river, and DEM will be overlaid using the coordinates and no compromise is given to the spatial accuracy, to create a 3D model. We are using software like ArcGIS, AutoCAD, Sketchup Pro, Lumion, Camtasia and using this software's 3D model and animation would be created.

STUDY AREA

Kerala gone through the heavy flood in the year 1924 which caused great damages to Property, Crops even it led to the loss of many lives. This flood started from 16th July 1924 and lasted till 18th Jul 1924 as 15th July 1924 south-west monsoon arrived in Kerala. Due to the arrival of south-west monsoon heavy rainfall occurred which led to the intense flood in many districts of Kerala. The affected regions recorded

maximum one-day rainfall on 17th July, maximum 2-day rainfall on 16th July 1924 and 17th July 1924 and maximum 3-day rainfall on 16th July 1924 to 18th July 1924. Devikulam is the place in Kerala which experienced rainstorm with 484 mm and 751 mm of rainfall on 1-day and 2-day respectively. Munnar experienced a 3-day rainstorm of 897 mm rainfall which lasted for 3 days [10]. After the tragic flood occurred in 1924, Kerala again went through a heavy flood in the year 1961. Generally, 7 to 10 days of the monsoon is the time period when water in the rivers rises than their banks which causes an overflow. But in the year 1961, there was an unexpected overflowing of rivers not only in the expected duration and intensity which resulted in a heavy flood in the State. Towards the end of July, monsoon became violent and persisted till the early days of August which affected the southern part of the State. The intensity of rainfall was gradually increased from the first week of July and it took a disastrous phase by the mid of the July in which Kerala suffered a lot. Periyar sub-basin was affected to a greater extent by the continuous and heavy rainfall which also influenced some sub-basins in Kerala. The highways were submerged in water during this period. Both the northern and southern part of Kerala was affected by this flood since the rainfall recorded was 56% more than the normal. Surveys concluded that 115 people died, more than 50,000 houses were damaged and 1,15,000 acres of fields in which paddy cultivated were affected by this flood and landslides which shows that the damage caused to a great extent (Centre water commission 2018).

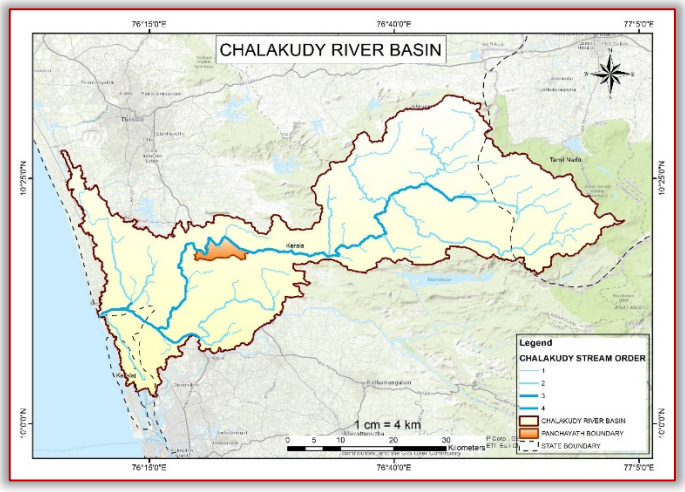

Figure 1. Study area map depicting streams and panchayat boundary

The study area is Meloor Panchayath, which is a small village in Chalakudy block. Meloor comes under the Thrissur district in Kerala State. Meloor lies on the banks of Chalakudy River, northern side boundary is completely facing Chalakudy River, which exactly measures 15.52 km^2. Geomorphologically, the stretch of Chalakudy river is characterized by a hilly area, highly undulating terrain, moderately undulating terrain, low rolling terrain, transitional plain and floodplain (Figure 1).

METHODOLOGY

— Realistic 3D GIS Workflow

There is no GIS software with good quality 3D Visualisation ability. Vice-versa, there is software with good 3D visualization capabilities, but GIS abilities are not available. So for using the abilities of GIS software and 3D modeling software together, they should be interoperable. But currently, that is an issue, to solve this multiple software is used. While thinking about the basics, both GIS and 3D architectural designing is evolved from the CAD environment. So both software is good in CAD interoperability, CAD format can be converted to GIS formats or to 3D formats. Thus we selected AutoCAD as our CAD software and Sketch-up and Lumion as our 3D modeling and animation software. Then GIS layers in ArcGIS are converted to CAD and further procedure summarised below (Figure 2).

— GIS

≡ Data collection

Data used are SRTM DEM, Panchayat boundary, OSM River & building footprint polygon and flood inundated area as raster layer. SRTM DEM was downloaded from the NASA Earthdata website. Flood inundated area raster was used to check the flood heights.

≡ OSM Data Download

OSM Data is open source data hosted by an open street map. They are mainly crowd sourced data and now big multinational companies like Facebook are also funding them to create a quality map because they are also using OSM base maps in their services. OSM has roads, amenities, and Building polygons, placemarks, etc. All data is created either by crowdsourcing or by satellite image processing. Building footprints are created using satellite image processing. For this project, OSM data was downloaded using QGIS 3.4 plugin. The name of the plugin is "OSM downloader", where all data can be downloaded by drawing area of interest rectangle around our study area. The downloaded file will be in '.osm' format and it will be loaded in the QGIS interface, after downloaded from OSM servers. The downloaded file will contain lines, multiline strings, multi polygon, other relations and points.

Lines and multiline-strings include roads, river centrelines, transmission lines, etc., Multipolygons include building footprints, land use, water bodies, etc. So lines and multiline- strings are exported by right click and go to export, then select ESRI Shapefile as format and give the WGS1984 projection, then download. Building polygons and river polygons are separated using the attribute information and

separate feature class was created in ArcMap, Select by attribute and export tools were used for that purpose. Road data was also separated from transmission lines and river centrelines, and separate feature class was made.

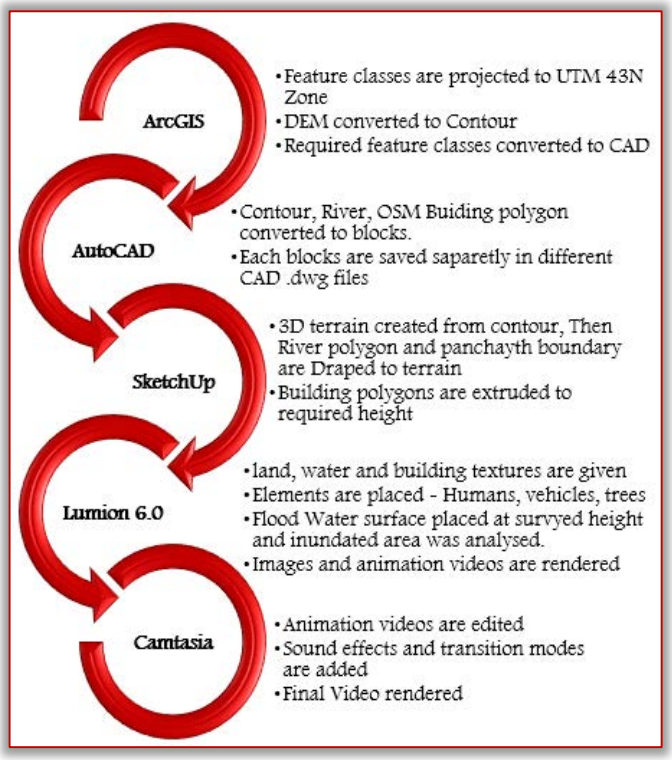

Figure 2. Workflow of 3D Flood animation

≡ Data preparation

OSM data was not enough, because some roads were not mapped. Road data was updated using base map services of ArcGIS and also field survey was also done. This digitized data need to be projected for every step ahead. So all the feature classes were projected to "UTM 43N Zone". AutoCAD software can handle all coordinate systems but Sketchup and Lumion are not capable of that. We need to convert the Coordinate to 2d coordinate in Meters, thus Lumion and sketch up will access the data by assuming it in the local coordinate system in the meter. The contour was created from SRTM DEM using the "Create contour" tool because DEM cannot be directly accessed in Sketchup. Required Feature classes were converted to CAD files using the "Export to CAD" tool in the conversion toolbox.

— AutoCAD

AutoCAD is a computer-aided designing and drafting software owned by Autodesk. It is mainly used in 2D drafting purposes. The native file format of AutoCAD is ".dwg" (drawing). The version used for this project was AutoCAD 2015. In AutoCAD, the separate .dwg files of individual feature classes were opened and it was converted into Blocks using the "blocks" command. This is done because when we import the .dwg files into Sketchup, they will behave like 'components'. Each component is meant to be in a union, without interfering with other components, so that component-wise editing is possible just like blocks in AutoCAD. The coordinates of AutoCAD space should be the same as the UTM coordinate values, cross-checking should be done.

— SketchUp

Sketchup, earlier known as Google Sketchup, when owned by Google, now it's acquired by Trimble inc., a mapping, and surveying the solution company. It is a 3D modeling computer program used for many drawings and 3D modeling purposes in architectural, interior designing, landscape designing, etc. We use Sketchup pro-2015, which is an advanced version with greater capabilities.

Sketchup is capable to import AutoCAD .dwg files directly using the "import" option in the File menu. Firstly, Contour was imported, which was imported and visualized as a component. Go inside the component and contour was used for the creation of Land-surface mesh or DSM. Sketchup has a "Sandbox" tool for that. So select the contours and run the "Sandbox" tool. Then, imported the river polygon and Panchayat boundary into Sketchup (Figure 3).

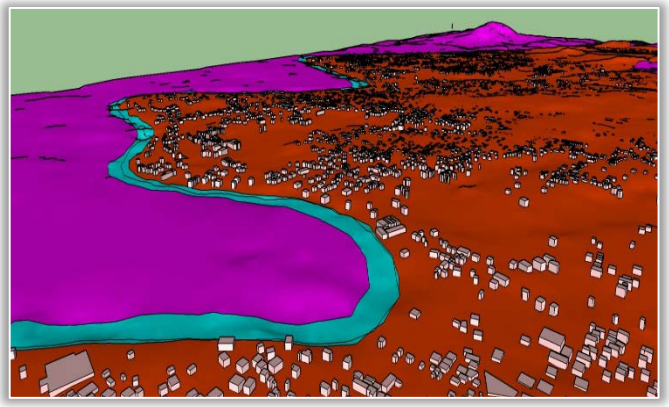

Figure 1. Sketchup 3D model

It was overlaid above the contours using the coordinates, thus it shows the GIS capability of layer overlay. Select Component of Panchayat boundary runs the "Drape" tool in the Sandbox toolset. Drape tool enables us to draw a polygon on Surface which can be differentiated by colors because, in Lumion, we can only give textures on the basis of unique colors. So Different colors were given to the river, Study area and outside study area portions. OSM Building Footprint was imported into Sketchup. Building polygon also overlaid above other layers using the coordinates, which was spatially referenced. This building polygon component was hollow polygons, so for extrusion for height, a face was needed. So Polygons are filled with face surface and all face are selected together and extruded upwards, intersecting the DSM surface, "Push/Pull" tool was used for extrusion. The extruded building polygons was having the same height, so in DSM with higher

altitude areas, building height seems to be less compared to the lower altitude region. This problem was solved by manually adjusting the height of each polygon using the "Push/Pull" tool. Colour was also given to buildings for giving textures in Lumion.
This Finished Sketchup file is saved as ".skb", which is not supported in Lumion. So it was exported to "COLLADA, .dae" file format. Sketchup was also able to create animation videos and good realistic rendering, but Lumion was added into workflow because of the better performance and availability of stock 3D elements like Trees, plants, vehicles, humans and specifically the perfect realistic water body rendering.

— Lumion

Lumion is a fast 3D rendering software with realistic outputs, they also have close to reality 3D library of many features like people, vehicles, trees, etc. It also has the sound effects and physical motion of each feature, like the movement of water waves, rain and trees leave in wind. Lumion is owned by Act 3D B.V. Lumion 6.0 was used in this project. Collada file created in Sketchup was imported into Lumion using the "import" tool in the "Objects" tab. The model will be placed in space according to the coordinate given, so it may face difficulty in moving to the coordinates which may far away from the origin, for avoiding that situation, the final stage of Sketchup file the entire 3D model should be moved close to the origin. Because in Lumion, coordinates don't matter, it is a visualization software. Textures for the ground, River, and Buildings are given from the library, it can be accessed from the "Material" tab. Categories of material textures available are nature, indoor, outdoor and custom. The colors given in Sketchup will act as the base for texture input, each color will act as a homogenous base while giving textures. Select each color and given the material color.

— Floodwater surface

The floodwater surface was created using the "Landscape" tool, where the "Water" tool is available. A Rectangle area of interest was drawn and the software renders water below that. So the water surface was drawn for the entire study area and it was raised up to the flood level. A particular reference location was selected and "Flood inundated raster" was checked for the flood height of that location. Then the surface height of that location from the origin in Lumion space is measured, there is no direct measurement tool available in Lumion, so an object was placed above the surface, which will show the height and that height was noted. Then, "Floodwater surface height = Surface height + Flood height" Thus flood water surface height was found out and previously created water surface was raised to that surface, assuming that water level is the same in all inundated area. The water surface will cut through the terrain giving a visualization of the flooded area.

— Animation

The animation is created using movie maker tool in Lumion. Fly through using mouse and keyboard is perfect for creating the moving shots. Cinematic frames are possible to make using Lumion. The camera path was set using creating multiple snapshots that define the different camera positions. Weather effects were given from "New effects", then under the weather category, rain is available. So basically different clips were made using different weather conditions and flood levels. First, clear weather was used to create a clip for showing the conditions before the flood. Then slowly weather conditions are changed, like small rain events to thunderstorms and also temporal flood level rise also showed using the data obtained in the flood mapping section. The flood surface was raised according to the results obtained during the flood mapping. The camera focal length was adjusted to occupy maximum details. Sound effects were also added from the sound library, Thunderstorm sound and other background sounds are so realistic in Lumion environment. Each clip was rendered out of Lumion in the ".avi" format.

— Camtasia

Camtasia is primarily a screen recording software for creating video tutorials, it is owned by Techsmith. It also has video editing capabilities with good tools for inputting in video text and images. In this research, Camtasia Studio 8.4 was used. Camtasia editor has the industry-standard facility like the "timeline" interface, which enables drag and drops facilities for multiple tracks. Rendered clips were added into the timeline, then it was joined together using transitions for continuity.

RESULTS AND DISCUSSIONS

— 3D model

The 3D model is as shown in Figure 4 the buildings, river, and Topography are everything spatially accurate, it was created from the shapefile/Feature class from the GIS platform.

Figure 2. Final output of the 3D model

But Trees and all other elements are placed randomly to boost the visual appearance and to get the relative size comparison while flood happens, forgetting the impact of the flood.
The floodwater surface was the same as the flood inundated area found in the field.

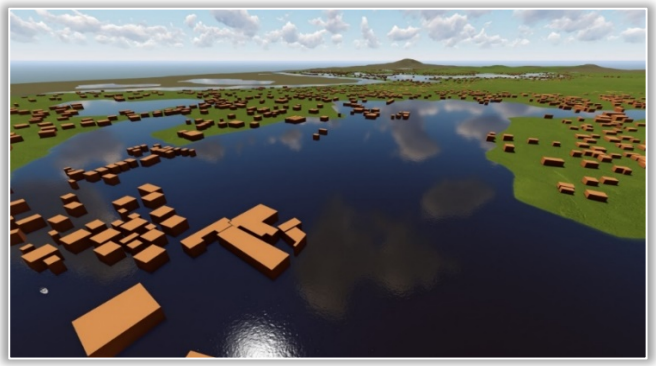

Figure 3. Floodwater surface

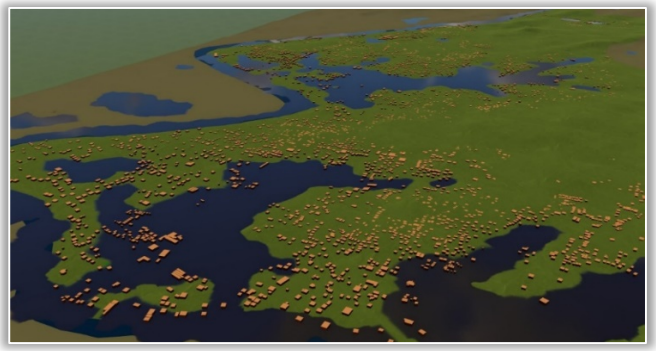

Figure 4. Flood inundation visualization

— Beneath a Flood

Where flood mapping gives the 2D map and spatial variation of a flood, suppose we need to analyse the height aspect and feature submerged by water, a 3D model is a great tool. By placing elements like peoples and vehicles, we can compare and analyse the impact of the flood (Figure 5). All 3D elements in Lumion are in scale with the real environment, if the model from Sketchup is saved in meter, then every element placed in Lumion will be proportionate to the environment. .We are able to measure the flood height of every area as shown in Figure 6. This will help to understand the dangerous situation of floods. The elements placed like 3D human and Car will communicate the flood height and its impact, every element in Lumion are in standard size according to the unit selected in the SketchUp model. Flood underwater visualization can also be created using Lumion (figure 7). This visualization helps to communicate the impact of the flood on the masses. This visualization demonstrates the destruction happened. Weather condition, sun angle and cloud thickness, etc. can also be changed according to match the situations during flood events. The above images were rendered out of Lumion using an image rendering tool (figure 8).

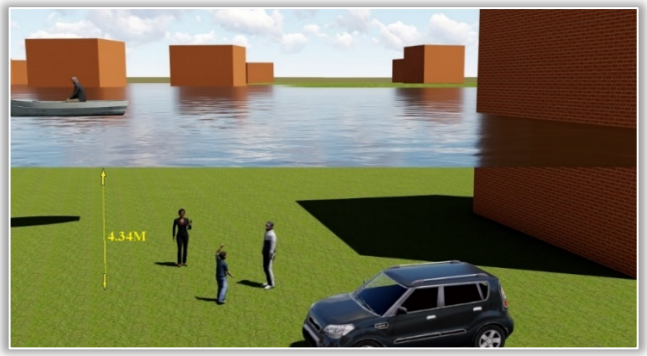

Figure 5. Analysis of features drowned by the flood

Figure 6. Flood inundation visualization

— Animation

Animation showing the temporal change of water level and flood inundated area was created using Lumion and Camtasia software. Rain effects and required sound effects where created in Lumion and Camtasia. Few frames of the animation are showed in figure 9 and figure 10.

Figure 9. 3D Visualization

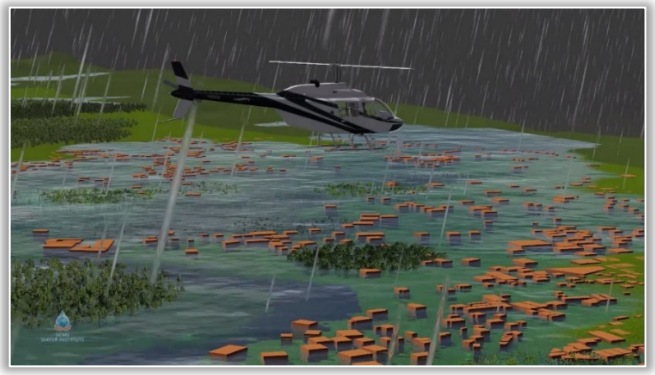

Figure 10. Final Animation video

CONCLUSIONS

Using 3D GIS it was successful to recreate the flood and analyse the situation and losses during the flood. It was very helpful in analysing disaster events. Capable 3D GIS software was not available in the market and this workflow will help several enthusiasts for future research. In disaster preparedness, taking recent flood as a benchmark, planning for flood events was done. Relief camp location and Evacuation priority were calculated and according to that safest route avoiding flood was developed. This system can be used in future flood events for evacuation planning and it will help the disaster preparedness planning for Panchayat. This research found the flood inundated area and temporal change of flood, using that map was prepared. This map will facilitate future uses in disaster preparedness and land use planning for effectively using the flood plain

References

[1] Dimitriou, E.,: Overland Flow, Encyclopedia of Agrophysics. Encyclopedia of Earth Sciences Series, 2011: 536–536.
[2] Khanna, K. R., Agarwal, C. K., P Kumar.: Remote Sensing and GIS applications in Flood Management. New Delhi, 2006, 11.
[3] Shanley, L. A., Bellovary,T., Lulloff, A., Schwoegler-Boos P.A L.,: GIS Data Sharing and Flood Hazards in Wisconsin. Wisconsin: Wisconsin Land Information Association, 2006.
[4] Evans, S.Y., Todd, M., Baines, I., Hunt, T., Morrison G.: Communicating flood risk through three-dimensional visualization. Proceedings of the Institution of Civil Engineers 167 (2014): 48-55.
[5] Kjellin, A., Pettersson, L.W., Seipel, S., Lind, M,: Evaluating 2D and 3D visualizations of spatiotemporal information. ACM Transactions on Applied Perception 7 (2010)
[6] Kolbe, T. H., Gröger, G., Plümer L.: Geospatial Information Technology for Emergency Response. Taylor & Francis, 2007.
[7] Kemec, Serkan., Sebnem Duzgun, H., Zlatanova Sisi.: A Conceptual Framework For 3d Visualisation To Support Urban Disaster Management . 2010.
[8] Liang, J., Gong, J. Li,Y.: Realistic rendering for physically based shallow water simulation in Virtual Geographic Environments (VGEs). Annals of GIS 21 (2015): 301-312.
[9] Tully, D., Rhalibi, A.E., Carter,V., Sudirman, S.: Hybrid 3D rendering of large map data for crisis management. ISPRS International Journal of Geo-Information 4 (2015): 1033-1054.
[10] Centre water commission, Government of India. "Kerala floods 2018." 2018.

ACTA TECHNICA CORVINIENSIS – Bulletin of Engineering
ISSN: 2067-3809

[1.]Muhammad Asif RABBANI

SOLAR POWER SYSTEMS AND DC TO AC INVERTERS

[1.] Department of Electrical & Electronics Engineering, Faculty of Engineering, Cyprus Science University, Ozanköy/Kyrenia, North Cyprus, CYPRUS

Abstract: In this article solar power systems architecture along with the brief overview of the DC to AC inverters and their utilization as a power electronics device in solar photovoltaic systems is provided. The study provides details regarding the types of the inverters, single phase half bridge inverters, single phase full phase inverters and three phase inverters. As pulse width modulation (PWM) is widely used in inverters which works as a solar charge controllers so the principles of PWM along with carrier based and carrier less modulation techniques is also mentioned. A comprehensive simulation and implementation of a three phase PWM inverter in Simulink Matlab is also provided.
Keywords: solar power systems, inverters, pulse width modulation, smart grids, control strategies, simulation model

INTRODUCTION

The major sources of producing electricity in the world include fossil fuels and coals which are increasing the greenhouse gases (GHG) emissions. These GHG emissions are the main reason behind the climate change. As the population of world is increasing this is also resulting in increase in demand of the electricity as well. After the Paris agreement on climate change, the countries have decided to cap the carbon emissions up to certain levels and to reduce the production of the GHG gases by stop using conventional fossil fuels to produce electricity.

One of the clean options was the Nuclear power but after the meltdown of the Fukushima Daiichi nuclear plant in Japan due to the tsunami caused by severe earthquake on March 2011 the governments around the world are now no more considering Nuclear as an option for environmental production of energy instead the only option for the clean energy production with the unlimited natural resources left is through the renewable energies [1]. The incentives provided by the governments is helping in more installations of solar power plants around the world at residential and commercial levels.

Therefore in order to achieve the targeted goals regarding climate change set by UNFCC [2] the increase in PV generation facilities can be play an important role. As there is abundance of sun and solar energy in the world so we can consider photovoltaic (PV) energy effect to be an important sustainable resource because of this the photovoltaic systems are widely used, as the source of electricity in urban and rural areas. In this study, solar power system types are discussed with the types and classifications of DC to AC inverters and their importance regarding the integration of DC solar power systems with the AC side of the utilities as well is discussed. Also in this paper using Matlab model simulation of the PWM inverters is discussed.

TYPES OF PHOTOVOLTAIC SYSTEM

The solar power systems can be branded into different types depending upon the electric production ability and according to the end user energy requirements.

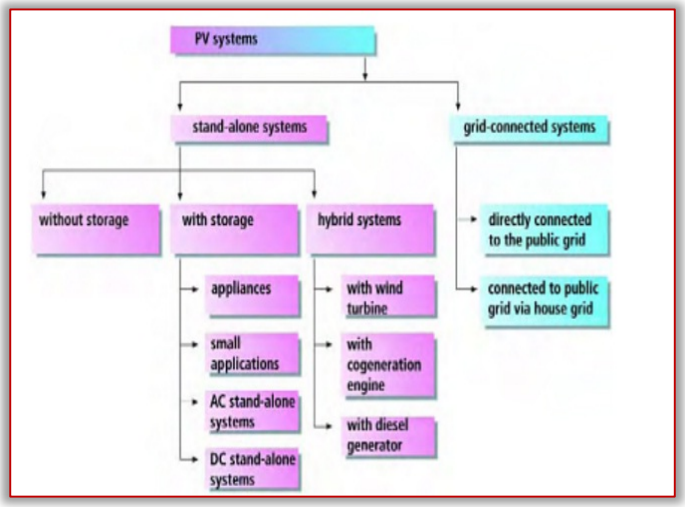

Figure 1. Types of PV systems source (The German Energy Society, Deutsche Gesellschaft für sonnen energie (DGS LV Berlin BRB), 2008)

— Standalone systems

The other term used for standalone systems is "off-grid solar power systems" as they are commonly used in areas where grid or utility power is not available. These systems are independent of any other source of energy and the energy produced by sun is not only utilized during the day but access is stored in battery banks to be used when there is no sun available. These systems are used where supply of electricity is immediately required and with minimum price.

The systems can be installed in shortest time periods and no hassle or rustle is needed like the provision of high transmission lines and the transformers. These systems are mostly being used in rural electrification projects and in remote areas where the grid is not available. The OFF-Grid solution is the solution in which you can simply live without the GRID and produce and use your own produced energy according to your requirements.

Following are the main components required for such kind of systems:

1. PV modules
2. Charge controllers
3. Battery bank
4. Load
5. Ac inverter for systems where alternate current is required at the loads

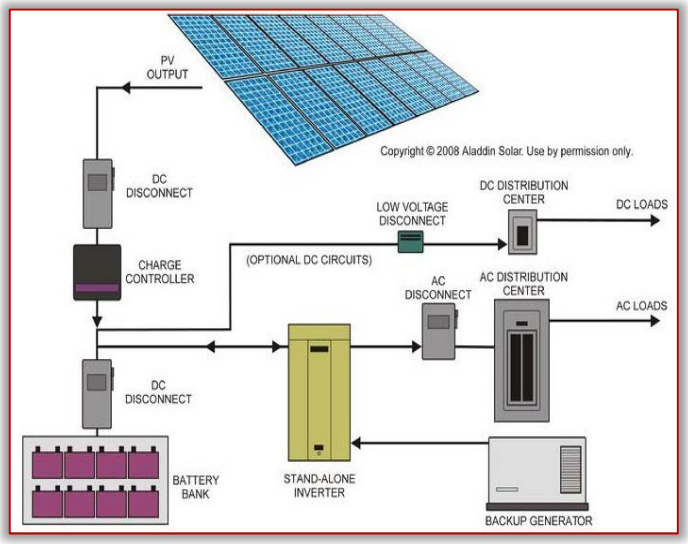

Figure 2. Schematic diagram of solar off grid system

—Grid connected systems

This is a solar power system which is linked to the utility grid. In unconnected systems (standalone systems) we need battery bank for energy storage but in grid connected systems the energy which is produced more than the requirement of end user is transported back to the utility grid to be used where there is shortage of energy. In grid-connected systems the community electricity grid is used as an energy store as well.

Many countries around the world prefer mostly solar PV systems to be connected to the utility grid because that helps their national grids is getting access energy from the solar systems, reduce production of cost of energy production by use of fossil fuels and in return the citizens with solar installations enjoy rebates. Feed-in tariff for production of solar electricity also helps the user to get back the initial investment on the system at the earliest.

The standard grid-connected PV systems are mostly made up of the following components:

1-PV modules/array

2-PV array combiner/junction box

1. 3-Direct current (DC) cabling
2. 4-Inverter
3. 5-AC cabling
4. 6-Meter cupboard with power distribution system, supply and feed meter, and electricity connection.

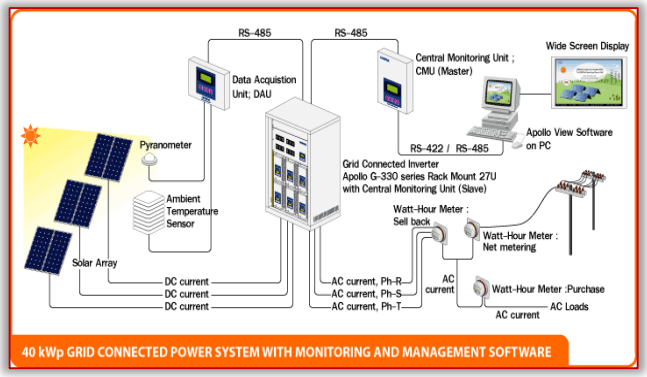

Figure 3. Grid connected PV system (source: http://www.leonics.com)

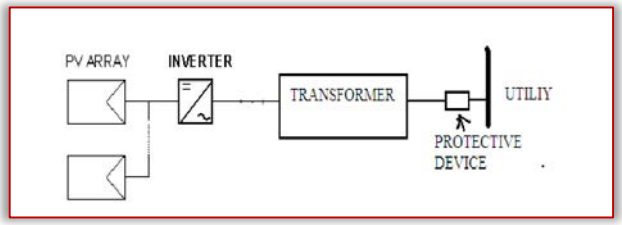

Figure 4. Block diagram Grid-Connected System

The use of transformers increases the ac output voltage when needed. Where there is no boost up of ac current required, transformer less designs are preferred. In order to prevent resistive power flow from utility to the solar system protective devices like under voltage relay, circuit breakers etc are installed. Grid-connected photovoltaic (PV) energy is one of the fastest growing and most promising renewable energy sources in the world.

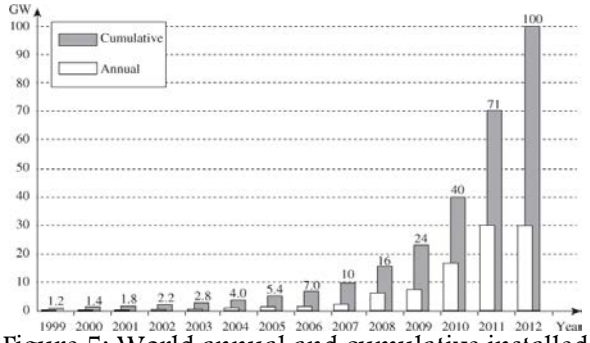

Figure 5: World annual and cumulative installed photovoltaic capacities Source: (Abu-Rub, Malinowski, & Al-Haddad, 2014

According to London based research and consulting firm GlobalData, the global collective installed solar photovoltaic (PV) capacity would increase from 175.4 Gigawatts (GW) in 2014 to approximately 223.2GW in 2015. According to GlobalData's recent report China is considered as the major market leader in PV installations with about 17.6 GW in 2015.

—Hybrid Systems

In hybrid systems the required output power is obtained by two or more different power generating sources. A system can be hybridized by combining different renewable energy sources such solar and wind together to get the common output required by

the end user. Solar power system can also be joined together with the diesel generator in areas where there is needed and for better performance. The main aim of hybridization is to get the stable output from the renewable energy sources and cater for fluctuations caused because of the environmental conditions while using solar and wind generation.
Sometimes hybrid systems are also known as "Integrated renewable energy systems".
Hybrid systems are generally planned to meet the peak demand when they run in combination with conventional power generation systems. For example in case of wind and PV hybrid power plant these two separate systems share a single inverter for power conversion and a single storage facility depending upon the case of grid connected system [3].

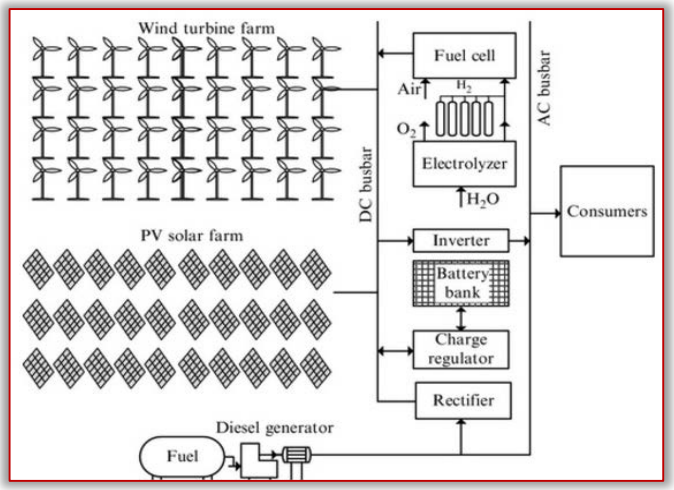

Figure 6. Hybrid Solar-PV, Wind Turbine, and Diesel Power Integrated System

DC TO AC INVERTERS

The conversion circuits that run from a DC voltage source or a DC current source and convert it into an AC voltage or Current are known as inverters. In this case the input to the inverter is a DC source or DC source produced from an AC voltage source. The principle source of input power is possibly utility ac voltage source that is transitioned to DC by an AC-DC rectifier with capacitor filter and then converted into ac supply using an inverter [4].
The dc-ac converter, also known as the inverter, converts dc power to ac power at required output voltage and frequency. We can use existing power supply network or form a rotating alternator through a rectifier or a battery, fuel cell, photovoltaic array or magneto hydrodynamic generator to provide DC power input to the inverter. We can get the constant DC link voltage by adding a filter capacitor across the input terminals of the inverter hence the inverter can be considered as an adjustable-frequency voltage source. The configuration of ac to dc converter and dc to ac inverter is called a dc-link converter.

— Classification of Inverters

Inverters can be broadly classified into two types, voltage source and current source inverters.

» Voltage Source Inverters

A voltage–fed inverter (VFI) or a voltage–source inverter (VSI) is one in which we have a dc source with a very small impedance which is negligible. The input terminals have a constant voltage. In the voltage source inverter the main input supply is voltage. The VSI are used to control the output voltages. Also the shape of the ideal VSI output voltage waveform should be autonomous of the load connected to the inverter. DC to AC inverter generates an AC output waveform from a DC source. The VSI are used in various applications such as adjustable speed drives (ASD), uninterruptible power supplies (UPS), active filters, Flexible AC transmission systems (FACTS), voltage compensators, and photovoltaic generators.
Voltage source inverters are applied in three phase or single phase applications. The half-wave and full wave Single-phase VSIs are widely used for power supplies, single-phase UPSs, and intricate high-power topologies when used in multilevel arrangements. Whereas for the sinusoidal voltage waveforms, such as adjustable speed drives(ASDs), uninterruptible power supplies (UPS), and some types of Flexible AC transmission systems (FACTS) devices such as the STATCOM we use three-phase VSIs. Commonly voltage inverters are used in the applications where arbitrary voltages are required [5]

» Current Source Inverters

In current source inverters (CSI) the input is changeable current from the dc source of high impedance that is from a constant dc source so in the current source inverter the supply to the inverter is the current source. In case of the current source inverter we control the current output. We use CSI with transistor or thyristor switches. The polarity of input current does not change and the direction of flow of power is determined by the input voltage. The AC (alternating current) wave form with fixed magnitude is produced for a given input. An inductor is connected at the input side of CSIs to maintain the current [6]. The CSIs are used in many applications such as a very high power and high voltage AC motor drives. CSIs can be also applied in motion control systems.

SINGLE PHASE INVERTERS

The voltage source inverters (VSI) are classified on the basis of their construction and their output voltage and their level of implementation. There are three main types of the VSI on the basis of their output voltage as [5]:
1) Single-phase half-bridge inverter
2) Single-phase full-bridge inverter
3) Three phase voltage source inverter

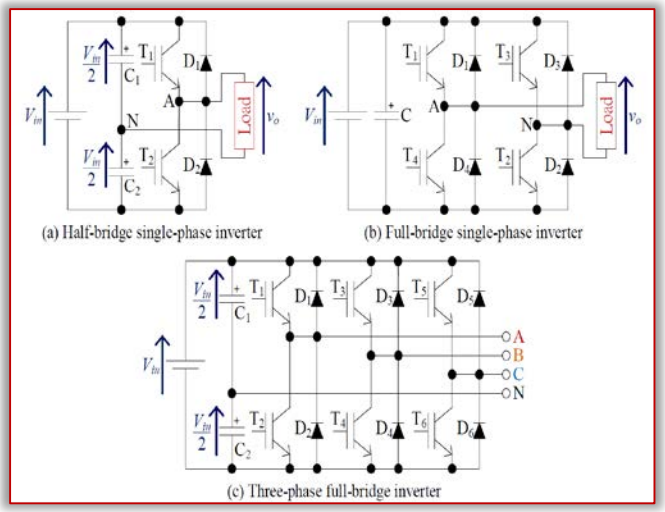

Figure 7. Circuit diagrams for power inverters

— Single phase half bridge inverter

For low power applications we use a Single-phase half-bridge. Fig.6 (a) shows the circuit diagram of a single-phase half-bridge inverter. This inverter consists of two switching devices, T1 and T2 and two diodes, D1 and D2. In this case, IGBTs (insulated gate bipolar transistors) are the switching devices. These two IGBTs and these two diodes build a one-leg or called a half-bridge. D1 and D2 are called anti-parallel diodes of T1 and T2, respectively. If the switching devices are MOSFETs, these diodes are built internally. The input capacitors, C1 and C2, share the input equally. Their voltage is the same and equal to Vin/2. The node between these two capacitors is the neutral point of the output of the inverter, N, and the node between two IGBTs is the live point of the output of the inverter, A. The T1 and T2 are switched ON and OFF alternatively in order operate this inverter. The duty of the gate signal of each IGBT in the ideal case is 0.5 which is the dead-time between each switching is applied to avoid short circuit in practice. The single phase half bridge inverter can be with purely resistive load and with resistive and inductive load. The idealized wave forms are shown below:

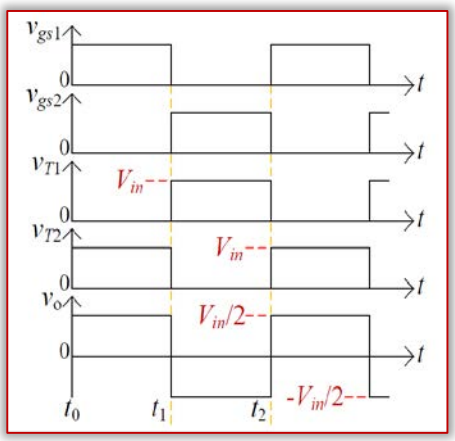

Figure 8. Idealized waveforms of a single-phase half bridge inverter with a purely resistive load

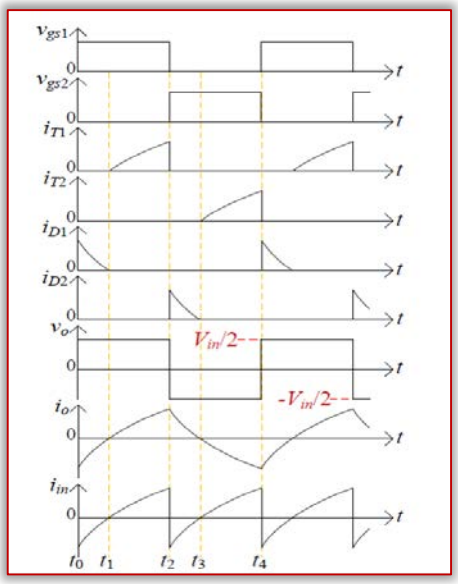

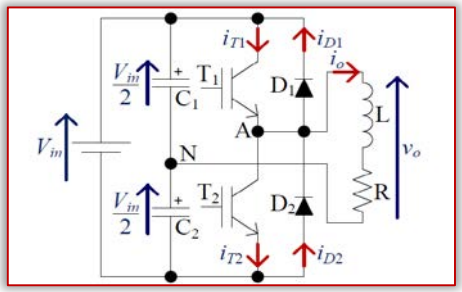

Figure 9 (a). Idealized waveforms of a single phased half bridge inverter with a resistive and inductive load (b) Circuit Diagram of a single-phase half bridge inverter with a resistive and inductive load

— Single phase full bridge inverter

When the connect parallel three single-phase half-bridge inverters operating with 120 degrees phase difference we make a single phase full bridge inverter. As a result, there are 3 legs built with six switching devices and six anti-parallel diodes.

This type of inverter is able to produce three-phase line voltages and phase voltages to the load. This converter is commonly operated with 180° and 120° conduction; i.e., 50% duty ratio and 33.33% duty ratio of the gate signals, respectively.

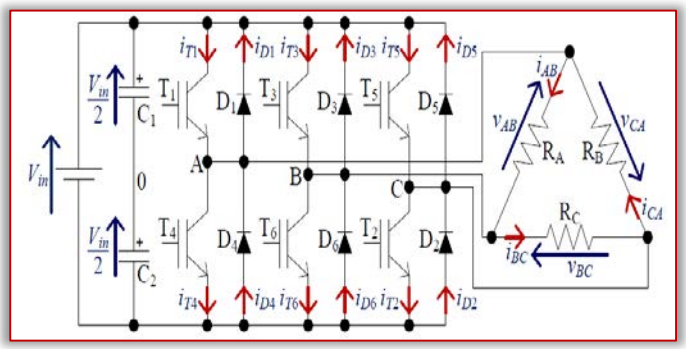

Figure 10. Circuit diagram of a three-phase full-bridge converter

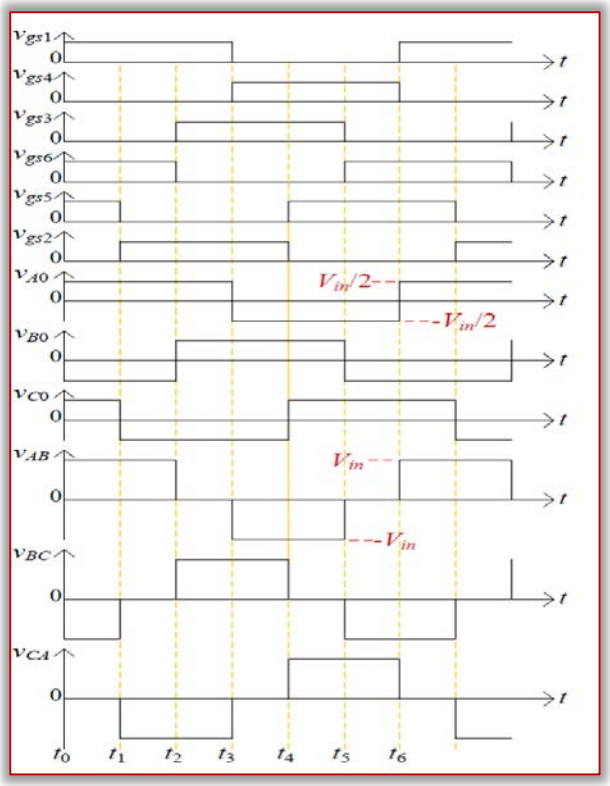

Figure 10. Idealized waveforms of a three-phase full-bridge inverter with a delta-connected resistive load for 180° conduction

The duty ratio of the gate signals of each switching devices are 50%. All the three resistors, RA, RB, and RC, are having the same resistance, R. The peak output line voltage of each phase of the inverter is Vin although the peak values of vA0, vB0, and vC0 are Vin/2. The on-state sequence is T1 & T2, T2 & T3, T3 & T4, T4 & T5, T5& T6, T6 & T1 so that each leg is like a single-phase half-bridge inverter operating with 120 degrees phase difference.

INVERTERS AS MAIN COMPONENTS OF GRID CONNECTED PV SYSTEMS

The components of grid connected systems include the PV array which converts the solar energy into DC power and an inverter which converts the DC power to AC power. The produced power can then be either used up by the load or transferred back to the utility grid. Hence array of solar panels and the inverters are considered as the building blocks of the grid connected system and their study and design is important for installation of any kind of grid connected system.

The performance of grid connected system is highly dependent upon the type of inverter used in solar power design. The inverter converts the dc current into ac for the use by the end user and the access current not required at the load flows back to the grid. When the current starts flowing from PV source to the grid the electric meter starts moving in backward direction and the phenomenon is known as "Net Metering".

The "Islanding" is a state in which part of the utility system taking care of both the loads and the distributed resources remains energized even after being cut off from the main utility.

Hence it is the major need according to the standards that grid connected inverters of solar power systems should always seize transfer of power into the grid under exact abnormal operating conditions of the grid including those leading to the islanding [7].

It is necessary for a solar power grid connected system to have inverters with an anti-islanding protection so that in case the grid fails it shuts down immediately. Also in case of fluctuations in frequency or voltage of grid power inverter must stop working. This helps the equipment to be safe from potentially damaging events from the grid or the solar grid ties system site. It is highly recommended to use an inverter with fault condition reset which turns the inverter on when grid is operating properly again or can sense and adjust voltages/frequencies appropriately. Latest grid connected inverters are available with all above features along with the internal battery backup, LCD display and maximum power point tracking (MPPT) software examine in real time the voltages and amperes.

The input values of voltages and currents have been increased along with the introduction of automatic morning wake-up and shut down in grid tied inverters. The automatic morning wake-up and shut down functions permits inverter to sleep, reducing its power requirements when there is least or no demand of power [8]

The major task of the inverter includes the control of the output voltage or current of the PV array to produce maximum power at a certain irradiance and temperature. This is called maximum power point tracking (MPPT). The grid tied systems using MPPT inverters are more stable and efficient. The grid tied inverter also controls the sinusoidal current that is transferred into the grid to have the same frequency as that of the grid and a phase shift with the voltage value between the acceptable limits is allowed at the point of connection. Currently, the research is going on to control the quality of injected power and the power factor at the grid interface [7].

The extra functions of grid tied inverter are to take into account voltage amplification in order to be matched with the voltage produced by the PV array and the grid voltage which reduces power losses.

— Inverter connection topologies of grid-connected PV system

Photovoltaic systems have various topologies based on the way PV modules are connected with power conditioning unit (PCU). Some of frequently used topologies are [9]

a. Centralized topology

In centralized topology, the centralized inverter is controlling the outputs from a huge number of different solar arrays connected to it. The high power photovoltaic systems where production is in MW can use this topology.

In such connections the cost is minimized and also the maintenance of system becomes easier. The disadvantage is the reliability, which is very low in this case as when a single inverter fails it shuts down the whole solar power system. As only one inverter is used therefore there is considerable power loss of mismatch between the modules and due to shading as tracking is done using MPPT. In effort to minimize these disadvantages and improve the reliability and performance of centralized topology a number of parallel inverters are connected to array so in case one inverter fails the other inverters can still operate and deliver power and prevents system to be shut down. This type of arrangement is called "Master –Slave" topology.

b. String topology

In string topology, single inverters are being connected to individual strings of modules separately. Therefore the combined output from number of strings is not controlled by just a single centralized inverter only. This helps to minimize the losses and increase the reliability of overall system as each string independently operate at its own maximum power point and thus overcoming the drop in power due to the shading issues.

By this kind of typology the mismatch losses are also reduced and there is always a room to add up more modules in a system and thus increasing its size any time according to the requirement. The power rating of each string can be up to 2-3KW. As we use more inverters in this topology so the cost is also increased. When string topology is combined with master slave concept we call such a combination as "team concept topology".

c. Multi string topology

This type of topology uses advantages of both previously discussed topologies to provide maximum power output. Multiple strings are connected together with their own dc-dc converters and then to a common dc-ac inverter. We can use dc-dc converters for maximum power point tracking which results in voltage amplification. The major disadvantage of using dc-dc converter is that it reduces the reliability and performance.

d. Modular topology

The modular topology is also famous as AC modules. In AC modules an inverter is embedded in each module and one large PV-Cell is connected to dc-ac inverter. The main requirement for grid connection is to have an inverter that can amplify very low voltages 0.5-1.0V and 100W per square meter up to the grid level along with acquiring higher efficiencies. The modular inverter or micro inverter topologies are used for intelligent PV system interface as shown in figure 11.

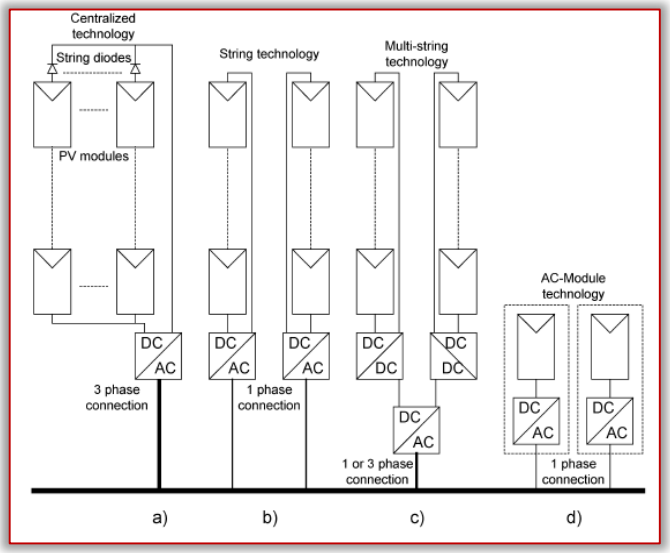

Figure 11. Connection Topologies
a) Centralized Topology b) String Topology c) Multi-String Topology d) AC-Module

— Categorization of grid connected inverters

The inverters whether single or three phased are categorized depending on the following basis:

» **Number of processing stages**

There are usually three kinds of stages in terms of processing. In the single stage all parameters such as maximum power point tracking, control of grid current, and voltage amplification all are handled by the inverter itself. In dual stage inverters we use additional DC/DC converter for MPPT. Pulse width modulation (PWM) is used to control the grid current and in third case, each module is independently connected to its own DC/DC converter and all are joined together to the same inverter which controls the grid current.

» **Use of decoupling capacitors**

In order to keep the capacitor as small as possible, electrolytic capacitor can be replaced by thin film capacitor. In case of three phase inverter the capacitor must be 10 times smaller [9].The capacitor determines the life of the inverter and it can be placed in parallel with the PV modules or in the DC link between the inverter stages.

» **Isolation between AC side and DC side**

It is very important to isolate the DC side of solar power system with the AC side of the Grid and that requirement is fulfilled by using isolated transformer installed at the output side of inverter. As transformer of a commercial frequency is required therefore that can increase the overall weight of the inverter. In order to reduce the weight of inverter, high frequency AC circuit is provided for inverter between the direct

current and the commercial AC system. The transformer is then used at high frequency part of the circuit and to achieve the isolation between AC and DC sides.

Transformer less inverters can also be used and in that case no isolating transformer is required instead a circuit for detecting the DC component at AC circuit and ground detection circuit in DC circuit is required. According to [10] a utility connected inverter which has a very high performance current control scheme can be used effectively in order to improve the power quality in grid connected distribution systems when there is a lot of instability.

— Inverters to synchronize Grid Tied systems with the Utility

The gird connected inverters are used to integrate the photovoltaic power system with the main utility Grid by using the topologies and the codes for Grid Integration. The standard of power provided by the photovoltaic system for the on-site AC loads and for the power delivered to the utility is judged and governed by practices and quality standards on voltage, flicker, frequency, harmonics and power factor as per recommended by ANSI/IEEE Std 519-1981

As these inverters are useful because they can convert ac to dc and dc to ac so this characteristic also changes the sinusoidal nature of the ac power current (and consequently the ac voltage drop), resulting in the flow of harmonic currents in the ac power system that can cause interference with communication circuits and other equipments. Therefore when reactive power compensation is used with converters, resonance conditions can cause high harmonic voltages and currents when they occur at a harmonic associated with the converter [11]. Hence it is very important to have minimum harmonics and same sinusoidal waveforms in the dc side of the inverters connected with the solar power system and the ac grid side connected with the utility.

In this paper we are discussing the use of inverters in solar power system as a power device.

THE PULSE WIDTH MODULATION INVERTERS

As discussed earlier the sinusoidal waveform at the inverter side should match the waveform at the output side therefore the voltage to frequency ratio at the inverter output terminals must be kept constant. This avoids saturation in the magnetic circuit of the device fed by the inverter.

The various methods for the control of output voltage of inverters can be classified as:

(a) External control of ac output voltage
(b) External control of dc input voltage
(c)Internal control of the inverter.

In the above mentioned methods the first two methods require the use of some external components however the third method requires no external components and we can use the pulse width modulation for the internal control of the inverter.

— Principles of PWM

The pulse width modulation signals are pulse trains with static frequency and scale but with variable pulse width. There is one pulse of fixed magnitude in every PWM period. According to the same modulation signal the width of pulses changes depending on the requirements. When PWM is applied to the gate of transistor. The change in PWM period results in ON and OFF states of the transistors. It is to be noted that the frequency of a PWM signal must be much higher than that of the modulating signal, the fundamental frequency. The energy supplied to the load is mostly depend on the modulating signal.

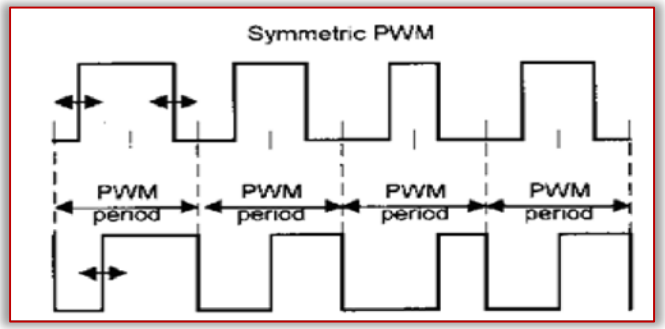

Figure 12. Symmetric and Asymmetric PWM Signals

There are basically two types of PWM signals, symmetric and asymmetric. The pulses of a symmetric PWM signal are always symmetric with respect to the center of each PWM period. The pulses of an asymmetric PWM signal always have the same side associated with one end of each PWM period. Mostly symmetric PWM signals are considered as they result in less harmonics in the output voltages and currents.

— PWM techniques

The most common method of controlling the output voltage from the inverter is termed as Pulse-Width Modulation (PWM) Control. The benefits possessed by PWM techniques include lower power dissipation, easy to implement and control, no temperature variation and aging-caused drifting or degradation in linearity, Also the output voltage control can be obtained without any additional components and with this method, lower order harmonics can be eliminated or minimized along with its output voltage control. The main drawback of this method is that silicon controlled rectifiers (SCRs) most commonly known as thyristors are expensive as they must possess low turn-on and turn-off times. PWM techniques are characterized by constant amplitude pulses. The width of these pulses is however modulated to obtain output voltage control and to reduce its harmonic content. The modulation techniques can be classified into two types mainly carrier based modulation and carrier less modulation. The main purpose of designing these techniques is to control the PWM

inverter switches so we can get the AC voltage or current very close to the sine wave form. We can say that by switching ON and OFF the dc supply at regular intervals is considered as the basic method to convert a fixed DC voltage to an AC voltage that is in pure sine wave form. We use PWM in order to achieve this. The quality of these, PWM techniques, depends on the amplitude of the fundamental component, the harmonic content in the inverter output, the effect of harmonics on the source, the switching losses, controllability and implementation.

According to [12] and [13], the main basic idea of the PWM technique is to compare a carrier signal usually a triangular signal with frequency fs with the a reference signal which is a low frequency signal known as modulating signal with frequency fm. The frequency of the reference-modulating signal fm is set the desired output frequency. In Sinusoidal Pulse width modulation technique for getting the pulses, it is required to compare sine wave with triangular wave and in similar way Trapezoidal modulation is a technique to advance the control ability by using computation of PWM patterns. The output frequency of the converter is decided with the frequency of the modulating wave. Space vector PWM (SVPWM) is a digital modulating technique because its control strategies are implemented in digital systems. The purpose of this technique is to produce PWM load line voltages which are in average equal to given (or reference) load line voltages.

Inverter with PWM is three stage separate push pull driver, which produces phase waveform independently. SVPWM inverter is used to offer 15% increase in the utilization of dc-link voltage and output which have low harmonic distortions in comparison to conventional sinusoidal PWM inverter. In SVPWM inverter is considered as single unit; specifically, the inverter can be driven to eight unique stages.

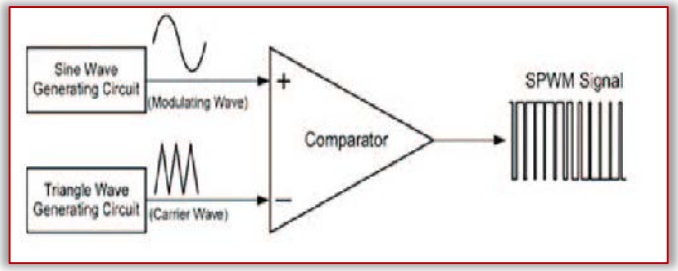

Figure 13. PWM using comparator

In order to get pure sine wave AC output voltage the multi-level PWM technique was developed and is classified as 1) 3-level PWM 2) 5-Level PWM 3) 7 level PWM 4) 9 level PWM and so on. The comparison of different PWM techniques is in following table 1.

Table 1. Comparison of different PWM techniques

No.	PWM Techniques	THD	Complexity	Efficiency
1.	PWM	High	Simple	Low
2.	SPWM	Moderare	Simple	Moderate
3.	SVPWM	Low	Complex	High
4.	Phase Disposition PWM	Moderate	Moderate	Low
5.	Simple Boost Control	Low	Complex	High
6.	Phase shifted PWM	Low	Complex	Very High

PWM Converter in Simulink

The below figure shows how the PWM controller is used to generate the high voltage PWM wave form.

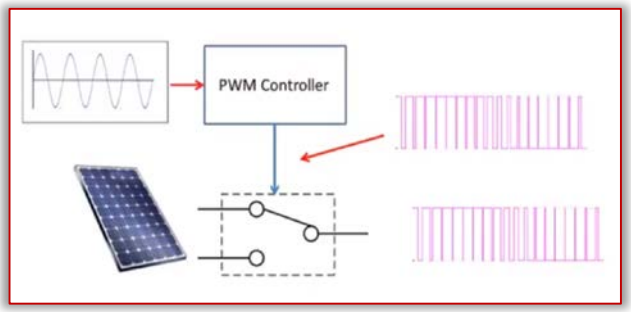

Figure 14. Generation of High Voltage PWM waveform in Solar Power System

The sine wave enters the PWM controller and a square wave signal form is generated. This signal waveform then by using the input signal waveform from the solar power panel is converted to high voltage PWM waveform using a single pole double throw (SPDT) switch. All we can vary is the time of the Switch resulting in Pulse Width Modulation.

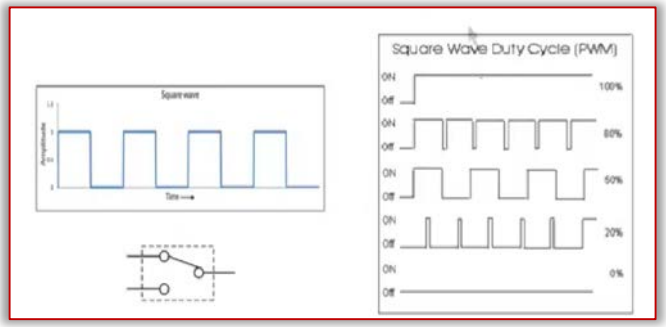

Figure 15. Square wave duty cycle and waveforms

The PWM square wave form obtained above is then passed through the LC filter in order to filter out the harmonics and generate a sine wave. It is seen that average value of the PWM is propositional to the sine wave.

The following figure shows the PWM converter in Simulink Matlab:

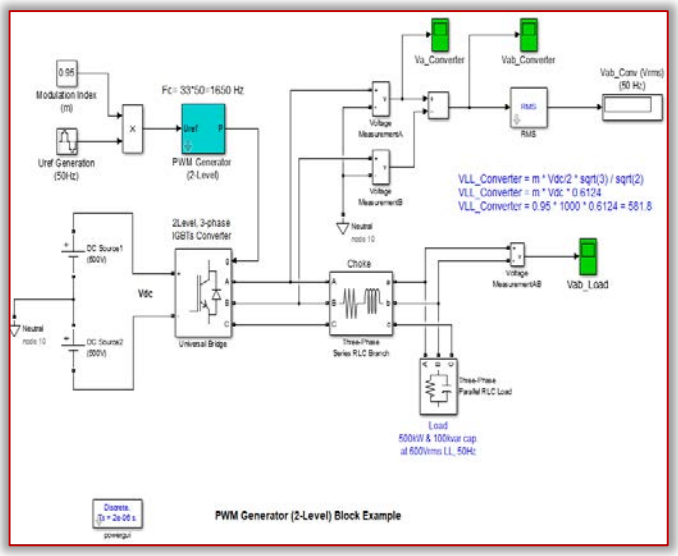

Figure 16. PWM converter in Simulink Matlab

The basic principle as discussed above is that we need a sine wave which is a reference signal at fundamental frequency(which is the frequency required at the output) and then we have a carrier wave which is at higher frequency (usually a sawtooth wave) and then reference is compared with Carrier wave. When Reference wave is greater than carrier wave, output will be high and when reference wave is less than the carrier wave the output will be low. The modulation of pulse is show below:

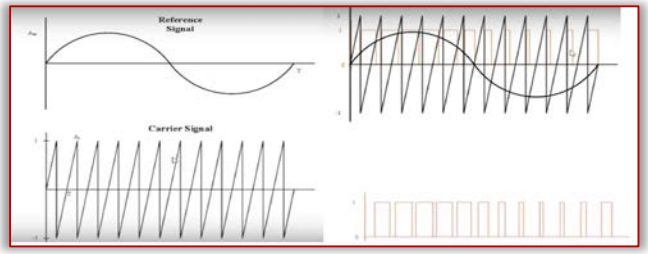

Figure 17. Generation of PWM

When we run the PWM inverter in simulink we get the following outputs for the Inverter.

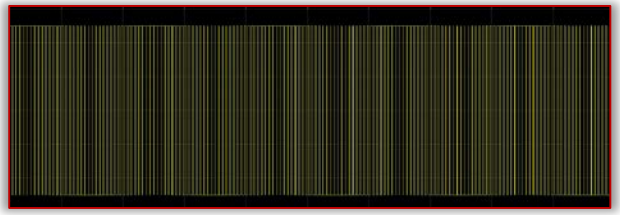

Figure 18. Inverter output

Figure 19. Inverter output after passing through Filter

The above outputs show that when modulated signal from the inverter is passed through the RLC filter, we get pure sine wave at the load side of the inverter.

Also in [14], the simulations in Matlab are done to check experimentally the power quality of an off-grid inverter and power quality of the utility network in the UK are discussed and it is observed that the power quality of off-grid system is better than that of the utility network.

CONCLUSION

In this article the inverters as integrators of the solar power system with the utility grids are discussed beside their use as DC to AC converters for the use in Off-grid solar power applications. In detail overview on PWM techniques and the inverters is also provided. The simulation has been done using PWM Generator (2 level block) in Matlab in order to see the output signal waveform at the inverter's output side with and without RLC filter. It can be seen that the output is pure sine wave (AC) after passing through RLC filer.

References

[1] Vlado Vivoda, (2012). "Japan's energy security predicament post-Fukushima",Energy Policy, Volume 46, pp.135-143

[2] Nation Framework Convention on Climate Change. (2016, April 29). Climate Change Newsroom from the UNFCCC. Retrieved from United Nation Framework Convention on Climate Change: http://unfccc.int/resource/docs/2015/

[3] Dincer, I., & Zamfirescu, C. (2014). Advanced Power Generation Systems. Amsterdam: Elsevier. Retrieved from http://proquestcombo.safaribooksonline.com

[4] M. H. Rashid, M. H. Rashid, and M. H. Rashid, Power electronics: circuits, devices, and applications, vol. 2. Prentice hall NJ, 1988.

[5] Instruments, T. (2015). Voltage Source Inverter Design Guide, (November), 1–45.

[6] Ziogas, P. D., Manias, S., & Wiechmann, E. P. (1984). Application of current source inverters in UPS systems. IEEE Transactions on Industry Applications, IA-20(4), 742–752

[7] AbdEl-Gawad, H., & Sood, V. K. (2014). Overview of Connection Topologies for Grid-Connected, PV Systems. (pp. 1-8). Toronto: IEEE

[8] Balfour, J. R. (2011). Introduction to Photovoltaic System Design. Burlington: Jones & Bartlett Learning.

[9] Kjær, S. B., Pedersen, J. K., & Blaabjerg, F. (2005, SEPTEMBER/OCTOBER). A Review of Single-Phase Grid-Connected Inverters for Photovoltaic Modules. IEEE TRANSACTIONS ON INDUSTRY APPLICATIONS, 41(05), 1292 - 1306

[10] Kim, K.-H. (2015). A Current Control Scheme of a Grid-connected Inverter to Enhance Power Quality, in Distributed Generation. International Conference on Circuits and Systems (CAS 2015) (pp. 139-743). Soul: Atlantis Press.

[11] Algaddafi, A., Brown, N., Gammon, R., Altuwayjiri, S. A., & Alghamdi, M. (2016). Improving off-grid PV system power quality, and comparing with grid power quality. International Conference on Electronics, Information, and Communications, ICEIC 2016, (Dc), 1–6
[12] Algaddafi, A., Brown, N., Gammon, R., Altuwayjiri, S. A., Alghamdi, M. (2016). Improving off-grid PV system power quality, and comparing with grid power quality. International Conference on Electronics, Information, and Communications, ICEIC 2016, (Dc), 1–6
[13] Kumar, R. R., Kumar, S., & Yadav, A. (2013). Comparison of PWM Techniques and Inverter Performance. IOSR Journal of Electrical and Electronics Engineering, 4(1), 18–22.
[14] Algaddafi, A., Brown, N., Gammon, R., Altuwayjiri, S. A., Alghamdi, M. (2016). Improving off-grid PV system power quality, and comparing with grid power quality. International Conference on Electronics, Information, and Communications, ICEIC 2016, (Dc), 1–6

ACTA TECHNICA CORVINIENSIS – Bulletin of Engineering
ISSN: 2067-3809

[1.]Elena GRESOVA, [2.]Jozef SVETLIK

COMPREHENSIVE USAGE OF DECISION TREES: THE COST-SENSITIVE MODELING

[1.]Institute of Control and Informatization of Production Processes, Faculty of Mining, Ecology, Process Control and Geotechnologies, Technical University of Kosice, Kosice, SLOVAKIA
[2.]Department of Manufacturing Machinery, Faculty of Mechanical Engineering, Technical University of Kosice, Kosice, SLOVAKIA

Abstract: The rate at which the societies globally evolve and change is immense. It entails a lot of difficult challenges in many areas. Decision trees are one of the tools that are suitable for offering the solutions for many of them. The issue of decision tree algorithms is quite extensive. Their possible implementation is extensive, as well. The present paper highlights importance, usefulness, high informative value, huge practical contribution, good interpretability and wide range of usage discussing decision trees topic with emphasis on the cost-sensitive modeling fraction. Some selected areas of their use have been specified in more detail.
Keywords: algorithm, classification, cost-sensitive, decision tree, modeling

INTRODUCTION

— Urgency of the research

Nowadays, when society develops rapidly day by day, many new pressing issues occur. Likewise a lot of long-time existing and well known matters become increasingly emergent. There are urgent topics as an information technologies, software engineering, fraudulent transactions or cost saving. Decision tree algorithms are absolutely supportive and frequently used in these domains. Thus, their research as well as applications appear to be highly actual.

— Target setting

An implementation of the cost-sensitive approaches gains benefits in solving of the numerous real-world tasks. Therefore, their modeling accompanied with proper improvements has a great potential. That is the reason why it is very important to raise awareness of the opportunities they offer.

— Actual scientific researches and issues analysis

The open source publications were reviewed for the purposes of the paper with emphasis on their thematic and empirical aspects jointly with temporal feature.

— Uninvestigated parts of general matters defining

There is still certain gap for increasing the efficiency of decision tree algorithms.

THE RESEARCH OBJECTIVE

The principal aim of this paper is to point out the broad spectrum utilization of decision trees. Specifically, the focus is on cost-sensitive decision trees. The research sphere along with practice prove a significant popularity of this tool. The dominant areas of the usage are for instance cloud computing, data mining, information security, fraud detection, direct marketing or medical science. What is more, another goals are raising awareness and stimulating progress and development in this field with link to the real applications.

THE STATEMENT OF BASIC MATERIALS

Decision trees are greatly employed in the connection with machine learning due to their understandable cognition mapping. Designing of the minimal cost decision tree signifies a key part in the context of cost-sensitive learning. Minimal cost classification is the eminent question in data mining, as well. The practice showed that it is necessary to deal with, inter alia, issues as imbalanced datasets, algorithms' performance efficiency or datasets extent.

— Wide utilization of decision trees

Decision trees represent probably the most favorite algorithms for the purposes of classification. Some instances of their employment are declared in Figure 1 (own interpretation based on [4]).

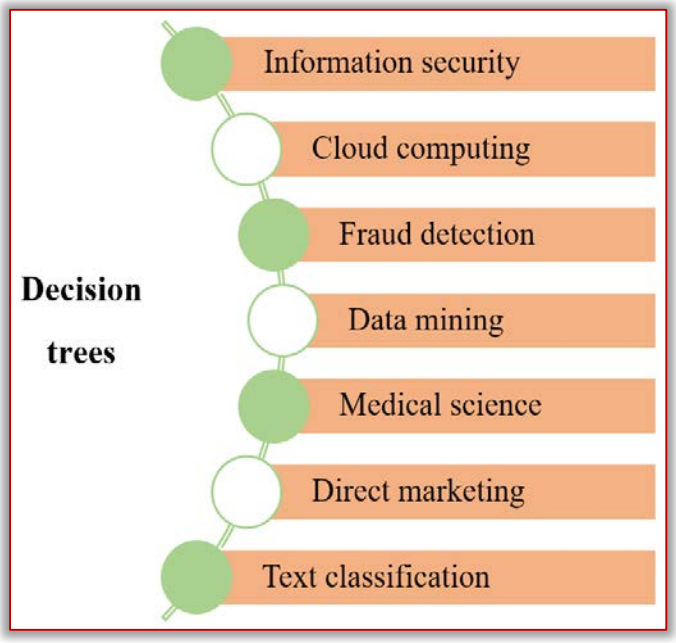

Figure 1. Selected fields of decision trees utilization

Naturally, there are additional areas of decision trees usage, as well. However, the areas above are characterized by very high incidence in scientific studies. The fact which enhances significance is the sort of these scientific studies - they do not deal only with theoretical analysis but also with real-world applications.

The great potential of modeling under decision tree algorithms highlight [2]. The connection between mathematics and economics is presented there on the trees basis. A matter of fact, the tree constitutes one of the elementary terms in a part of mathematics - combinatorics called graph theory (see e. g. [9] or [11]). Likewise the role of decision theory is pointed in this association.

— Cost-sensitive modeling

Nowadays, design of the minimal cost decision trees constitutes a decisive challenge in the context of the cost-sensitive learning. There exist numerous algorithms that deal with stated issue.

However, pursuant to [6], the algorithms proposed so far did not report adequate efficiency with regard on large datasets. Thus, the authors suggested a cost-sensitive decision tree algorithm accompanied by two adaptive mechanisms. They declared that such algorithm considerably enhances the problematical efficiency.

The subsequent research on this topic conducted by [14] provides a cost-sensitive decision tree algorithm formed by weighted class distribution with a batch deleting attribute mechanism. Based on realized experiments, the mean overall costs were diminished through using constructed algorithm in compare with using the existing ones. Therefore, same as by previous exploration, the efficiency rises.

Another sweeping question is imbalanced dataset. The real-world situations show imbalanced character of datasets in many cases. Mentioned task was undertaken for solving by [5]. Standard fixing integrates undersampling, oversampling and cost-sensitive classification. In the given paper, an effective group of cost-sensitive decision trees intended for imbalanced classification was presented. Core classifiers were built on the precise cost matrix and offered algorithm was rated on manifold benchmark datasets. Invented cost-sensitive ensemble grounded on decision trees supports improvement of the minority class cognizance plus brings handy solution for imbalanced datasets.

In connection with frequent imbalanced nature of datasets, the categorization of usually used techniques for such data is stated in Figure 2 (own interpretation based on [4]). The cost-sensitive learning with respective practices is shown there, as well.

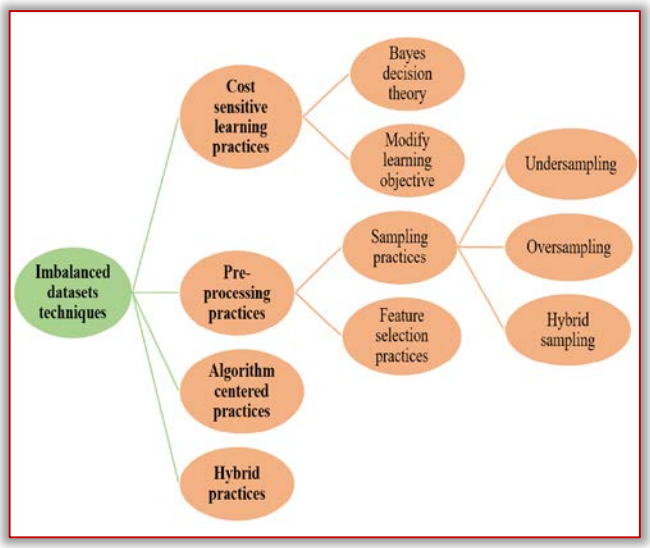

Figure 2. Categorization of the common practices applied on imbalanced datasets

— Cost-sensitive decision tree algorithms in computer technologies.

The extensive sphere where cost-sensitive decision trees can find their justification is software engineering. In the concrete, software development was discussed in the review of [7]. Vendors of the business software regularly stand face to face the situation when releasing the software outcome is needed regardless of missing some fixations of the announced defects.

The reasons are prosaic - constrained funds and deadlines, too. However, the clients escalate a minimum of proclaimed errors. The software vendors are thus forced to tackle them straightaway which entails very high expenses. The review brought original Escalation Prediction system. Its main aim was to find a solution for the maximum net profit dilemma. The cost-sensitive learning was used in relationship with meeting the aim. The conclusions of the exploration pointed that the cost-sensitive decision tree algorithm came out as the best choice. As a great success can be considered the flourishing implementation of the developed Escalation Prediction system in the product group of a business software vendor.

The software development was deliberated in the work of [12], as well. The software defect prediction was brought out there. One of the techniques suggested and consequently utilized for answering to this question was a cost-sensitive classification technique. It was represented by a collection of decision trees, so-called decision forest. The empirical verification ran and signaled the pros of all offered approaches.

The theme of software defect prediction also resonated in the research of [13] where the cost-sensitive learning was implemented. The goal was to mitigate the costs caused by forecasts. The algorithm

was based on decision forest principal what enabled taking out the information from each and every decision tree separately. What is very interesting, the execution was realized to NASA software defects.

— **Cost-sensitive decision tree algorithms in financial information technologies.**

From the financial point of view, damages are noted in relation with various kinds of frauds. Mainly information technologies expansion caused frequent and novel malpractice, inter alia, taking into consideration credit card systems. Fraud detection thus appears as highly alarming topic. Following [10] it is the key instrument for avoiding fraudulent behavior. Described current issue served as subject of interest for these researchers who developed yet unknown cost-sensitive decision tree approach. Its fulfillment was matched with the multiple popular models aimed on classification. The comparison was realized through using a feasible credit card dataset obtained from practice. Such selection underlines the relevancy hand in hand with benefits of the study. As a result of investigation and consecutive construction of the particular cost-sensitive decision tree the financial losses are expected to a lesser extent when dealing with frauds. Hence, researchers recommend the application of this technique in the fraud identification systems.

In the financial domain, another novel algorithm was suggested [1] which was typical of its example-dependent cost-sensitive nature. The fundament was constituted over the decision tree structure. Assorted example-dependent costs were included to an upstart cost-based impurity measure as well as an upstart cost-based pruning standards. The designed approach´s appreciation was done handling the real-life databases. Specifically, they were related to credit scoring, credit card fraud detection together with direct marketing. In compliance with findings presented in the paper the new algorithm reported the finest records for every single database.

— **Cost-sensitive decision tree algorithms in medicine.**

The usefulness of decision trees is striking in another field - medicine. Classification accompanied with cost reflection is enormously important in this domain. Its part, mainly in diagnostics, underline [3]. The authors attempted to identify, execute and screen an action plan of the cost-sensitive learning. They constructed an algorithm for decision tree induction which involved a several types of costs such as delayed costs, test costs or costs arising from risks. Next step was the action plan implementation with intention to practice and appraise cost-sensitive decision trees using medical data. Modeled trees serve for verification in accordance with particular action plans that incorporate special costs, ordinary costs and group costs.

The practicability of cost-sensitive decision trees is confirmed also by [8] in medical diagnosis. The effort was costs reduction concerning misdiagnosis as well as medical tests. To support this effort, the cost-sensitive machine learning algorithms were proposed for subsequent diagnosis modeling. Medical tests figured as attributes - the attribute costs were bounded there. Misdiagnosis represented misclassifications with corresponding misclassification costs. In this connection, various test strategies were processed. What is important, mentioned strategies accorded with diverse cases from diagnosis practice. Even more, they have undergone an empirical assessment and declared their effectiveness. This results to the instantaneous possibility for usage in real medical diagnosis.

CONCLUSION

In the sphere of classification, decision trees represent one of the most favorite and used algorithms. The presented paper dealt with decision trees and their comprehensive usage. Mentioned theme was examined from the cost-sensitive point of view. The numerous fields of decision trees utilization were stated and some of them were afterward analyzed. The modeling under cost-sensitive regard was disclosed and selected associated problems were outlined. The central attention was dedicated to the cost-sensitive decision tree algorithms in computer technologies, financial information technologies and medicine.

Acknowledgment

This work was supported by the Slovak Research and Development Agency under the Contract no. APVV-18-0413.

References

[1] Bahnsen, A.C., Aouada, D., Ottersten, B. (2015). Example-dependent cost-sensitive decision trees. Expert Systems with Applications, 42(19), 6609-6619.

[2] Drabiková, E., Škrabul'áková, E.F. (2017, May). Decision trees-a powerful tool in mathematical and economic modeling. In 2017 18th International Carpathian Control Conference (ICCC) (pp. 34-39). IEEE.

[3] Freitas, A., Costa-Pereira, A., Brazdil, P. (2007, September). Cost-sensitive decision trees applied to medical data. In International Conference on Data Warehousing and Knowledge Discovery (pp. 303-312). Springer, Berlin, Heidelberg.

[4] Kaur, H., Pannu, H.S., Malhi, A. K. (2019). A Systematic Review on Imbalanced Data Challenges in Machine Learning: Applications and Solutions. ACM Computing Surveys (CSUR), 52(4), 36 pp.

[5] Krawczyk, B., Woźniak, M., Schaefer, G. (2014). Cost-sensitive decision tree ensembles for effective imbalanced classification. Applied Soft Computing, 14, Part C, 554-562.

[6] Li, X., Zhao, H., Zhu, W. (2015). A cost sensitive decision tree algorithm with two adaptive

mechanisms. Knowledge-Based Systems, 88, 24-33.
[7] Ling, C.X., Sheng, V.S., Bruckhaus, T., Madhavji, N. H. (2006, August). Maximum profit mining and its application in software development. In Proceedings of the 12th ACM SIGKDD international conference on Knowledge discovery and data mining (pp. 929-934). ACM.
[8] Ling, C.X., Sheng, V.S., Yang, Q. (2006). Test strategies for cost-sensitive decision trees. IEEE Transactions on Knowledge and Data Engineering, 18(8), 1055-1067.
[9] Peterin, I., Schreyer, J., Škrabul'áková, E.F., Taranenko, A. (2018). A note on the Thue chromatic number of lexicographic products of graphs. Discussiones Mathematicae Graph Theory, 38(3), 635-643.
[10] Sahin, Y., Bulkan, S., Duman, E. (2013). A cost-sensitive decision tree approach for fraud detection. Expert Systems with Applications, 40(15), 5916-5923.
[11] Schreyer, J., Škrabul'áková, E. (2015). Total Thue colourings of graphs. European Journal of Mathematics, 1(1), 186-197.
[12] Siers, M.J., Islam, M.Z. (2015). Software defect prediction using a cost sensitive decision forest and voting, and a potential solution to the class imbalance problem. Information Systems, 51, 62-71.
[13] Siers, M.J., Islam, M. Z. (2018). Novel algorithms for cost-sensitive classification and knowledge discovery in class imbalanced datasets with an application to NASA software defects. Information Sciences, 459, 53-70.
[14] Zhao, H., Li, X. (2017). A cost sensitive decision tree algorithm based on weighted class distribution with batch deleting attribute mechanism. Information Sciences, 378, 303-316.

ACTA TECHNICA CORVINIENSIS – Bulletin of Engineering
ISSN: 2067-3809

[1.]Osama Mohammed Elmardi Suleiman KHAYAL

RELATION BETWEEN HUMAN FACTORS AND ERGONOMICS

[1.] Mechanical Engineering Department, Faculty of Engineering and Technology, Nile Valley University, Atbara, SUDAN

Abstract: Ergonomics offers a wonderful common ground for labor and management collaboration, for invariably both can benefit managers, in terms of reduced costs and improved productivity, employees in terms of improved safety, health, comfort, usability of tools and equipment, including software, and improved quality of work life. Of course, both groups benefit from the increased competitiveness and related increased likelihood of long-term organizational survival that ultimately is afforded. Clearly, to enable our profession to approach its tremendous potential for humankind, the professional human factors against ergonomics community, must better document the costs and benefits of their efforts and proactively share these data with their colleagues, business decision makers, and government policymakers. It is an integral part of managing their profession.
Keywords: Human factors, ergonomics, areas of application, theories and models, methodologies

INTRODUCTION

The first initiatives of the new discipline was found in 1914. The design of new machines revealed the importance of taking into account the characteristics of people who should operate them. It was found that many people had difficulties to operate with more complex machines. This led the community to recruit psychologists who were assigned the task of developing and administering tests to select personnel and to assign them to different tasks. These applied psychologists were the first human factors laboratories. But in 1940 ergonomics was developed as a discipline with industrial and academic recognition.

The focus of ergonomics is to be found in industry and it has been linked to an interest in improving worker performance and satisfaction. The discipline began with an emphasis on the design of equipment and workplaces although in principle themes were related to biological, rather than to the psychological aspects. In this way, studies began on anthropometry, work medicine, architecture, lighting, etc. In the 1980s, the ergonomists began to worry largely about advanced psychological aspects and therefore, they emerged leading to a confluence of interests with human factors and cognitive science professionals.

The definition of ergonomics is extended today to all human activities in which artefacts are implemented. Ergonomists are in a permanent search for comprehensive approaches in which physical, cognitive, social and environmental aspects of human activities can be considered. Although ergonomists often work on different economic sectors or particular tasks, these application domains are constantly evolving, creating new ones and changing the perspective of the old ones.

Accordingly, one can recognize today four main domains of expertise which are crucial for investigating interaction between humans and socio-technical systems which are: physical ergonomics, cognitive ergonomics, Neuroergonomics and social or organizational ergonomics.

APPLICATION DOMAINS

— Industrial areas

≡ Human Computer Interaction

In most of the cases, computers are only parts serving to the functioning larger technical systems, so our interaction with them is not as explicit as when a personal computer is in use. For this reason, one should talk rather about Cognitive Ergonomics of Human Machine Interaction and rethink interaction with computer as interaction with everyday computerized artefacts (Sellen et al., 2009).

≡ Control processes

A processing industry is one where energy and matter interact and transform one into another (Woods, O'Brien and Hanes, 1987). There is one ergonomically relevant characteristic that distinguishes among processing industries.

One can say that the various process industries differ in the degree of dependence on the artefacts that play a mediating role between the operators and the physical processes that they control. In many cases, there may be a relatively direct relationship between human control operations of the physical process.

Therefore, in general terms, in the process control domain one or more persons work to control a physical system using one or more artefacts. These individuals interact directly with the mediating artefacts, but not with the physical system that they are controlling.

Unlike what happens in the interaction of a person with a computer when she is writing a text, in process control there is an external world which is the physical industrial system that the persons perceive and control through the mediating artefact, which, of course, can be a computer (Ken'ichi, Kunihide, Seiichi, 1997).

— Intervention areas

≡ Design

Design is the core of the profession of ergonomists (Dowell and Long, 1998). The design of a new system is the process that happens from the conceptualization of the artefact until when it is used by the people for whom it is intended. From the point of view of cognitive ergonomists, there are two aspects of interest in system design (Carroll, 1991). On the one hand, they are interested in the process of design itself. That is, cognitive ergonomists want to understand how people devise a new system, and what are the individual and group factors involved in making decisions that lead to certain solutions defining the system.

Furthermore, cognitive ergonomists would like to know whether the solutions adopted suit the needs and characteristics of users. Their main role in this sense is to describe the human being at all levels of functional organization appropriate for the system being designed (Velichkovsky, 2005; Wickens and Hollands 2000). Therefore, cognitive ergonomists are interested in the human being who designs and the humans being interacting with the system that has been or has to be designed. The work of cognitive ergonomists in the design process has undergone serious changes over the last decades.

In the early times of human factor engineering, they were called to explain why the particular design had not worked. Later on, they were called to intervene directly in the design process (Wickens and Hollands, 2000).

Today, the processes of innovation requires that ergonomists proactively supply ideas and empirical data for the design of future artefacts improving human performance and public acceptance of new technologies (Akoumianakis and Stephanidis, 2003; Kohler, Pannasch and Velichkovsky, 2008).

≡ Technological innovation

The concept of user centered design was developed during the 1980´s in the design of technologies (Norman, 1986). User centered design aims at describing the human being who interacts with the system from the viewpoint of cognitive science. Then, based on those characteristics cognitive ergonomists provided engineers with a set of principles to be considered in the design.

This paradigm has led to the establishment of usability research that has contributed greatly to the effectiveness, efficiency and satisfaction of users in their interaction with the technologies and to a better interaction between users through technology (Holzinger, 2005).

The change is motivated by the design of new applications and services under the influence of increasingly fast convergence of nano, bio and information technologies with cognitive science (NBIC Report, 2006).

≡ Safety and accident investigation

The objective is to predict the likelihood of human error and evaluate how the entire work system is degraded as a result of this error alone or in connection with the operation of the machines, the characteristics of the task, the system design and characteristics of individuals (Swain and Guttmann, 1983). This approach has led to a considerable progress in the efforts to predict the occurrence of human error. However, it has been criticized as insufficient. (Reason, 1992) particularly notes that the main difficulty is the estimation of error probability. In designing new systems, there are no prior data on the error probabilities.

One can count on data from simple components, such as errors that are committed to read a data into a dial or enter them into a keyboard, but not the errors that may be committed by interacting with the system. The second approach was adopted from cognitive psychology. In this, ergonomics seek to know the mental processes responsible for committing an error (Norman 1981; Reason, 1992). They assume that errors are not caused by irresponsible behavior or defective mental functioning. They may be rather the consequence of not having taken into account how a person perceives, attends, remember, makes decisions, communicates and acts in a particularly designed work system.

This standpoint suggests investigating the causes of human errors by analyzing the characteristics of human information processing. Here, the first step has been the classification of errors according to the level of processing involved in the behavior that led to the error. Although there are more elaborated classifications today, it is possible to make a synthesis based on the classical scheme proposed by Jens Rasmussen (1983).

He distinguishes three types of errors depending on the level and degree of cognitive control involved in the erroneous behavior. The three types of errors can be largely attributed to the familiarity that the person has with the system are: Errors based on skills, Errors based on rules and Errors based on knowledge. Another approach has been developed recently to combine the reliability analysis developed by engineers with cognitive modeling. This approach starts from the basic assumption that the behavior of a person is determined by the context in which it occurs.

The work system creates dynamic, ever changing situations. It is therefore necessary to take into account the context and all levels of organization that contribute to system safety: the system's technology, the individual, the group, the organizational management and cultural factors. In other words, it is

not sufficient to estimate errors only from the perspective of human information processing (Wilpert, 2001).
According to this new approach, the person and the working environment should be considered as a highly interactive joint cognitive system (Hollnagel and Woods, 2007). The interaction between the two components is of a crucial importance for any ergonomic analysis. Based on these assumptions, several authors have proposed methodology for estimating the probability of human errors depending on specific situation in which human machine interaction occurs.
The methodology presupposes two steps of analysis: to identify the types of errors that are possible for a specific task in a given scenario of event development; to classify these types of errors by their ranges of probability to identify which are the most probable and which are the least probable within the given joint cognitive system (Cacciabue, 2004).

THEORIES AND MODELS

In their everyday practical work ergonomists may well be more interested in improving what people do rather than what people know or feel.
However an enduring improvement of performance seems to be possible only if the underlying cognitive representations as well as attitudes and competences of participating persons are known. This is why, the Chomskian distinction between competence and performance become very important for cognitive ergonomists (Amalberti, 2001).
In addition to this theoretical distinction, influential concepts are being borrowed, on the one hand, from ecological psychology and activity theory (Gibson, 1979; Leontiev, 1978) and, on the other hand, from the rapidly growing field of cognitive neuroscience (Hancock and Parasuraman, 2003).

— Conceptual developments

With reference to Herbert Simon (1969), cognitive ergonomics had an enormous influence on the development of the discipline in the early 1970s. It was argued that cognitive science must have its own area of application. Cognitive engineering deals with the problems of designing an effective mental work and the tools with which this work is done (Hollnagel and Woods, 1983).
Therefore, the object of cognitive ergonomics is formulated around the concepts of mental work and cognitive tool. Donald Norman (1986) was the one who also argued for a combination of knowledge from cognitive science and engineering to solve design problems. According to him, the objectives of such a strategy would be twofold: to understand the fundamental principles of human actions that are relevant to the development of principles of engineering design, and to build systems that are pleasant to use.
The first goal suggests a slight change in accents with respect to the original proposal of Simon. In fact, it put the discipline in line to the vision of some advanced experts in engineering (Vincenti, 1990): the establishment of cognitive engineering as a discipline of human action independent from albeit related to cognitive science from which it could borrow knowledge about cognitive processes.
However, this proposal remained unattended for a decade, and ergonomics evolved according to Simon's idea of understanding the cognitive engineering as an applied pendant to cognitive science. An example of this view can be found in some textbooks on human factors engineering (Wickens and Hollands, 2000), which are organized according to topics of human information processing. In this way, the list of sections is the same as the list of sections that can be found in any textbook of cognitive psychology.
In the classical conceptualization, the artefact and the human being were considered independent from the context where the interaction between them took place. These considerations have been laid down into paradigm of the joint cognitive systems (Dowell and Long, 1998; Hollnagel and Woods, 2007).
The main message of the proponents of this approach is a broad interactionism: for a solution of cognitive design problem human behavior must be modeled as activity, in its interaction with the environment and with other cognitive systems – both human and artificial – that there are in the environment.
Therefore, in this new conceptualization of cognitive engineering the meaning of cognition itself is being reformulated in more dynamic and situational terms.

— Definition of cognition

In the traditional understanding, cognition refers to the acquisition, maintenance and use of knowledge as examples of operations within the realm of human information processing. However, within dissident conceptions such as the joint cognitive paradigm, cognition should be understood in a broader sense, exceeding the limits of individual's brain or body.
An example is the Gibsonian notion of affordance, which refers to all aspects of the environment supporting specific actions of individuals (Gibson, 1979). This notion is of obvious significance for cognitive engineering, to such a degree that some authors declare the design of affordances to the main goal of human factors engineering (Vicente, 1999). In a similar vein, Norman (1986) stresses the importance of external memory.
Under influence of these ideas, the meaning of cognition in cognitive ergonomics now refer to a highly organized distributed systems such as the military, air traffic control, aircraft cabins or navigation systems for large ships.

Both people and artefacts are jointly regarded as agents within such a system. The focus is placed on the transfer and processing of information within and between agents. In this framework, cognition is viewed as a phenomenon that emerges from the work of the system as a whole (Hutchins, 1995).
One consequence of this redefinition has been the incorporation of theories that have been developed outside the mainstream cognitive research. This is the explanation for a discovery of activity theory (Leontiev, 1978), which has its roots in the European romanticism and Marxist philosophy. Activity theory, with its focus on sociocultural origins of human thought and action, is now considered as a promising starting point for doing research in cognitive ergonomics (Nardi, 1996).
Accordingly, there are no sharp distinction between consciousness and behavior, and thus between external actions and internal thoughts, a distinction that is common for traditional cognitive science and ergonomics. Thoughts without external actions are considered as internalized social actions, similar to corresponding external actions (Vygotsky, 1978). As soon as the socio-cultural context is considered, the scope of analysis becomes broader than in cognitive science.
The incorporation of new approaches and theories of cognition into ergonomics let to a discussion on the relative merits of macro and micro theories whereby the dominating view stressed the importance of the overarching explanations. Cognitive ergonomists should create macro theories that incorporate all the complexity of interaction within a socio-technical system.
Simultaneously to this holistic trend, one can testify a growing influence of concepts borrowed from the field of cognitive neuroscience. Being closely related to the progress in methods of brain and behavioral research, the second trend recently let to development of Neuroergonomics (Parasuraman and Wilson, 2008; Velichkovsky and Hansen, 1996).
This tendency is especially evident, in the analysis of several traditional topics of human factors studies which are discussed below.

— Conceptual topics

≡ Situation awareness and attention

One of the reasons for this rapidly growing interest to situation awareness is instability of human performance related to the automation of work processes. The problems or ironies of automation were first noted by Lisanne Bainbridge in a seminal paper (Bainbridge, 1983).
With a high degree of automation, human operator is out of loop of controlling processes. As a result, operators are less well practiced in their abilities to take over the process when an automatic unit fails. This deterioration results from the fact that the manual and cognitive skills decline due to the absence of active participation in the process.
Furthermore, it becomes more difficult with progressing automation to gain access to knowledge about the system behavior.
Many authors see the solution of such problems in adaptive automation, which could take the current state of knowledge of human operator into account and, in this way, support a better division of labor between humans and machines.
However, the solution presupposes reliable and timely feedback information about human understanding of the situation. This is the area where Neuroergonomics seems to have serious chances for a success (Parasuraman and Wilson, 2008). In particular, neurocognitive studies of attention build the main source of knowledge about mechanisms of situational awareness.
These studies have elucidated three different attention networks in the human brain (Posner, Rueda and Kanske, 2007) and up to six levels of cognitive organization (Velichkovsky, 2005). Changing balance of these networks can explain fluctuation in the level of human performance over time, as in the case of driver's behavior in hazardous situations (Velichkovsky et al., 2002).
There seems to be a new understanding in the ergonomics that some degree of attention and situational awareness is always required to control the performance of any task, no matter how seemingly simple and safe it is. Today this is a topic of vital importance in many areas of ergonomics from military applications, industry, and transportation to the work of medical professionals.
A recent world health organization founded study has shown that the rate of postoperative mortality in a number of hospitals across the world could be reduced by nearly 40% if before the surgery medical personnel answered questions like the determination the right place, the right patient and the type of operation needed (Haynes et al., 2009).

≡ Mental models

When interacting with a system, people normally have some knowledge of its structure and functioning. This small scale subjective representation of system's structure and functioning is called a mental model (Johnson-Laird, 1983).
Taking into account the peculiarities of users' mental models in the design of artefacts is considered to be crucial for an efficient interaction. Therefore, the investigation of mental models is one of the central themes in cognitive ergonomics (Cañas, Antolí and Quesada, 2001; Ken'ichi, Kunihide, and Seiichi, 1997).
Computational analysis of mental models complexity has been widely used to predict the understanding of instructions that describe how to deal with a technical

system. Finally, in the area of HCI, researchers have consistently proven that when a person interacts with the computer she acquires knowledge about its structure and operation.
Interestingly, this acquisition may be less efficient with relatively easy to use graphical user interfaces than with old fashioned command line interfaces. Other research has shown that acquisition of an adequate mental model of the computer facilitates learning a programming language (Cañas, Bajo and Gonzalvo, 1994; Kieran and Bovair 1984; Navarro and Cañas, 2001).

≡ Decision making

Ergonomists have been using several terms that could be considered at least partial synonyms: command and control, dynamic decision making, distributed decision-making, natural decision-making and decision science (Artman, 1998; Brehmer, 1992; Zsambok and Klein, 1997).
The training of professionals, which is based on formal algorithms of decision-making, can be rather misleading as the need to take a quick and obvious solution leaves no time to contract it with other theoretically possible moves (Salas, Cannon-Bowers, and Johnston, 1997).
The combination of time pressure and the highly significant outcomes explains the interest that decision science demonstrates to 'hot', i.e. affectively loaded, rather than to 'cold' cognition (Kahneman, 2003).

≡ Mental workload and stress

It would be important to have an exact and measurable definition of human cognitive limitations during engineering of new systems allowing designers to predict which implementation will maximize the effectiveness and still leave the user a residual capacity to cope with unexpected demands (Yeh and Wickens, 1988).
In addition, the labor legislation of industrialized countries recognizes that mental workload affects the mental and physical health.
Therefore, the law requires companies to evaluate the mental workload to which workers and employers are exposed. It has been argued that many of the mistakes made when interacting with a computer are caused by an excessive load of working memory (Olson and Olson, 1990; Gevins et al., 1998). There are some persistent problems with the notion of mental workload. First, this is an overtly mentalist concept. Second, the nature of cognitive resources and their relations to structural and operational constrains of processing remain unknown.
Numerous hypotheses, models and theories have been proposed to clarify these issues (Meyer and Kieran, 1997). One of the widely accepted is the model of multiple resources by Christopher Wickens (1984).
Accordingly, there is more than one kind of resources such as enabling verbal and non-verbal processing. The hopes on a progress in understanding limitations of human information processing are currently related to functional brain imaging studies (Hancock and Parasuraman, 2003).
Any limitation in performance should also be considered from the perspective of a variety of human functional states such as fatigue, monotony and stress (Leonova, 1998).

METHODOLOGIES

— Ethnographic method and field studies

The ethnographic method is applied when ergonomists have to analyze a completely unknown situation (Garfinkel, 1967). Being initially used in anthropology and sociology, it represents a kind of immersion of the researcher in the environment to describe and explain the observed phenomena.
The emphasis is on observation relatively free of theory and on a 'qualitative' rather than 'quantitative' description of what is observed. This approach emerged to replace methods based on structural interviews and questionnaires.
Researchers using the ethnomethodology often argue that their observations are not driven by any assumptions.
However, it is difficult to believe that ergonomists could be able to shed all their prior knowledge to observe a situation without bias (Shapiro, 1994). Without going into details of a methodological discussion that storms in the philosophy of science, many ergonomists prefer to use a well-established method, called field study, in which as in the ethnographic method, one observes and describes a situation without seriously interfering with it, but the observations are guided by assumptions that are explicitly established from the outset.

— Standards and evaluation testing

When introducing a new software application within the common platform of graphical user interface, one has to consult the corresponding guidelines on the designing dialogues and overall requirements to human-computer interaction (Karwowski, 2005). Even if the application of standards is not immediately possible, the theoretical and empirical development of human factors and ergonomics allows doing analysis of artefacts by use of known principles and data without carrying out experimental research.
There is sufficient documented knowledge about human sensory and motor systems that make unnecessary to conduct a new experiment every time there is a need to design a new display or a mouse (Boff, 1986). In addition, there are a large number of reference sources that responds to the growing need for specific instruments and methods for testing the usability of human-system interfaces (Charlton and O'Brien, 2002; Holzinger, 2005).

— Experiment

Still, there seems to be no method in the immediate and middle-term perspective that could better fulfill the task of scientifically-based human factors and ergonomic research than experiment.

Paradoxically, one can achieve a higher applicability of experimental data by a more in-depth laboratory research. The promises of Neuroergonomics are related to establishing the brain mechanisms of different forms of attention (Posner, Rueda and Kanske, 2007).

The success of direct diagnostics of their state of activation and emerging techniques of brain computer interfaces depends on the progress made in cognitive science. In a longer run, one can hope to replace the most of real experimental work by running computational experiments with virtual artefact and virtual users.

— Simulation

Ergonomists study complex behaviors that are difficult to dissect (Klein et al., 2003). They are also interested in a broad range of phenomena to predict human behaviour and functional states under sometimes hazardous conditions. In addition, many industrial artefacts now-days are firstly produced in a fast-prototype manner, as a virtual mock-up suitable for some forms of usability testing.

An ideal counterpart of this partially virtual world would be, of course, a virtual human dummy that implements some of the essential characteristics of potential user. The contemporary efforts along these lines concentrate themselves on the biomechanical and optical features of human beings (Duffy, 2008).

CONCLUSIONS

The future agenda of human factors research and applications is set up by how technology will be developed and used in society. At the high-end of technological development, there will be many options to meet the human factors challenges as they were carefully listed on eve of the new millennium (Nickerson, 1992).

First of all, it will inevitable come to a further convergence of the basic technologies with the resulting enhancement of human performance. One can expect that usability evaluation will be soon evolved to a more scientifically based and predictive endeavor.

Another expectation is that of a proliferation of completely new forms of interfaces. Some of them may have nano-dimensions fulfilling their roles within the molecular machinery of human cognitive-affective processes. With a high probability, Neuroergonomics will not long have the status of the youngest science of artificial perhaps being combined with something like computational ergonomics.

Due to uneven pace of these processes, there however, will be regions and domains, where people will still have to perform hard, dirty, unpleasant physical tasks round the clock and without proper gratification.

Here human factors experts and ergonomists, along with politics and social workers, should seek to improve the work environment of such individuals with more traditional means (Hancock and Parasuraman, 2003).

References

[1] Akoumianakis, D. and Stephanidis, C. (2003). Blending scenarios of use and informal argumentation to facilitate universal access. Behaviour and Information Technology, 22, 227–244.

[2] Amalberti, R. (2001). La conduite de systèmes à risques. Paris: Presses Universitaires de France. Anderson, J.R., Bothell, D., Byrne, M. D., Douglass, S., Lebiere, C., and Qin, Y. (2004). An integrated theory of the mind. Psychological Review, 111(4), 1036- 1060.

[3] Artman, H. (1998). Co-operation and situation awareness within and between timescales in dynamic decision making. In Y. Waern (Ed.) Cooperative process management (pp. 117-130). London: Taylor and Francis.

[4] Bainbridge, L. (1983). Ironies of automation. Automatica, 19 (6), 775-779. Beach, L.R., and Lipshitz, R. (1993). Why classical theory is an inappropriate standard for evaluating and aiding most human decision making. In G.A. Klein, J. Orasanu, R. Calderwood, and C.E. Zsambok (Eds.), Decision making in action (pp. 21-35). Norwood, NJ: Ablex.

[5] Brehmer, B. (1992). Dynamic decision making: Human control of complex systems. Acta Psychologica, 81, 211-241.

[6] Cacciabue, P.C. (2004). Guide to applying human factors methods. London: Springer- Verlag.

[7] Carroll, J.M. (1991). Designing interactions. New York: Cambridge University Press.

[8] Duffy, V.G. (Ed.). (2008). Handbook of digital human modeling. Boca Raton, FL: CRC Press.

[9] Garfinkel, H. (1967). Studies in ethnomethodology. Englewood, N.J.: Prentice-Hall.

[10] Gibson, J.J. (1979). An ecological approach to visual perception. Boston: Houghton Mifflin.

[11] Hancock, P.A., and Parasuraman, R. (2003). Human factors and ergonomics. In: L. Nadel (Ed.). Handbook of cognitive science (Vol. 2, pp. 410-418). London: Nature Publishing.

[12] Haynes, A.B., Weiser, T.G., Berry, W.R., Lipsitz, S.R., Breizat, A.S., Dellinger, E.P., Herbosa, T., Joseph, S., Kibatala, P.L., Lapitan, M.C.M., Merry, A.F., Moorthy, K., Reznick, R.K., Taylor, B., and

Gawande, A. (2009). A surgical safety checklist to reduce morbidity and mortality in a global population. New England Journal of Medicine, 360, 491-499.
[13] Hollnagel, E. and Woods, D.D. (1983). Cognitive systems engineering: New wine in new bottles. International Journal of Man-Machine Studies, 18, 583-600.
[14] Hollnagel, E. and Woods, D.D. (2007). Joint cognitive systems: Foundations of cognitive systems engineering. New York: Taylor and Francis.
[15] Holzinger, A. (2005). Usability engineering methods for software developers. Communications of the ACM, 48, 71-74.
[16] Hutchins, E. (1995). Cognition in the wild. Cambridge, MA: MIT Press.
[17] Kahneman, D. (2003). Maps of bounded rationality. The American Economic Review, 93(5), 1449-1475.
[18] Karwowski, W. (Ed.). (2005). Handbook of standards and guidelines in ergonomics and human factors. Boca Raton, FL: CRC Press.
[19] Ken'ichi, T., Kunihide, S., and Seiichi, Y. (1997). Structure of operator's mental models in coping with anomalies occurring in nuclear power plants. International Journal of Human-Computer Studies, 47, 767-789.
[20] Kohler, P., Pannasch, S., and Velichkovsky, B.M. (2008). Enhancing mutual awareness, productivity and feeling: Cognitive science approach to design of groupware systems. In P. Saariluoma and H. Isomäki (Eds.), Future interaction design (Vol. 2, pp. 31-54). London: Springer-Verlag.
[21] Leonova A.B. (1998). Basic issues in occupational stress research. In J.G. Adair, D.B. Belanger and K.L. Dion (Eds.), Advances in psychological sciences. (Vol. 1, pp. 307-332). Hove, UK: Psychology Press.
[22] Leontiev, A.N. (1978). Activity, consciousness, personality. Englewood Cliffs, NJ: Prentice Hall.
[23] Meyer, D., and Kieras, D. (1997). A computational theory of executive cognitive processes and multiple-task performance. Psychological Review, 104, 3-65.
[24] Nardi, B. (1996). Context and consciousness: Activity Theory and Human-Computer Interaction. Cambridge, MA: MIT Press.
[25] Navarro, R., and Cañas, J.J. (2001). Are visual programming languages better? The role of imagery in program comprehension. International Journal of Human- Computer Studies, 54, 799-829.
[26] NBIC Report: Converging technologies for improving human performance (2006). Washington, DC: NSF and U.S. Department of Commerce.
[27] Nickerson, R.S. (1992). Looking ahead: Human factors challenges in a changing world. Hillsdale, NJ: Lawrence Erlbaum Associates.
[28] Norman, D.A. (1981). Categorization of action slips. Psychological Review, 88, 1-15.
[29] Norman, D.A. (1986). Cognitive engineering. In D.A. Norman and S.W. Draper (Eds.), User centered system design. Hillsdale, NJ: Lawrence Erlbaum Associates.
[30] Olson, J.R, and Olson, G.M. (1990). The growth of cognitive modeling in human computer interaction since GOMS. Human-Computer Interaction, 5, 221-265.
[31] Parasuraman, R. and Wilson, G.F., (2008). Putting the brain to work: Neuroergonomics past, present, and future. Human factors, 50(3), 468-74.
[32] Posner, M.I., Rueda, M.R., and Kanske, P. (2007). Probing the mechanisms of attention. In J.T. Cacioppo, L.G., Tassinary, and G.G. Berntson (Eds.), Handbook of psychophysiology (pp. 410–432). New York: Cambridge University Press.
[33] Rasmussen, J. (1983). Skills, rules, knowledge: signals, signs and symbols and other distinctions in human performance models. IEEE Transactions: Systems, Man and Cybernetics, 13, 257-267.
[34] Reason, J. (1992). Human error. New York: Cambridge University Press.
[35] Salas, E., Cannon-Bowers, J.A. and Johnston, J.H. (1997). How can you turn a team of experts into an expert team? In C.E. Zsambok and G. Klein (Eds.), Naturalistic decision making (pp. 359-370). Mahwah, NJ: Lawrence Erlbaum Associates.
[36] Shapiro, D. (1994). The limits of ethnography. In R. Furuta and C. Neuwirth (Eds.), Proceedings of the conference on Computer Supported Cooperative Work. Chapel Hill, NC: ACM Press.
[37] Swain, A.D., and Guttmann, H.E. (1983). Handbook of human reliability analysis with emphasis on nuclear power plant applications. Albuquerque, NM: Sandia National Laboratories.
[38] Velichkovsky, B.M. (2005). Modularity of cognitive organization: Why it is so appealing and why it is wrong. In W. Callebaut & D. Rasskin-Gutman (Eds.), Modularity: Understanding the development and evolution of natural complex systems (pp. 335-356). Cambridge, MA: MIT Press.
[39] Velichkovsky, B.M., and Hansen, J.P. (1996). New technological windows into mind. In CHI-96: Human factors in computing systems (pp. 496–503), New York: ACM Press.

[40] Velichkovsky, B.M., Rothert, A., Kopf, M., Dornhoefer, S.M. and Joos, M. (2002). Towards an express diagnostics for level of processing and hazard perception. Transportation Research, Part F. 5(2), 145-156.
[41] Vicente, K. (1999). Cognitive work analysis. Mahwah, NJ: Lawrence Erlbaum Associates.
[42] Vincenti, W.G. (1990). What engineers know and how they know it. Baltimore: Johns Hopkins University Press.
[43] Vygotsky, L.S. (1978). Mind in society. Cambridge, MA: Harvard University Press.
[44] Wilpert, B. (2001). The relevance of safety culture for nuclear power operations. In B.
[45] Woods, D.P., O'Brien, J.F. and Hanes, L.F., (1987). Human factors challenges in process control. In: G. Salvendy (Ed.), Handbook of human factors (pp. 1724-1770). New York: Wiley.
[46] Zsambok, C.E., and G. Klein (1997). Naturalistic decision making. Mahwah, NJ: Lawrence Erlbaum Associates.

ACTA TECHNICA CORVINIENSIS – Bulletin of Engineering
ISSN: 2067-3809

[1.]Asmita Mayuresh MARATHE, [2.]Anagha PATHAK

EVALUATION OF SNAKING ISSUES IN 250KWe POWER PLANT BASED ON DIRECT STEAM GENERATION USING PARABOLIC TROUGH COLLECTOR

[1.]Department of Technology, Savitribai Phule Pune University, Ganeshkhind Road, Pune, INDIA
[2.]School of Energy Studies, Savitribai Phule Pune University, Ganeshkhind Road, Pune, INDIA

Abstract: A Direct Steam Generation (DSG) 256 KWe plant based on parabolic trough solar collector at Shive, Pune, and India is studied. During operation of the plant the snaking of Heat Collection Element (HCE) is observed resulting in plant instability and damage of glass cover. The thermo-hydraulic analytical model has been developed for the performance prediction of DSG process under actual operating conditions. Various controlling parameters causing the snaking problem and the effects of the Flow variation, heat input, internal working pressure and amount of sub-cooling has been simulated in the model. The analysis shows that the higher pressure and lower sub-cooling at the constant mass flow rate and heat input will lead to the stable system.
Keywords: Direct Steam Generation (DSG), Heat Collection Element (HCE), Instabilities, parabolic trough collector (PTC), Solar Thermal Concentrators

INTRODUCTION

A solar thermal power generation demonstration plant was commissioned in 2011 under grant from Department of Science and Technology, Government of India to explore as renewable energy generation in rural areas. The plant uses parabolic trough collector (PTC) to generate low pressure saturated steam at low pressure to drive turbine. A unique phenomenon of bending of receiver tube was observed after commissioning of the plant. It is observed that at noon the wave is passing through the series of HCE from one end to the other, the bending of the HCE is more than 12.5mm on either side. From outside, the HCE looked like a moving snake and hence local operators called it as snaking effect and making system unstable and unsafe. Over 10 % of the glass tubes are broken due to the movement of receiver tube or HCE in the glass envelopes. Maximum bending observed in past is 50mm, [1-3]. The detailed study to understand this bending process is taken up which is explained in this paper through a Thermo-hydraulic model. Based on the understanding of the system and the model, corrective action was taken and the issue got resolved. All the DSG plants as per the literature available are operating at DSG systems operating at pressures minimum at 30 bar, 34 bar, 100 bar, 112 bar are analyzed for prediction of its behavior and also for the lab scale models minimum 30 bar pressure. However the plant under study is a low pressure low temperature plant. It is operating in the range of 14-17 bar and saturation temperature. Complex phenomenon of flow interactions, non-uniform circumferential heating of HCE and transient temperature distribution causing snaking is addressed in this paper. It is observed experimentally that there exists a temperature difference of maximum 80°C [4-5] and the gradient on the wall tubes up to 30 °C [4].

The state of art has less predicted the thermo-hydraulic behavior of the DSG process. In this context, the prediction of the thermal performance of parabolic trough solar collectors used for hot water and steam generation is essential for the observation, operation, safety monitoring and certification of these solar collectors

Different flow patterns such as: bubbly flow, plug flow, slug flow, stratified flow and annular flow are observed inside the HCE [6]. It is the result of the interaction between phases the instabilities occurring during the DSG process [2]. In practice, the stratified flow, at low liquid and gas velocities, complete separation of the two phases occurs. Causes the overheating in the dry section causes highest thermal stress risk due to the which may lead to the bending of the absorber tube [1-2,7-8]. The annular flow represents the most favorable flow pattern as it maintains the contact between water and the absorber pipe.

Despite the numerous studies by various authors about DSG systems, mathematical modeling of water-steam two-phase flow in solar receivers still has considerable challenges. Basic, numerical and experimental research is still needed

Thermo-hydraulic behavior inside a DSG collector has been analyzed using in several software [7,9-10], commercial computational fluid dynamic CFD models were used to solve the superheated steam section [10-11] and for the whole DSG loop, other DSG models were based on numerical tools such as Modelica language [12], RELAP , ATHLET [7,10] and TRNSYS [13] for dealing with the dynamic simulation of DSG parabolic trough solar collectors. Hydrodynamic model for Once though system based direct steam generation is developed [14], Elsafi presented a complete flow pattern analysis along the DSG

absorber tube and discussed the flow transitions in different sections of the DSG loop considering a constant heat flux distribution around the receiver. In his work, the flow pattern map proposed by Wotjan [15] was used to predict the flow pattern in the DSG loops. Despite the various numerical studies to predict the thermo-hydraulic behavior of the DSG process, the modeling of water-steam flow in parabolic trough collectors is still challenging [9]. According to the state of the art of DSG modeling, no previous work has been conducted to predict the thermo-hydraulic behavior and performance of the DSG process under the conditions of the Shive plant i. e for the low pressure and mass flow rates. It becomes obvious from the aforementioned literatures that modeling the thermo-hydraulic process of DSG at lower temperature and pressure operating parameters to understand the stability of the 250 KWe direct steam generation plant facility under study.

Current numerical model is heat input based proposed to solve the two-phase flow under uniform heat flux, for heat transfer calculation using the correlation of Gunger and Winterton model [16]. This model was based on the correlation of Friedel [6] for the two-phase pressure drop calculation and the correlation of Gunger and Winterton [16].

PLANT CONFIGURATION

The configuration of the plant for the analysis presented here has main steam parameters of 250°C and 17 bar. The following sections cover the plant's layout as well as models and assumptions of the solar field and the power block.

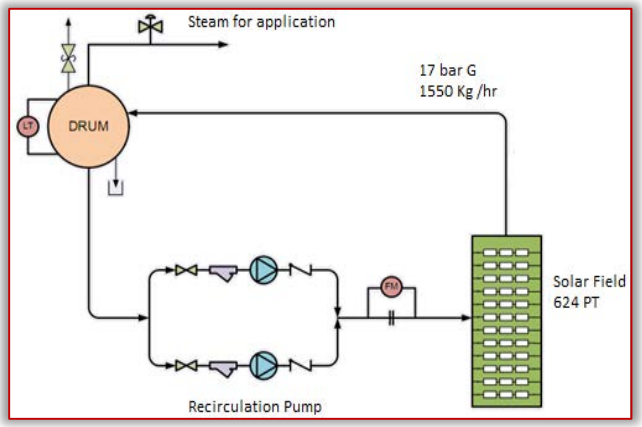

Figure 1. Direct steam generation Demonstration plant, Shive, Maharashtra, India

The power plant is designed for a gross electricity output of 250 KWe. The solar field consists of 624 parabolic troughs E-W or N-S orientated based on the space availability. The plant was operated in recirculation mode. The solar heat collectors are non-evacuated type, though it drops over the evacuated receiver the cost of the project reduces and collector field reliability would increase [17]. Tracking mechanism is so designed that it tracks 2 modules of 8 collector each at a time [18]. The Solar field has 39 parallel loops. Parabolic trough focal length is 0.5 m with the width 1.8m and the length is 3.8m. The diameter of absorber tube is 25.4mm. Water passes through 16 collectors in series. Such 39 loops are connected in parallel. The heated water and steam mixture is then fed to the drum. The saturated steam from the drum is passed through the turbine to generate electricity, which is fed to the grid depending upon the requirements.

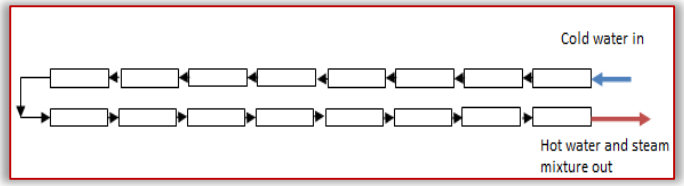

Figure 2. Solar HCE loop at site

ANALYTICAL MODEL

The analytical model based on separated flow model, is simplistic method for calculating the frictional pressure drop, understanding the flow pattern that may be causing the bending of the heat collection element of the parabolic trough. The flow properties are calculated using REFPROP based on the NIST properties. The model assumes, across the entire parallel channel, mass flow rate is equal, but in reality due to cloud cover the flow rate in parallel channels will vary, varying the pressure drop that needs more sophisticated approach and modeling.

The analytical model to evaluate the Flow pattern is based on the following working parameters. Operating pressure, heat input, mass flow rate and amount of subcooling are the variables used to simulate the effect of each parameter.

Table 1. Cases under Study

Mass flow rate kg/hr	Inlet pressure effect Pressure in bar	Heat input effect (Collector length is 3.8 m.) Heat input: KW/collector	Amount of Sub cooling °C
100–1200kg/hr with increments of 50	2, 3, 4, 5, 8, 11, 14, 17	0.25 ,0.50 0.75 , 1	0, 10 20

The total length of the complete segment of 16 collectors is 61.2m i.e. each segments of 8 collectors is divided into three sections, a section where the sub cooled liquid enters (x<0), second where the liquid is evaporates (0<x<=1) and third where the saturated vapor is superheated (x=1). The steam quality more than 1 is not expected with the considered mass flow rate and the input heat flux. The exit enthalpy of each segment is calculated to confirm the quality of the

flow. The exit flow of first segment forms the inlet flow of the second segment.
The piping, valves and connections from pump outlet to the economizer (i.e. first segment) is considered while calculating the pressure drop due to single phase mass flow. Also the pressure drop in the piping, valves and connections from the segment 2, outlet to the solar boiler is considered while calculating the total pressure drop due to two phase flow.

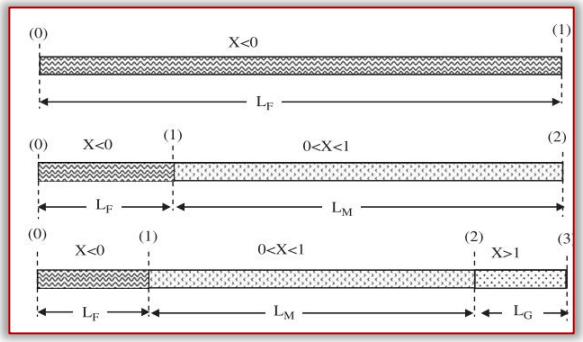

Figure 3. The three possible flow sections for the evaporation in a single pipe [19]

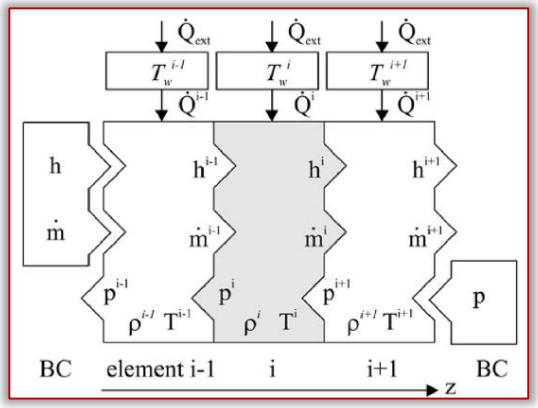

Figure 4. Axial discretization of fluid and pipe sections [20]

Separate pressure drop equations are used with the economizer, evaporator, piping and valves. The first step of the analysis is to get mass flow rate vs. pressure drop curve for the system. As the 39 different entries are parallel to each other and connected to common manifolds, at the entry and exit of the segments. The pressure drop is considered in only 1 section of 2 segments of 8 collectors each. It is assumed that all the parallel channels observe equal flow.
A one dimensional step by step approach has given to determine the outlet enthalpy as follows,

$$h_{out} = h_o + \frac{qL}{\dot{m}} \quad (1)$$

where q is the total average heat rate per unit length absorbed by the fluid, L is the length of the pipe and $\dot{m}$ is the mass flow rate in the pipe. After calculating the enthalpy the quality of the flow x_{out}can be calculated as,

$$x_{out} = \frac{h_{out} - h_{F,sat}}{h_{G,sat} - h_{F,sat}} \quad (2)$$

For sub-cooled region $x_{out} < 0$, for the two phase flow during the evaporation $0 < x_{out} < 1$, after the evaporation is complete the quality of exit vapor increases more than 1 ie for the superheated region $x_{out} > 1$.
The total heat input is assumed after the heat loss to the surrounding. Heat flux is taken to be uniform along and around the pipe.

—Finalization of the pressure drop equation to be used effectively for the DSG application

The pressure drop of the DSG process is dominated by the water/steam two-phase flow pressure drop. Different models known from literature predicting the pressure drop of a two phase flow that fulfill the specific requirements of the DSG process have been identified [6].

—For Single phase flow modeling

The pressure drop is estimated using experimental correlation system under consideration has not been designed for superheating; hence the pressure dropΔP_{1ph} in preheating section is only evaluated using Blasius equation.

$$\Delta P_{1ph} = 4f_{1ph}\left(\frac{L}{d_i}\right)\dot{m}_{total}^2\left(\frac{1}{2}\rho_{1ph}\right) \quad (3)$$

where f_{1ph} is the friction factor for turbulent flow, which is determined by using Moody's friction factor correlation considering the relative surface roughness $(\frac{\varepsilon}{d_i})$:

$$f_{1ph} = 0.0055\left[1 + \left(20000\frac{\varepsilon}{d_i} + \frac{10^6}{Re_{1ph}}\right)^{\frac{1}{3}}\right] \quad (4)$$

—For two phase flow modeling

Friedel correlation has been used (6) for calculating the two phase flow, it was the most accurate model used in European DISS Project (9). The correlation method of Friedel (1979) utilizes a two-phase multiplier

$$\Delta P_{2ph} = \Phi_{fr}^2\,\Delta P_{1ph} \quad (5)$$

Using the liquid dynamic viscosity μL, two-phase multiplier is

$$\Phi_{fr}^2 = E + \frac{3.24\,FH}{Fr_H^{0.045}\,We_L^{0.035}} \quad (6)$$

The dimensionless factors Fr_H, E, F and H are as follows:

$$Fr_H = \frac{\dot{m}_{total}^2}{g d_i \rho_{1ph}^2} \quad (7)$$

$$E = (1 - x^2) + x^2\frac{\rho_L f_G}{\rho_G f_L} \quad (8)$$

$$F = x^{0.78}(1 - x)^{0.224} \quad (9)$$

$$H = \left(\frac{\rho_L}{\rho_G}\right)^{0.91}\left(\frac{\mu_G}{\mu_L}\right)^{0.19}\left(1 - \frac{\mu_G}{\mu_L}\right)^{0.7} \quad (10)$$

The liquid Weber We_L is defined as:

$$We_L = \frac{d_i \dot{m}_{total}^2}{\sigma \rho_H} \quad (11)$$

Homogeneous density ρ_H is based on the vapor quality.

$$\rho_H = \left(\frac{x}{\rho_G} + \frac{1-x}{\rho_L}\right) \quad (12)$$

— **Finalization of the Heat Transfer coefficient equation to be used effectively for the Direct Steam Generation application.**

The heat transfer coefficient under the single-phase flow condition can be obtained from the Nusselt number ash$_{c1ph} = \frac{N_u K}{d}$. Odeh [21] developed the map based on which the heat transfer coefficient for two phase flow is evaluated. The flow transition is determined using the dimensionless Froud number. Froud number is the ratio of the flow inertia to the gravity force.

$$F_r = \frac{G^2}{\rho_{1ph}^2 \, g \, d_i} \quad (13)$$

If Fr < 0.04, the flow is stratified. If Fr > 0.04, annular flow occurs inside the absorber tube. The heat transfer coefficient for two phase flow can be evaluated using appropriate co-relations depending upon the type of flow.

In the thermo-hydraulic model, the properties of the heat transfer fluid (water/steam) are determined using the NIST Properties. A spreadsheet-based parabolic trough performance model. The model has been developed in Microsoft Excel® spreadsheet program was developed during the study. The spreadsheet is used for data input and output. The model uses the Visual Basic for applications language built into Excel for programming the hourly performance simulation.

It is observed that the simulation results are in good agreement with the literature.

RESULTS

— **Effect of operating pressure and mass flow rate:**

As shown in figure 5, at low mass flow rates, low pressure and constant heat input the boiling zone is observing higher pressure drop due to two phase flow. Higher pressure drops due to flow transition may lead to instability such as Ledinegg instability (or flow excursion) and the flow-pattern transition instability as defined by various researchers, [22], H T Liu et al.[23], Naik and Vijayan [24]. The Current plant under study is observing snaking in the 80% of the collectors in segment 2 of each loop.

— **Flow Pattern map:**

In this section, the present flow distribution model is compared against experimental data and numerical results for single and two-phase flow manifold systems reported in the technical literature. At higher pressures the flow inside the HCE will be intermittent. State of the art has suggested various transition models for two phase flow. Taitle [25] has summarized the models. Unified model for flow transition prediction used by Odeh [21] is used in this study. In the current analysis flow pattern maps are generated. The flow regimes considered are annular flow, stratified, bubbly dispersed and intermittent flow. Flow pattern maps for 25.4 mm tube at 17 bar and 3 bar are plotted as shown in the figure 6.

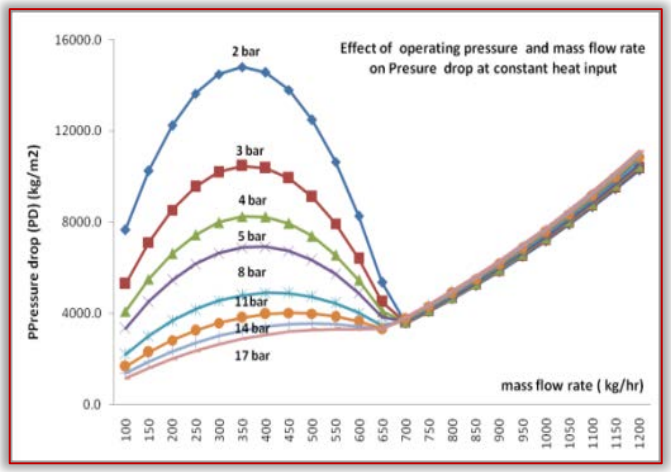

Figure 5. Two Phase Flow pressure drop in the HCE, this work

— **Effect of operating condition on pressure drop**

In DSG feed water flow rate, operating pressure, absorber tube diameter and tube inclinations are the major factors affecting the pressure drop. This collector would generate the steam when feed water flow rate is.

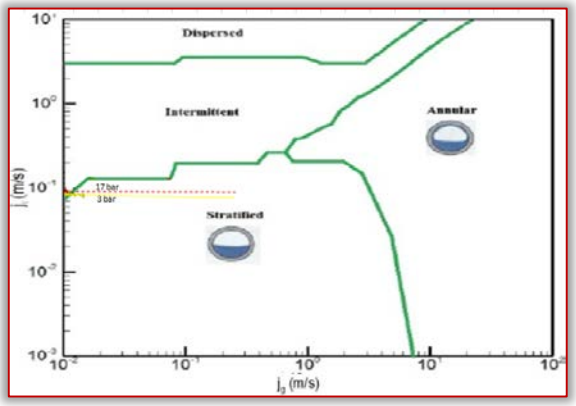

Figure 6. Surface velocities of two pressures 17bar and 3 bar in a DSG flow pattern map by Zarza [15]

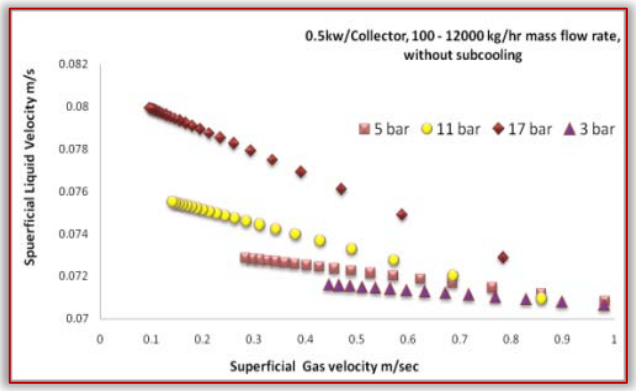

a. without subcooling

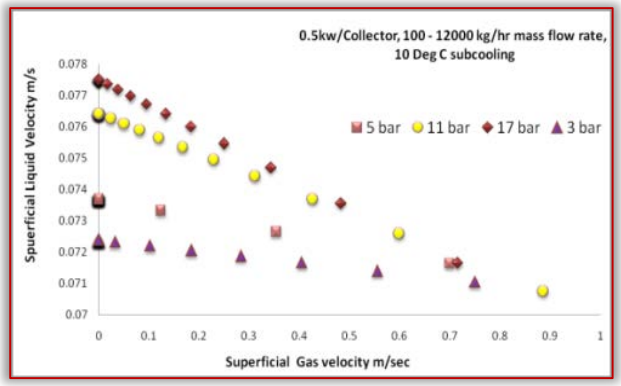

b. with 10°C subcooling

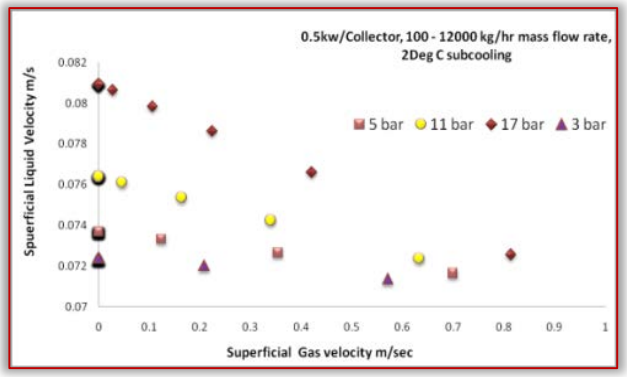

c. with 20°C subcooling

Figure 7. Flow pattern map with pressure and subcooling as a variable

CONCLUSION

The model has been prepared to analysis the instability in the plant under study. All the results are the confirmation of the actual plant study, theoretical study by Rafael et al. [1-2], Sourav Khanna et al. [3], Murphy et al. [22], Flores et al.[26].

It was observed that if the current system is operating at 14bar or below pressure and mass flow rates below 1200kg/hr the flow pattern is observed as stratified flow which is causing maximum temperature variation around the perimeter of the HCE. . The analysis is in line with the site conditions and results stated by Saad [14]. The plant is operating at the pressure range 0-10 bar and at 780 kg/hr mass flow rate and facing snaking issues.

It was suggested to operate the plant in full capacity at higher pressures more than 12 bar and flow rates more than 1200 kg/hr at high solar insolation hours with less subcooling it to avoid the instabilities.

It has improved the performance of plant and the snaking issue is resolved upto 80%.

As the DSG at low pressure is still facing various challenges as static and dynamic instabilities, the future efforts should be done to build a model for complete power plant to simulate the operating conditions and find the stable operating range for DSG. Also r the non-uniform Heat flux modeling needs to be assessed to make the model more accurate.

Acknowledgment

The valuable inputs and support extended by Thermax, India and School of Energy Studies, Savitribai Phule Pune University is acknowledged. This research did not receive any specific grant from funding agencies in the public, commercial, or not-for-profit sectors.

NOMENCLATURE

A	Cross section area, m^2
d	Diameter, mm
e	Thickness, mm
Fr	Froude number
G	Mass flux,
g	Gravity field, m/s^2
h	Convective heat transfer coefficient, $W/(m^2 \cdot K)$
K	Thermal conductivity,
L	Length, m
ṁ	mass flow rate, kg/hr
Nu	Nusselt number
P	Pressure, bar
Pr	Prandtl's Number
q	Heat flux, W
Re	Reynolds number
We	Weber Number
T	Temperature, °C
x	Steam quality
σ	Absorptance, void fraction
ρ	density, kg/m3
Δ	Difference
a	Absorber tube
cond	Conduction
conv	Convection
f	Fluid
g	Gas
h	Homogeneous
l	Liquid
rad	Radiation
o, out	Out
sat	Saturation
sky	Sky
DSG	Direct steam Generator
HTF	heat transfer fluid
PTC	Parabolic trough collector
HCE	Heat collection Element
DISS	Direct Solar Steam
NIST	National Institute of Standards and Technology

References

[1] Receiver Behavior in Direct Steam Generation with Parabolic Troughs. Rafael Almanza, Alvaro Lentz , gustavo Jimenez. 1997, Solar Energy Vol. 61 No. 4, pp. 275-278.

[2] DSG Under Two Phase and Stratified Flow in a steel receiver of a Parabolic Trough collector . Rafael Almanza, Gustavo Jimenez , Alvaro Lentz , Alberto Valdes , Alberto Soria. 2002, ASME Vol. 124, pp. 140-144.

[3] Analytical expression for circumferential and axial distribution of absorbed flux on a bent absorber tube of solar parabolic trough concentrator. Sourav Khanna, Shireesh B. Kedare, Suneet Singh. 2013, Solar Energy 92, pp. 26-40.

[4] Receiver behavior in Direct Steam Generation with PArabolic Trough . Rafael Almanza, Alvaro Lentz , Gustavo Jimenez. 1997, Solar Energy, 61, pp. 275-278.

[5] Developement of receivers for the DSG process. Nikolaus Benz, Markus Eck, Thomas Kuckelkorn, Ralf Uhlig. 2005. SolarPACES2006 A2-S6. pp. 1-7.
[6] WOLVORINE TUBE, INC. Design consideration for enhanced heat exchangers. Engineering Data Book III.
[7] Modeling direct steam generation in solar collectors with multiphase. David H. Lobón, Emilio Baglietto, Loreto Valenzuela, Eduardo Zarza. s.l. : Applied Energy , 2014, Vol. 113.
[8] Experimental investigation of thermo and fluiddynamics in a Horizontal evaporator tube with injection. Laufs, L and F. Mayinger (Lehrstuhl A Fur Thermodynamik, Technische Universitat Munchen, Germany. Germany : s.n., 1996. he 9th International symposium on transport Phenomena in thermal Fluids Engineering, Singapore, June 25-28,1996. pp. 1-6.
[9] Thermo-hydraulic analysis and numerical simulation of a parabolic trough solar collector for direct steam generation. Ahmed Amine Hachicha, Ivette Rodríguez,Chaouki Ghenaia. s.l. : Applied Energy, 2018, Vol. 214, pp. 152–165. Applied Energy 214 (2018) 152–165.
[10] Modelling and simulation tools for direct steam generation in parabolic trough solar collectors: A review. Antonio Sandáa, Sara L. Moyaa, Loreto Valenzuelab. 109226, s.l. : Renewable and Sustainable Energy Reviews, 2019, Vol. 113.
[11] Numerical study of heat transfer enhancement in the receiver tube of direct steam generation with parabolic trough by inserting metal foams. P. Wang, D.Y.Liu, C. Xu. 2013, Applied Energy 102, pp. 449-460.
[12] Simulation of transient two-phase flow in parabolic trough collectors using Modelica. Tobias Hirsch, Markus Eck, Wolf-Dieter Steinmann. Germany : s.n., 2005.
[13] A quasi-dynamic simulation model for direct steam generation in parabolic troughs using TRNSYS. Mario Biencinto, Lourdes González, Loreto Valenzuela. s.l. : Elsevier, 2016, Applied Energy, Vol. 161, pp. 133-142.
[14] Hydrodynamic Analysis of Direct steam Generation Solar collectors. S.D. Odeh, M. Behnia, G.L.Morrison. 2000, ASME Vol. 122, pp. 14-22.
[15] Direct Steam Generation in Parabolic troughs:Final results and conclusions of the DISS project. Eduaro Zarza, Loreto Valenzuela , Javier Leon ,Klaus Hennecke , Markus Eck ,Dieter Weyers, Martin Eickhoff. 2004, ENERGY, pp. 635-644.
[16] A general correlation for flow boiling in tubes and annuli. K. E. GUNGOR, R. H. S. WINTERTON. 3, Great Britain : hr. .I. Hear Mass Transfer, 1986, Vol. 29, pp. 351-358.
[17] Modular trough Power plant. Hasanni, Vanab and Price, Henry. 2001, ASME , Solar enginnering, pp. 437-443.
[18] Thakur Deepak, Jangada Jayprakash, Ahmed Tanveer. Multi Dish Tracking system through Image Processing. 2938/MUM/2011 India, 10 19, 2011.
[19] L M Murthy, E Kenneth May. Steam Generation in Line-Focus Solar Collectors : A Comparative Assessment of Thermal Performance , Operating Stability , and Cost Issues. Colorado : Solar energy research Institute, 1982.
[20] Simulation of transient two-phase flow in parabolic trough collectors using Modelica. Tobias Hiesch, Markus Eck, Wolf Dieter Steinmann. 2005, Modelica, pp. 403-411.
[21] Hydrodynamic model for Horizontal and inclined Solar Absorber Tubes for Direct steam generation collectors. Saad Odeh, Masud Behnia, Graham L Morrison. Melbourne : s.n., 1998. 13th Australasian Fluid Mechanics Conference.
[22] L.M.Murphy, E.Kenneth May. Steam Generation in Line-Focus Solar Collectors : A Comparative Assessment of Thermal Performance , Operating Stability , and Cost Issues. 1982.
[23] Dynamic analysis of pressure drop type oscillations with planar model. H T Liu, H Kocak, S Kakac. 1995, International journal of Multiphase flow, pp. 851-859.
[24] A. K. Nayak, P. K. Vijayan Reactor. FlowInstabilities in Boiling Two-Phase Natural Circulation Systems: A Review. Science and technology of the nuclear articles . 2008, Vol. 2008.
[25] Transient solution for flow of evaporating fluid in parallel pipes using analysis based on flow patterns. Yehuda Taitel, Mordechai Baikin , Dvora Barnea. 2011, International Journal of Multiphase Flow, vol. 37 , pp. 469-474.
[26] Behavior of the Compound Wall Copper-Steel Receiver with Stratified Two-Phase Flow Regimen in Transients States when Solar Irradiance is Arriving on One Side of Receiver. V. Flores, R. Almanza. 2001. ISES 2001 Solar World Congress. pp. 805-810.
[27] Direct steam generation : Technology Overview . Feldhoff, Fabian. Almera, Spain : s.n., 2012. SFERA summer sshool 2012. pp. 1-66
[28] Fernández-Garcíaa A, Zarza E, Valenzuela L, Pérez M. Parabolic-trough solar collectors and their applications. s.l. : Science Direct, 2010. pp. 1695-1721. Vol. 14.

ACTA TECHNICA CORVINIENSIS – Bulletin of Engineering
ISSN: 2067-3809

[1.]S. HEMAJOTHI, [2.]S. ABIRAMI, [3.]S. AISHWARYA

A NOVEL COLOUR TEXTURE BASED FACE SPOOFING DETECTION USING MACHINE LEARNING

[1-3.]Department of ECE, Prince Shri Venkateshwara Padmavathy Engineering College, Chennai, INDIA

Abstract: Research on noninvasive software's based on face spoofing detection schemes has mainly been given focus on the analysis of the luminance information of the face images, hence removing the chroma component can be very much useful for discriminating photo faces from genuine faces. This brings us a novel and an appealing approach for detecting face spoofing using color texture analysis. The combined texture information and data of colors from the luminance and the chrominance channels by taking out complementary low-level feature descriptions from different color spaces are used. The color local binary patterns (LBP) descriptors, finds the facial color texture content using four other descriptors: the co-occurrence of adjacent local binary patterns (CoALBP), local phase quantization (LPQ). Here by using these features and characteristics the color texture is analyzed and extracted by face descriptors from different color bands. To gain insight into which color spaces are most suitable for discriminating genuine faces from fake ones, considered three color spaces, namely RGB, HSV and YCbCr. A new and appealing approach using color texture analysis and demonstrate that the chroma component can be very useful in discriminating fake faces from genuine ones. First, the face is detected, cropped and normalized into an M×N pixel image. Then, holistic texture descriptions are extracted from each color channel and the resulting feature vectors are concatenated into an enhanced feature vector in order to get an overall representation of the facial color texture. The final feature vectors are given to a binary classifier and the output score value describes whether it is a real or a fake image.

Keywords: spoofing detection schemes, noninvasive software, luminance information

INTRODUCTION

Compared with traditional authentication approaches including password, verification code and secret question, biometrics authentication is more user-friendly. Since the human face preserves rich information for recognizing individuals, face becomes the most popular biometric cue with the excellent performance of identity recognition. Currently, person identification can easily use the face images captured from a distance without physical contact with the camera on the mobile devices, e.g. mobile phone. As the application of face recognition system becomes more and more popular with the widespread of the Mobile phone, their weaknesses of security become increasingly conspicuous. For example, owing to the popularity of social network, it is quite easy to access a person's face image on the Internet to attack a face recognition system. Hence, a deep attention for face spoofing detection has been drawn and it has motivated great quantity of studies in the past few years. In general, there are mainly four types of face spoofing attacks: photo attack, masking attack, video replay attack and 3D attack. Due to the high cost of the masking attack and 3D attack, therefore, the photo attack and video reply attack are the two most common attacks. Photo and video replay attacks can be launched with still face images and videos of the user in front of the camera, which are actually recaptured from the real ones. Obviously, the recaptured image is of lower quality compared with the real one in the same capture conditions. The lower quality of attacks can result from: lack of high frequency information image banding or more effects, video noise signatures, etc. Clearly, these image quality degradation factors can work as the useful cues to distinguish the real faces and the fake ones. Face spoofing detection, which is also called face liveness detection, has been designed to counter different types of spoofing attacks.

The real and fake faces can be very distinctive in the chrominance channels. For instance, Burkinabe analyzed the impact of different color spaces on face anti-spoofing and presented a shallow model based on color features, achieving fairly good performance. To exploit and combine the effectiveness of color and deep learning, we utilize a deep learning framework combined with LBP features extracted from different color spaces (such as RGB, HSV, YCbCr). Among the significant contributions of our present work:

- While most previous methods based on deep learning suffer from the lack of face training samples, we introduce a new deep learning model by fine tuning the VGG-face model.
- We combine deep learning with handcrafted features by extracting the LBP descriptions from the convolutional feature maps.
- We explore how well different color spaces can be used for describing the intrinsic disparities in deep learning between genuine faces and fake ones. We also perform a fusion study to analyze the complementarity of different color space.

BINARY PATTERNS AND FACE QUANTAIZATION ALGORITHM

Here Texture descriptors originally designed for gray-scale images can be applied on color images by

combining the features extracted from different color channels. Color texture of the face images is analyzed using three descriptors: Local Binary Patterns (LBP), Co-occurrence of Adjacent Local Binary Patterns (CoALBP), Local Phase Quantization (LPQ) have shown to be effective in gray-scale texture-based face anti-spoofing.

— LBP (Local Binary Pattern)

Local Binary Pattern (LBP) is a simple yet very efficient texture operator which labels the pixels of an image by thresholding the neighborhood of each pixel and considers the result as a binary number. Parameters: the LBPH uses 4

The first computational step of the LBPH is to create an intermediate image that describes the original image in a better.

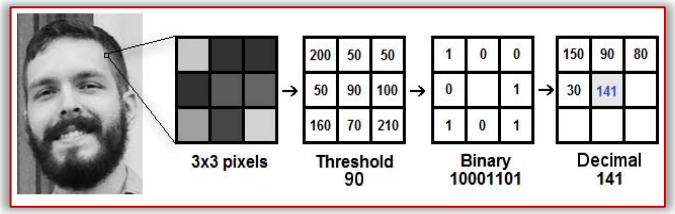

Figure 1. LBP image

For each neighbor of the central value (threshold), we set a new binary value. We set 1 for values equal or higher than the threshold and 0 for values lower than the threshold. Now, the matrix will contain only binary values (ignoring the central value) figure 1. We need to concatenate each binary value from each position from the matrix line by line into a new binary value (e.g. 10001101). Note: some authors use other approaches to concatenate the binary values (e.g. clockwise direction), but the final result will be the same. Then, we convert this binary value to a decimal value and set it to the central value of the matrix, which is actually a pixel from the original image. At the end of this procedure (LBP procedure), we have a new image which represents better the characteristics of the original image. The LBP procedure was expanded to use a different number of radius and neighbors, it is called Circular LBP. It can be done by using bilinear interpolation. If some data point is between the pixels, it uses the values from the 4 nearest pixels (2x2) to estimate the value of the new data point.

— LPQ (Local Phase Quantization)

In recent years, high elongation materials are widely used. Therefore, it is important to investigate the tensile properties of high elongation materials for engineering applications. Video extensometer is equipment for measuring the materials' tensile properties. It uses image processing technology to match data points and measures the actual deformation. However, when measuring high elongation materials, motion blur will appear on the collected images, which can affect the accuracy of image matching. In this paper, we proposed an image matching method which is based on Local Phase Quantization (LPQ) features to reduce the interference of the motion blur and improve the accuracy of the image matching algorithms as well. The experimental results on simulations show that the proposed initialization method is sufficiently accurate to enable the correct convergence of the subsequent optimization in the presence of motion blur. The experiment of uniaxial tensile also verifies the accuracy and robustness of the method. High elongation materials are an important class of materials for structural applications such as transportation, civil infrastructures, and biomedical applications. In actual service conditions, these materials are often subject to both mechanical and environmental loads. These factors will change the material properties and thus have a great influence on the service life and safety performance of these materials. In order to study these factors, the tensile mechanical test should be carried out on these materials. At present, the most commonly used equipment for the tensile mechanical test is the mechanical extensometer and video extensometer. For the high elongation materials, the mechanical extensometer which is mounted directly onto the material via blade causes many problems such as the following:

- mutual friction will reduce the measurement accuracy;
- the total deformation cannot be easily measured in the uniaxial tensile test;
- the measuring range is limited.

Compared with mechanical extensometer, the video extensometer has the following advantages. However, if higher accuracy is pursued, some influence factors cannot be ignored, such as out-of-plane displacement, self-heating of the camera, lens distortion, and image blur induced by motion. Reference [2] theoretically describes the measurement errors caused by out-of-plane displacement and self-heating of the camera; it further establishes a high-accuracy two-dimensional digital image correlation (2D-DIC) system using a bilateral telecentric lens to minimize the errors.

Reference [3] investigates the systematic errors due to lens distortion using the radial lens distortion model and in-plane translation tests; it finds out that the displacement and strain errors at an interrogated image point not only are linear proportion to the distortion coefficient of the camera lens used but also depend on the distance relative to distortion center and its magnitude of the displacement; the paper also proposes a linear least-squares algorithm to estimate the distortion coefficients and then to eliminate the errors.

It proposes an off-axis digital image correlation method for real-time, noncontact, and target less measurement of vertical deflection of bridges to achieve subpixel accuracy. Despite these advances, few works about eliminating extensometer's measurement errors caused by motion-induced image blur to improve the accuracy have been reported.
In this paper, we will propose an image matching method for video extensometer to measure the parameters by utilizing Local Phase Quantization (LPQ) feature. This method is robust and performs well on images with serious motion blur and deformation.
The phase information in the Fourier coefficients is recorded by examining the signs of the real and imaginary parts of each component in.This is done by using a simple scalar quantization, where is the component of the vector. The resulting eight binary coefficients are represented as integer values within 0–255 using binary coding:
Finally, a histogram is formed by all the positions in the rectangular region and used as a 256-dimensional feature vector in the match.

— CoLBP (Co-Occurrence Local Binary Pattern)

The new image feature based on spatial co-occurrence among micropatterns, where each micropattern is represented by a Local Binary Pattern (LBP). In conventional LBP-based features such as LBP histograms, all the LBPs of micropatterns in the image are packed into a single histogram in figure 2. Doing so discards important information concerning spatial relations among the LBPs, even though they may contain information about the image's global structure. To consider such spatial relations, we measure their co-occurrence among multiple LBPs. The proposed feature is robust against variations in illumination, a feature inherited from the original LBP, and simultaneously retains more detail of image. The significant advantage of the proposed method versus conventional LBP-based features is demonstrated through experimental results of face and texture recognition using public databases. Spatial co-occurrence could boost the discriminative power of the features, but it always suffers from the geometric and photometric variations. In this work, we investigate rotation invariant property of co-occurrence feature, and introduce a novel pairwise rotation invariant co-occurrence local binary pattern (PRI-CoLBP) feature which incorporates two types of context, spatial co-occurrence and orientation co-occurrence. Different from traditional rotation invariant local features, pairwise rotation invariant co-occurrence features preserve the relative angles between the orientations of individual features. The relative angle depicts the local curvature information, which is discriminative.

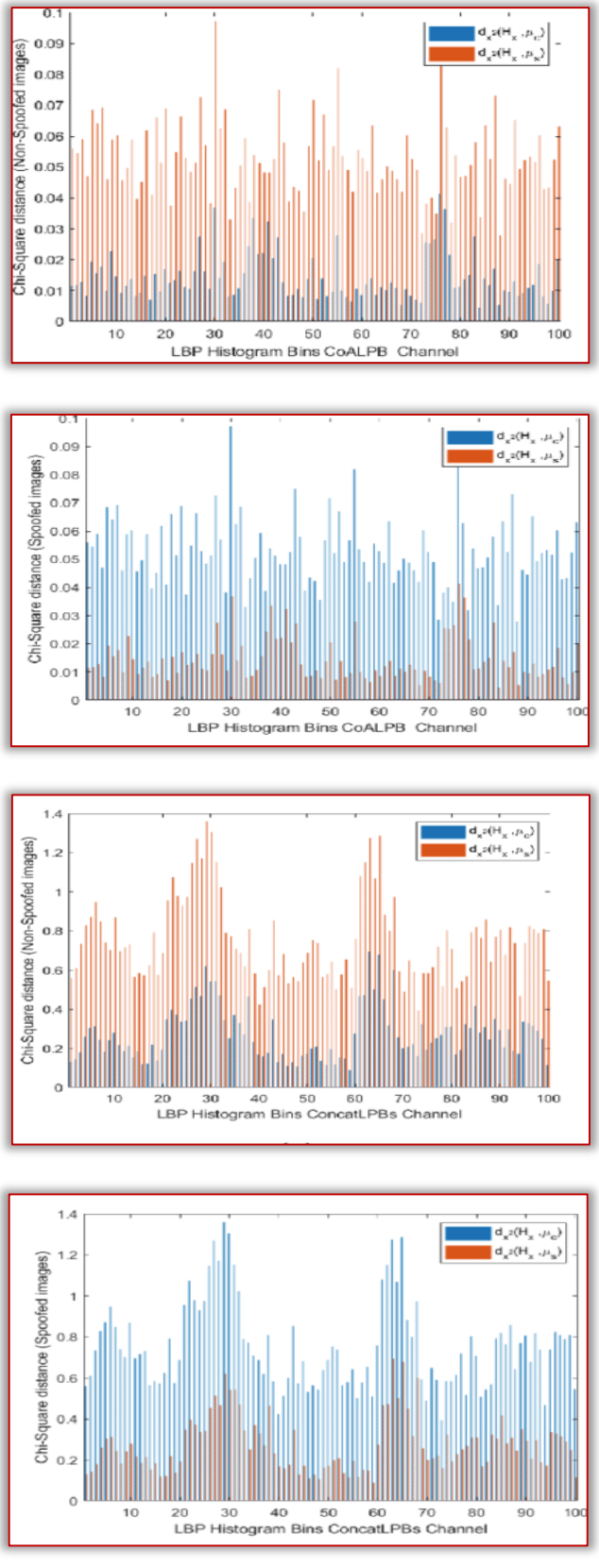

Figure 2. CoLBP image

METHODOLOGY

— Input image

Read and Display an input Image. Read an image into the workspace, using the misread command. In image processing, it is defined as the action of retrieving an image from some source, usually a hardware-based

source for processing. It is the first step in the workflow sequence because, without an image, no processing is possible. The image that is acquired is completely unprocessed.

— RGB colour image

The RGB color model is an additive color model in which red, green, and blue light are added together in various ways to reproduce a broad array of colors. The name of the model comes from the initials of the three-additive primary colors, red, green, and blue.

The main purpose of the RGB color model is for the sensing, representation, and display of images in electronic systems, such as televisions and computers, though it has also been used in conventional photography. Before the electronic age, the RGB color model already had a solid theory behind it, based in human perception of colors' is a device-dependent color model: different devices detect or reproduce a given RGB value differently, since the color elements (such as phosphors or dyes) and their response to the individual R, G, and B levels vary from manufacturer to manufacturer, or even in the same device over time in figure 3. Thus an RGB value does not define the same color across devices without some kind of color management. Typical RGB input devices are color TV and video cameras, image scanners, and digital cameras. Typical RGB output devices are TV sets of various technologies (CRT, LCD, plasma, etc.), computer and mobile phone displays, video projectors, multicolor LED displays, and large screens such as Jumbotron. Color printers, on the other hand, are not RGB devices, but subtractive color devices (typically CMYK color model).

Figure 3. RGB image

— Grayscale

In photography and computing, a grayscale or greyscale digital image is an image in which the value of each pixel is a single sample, that is, it carries only intensity information. Images of this sort, also known as black-and-white, are composed exclusively of shades of gray, varying from black at the weakest intensity to white at the strongest. Grayscale images are distinct from one-bit bi-tonal black-and-white images, which in the context of computer imaging are images with only the two colors, black, and white (also called bilevel or binary images). Grayscale images have many shades of gray in between. Grayscale images are also called monochromatic, denoting the presence of only one (mono) color (chrome). Grayscale images are often the result of measuring the intensity of light at each pixel in a single band of the electromagnetic spectrum (e.g. infrared, visible light, ultraviolet, etc.), and in such cases they are monochromatic proper when only a given frequency is captured. But also, they can be synthesized from a full colour image; see the section about converting to grayscale in figure 4. Example of gray scale image is given below.

Figure 4. Gray scale image

— Colour convertion

A color space is a specific organization of colors. In combination with physical device profiling, it allows for reproducible representations of color, in both analog and digital representations. A color space may be arbitrary, with particular colors assigned to a set of physical color swatches and corresponding assigned color names or numbers such as with the Pantone collection, or structured mathematically as with the NCS System, Adobe RGB and sRGB. A "color model" is an abstract mathematical model describing the way colors can be represented as tuples of numbers (e.g. triples in RGB or quadruples in CMYK); however, a color model with no associated mapping function to an absolute color space is a more or less arbitrary color system with no connection to any globally understood system of color interpretation. Adding a specific mapping function between a color model and a reference color space establishes within the reference color space a definite "footprint", known as a gamut, and for a given color model this defines a color space. For example, Adobe RGB and sRGB are two different absolute color spaces, both based on the RGB color model. When defining a color space, the usual reference standard is the CIELAB or CIEXYZ color spaces, which were specifically designed to encompass all colors the average human can see. Since "color space" identifies a particular combination of the color model and the mapping function, the word is often used informally to identify a color model. However, even though identifying a color space automatically identifies the associated color

model, such a usage is incorrect in a strict sense. For example, although several specific color spaces are based on the RGB color model, there is no such thing as the singular RGB color space.

— Pre-processing

Pre-processing is a common name for operations with images at the lowest level of abstraction both input and output are intensity images.

The aim of pre-processing is an improvement of the image data that suppresses unwanted distortions or enhances some image features important for further processing. Image pre-processing methods use the considerable redundancy in images. Neighboring pixels corresponding to one object in real images have essentially the same or similar brightness value. Thus, distorted pixel can often be restored as an average value of neighboring pixels.

— Feature extraction

In machine learning, pattern recognition and in image processing, feature extraction starts from an initial set of measured data and builds derived values (features) intended to be informative and non-redundant, facilitating the subsequent learning and generalization steps, and in some cases leading to better human interpretations. Feature extraction is related to dimensionality reduction. When the input data to an algorithm is too large to be processed and it is suspected to be redundant (e.g. the same measurement in both feet and meters, or the repetitiveness of images presented as pixels), then it can be transformed into a reduced set of features (also named a feature vector). Determining a subset of the initial features is called feature selection. The selected features are expected to contain the relevant information from the input data, so that the desired task can be performed by using this reduced representation instead of the complete initial data.

- ≡ Shape features
- ≡ color features

— Classification

Image classification refers to the task of extracting information classes from a multiband raster image. The resulting raster from image classification can be used to create thematic maps. The recommended way to perform classification and multivariate analysis is through the Image Classification toolbar. There are many classification algorithms are available and some classification algorithm that are given below.

In pattern recognition, the k-nearest neighbors' algorithm (k-NN) is a non-parametric method used for classification and regression.[1] In both cases, the input consists of the k closest training examples in the feature space. The output depends on whether k-NN is used for classification or regression.

In k-NN classification, the output is a class membership. An object is classified by a plurality vote of its neighbors, with the object being assigned to the class most common among its k nearest neighbors (k is a positive integer, typically small). If k = 1, then the object is simply assigned to the class of that single nearest neighboring k-NN regression, the output is the property value for the objecting figure 5. This value is the average of the values of k nearest neighbors. k-NN is a type of instance-based learning, or lazy learning, where the function is only approximated locally and all computation is deferred until classification. Both for classification and regression, a useful technique can be to assign weights to the contributions of the neighbors, so that the nearer neighbors contribute more to the average than the more distant ones. For example, a common weighting scheme consists in giving each neighbor a weight of 1/d, where d is the distance to the neighbor.

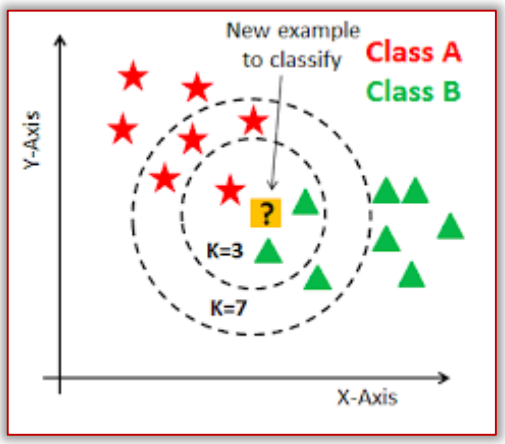

Figure 5. KNN

CONCLUSIONS

To approach the problem of face anti-spoofing from the color texture analysis point of view. We investigated how well different color image representations (RGB, HSV and YCbCr) can be used for describing the intrinsic disparities in the color texture between genuine faces and fake ones and if they provide complementary representations. The effectiveness of the different facial color texture representations was studied by extracting different local descriptors from the individual image channels in the different color spaces. The facial color texture representation seems be more stable in unknown conditions than texture descriptions extracted from gray-scale images. Thus, the use of color texture information provides a way to improve the unsatisfying generalization capabilities of texture-based approaches. In order to benefit from the potential complementarity of the CoALBP and the LPQ face descriptions, to fuse them by concatenating their resulting histograms. The facial representations extracted from different color spaces using different texture descriptors can also be concatenated in order to benefit from their complementarity. The effectiveness of different texture descriptors more

closely in detecting various kinds of face spoofs by extracting holistic face representations from luminance and chrominance images in different color spaces. In future, the T test is use for feature selection to reduce high time consumption due to high feature size, second the Classifier need high training sample so by applying sparse classifier it will be reduced.

References

[1] Y. Li, K. Xu, Q. Yan, Y. Li, R.H. Deng, "Understanding OSN-based facial disclosure against face authentication systems," in Proceedings of the 9th ACM Symposium on Information, Computer and Communications Security, ser. ASIA CCS '14. ACM, 2014

[2] J. Li, Y. Wang, T. Tan, A.K. Jain, "Live face detection based on the analysis of Fourier spectra," in Biometric Technology for Human Identification, 2004.

[3] X. Tan, Y. Li, J. Liu, L. Jiang, "Face liveness detection from a single image with sparse low rank bilinear discriminative model," in Proceedings of the 11th European conference on Computer vision: Part VI, ser. ECCV'10, 2010.

[4] Z. Zhang, J. Yan, S. Liu, Z. Lei, D. Yi, S.Z. Li, "A face antispoofing database with diverse attacks," in 5th IAPR International Conference on Biometrics (ICB), 2012, pp. 26–31.

[5] J. Galbally, S. Marcel, "Face anti-spoofing based on general image quality assessment," in Proc. IAPR/IEEE Int. Conf. on Pattern Recognition, ICPR, 2014.

[6] D. Wen, H. Han, A. Jain, "Face spoof detection with image distortion analysis," Transactions on Information Forensics and Security, vol. 10.

[7] J. Bai, T.-T. Ng, X. Gao, Y.-Q. Shi, "Is physics-based liveness detection truly possible with a single image?" in IEEE International Symposium on Circuits and Systems (ISCAS), 2010.

[8] J. Mahatma,¨ A. Hadid, M. Pietikainen, "Face spoofing detection from single images using micro-texture analysis," in Proceedings of International Joint Conference on Biometrics

[9] J. Komulainen, A. Hadid, and M. Pietikainen, "Face spoofing detection from single images using texture and local shape analysis," Biometrics, IET, vol. 1, no. 1, pp. 3–10, March

[10] J. Yang, Z. Lei, S. Liao, S. Z. Li, "Face liveness detection with component dependent descriptor," in IAPR International Conference on Biometrics, ICB, June 2013.

[11] T. d. F. Pereira, J. Komulainen, A. Anjos, J. M. De Martino, A. Hadid, M. Pietikainen, S. Marcel, "Face liveness detection using dynamic texture", EURASIP Journal on Image and Video Processing, 2013

ACTA TECHNICA CORVINIENSIS – Bulletin of Engineering
ISSN: 2067-3809

[1.]Rasheed Uthman OWOLABI, [2.]Mohammed Awwalu USMAN, [3.]C.E. WISDOM

TRANS-ESTERIFICATION OF CASTOR OIL USING HETEROGENEOUS BIO-CATALYST OBTAINED FROM BOVINE BONE

[1.]University of Lagos, Chemical and Petroleum Engineering Department, Akoka, Yaba, Lagos State, NIGERIA

Abstract: Bones obtained from bovine species of animal was investigated in this study as heterogeneous bio-catalyst for trans-esterification process. The bones were washed, dried,comminuted and calcined at a temperature around 500-900°C. A solution of 10 wt% aqueous KOH was prepared to soak the comminuted calcined bones to enhance their surface chemical properties. The obtained bio-catalysts were characterized physico-chemically using x-ray diffraction (XRD) for phase identification of the synthesized biocatalyst, differential thermal analysis (DTA) for the measurement of the mass changes in materials as function of temperature, Fourier transform infra red spectroscopy (FTIR) for the identification of the functional groups and gas chromatography mass spectrometry to identify the fatty acid profile of the synthesized biodiesel. The biodiesel was synthesized using establised optimum conditions of 60°C reaction temperature, methanol to oil molar ratio of 6:1, catalyst concentration of 1% weight of the oil, and at one hour reaction time and a maximum yield of 95.12% was obtained. After the 4th cycle of trans-esterification, a further yield of 78.40 % was obtained. The biodiesel produced was found to meet most of the ASTM specifications and more importantly, bovine bone derived catalyst has been identified as a promising and competing catalyst for the synthesis of green fuel through trans-esterification process.
Keywords: bovine, heterogeneous, bio-catalyst, trans-esterification, green fuel

INTRODUCTION

Trans-esterification reaction for the synthesis of biodiesel has gained mass and impressive attention of researchers particularly over the past two decades. For instance, researchers such as Folasegun et al., 2014; Yordanov et al., 2013; Kang and Rui, 2013; Owolabi and Osiyemi, 2013; Owolabi et al., 2011; Porte et al., 2010; Shu et al., 2010; Kasendo et al., 2009; Singh and Singh, 2009; Lapuerta et al., 2009; Canoira et al., 2008; Canoira et al., 2007; Kumar et al., 2007; Canoira et al., 2006; among others successfully trans-esterified various bio-sourced oil respectively, for biodiesel synthesis under varied catalyzed medium with each obtaining interesting results.

Gernerally, a catalyst offers safer and milder reactions, increases chemoselectivity and functional group tolerance, involves simple work procedure, reduces waste and also exhibits wide substrate scope (Gusev, 2013) still, over the years, only the use of homogeneous acids and bases as catalysts for trans-esterification reaction remained the common practise among researchers. The commonly used homogeneous catalyst is H_2SO_4 (Leung et al., 2010; Meher et al., 2006; Barnwal and Sharma 2005; Fukuda et al.,2001 and Ma et al.,1999) while commonly used homogeneous bases are lyes such as NaOH, KOH etc (Owolabi et al., 2012). Lye catalysts are corrosive to glass apparatus and also prone to saponification wiith a bye product that poses separational issues both in terms of technicalities and cost (Wen et al., 2010 and Song et al., 2011). The homogeneous acid catalysts have also been reported to consume excess reactants coupled with its strong affinity for high methanol oil ratio (Canakci and Van Gerpen, 1999). All these traits of homogeneous catalysts are not in favour of low cost biodiesel production especially at a scaled up level. Other recent studies have focused on some heterogeneous catalyst with some degree of successes. For instance, micro- crystalline cellulose was used by Ayodele and Dawodu, 2014; Beta-Zeolite (Sathyaselvabala et al.,2011); Ferric Sulfate (Patil et al.,2010); Calcium oxide (Zhang et al., 2010) and sulfunated Zirconia (Garcial et al., 2008) but with varied degree of successes.The last half decade has also witnessed synthesis of heterogeneous catalyst for trans-esterification process from agro-related materials such as palm trunk, sugar cane bagasse, coconut husk , coco pod husk and oyster shell waste (Ezebor et al., 2014a-b; Vadery et al.,2014; Ofori-Boateng and Lee, 2013; Nakatani et al., 2009) respectively.These forms of catalyst were reported by Gryglewicz, 1999; and Suppes et al., 2004 to facilitate post reaction mixtures separation but reaction progresses at relatively slower rate. Moreover, bones have been found to contain hydroxyapatite [$Ca_{10}(PO_4)_6(OH)_2$] which are porous with large surface area that facilitate catalytic actions (Nisar et al., 2017). Their report was based on the use of an unspecified but calcined waste animal bones as catalyst for biodiesel synthesis.They further ascertained the reasonable performance of the catalyst only at high proportion coupled with longer reaction time.These limitations require enhancement of the surface chemical properties for effective catalytic activity on the bone surface which this present study incorporates. It is therefore our focus in this study to synthesize, characterize and test run the functionality of the new set of catalysts from bovine animal bones for possibilities of improved catalytic

actions over the earlier catalysts. The study also focuses on the operational strength of the bio-catalyst in terms of its recycliability, overall biodiesel yield obtainable and quality.

SYNTHESIS AND ACTIVATION OF BIO-CATALYST

Bovine bones with particular focus on the leg were obtained fresh from an abbattoir in Lagos state, Nigeria with 6.5244° N, 3.3792° E. They were washed with hot water to remove impurities and dried in day light for two weeks consecutively.The bones were then crushed, comminuted and pulverised using an industrial grinder while some were left as granules as shown in Figure 1. The bovine bones were calcined at a temperature around 500 - 900 °C in a furnace (Nisar et al.,2017; Madhu et al., 2016; Chopade et al., 2012). A solution of 10 wt% aqueous KOH was prepared to soak the calcined pulverised bones to enhance its surface chemical properties (Nisar et al., 2017).The admixture of the calcined pulverised bones and KOH were simultaneously heated and agitated at 500 rpm using a magnetic heater till cake formation and complete evaporation of water were observed (Alamu et al.,2007; Semwal,2011.). The hard cake was left to cool and dry. Samples of the virgin pulverised bovine bones, calcined bones and KOH treated bones were kept for subsequent biodiesel production.

Figure 1: Calcined Bovine Bones

— Characterization of the Bio-Catalyst

The synthesized bio-catalyst derived from bovine bone was characterized physico-chemically using x-ray diffraction (XRD) for phase identification of the synthesized biocatalyst, differential thermal analysis or thermogravimetric analysis (DTA/TGA) for the measurement of the mass changes in materials as function of temperature, Fourier transform infra red spectroscopy (FTIR) for the identification of the functional groups and gas chromatography mass spectrometry which utilizes the combined features of both gas chromatography and mass spectometry to identify the fatty acid profile of the synthesized biodiesel.

— Operation of Reactor

All reactions were performed in two neck batch reactor with reflux condenser, temperature sensor and controlled magnetic stirrer. The temperature was monitored by the digital display on the heating system.The reflux system was adopted to eliminate vapourization of methonal from the reacting system.

— Synthesis of Biodiesel (Green Fuel)

Castor oil for the synthesis of the green fuel was obtained from SIGMA ALDRICH with specification SKU-pack size 18722-1L and was used as obtained.The chemical composition of the castor oil in weight percent and other physico-chemical properties are contained in Tables 1 and 2. The biodiesel was initially synthesized using establised optimum conditions of 60 °C reaction temperature, methanol to oil molar ratio of 6:1, catalyst concentration of 1% weight of the oil, and at one hour reaction time (Kang and Rui,2013). The castor oil was initially pre-heated till desired temperature was reached. A prepared mixture of methanol and catalyst was introduced into the pre-heated oil for trans-esterification purpose and commencement of the reacton time (Banerjee et al., 2017; Kilic et al., 2013). Products were kept overnight for cooling and phases separation in a separating funnel. The desired upper phase consists of the castor oil biodiesel while the lower phase consists of glycerol, catalyst, unreacted reactants and other insignificant side reaction products. For the case of the synthesized bio-catalyst,the catalyst was separated and kept for further biodiesel production and yields were obtained using Eq.1

$$\text{Yield Biodiesel} = \frac{\text{Weight Fatty acid methy ester}}{\text{Weight of oil}} 100 \quad (1)$$

The recycliability of the synthesized bio-catalyst was examined for a number of experimental cycle under the same established optimum conditions. Yields of biodiesel obtained were calculated at the end of each cycle.

RESULTS AND DISCUSSION

— Characterization of the Castor Oil Feedstock

Table 1 and 2 contains the fatty acid profile and physico-chemical properties of the castor oil, respectively as directly obtained from the manufacturer.

Table 1. Fatty Acid Composition of Castor Oil

S/N	Fatty Acid	% Composition
1	Ricinoleic Acid	87
2	Oleic	7
3	Linoleic	3
4	Palmitic	2
5	Stearic	1
	Merck, 2019	

Table 2. Physico-Chemical Properties of Castor Oil

S/N Properties	Units	Value
Appearance (Light Yellow)		
Density (20 °c)	g//ml	0.952-0.965
Viscosity (25 °c)	Poise	1.6-2.8
Flash Point	°C	113
Peroxide Value	meq/g	≤ 5
Acid Value	mgKOH/g	≤ 5
Hydroxyl Value	mg/g	≥ 160
Iodine Value	mgI_2/g	82-90
Saponification Value	mgKOH/g	176-187

Activation and Characterization of the Synthesized Bio-Catalyst

Thermogravimetric analysis to monitor the influence of calcination temperature on weight loss of the cow bone is as depicted in Figure 2. The study was carried out over a temperature range of 32-900°C. A sharp drop in weight was recorded between temperature range of 32–500°C thereafter, it became approoximately steady. Madhu et al., 2016 attributed the sharp drop in weight to the decomposition of calcium carbonate to calcium oxide coupled with effervessence of carbon (iv) oxide (Eq.2)

$$CaCO_{3(s)} \rightarrow CaO_{(s)} + CO_{2(g)} \quad (2)$$

Steady weight loss was also observed between 500–900°C. Nisar et al., 2017 similarly observed this trend in their study and attributted such to the formation of gaseous fraction due to transformation of bone to hydroxyapatite (HAP). In Figure 2, no significant further loss in weight was observed. This is a confirmation of the high thermal stability of the calcined cow bone.

The scanning electron microscope of the synthesized biocatalyst (15,000 X and 10,000 X) are presented in Figure 3a-b and as specified are at different magnifications showing the surface morphology of the heterogeneous catalyst.The architecture observed seems porous which gives it a catalytic advantage.

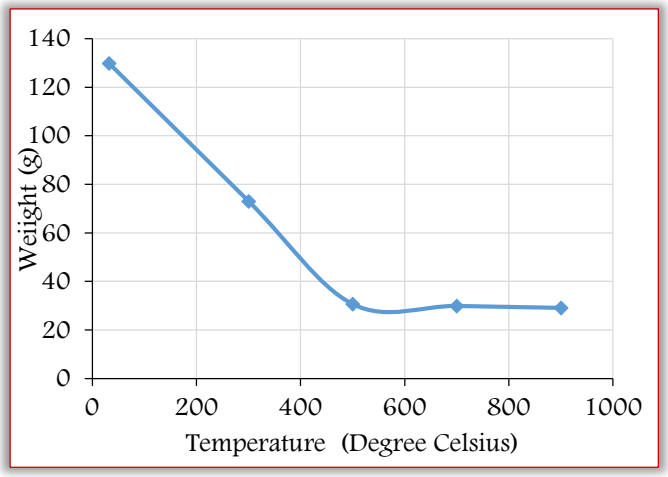

Figure 2: The TGA/DTA Profile of Cow Bone

The preparation of the bio-catalyst was supported with KOH(aq) which could be responsible for scattered particles on the catalyst surface. Though, effects of the calcination temperature was not studied but reports (Goli and Sahu,2018) confirmed that at high calcination temperature, the catalyst particles becomes smaller.

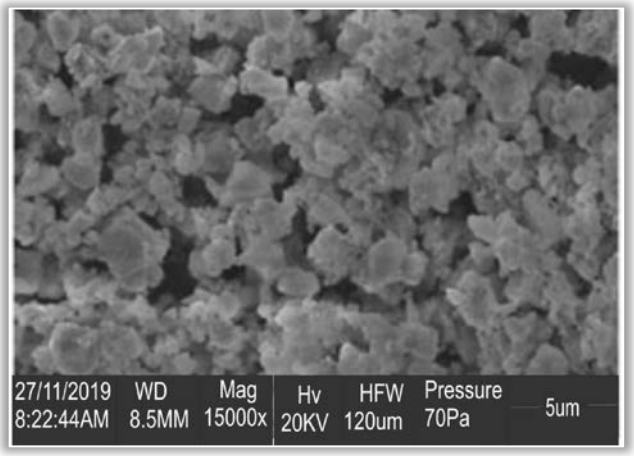

Figure 3 a : SEM Image of the Synthesized Biocatalyst (Magnification15000x)

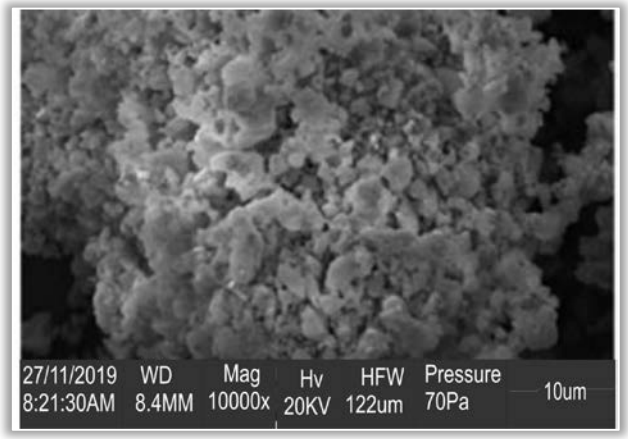

Figure 3b: SEM Image of the Synthesized Biocatalyst (Magnification10000x)

In another study, the reduced particle were found to be proportional to the specific surface area and depends on the catalyst surface area (Khemtong et al., 2012; and Viriya- Empikul et al., 2012). From the biodiesel yield obtained in this study,the bio-catalyst particles exhibited remarkable catalytic acitivty. Figure 4 shows results from the X-RD where just few peaks were observed.Similar to the report of Tahvildari et al., 2014, modified materials which are crystalline in nature are apparent. This could be by virtue of the reaction between calcined bone and KOH (Tahvildari et al., 2014).

From the spectral analysis of the bio-catalyst, the major absorption bands include ,the C-Cl stetch that was detected at the wave numbers 557 and 597 cm^{-1}, both the meta and para C-H bend that were detected at 871 cm^{-1} wave number, the C-H in plane bend that was also detected at the wavenumber 1388cm^{-1}.and finally, both the isolated and the conjugated C = C variable stretches were also detected.

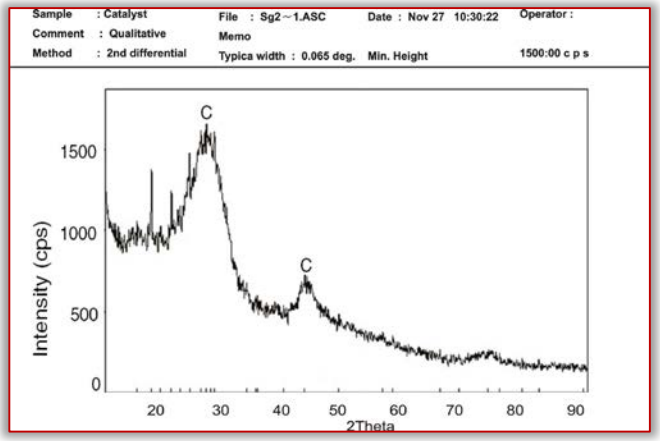

Figure 4: X-ray Diffraction of the Synthesized Bio-Catalyst

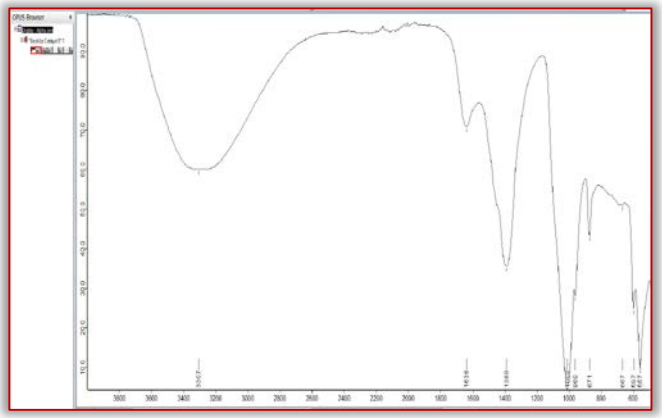

Figure 5: FTIR Spectrum of the Bio-Catalyst

— Bio - Catalyst Recyclability

The strength of the synthesized bio-catalyst was determined through the number of cycles it was used to catalyse trans-esterification reaction. The recyclability takes advantage of the heterogeneous nature of the catalyst which can be easily re-filtrated and reused. As shown in Figure 6, after 4 cycles of trans-esterification, the yield was still 78.40%.

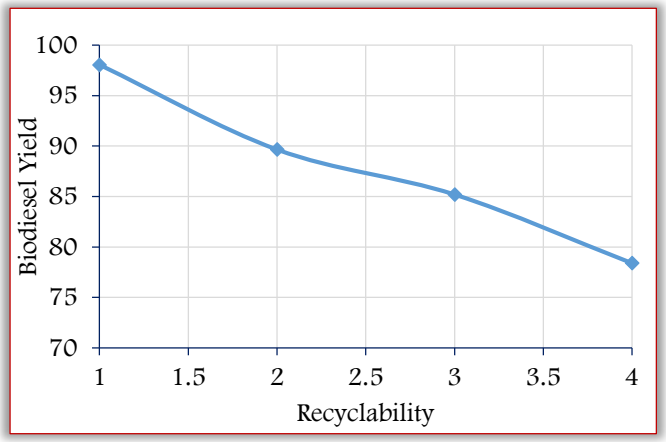

Figure 6: Recyclability profile of Bio-catalyst

The cycled reaction was carried out without further re-calcination of the used bio-catalyst. Obadiah et al., 2012 recorded 83.7% biodiesel yield after 5 cycles while Madhu et al., 2016, recalcined the used bio-catalyst and obtained 84% biodiesel yield after 5 cycles and a closely 83% biodiesel yield without further recalcination after 5 cycles.It can be surmised that wiith re-calcination, catalytic sites are further activated with improved biodiesel yield. The decline in the yield of biodiesel as the catalyst was recovered is due to catalyst loss as well as reduced catalytic activity (Sani et al., 2014).

CONCLUSION

In this study, animal derived biomass specifically from bovine species was used as major feedstocks for trans-esterification heterogeneous catalyst development and was found to synthesize biodiesel with a maximum yield of 95.12 % which was found to be the optimun and a further yield of 78.40 % after the fourth trans-esterification cycle thereby, proving the catalytic activities of the biomass derived catalyst as further supported by the prior analysis the synthesized catalyst was subjected to. The green fuel (biodiesel) produced was found to meet most of the ASTM specifications As an addition to knowledge, biomass derived catalyst from bovine species of animals has been identified as a promising and competing catalyst for the synthesis of green fuel through trans-esterification process.

Acknowledgement

This research work received full funding from the Professor Ayo Ogunye professorial chair in chemical engineering (Third Edition) through the office of advancement, University of Lagos Ref. No.: VC/OA/E.29/Vol.7.

References:

[1] Sigma, 2019 https://www.sigmaaldrich.com/
[2] Ayodele, O.O., Dawodu, F.A. 2014. Production of biodiesel from Calophyllum inophyllum oil using a cellulose-derived catalyst. Biomass and Bioenergy, 70, 239-248.
[3] Barnwal, B.K., Sharma M.P., Renew. Sust. Energ. Rev., 2005, 9, 363-378
[4] Canakci, M., Van Gerpen, J. 1999. Biodiesel production via acid catalysis. Transactions of the ASAE-American Society of Agricultural Engineers, 42(5), 1203-1210.
[5] Canoira L., Alcantara R., Garcı´a-Martı´nez M.J., Carrasco, J. (2006). Biodiesel from Jojoba oil-wax: transesterification with methanol and properties as a fuel. Biomass Bioenergy, 30,76–81.
[6] Canoira L., Alcantara R., Torcal S., Tsiouvaras N., Lois E., Korres, D.M. (2007). Nitration of biodiesel of waste oil: nitrated biodiesel as a cetane number enhancer. Fuel, 86, 965–71.
[7] Canoira L., Rodrıguez-Gamero M., Querol E., Alcantara R., Lapuerta M., Oliva F.(2008). Biodiesel from low-grade animal fat: production process assessment and biodiesel properties characterization. Ind. and Eng. Chem Research, 47: 7997–8004.
[8] Chopade, S. G., Kulkarni, K. S., Kulkarni, A. D., and Topare, N. S. (2012). Solid heterogeneous catalysts for production of biodiesel from transesterification of triglycerides with methanol: a review. In Solid heterogeneous catalysts for production of biodiesel

from transesterification of triglycerides with methanol: a review. Acta Chim Pharm Indica. 2(1):8-14).
[9] Ezebor, F., Khairuddean, M., Abdullah, A.Z., Boey, P.L. 2014a. Oil palm trunk and sugarcane bagasse derived heterogeneous acid catalysts for production of fatty acid methyl esters.Energy, 70, 493-503.
[10] Ezebor, F., Khairuddean, M., Abdullah, A.Z., Boey, P.L. 2014b. Oil palm trunk and sugarcane bagasse derived solid acid catalysts for rapid esterification of fatty acids and moisture assisted transesterification of oils under pseudo-infinite methanol. Bioresource technology, 157, 254-262.
[11] Folasegun, A.D, Olubunmi, A., Jiayu, X., Suojiang, Z., Dongxia, Y (2014) Effective conversion of non-edible oil with high free fatty acid into biodiesel by sulphonated carbon catalyst, Applied Energy,114,819-826.
[12] Fukuda, H., Kondo, A., Noda, H., J. Biosci. Bioeng., 2001, 92, 405-416.
[13] Garcia, C.M., Teixeira, S., Marciniuk, L.L., Schuchardt, U. 2008. Transesterification of soybean oil catalyzed by sulfated zirconia. Bioresource technology, 99(14), 6608-6613.
[14] Goli,J., Sahu,O. (2012). Development of Heterogeneous Alkali Catalyst from waste Chicken Egg Shell for Biodiesel Production, Renewable Energy,128, 142-154.
[15] Gryglewicz, S., 1999. Rapeseed oil methyl esters preparation using heterogeneous catalysts. Bioresour. Technol. 70, 249–253.
[16] Gusev., (2013). Discover Homogeneous Ester Hydrogenation with Gusev Technology, a Commercially Available Novel Catalyst, Angew Chem Int Ed. 52, 2538-2542
[17] Kang, L and Rui, W. (2013). Biodiesel production by tranesterification of duck oil with methanol in the presence of alkali catalyst, Petroleum and Coal, 55, 68-72.
[18] Kansedo, J., Lee, K.T., Bhatia, S., Cerbera, O. (2009). See mango oil as a promising non-edible feedstock for biodiesel production, Fuel, 88, 1148-1150.
[19] Khemthong, P., Luadthong, C., Nualpaeng, W., Changsuwan, P., Tongprem, P., Viriya-Empikul, N., Faungnawakij, K.\(2018). Industrial Eggshell Wastes as the Heterogeneous Catalysts for Micro-Wave Assisted Biodiesel Production, Catalyst Today,190(1), 112-116.
[20] Kumar, T.A., Kumar, A., Raheman, H., (2007). Biodiesel production from jatropha oil (Jatropha curcas) with high free fatty acids: an optimized process. Biomass Bionergy.31, 569-575.
[21] Lapuerta M, Rodrıguez-Fernandez J., Oliva F., Canoira L. (2009). Biodiesel from low grade animal fats: diesel engine performance and emissions. Energy Fuels, 23, 121–129.
[22] Leung, D.Y.C., Wu, X., Leung, M.K.H., Appl. Energ., 2010, 87, 1083-1095.
[23] Ma, F., Hanna, M.A., Bioresour. Technol., 1999, 70, 1-15.
[24] Madhu, D., Chavan, S.B., Singh, V., Singh, B., Sharma, Y.C. (2016). An Economically Viable Synthesis of Biodiesel from a Crude Millettia Pinnata Oil of Jharkhand, India as Feedstock and Crab Shell Derived Catalyst. Bioresource Technology, 214, 210-214.
[25] Meher, L.C., Sagar, D.V., Naik, S.N., Renew. Sust. Energ. Rev., 2006, 10, 248-268
[26] Nakatani, N., Takamori,H , Takeda,K ., Hiroshi Sakugawa.,2009, Transesterification of soybean oil using combusted oyster shell waste as a catalyst, Bioresource Technology 100, 1510–1513
[27] Nisar, J., Razaq, R., Farooq, M., Iqbal, M., Khan, R.A.,Sayed, M.,Shah, A.,Rahman, R.U. (2017). Enhanced Biodiesel Production from Jatropha Oil using Calcined Waste Animal Bones as Catalyst.Renewable Energy,101, 111-119.
[28] Obadiah,A., Swaroopa, G.A., Kumar, S.V.,Jeganathan, K.R, Ramasubbu,A (2012). Biodiesel Production from Palm Oil using Calcined Waste Animal Bone as Catalyst, Bioresource Technology,116, 512-516.
[29] Ofori-Boateng, C., Lee, K.T. 2013. The potential of using cocoa pod husks as green solid base catalysts for the transesterification of soybean oil into biodiesel: Effects of biodiesel on engine performance. Chemical Engineering Journal, 220, 395-401.
[30] Owolabi, R.U, Osiyemi, N.A, Amosa, M .K and Ojewumi, M.E. (2013). Biodiesel from Household/Restaurant Waste Cooking Oil (WCO), Journal of Chemical Engineering & Process Technology 2 ,1-4
[31] Owolabi R.U, Adejumo A.L and Aderibigbe A.F. (2012). Biodiesel: Fuel for the Future (A Brief Review), International Journal of Energy Enginering, 5, 223-231.
[32] Patil, P., Deng, S., Isaac Rhodes, J., Lammers, P.J. 2010. Conversion of waste cooking oil to biodiesel using ferric sulfate and supercritical methanol processes. Fuel, 89 (2), 360-364.
[33] Porte, A.F., Schneider, R., Kaercher, J.A., Klamt, R.A., Schmatz, W.L., Da Silva, W (2010) Sunflower biodiesel production and application in family farms in Brazil, Fuel, 89,3718-3724.
[34] Sani, Y. M., Daud, W. A., Aziz, A. R. (2014). Activity of Solid Acid Catalyst for Biodiesel Production: a critical review. Applied Catalysis: A General, 470, 140-61.
[35] Sathya Selvabala, V., Selvaraj, D.K., Kalimuthu, J., Periyaraman, P.M., Subramanian, S. 2011. Two-step biodiesel production from Calophyllum inophyllum oil: Optimization of modified β-zeolite catalyzed pre-treatment. Bioresource technology, 102(2), 1066-1072.
[36] Shu, Q., Gao, J., Nawaz, Z., Liao, Y., Wang, D., Wang, J (2010). Synthesis of biodiesel from waste vegetable oil with large amounts of free fatty acids using a carbon based solid acid catalyst, Applied Energy, 87:2589-2596.
[37] Semwal, S., Arora, A. K., Badoni, R. P., and Tuli, D. K. (2011). Biodiesel production using heterogeneous catalyst . In Biodiesel production using heterogeneous catalyst. Bioresource Technology 102: 2151-2161
[38] Singh, S.P and Singh, D. (2009). Diesel production through the use of different sources and characterization of oils and their esters as the

substitute of diesel: a review. Renewable and Sustainable Energy Review, 14, 200-216.
[39] Song, R., Tong, D., Tang, J., Hu, C., Energ. Fuel, 2011, 25, 2679-2686
[40] Suppes, G.J., Dasari, M.A., Doskocil, E.J., Mankidy, P.J., Goff, M.J., 2004. Transesterification of soybean oil with zeolite and metal catalysts. App. Catal. A 257, 213–223
[41] Tahvildari, K., Chitsaz, H.R., Mozaffarinnia, P. (2014). Heterogeneous Catalytic Modified Process in the Production of Biodiesel from Sunflower Oil. Waste Cooking Oil,and Olive Oil by Trans-estrification Method, 5, 4, 60-68.
[42] Vadery, V., Narayanan, B.N., Ramakrishnan, R.M., Cherikkallinmel, S.K., Sugunan, S., Narayanan, D.P., Sasidharan, S. 2014. Room temperature production of jatropha biodiesel over coconut husk ash. Energy, 70, 588-594.
[43] Viriya-Empikul, N., Krasae, P., Nualpeng,W.,Yoosuk, B., Faungnawakij, k. (2012). Biodiesel Production over Ca- Based Solid Catalysts Derived from Industrial Wastes,Fuel, 92 (1), 239-244.
[44] Wen, Z., Yu, X., Tu ST., Yan J., Dahlquist E., Bioresour. Technol., 2010, 101, 9570-9576.
[45] Yordanov, D.I., Tsonev, Z.B., Palichev, T.V., Mustafa, Z.A (2013) A new approach for production of coffee oil from waste coffee as a feedstock for biodiesel, Petroleum and Coal, 55, 74-81.
[46] Zhang, J., Chen, S., Yang, R., Yan, Y. 2010. Biodiesel production from vegetable oil using heterogenous acid and alkali catalyst. Fuel, 89 (10), 2939-2944.

ACTA TECHNICA CORVINIENSIS – Bulletin of Engineering
ISSN: 2067-3809

[1.]Mustefa JIBRIL, [2.]Tesfabirhan SHOGA

QUARTER CAR ACTIVE SUSPENSION SYSTEM DESIGN USING OPTIMAL AND ROBUST CONTROL METHOD

[1.] Department of Electrical & Computer Engineering, Dire Dawa Institute of Technology, Dire Dawa, ETHIOPIA
[2.] Department of Electrical & Computer Engineering, Jimma Institute of Technology, Jimma, ETHIOPIA

Abstract: This paper offers with the theoretical and computational evaluation of optimal & robust control problems, with the goal of providing answers to them with MATLAB simulation. For the robust control, μ -synthesis controller and for the optimal control, LQR controller are designed for a quarter car active suspension system to maximize the ride comfort and road handling criteria's of the vehicle. The proposed controllers are designed using Matlab script program using time domain analysis for the four road disturbances (bump, random sine pavement and white noise) for the control targets suspension deflection, body acceleration and body travel. Finally the simulation result prove the effectiveness of the active suspension system with μ -synthesis controller.

Keywords: Quarter car active suspension system, optimal control, robust control, linear quadratic regulator

INTRODUCTION

Active suspension system are designed to satisfy specific necessities. In suspension systems, normally two maximum vital capabilities are anticipated to be advanced – disturbance shocking up (i.e. Passenger consolation) and attenuation of the disturbance transfer to the road (i.e. Vehicle dealing with). The first requirement might be supplied as an attenuation of the damped mass acceleration or as a peak minimization of the damped mass vertical displacement. The second one is characterized as an attenuation of the pressure acting on the road or in simple vehicle model as an attenuation of the unsprung mass acceleration. It is apparent that there's a contradiction among those requirements. Effort devoted to passive suspension design is ineffective, due to the fact there is a contradiction among both requirements. The nice end result (in experience of necessities development) can be done by active suspension, this means that that a few additional force can act on system.

The concept of optimal control has been nicely advanced for over forty years. With the advances of computer technique, optimal control is now widely used in multi-disciplinary applications which includes biological structures, conversation networks and socio-monetary systems and so forth. As an end result, increasingly people will benefit greatly via gaining knowledge of to resolve the optimal control problems numerically. Realizing such growing desires, books on optimum control put extra weight on numerical strategies. Necessary situations for diverse systems had been derived and specific solutions were given whilst possible. LQR is a control system that gives the pleasant viable performance with admire to some given degree of performance. The LQR design problem is to design a state feedback controller K such that the objective function J is minimized. In this approach a remarks advantage matrix is designed which minimizes the goal characteristic as a way to obtain some compromise among the use of control effort, the significance, and the speed of reaction so that it will assure a stable system.

MATHEMATICAL MODEL

— Quarter Vehicle Active Suspension System Mathematical Model

Let's begin with the most effective active suspension system model as shown in Figure 1. It carries two springs (one in suspension and second representing vehicle tires), one dumper and source of energy as actuator.

The model is described by way of the differential motion equations:

$$m_b\ddot{y}_b = F - k_1(y_b - y_w) - D(\dot{y}_b - \dot{y}_w) \quad (1)$$

$$m_w\ddot{y}_w = -F + k_1(y_b - y_w) - k_2(y_w - y_r) + D(\dot{y}_b - \dot{y}_w) \quad (2)$$

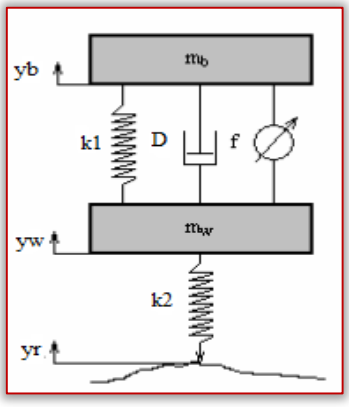

Figure 1: Quarter car active suspension model

Table 1: Parameters of Quarter vehicle Model

Model parameters	Symbol	Symbol Values
Vehicle body mass	m_b	300 Kg
Wheel assembly mass	m_w	40 Kg
Suspension stiffness	k_1	15,000 N/m
Suspension damping	k_2	150,000 N/m
Tyre stiffness	D	1000 N-s/m

ROAD DISTURBANCE INPUT SIGNALS

— Bump Road Disturbance

Bump input signal is a simple input to research the suspension system. It simulated a completely intense pressure for a very quick time, such as a car drive through a speed hump. This road disturbance has a maximum height of 5 cm as shown in Figure 2.

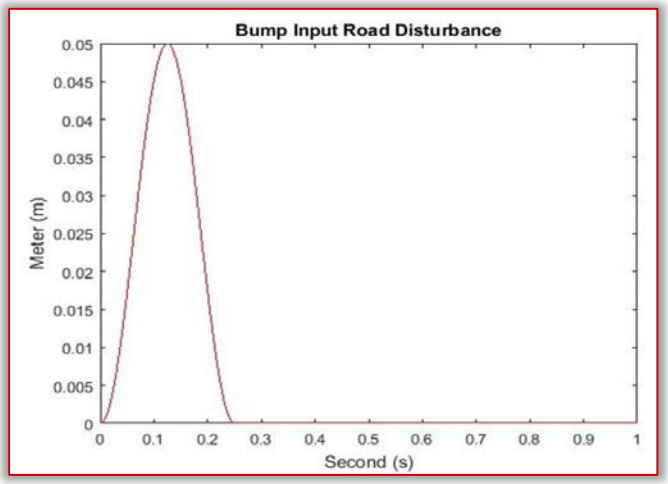

Figure 2: Bump road disturbance

— Random Road Disturbance

Numerous researches show that it's far vital to test a vehicle to a random road disturbance to test the spring and damper reply speedy and efficiently. The random road disturbance has a maximum height of 15 cm and minimum height of -15 cm as shown in Figure 3.

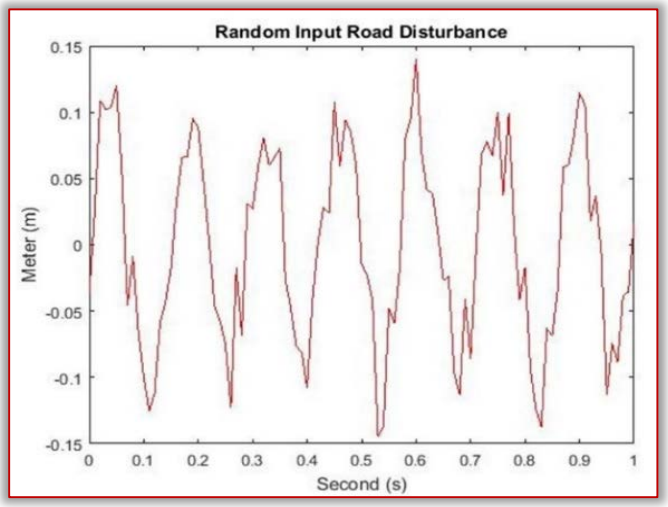

Figure 3: Random road disturbance

— Sine Pavement Road Disturbance

Sine wave input signal can be used to simulate periodic pavement fluctuations. It can take a look at the vehicle suspension system elastic resilience capacity whilst the vehicle reviews a periodic wave pavement. Sine input pavement test is made by means of each car industries before a new automobile drives on road. The sine pavement road disturbance has a height of -10 cm to 10 cm as shown in Figure 4.

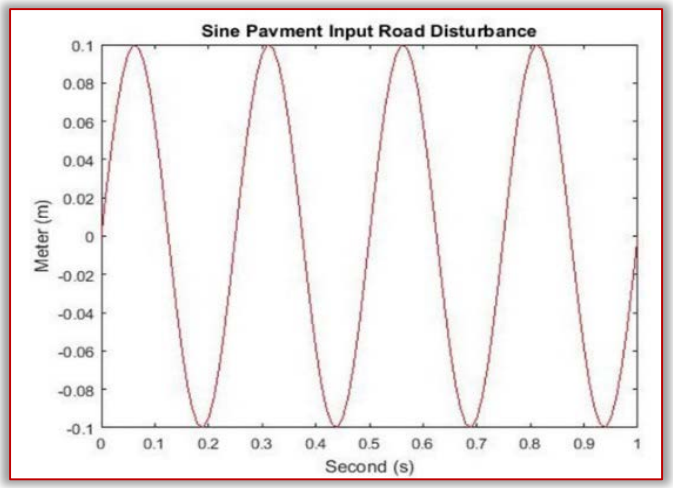

Figure 4: Sine pavement road disturbance

— White Noise Road Disturbance

Numerous researches display that once the automobile speed is consistent, the road roughness is a stochastic system that's subjected to Gauss distribution, and it can't be described accurately by means of mathematical model. The automobile velocity electricity spectral density is a constant, which correspond with the definition and statistical function of the white noise, so it is able to be virtually transformed to the road roughness time domain model as shown in Figure 5.

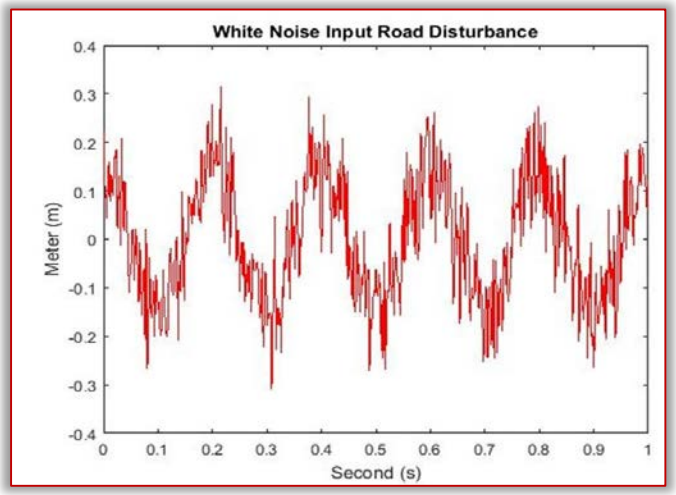

Figure 5: White noise road disturbance

THE PROPOSED μ-SYNTHESIS CONTROL DESIGN

— μ-Synthesis Controller Design

In the active suspension system, μ-synthesis design covered the hydraulic actuator dynamics. In order to account for the distinction between the actuator model and the real actuator dynamics, we used a second order model of the actuator dynamics as well as an uncertainty model. The active suspension system with μ-synthesis controller block diagram is shown in Figure 6.

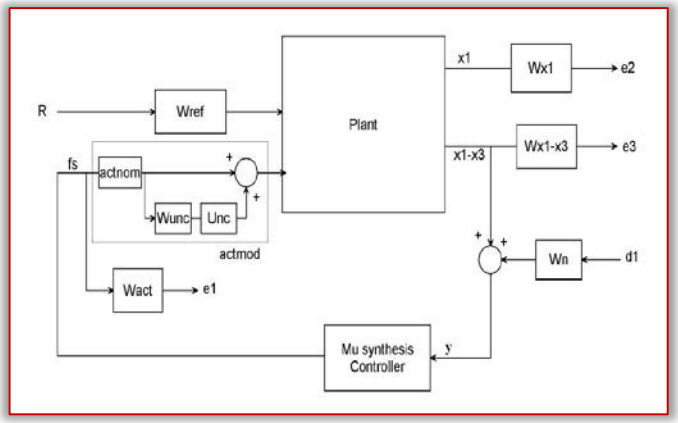

Figure 6: Active suspension system with μ - synthesis controller system interconnections block diagram

The output or feedback signal y is

$$y = \left(\left(x_1 - x_3 \right) + d_1 \times W_n \right)$$

The nominal model for the hydraulic actuator is

$$actnom = \frac{s+2}{s^2 + 4s + 1}$$

We describe the actuator model error as a hard and fast of viable models using a weighting function due to the fact the actuator model itself is uncertain. The model uncertainty is represented through weight Wunc which corresponds to the frequency variant of the model uncertainty and the uncertain LTI dynamics object Unc that is

$$W_{unc} = \frac{5s + 15}{67s^2 + 16s + 1}$$

Unc =Uncertain LTI dynamics"unc"with 1 outputs,1 inputs, and gain less than 1

— LQR Controller

In order to overcome a few problems that confronted via PID controller, the opposite sort of control strategies may be evolved such as Linear-Quadratic Regulator (LQR) most beneficial control. LQR is a control system that offers the satisfactory viable performance with recognize to some given measure of overall performance. The overall performance degree is a quadratic function composed of state vector and control input.

Linear Quadratic Regulator (LQR) is the most effective idea of pole placement technique. LQR set of rules defines the optimal pole location based on two cost function. To discover the optimal gains, one must outline the optimal performance index first off after which resolve algebraic Riccati equation. LQR does now not have any specific solution to outline the cost function to gain the most suitable gains and the cost function must be defined in iterative manner.

LQR is a control scheme that gives the high-quality viable overall performance with respect to a few given degree of performance. The LQR design hassle is to design a state feedback controller K such that the objective function J is minimized. In this technique a feedback gain matrix is designed which minimizes the objective function a good way to gain some compromise among the usage of control effort, the magnitude, and the speed of response on the way to assure a stable system. For a continuous-time linear system defined by means of

$$\dot{x} = Ax + Bu \qquad (3)$$

With a cost functional defined as

$$J = \int \left(x^T Q x + u^T R u \right) dt \qquad (4)$$

Where Q and R are the weight matrices, Q is required to be positive definite or positive semi-definite symmetry matrix. R is required to be positive definite symmetry matrix. One practical method is to Q and R to be diagonal matrix. The value of the factors in Q and R is associated with its contribution to the cost function J. The comments control law that minimizes the value of the cost is:

$$u = -Kx \qquad (5)$$

K is given by

$$K = R^{-1} B^T P \qquad (6)$$

And P can be located through solving the continuous time algebraic Riccati equation:

$$A^T P + PA - PBR^{-1} B^T P + Q = 0 \qquad (7)$$

The value of weighted matrix Q (state penalty) and R (control penalty) relies upon on designer. Designer pick the ideal cost of Q and R to locate an appropriate advantage matrix K the use of MATLAB. The State variable feedback configuration is shown below in Figure 7.

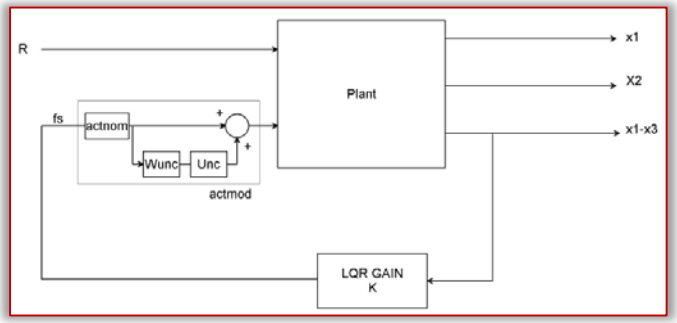

Figure 7: State variable feedback configuration

By taking

$$Q = \begin{bmatrix} 5 & 0 & 0 & 0 \\ 0 & 5 & 0 & 0 \\ 0 & 0 & 5 & 0 \\ 0 & 0 & 0 & 5 \end{bmatrix} \text{ And } R = \begin{bmatrix} 1 & 0 \\ 0 & 1 \end{bmatrix}$$

The value of obtained feedback gain matrix K of LQR is given by

$$K = \begin{bmatrix} -4.1189 & -0.1434 & 3.4141 & 0.2485 \\ -1.4657 & -0.0557 & 1.4983 & 0.0999 \end{bmatrix}$$

RESULT AND DISCUSSION: COMPARISON OF THE ACTIVE SUSPENSION SYSTEM WITH μ–SYNTHESIS AND LQR CONTROLLERS

The simulation outcomes for bump input road profile for suspension deflection, body acceleration and body travel is shown in Figure 8, Figure 9 and Figure 10 respectively.

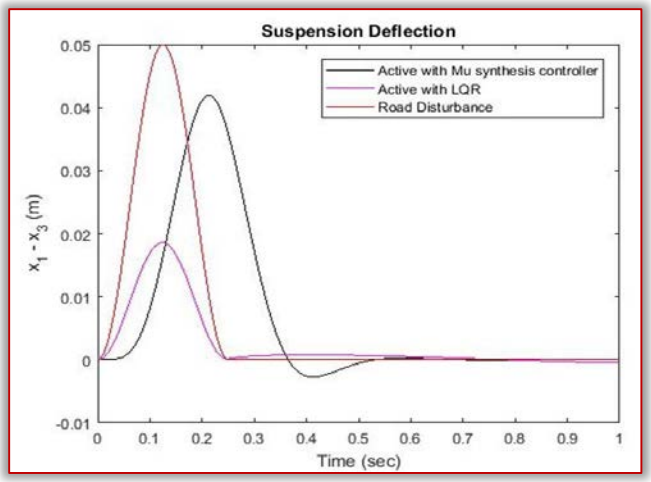

Figure 8: Suspension deflection for bump road disturbance

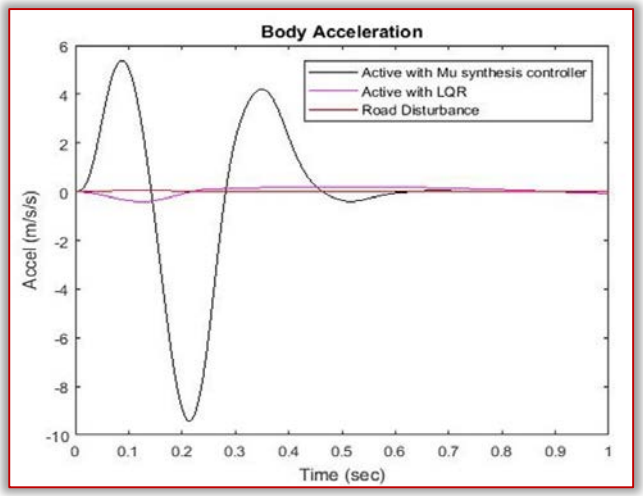

Figure 9: Body acceleration for bump road disturbance

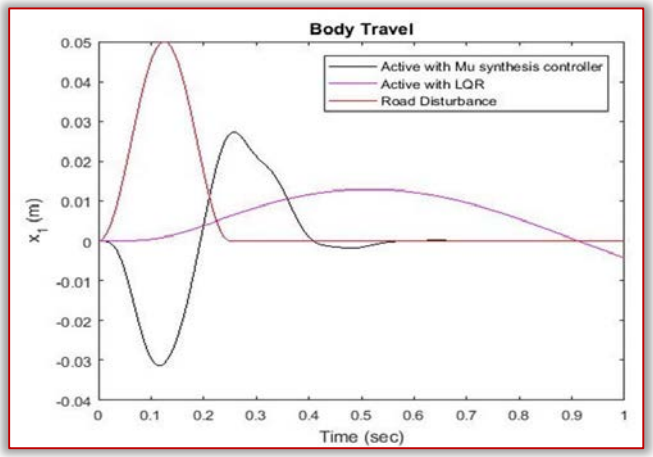

Figure 10: Body travel for Bump road disturbance

The simulation outcomes for random input road profile for suspension deflection, body acceleration and body travel is shown in Figure 11, Figure 12 and Figure 13 respectively.

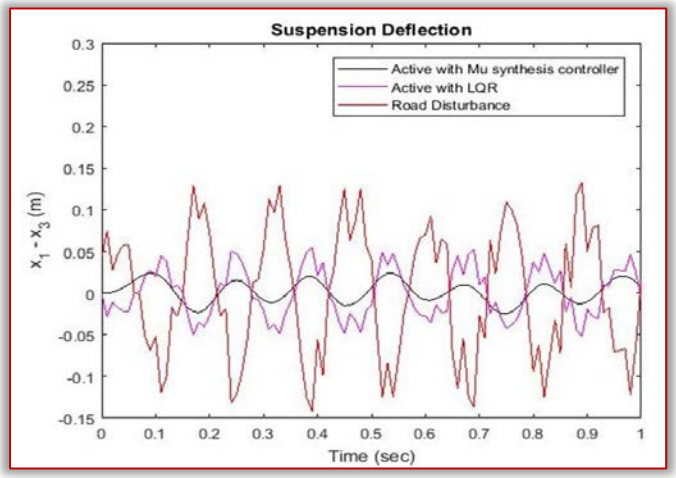

Figure 11: Suspension deflection for random road disturbance

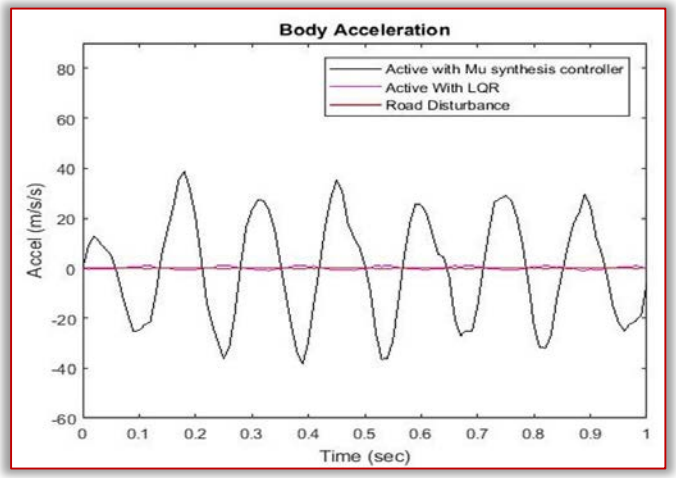

Figure 12: Body acceleration for random road disturbance

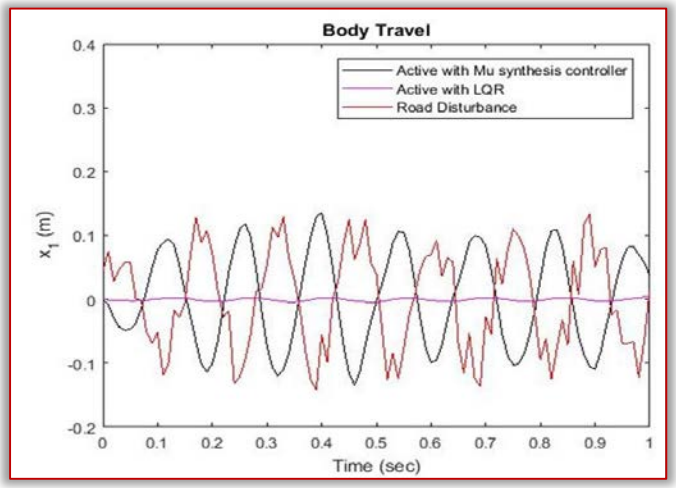

Figure 13: Body travel for random road disturbance

The simulation outcomes for sine pavement input road profile for suspension deflection, body acceleration and body travel is shown in Figure 14, Figure 15 and Figure 16 respectively.

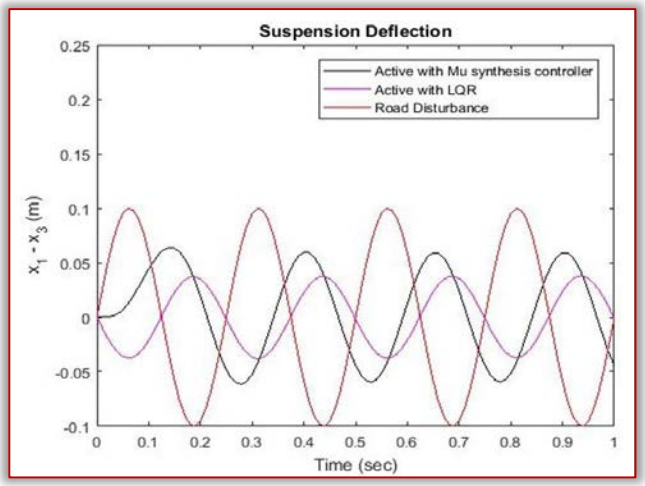

Figure 14: Suspension deflection for sine pavement road disturbance

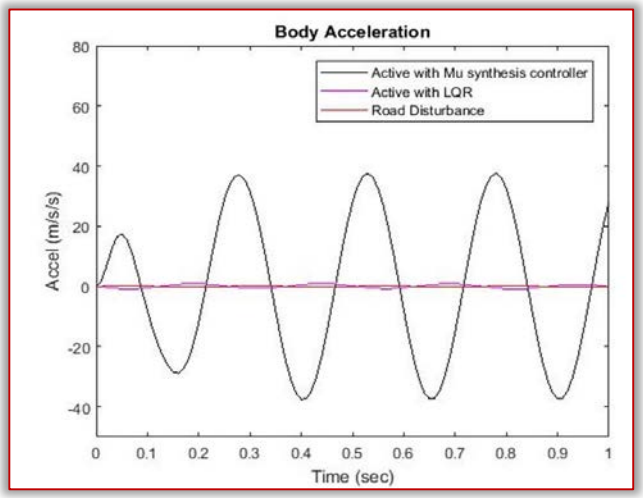

Figure 15: Body acceleration for sine pavement road disturbance

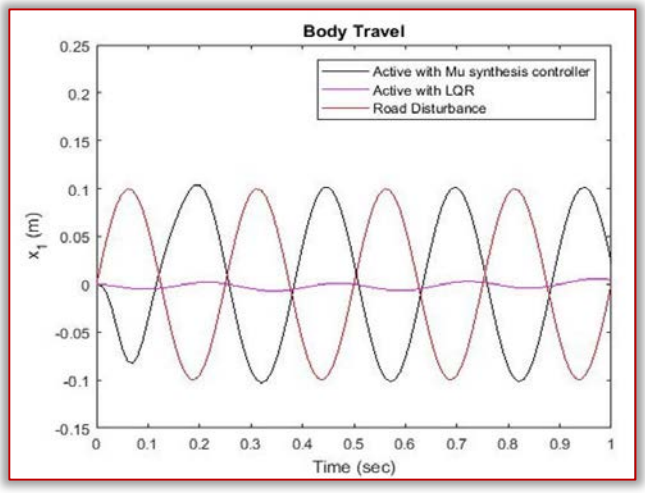

Figure 16: Body travel for sine pavement road disturbance

The simulation outcomes for white noise input road profile for suspension deflection, body acceleration and body travel is shown in Figure 17, Figure 18 and Figure 19 respectively.

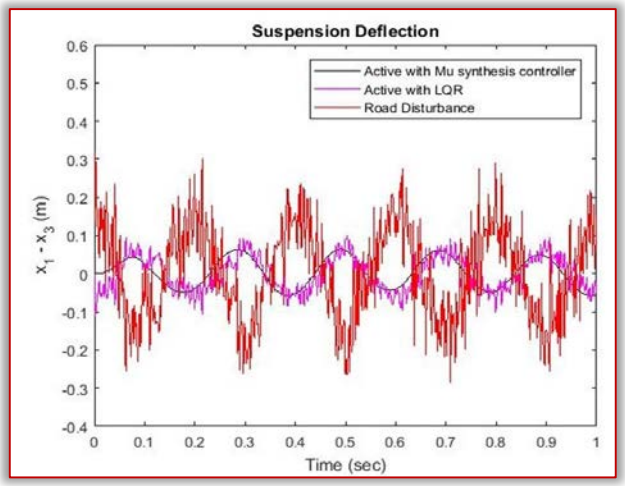

Figure 17: Suspension deflection for white noise road disturbance

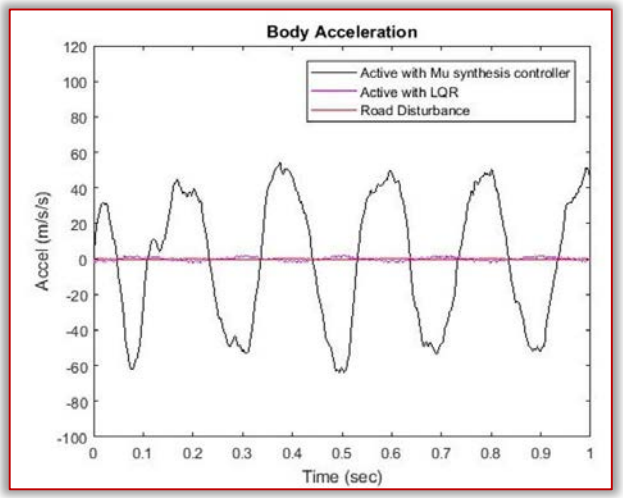

Figure 18: Body acceleration for white noise road disturbance

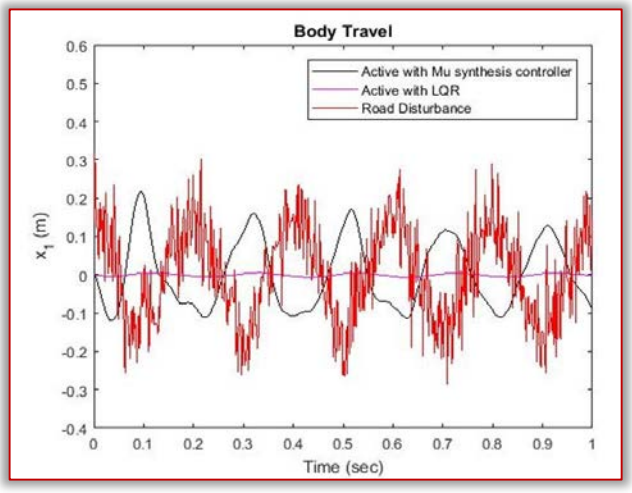

Figure 19: Body travel for white noise road disturbance

In the suspension deflection for the 4 road input profiles, Figure 8, Figure 14 and Figure 17 suggests that the active suspension system with μ-synthesis controller has the excellent overall performance and

Figure 11 suggests the active suspension system with LQR controller has the best performance.

In the body acceleration all of the simulation shows that the active suspension system with LQR controller has the best overall performance.

In the body travel all the four simulation indicates that the active suspension system with μ–synthesis controller has the best performance. From all of the simulation results, we conclude that the active suspension system with μ–synthesis controller has the best overall performance over the active suspension system with LQR controller.

CONCLUSION

In this paper, optimal control and robust control have been successfully designed (μ–synthesis and LQR controllers) using Matlab/Script program using time domain analysis using a control targets suspension deflection, body acceleration and body travel for a bump, random, sine pavement and white noise road profiles.

Finally, the simulation results prove the effectiveness of the active suspension system with μ–synthesis controller for improving the passenger ride comfort and road handling criteria for the suspension system.

Acknowledgment

First and formost, I would like to express my deepest thanks and gratitude to Dr.Parashante and Mr.Tesfabirhan for their invaluable advices, encouragement, continuous guidance and caring support during my journal preparation.

Last but not least, I am always indebted to my brother, Taha Jibril, my sister, Nejat Jibril and my family members for their endless support and love throughout these years. They gave me additional motivation and determination during my journal preparation.

References

[1] Sairoel Amertet "Design of Optimal Linear Quadratic Regulator (LQR) Control for Full Car Active Suspension System Using Reduced Order "National Academic Digital Respiratory of Ethiopia, 2019.

[2] Julian Asenov Genov et.al "A Linear Quadratic Regulator synthesis for a semi-active Vehicle Suspension Part-2 Multi-Objective Synthesis" AIP Conference Proceedings 2172, 110007, 2019.

[3] Haijing Yan et.al "The Optimal Control of Semi-active Suspension based on Improved Particle Swarm Optimization" Mathimatical Models in Engineering, Vol. 4 Issue 3, p.157-163, 2018.

[4] I.A Daniyan et.al "Design and Simulation of a Controller for an Active Suspension System of a Rail Car" Journal of Cogent Engineering, 2018.

[5] Satyanarayana et.al "Parameters Optimisation of Vehicle Suspension System for Better Ride Comfort" International Journal of Vehicle Performance, Vol.4 No.2, 2018.

[6] Jeng-Lang Wu "A Simultaneous Mixed LQR/H∞ Control Approach to the Design of Reliable Active Suspension System" Asian Journal of Control, March, 2017.

[7] Van Tan Vu "Using the LQR Control Method on the Active Suspension System of Automobiles" National Conference on Mechanics, 2017.

[8] Huan XIE, Hong-yan WANG and Qiang RUI "Research on Optimal Control Method of Active Suspension Based on AMEsim Modeling" 2017 2nd International Conference on Mechanical Control and Automation (ICMCA 2017), 2017.

[9] Fumiaki Yamada and Kohei Suzuki "Robust Control of Active Suspension to Improve Ride Comfort with Structural Constraints" IEEE Advanced Motion Control, Auckland New Zealand, April 22-24, 2016.

[10] Mohammed Jawad Aubad and Hatem Rahem Wasmi "A New Proposed Variable Stiffness of the Vehicle Suspension System Passive Case: I" Innovative Systems Design and Engineering www.iiste.org Vol.7, No.5, 2016.

[11] K. Dhananjay Rao and K. Pavani "Modelling and Vibration Control of Suspension System for Automobiles using LQR and PID Controllers" IJLTEMAS, Volume IV, Issue VIII, August 2015.

[12] B. Sepehri and A.Hemati "Active Suspension vibration control using Linear H-Infinity and optimal control" International Journal of Automotive Engineering Vol. 4, Number 3, Sept 2014.

[13] Md. Kaleemullah and Waleed F. Faris "Active Suspension Control of Vehicle with Uncertainties using Robust Controllers" Int. J. Vehicle Systems Modelling and Testing, Vol. 9, Nos. 3/4, 2014.

ACTA TECHNICA CORVINIENSIS – Bulletin of Engineering
ISSN: 2067-3809

[1.]S. KANNAPPAN, [2.]S. Aruna MASTANI

A SURVEY ON MULTI-OPERAND ADDER

[1-2.]Jawaharlal Nehru Technological University (JNTUA), Ananthapuramu, INDIA

Abstract: The processors are required to perform computationally intense operations in the modern data world and an Arithmetic Unit (AU) is the heart of the processor that contributes for its performance. It's an ever ending research to optimize the AU w.r.t. architecture area and latency for improving the performance of the processor. Adder forms the basic Building block of any AU, and in particular addition of multiple operands is required in complicated arithmetic operations like multiplication, convolution, Transforms etc. Hence existing circuits for efficient Multi-operand adder in terms of circuit area and delay are discussed. The Multi-Operand Adders is optimized in many ways; the most popular methods are discussed in brief with respect to their performance. Memory-based computing is becoming an important approach to achieve fastness and cost effectiveness in contrast to conventional logical approach, and Distributed Arithmetic (DA) is a process of replacing logic elements with small memories or LUTs to optimize the circuit complexity. This paper presents various methods of Multi-Operand Adders and various optimizations for Multi-Operand Addition.
Keywords: carry save adder, compressor, generalized parallel counter, adder tree

INTRODUCTION TO OPTIMIZATION OF ARITHMETIC COMPUTATIONS

The optimization of Arithmetic Units are started with the adder more particularly Multi-Operand Adder in case of computationally intense applications. Most of the Multi operand adder implementations are based on optimizing either compressor logic for reduction in partial sum or the optimization of tree structure for reducing the carry propagation. The existing techniques are effective for addition of less number of operands only. The Area and delay of the circuit increase linearly for addition of large number of operands. The addition of large operands was implemented using bit partition technique. In 1973, S. Singh and R. Waxman described a scheme for multiple operand addition and multiplication [16], applying the bit-partitioning technique for adding 'K' number of operands of N bits each. In this scheme each partition contains m-bits, where $m = \lceil \log_2(K-1) \rceil$. The final sum is obtained in $m + 1$ addition cycles; the overall delay depends on delay of addition cycle. It is inefficient for addition of large number of operands.

In the tree structured adder the delay is reduced but area increased with number of operands. In serial addition of multi operands the number of clock cycles (called Latency) increase with increase in number of operands so, the existing implementations of multi operand adders are not effective in optimizing area and delay for large number of operands. The various techniques of Multi-Operand Adders using Tree structure is discussed in Section II & III, the Multi-Operand Adder using Generalized Parallel Counters is discussed in Section-IV.

COMPRESSOR TREE STRUCTURE OF ADDERS

The Multi-Operand Adders are generally implemented in two methods i.e Array Adders and Adder Tree structure. In Array Adder structure, two operands are added and output is added with third operand and continues the chain of addition until to get final sum output. It requires 'K' number of adder levels for addition of 'K' operands. But in case of Adder Tree structure the number of levels to add 'K' operands is less than that of Array Adders. It groups 'K' number of operands into sets of two operands. All the sets are added parallel in one level. The sum outputs from first level again grouped into sets of two operands and perform addition. This process continues until to get two operands and added in last level to obtain final sum. In each level it reduces number of operands to half. Therefore it requires $\log_2 K$ levels. The Adder Tree structure is faster than Adder Array structure with same resources consumed by both configurations. But the Array Adder is having regular routing than Adder Tree structure.

The Ripple Carry Adder (RCA) or Carry Look Ahead Adder (CLA) are two general Carry Propagate Adders used in the above methods i.e. Array Adder, Adder Tree is Carry Propagate Adder. The delay of their CPA depends on bit length of operand. For N-bit operand the of RCA proportional to N and for CLA it is proportional to$\log_2 N$. To reduce the delay these adders where implemented on FPGA by using dedicated carry chains [8]. The RCA on FPGA using fast carry chain is simpler than any other CPA topologies at an expense of high hardware cost [9]. The pipelining technique can be applied more effectively RCA [1]. The delay of Adder Tree using CPA is high due to carry propagation along the bit length.

Carry Save Adder tree is used as another approach for implementing Multi-Operand Adders. Here the carry is directly propagated to next level instead of propagating in the same as in case of CPA. The advantage of Carry Save Adder (CSA) tree is utilized in ASIC implementation due to flexible routing. The critical path delay can be minimized by optimizing the interconnection between Full Adders. But to implement on FPGA the Ripple Carry Adder tree is

preferred than CSA adder tree. When CSA tree is implemented on FPGA it become slower than RCA tree due to routing delay of CSA. However, a straightforward implementation on FPGAs [6] roughly requires double hardware than a carry-ripple adder, and does not exploit the fast carry chain to improve speed. This was partially solved by the compressors which compress the operands more than CSA tree [5], [7].

In 2005, R. D Kenney et al. [10] introduced and analyzed three techniques for performing fast operands addition [10]. Multi-operand adder designs are constructed and synthesized for 6 to 12 input operands. In 2005, J. Villalba et al. have studied the on–line addition of multiple operands for conventional, carry–save (CS) and/or Signed–Digit (SD) numbers [11]. They have proposed a new and key element called on-line Full Adder which is used in CSA tree to perform Multi-Operand Addition serially. The on-line Full Adder contains a 1-bit delay register at the sum bit output of FA. An external delay element also inserted at every skipped level in tree structure to maintain proper timing. The on-line Full Adder is used to reduce the hardware resources and cycle time.

In 2009, Manuel Ortiz et al. [12] have implemented 3:2 and 4:2 compressors using Dedicated carry chain in FPGA. When more than three operands are to be added the 4:2 compressors is preferred because it fully utilizes the logic of the slice and achieves high speed than 3:2 compressor with same resources. In 2009, William Kamp et al. [13] has implemented the basic 3:2 and 4:2 compressors using dedicated carry chain for redundant numbers to eliminate carry propagation. So that the delay is maintained nearly constant even for large operand width targeting low cost FPGAs.

In 2013 J. Harmigo et al. [14] was proposed a complete compressor tree using the dedicated fast carry chain unlike basic compressors developed in [12], [13]. They developed a linear array of carry save adder by mapping to preceding stages of FAs to conventional Ripple Carry Adders (RCA) or ternary adders. The delay is much smaller with equivalent resources compared to Adder Tree using RCA. Due to shorter carry chain it would be fastest choice for combinatorial multiple operand adders but it is inefficient as it is has irregular shaped compressor trees.

WALLACE TREE ADDER

In 2017, S.D. Thabah et al. [15] have analyzed different types of Multi-Operand adders in terms of propagation delay, power consumption and resource utilization. From the synthesis reports they have concluded that Wallace Tree Adders are the high speed and less power consuming circuit.

Even though the Carry Save Adder tree based on Carry Propagate Adders provide easy for implementation, Wallace tree adder is an efficient architecture for implementing Multi-Operand Adder tree which gives lowest propagation delay and least power consumption compared to other implementations even for increasing number of operands and bit size. However Wallace tree architecture is not a regular structure so, for large number of operands the circuit complexity increases along with routing Delay.

MULTI-OPERAND ADDERS USING GENERALIZED PARALLEL COUNTERS

The concept of using Compressor trees has a history in the design of arithmetic units for microcomputers since 1964. C. Wallace has proposed a compressor tree structure called Wallace tree [17] to optimize the multiplier, and L. Dadda in 1965 has given with the concept of counting number of ones in a column of binary bits by a tree structure called Dadda tree [18]. The concept of compressor is to avoid the slow carry propagation by passing the carry to the next compressor stage instead of propagating it within the same stage, which guarantees speed-up in Application Specific Integrated Circuits (ASICs) or custom ICs. The carry save arithmetic is not suitable for implementation on FPGA for a long time. As the CSA tree has large routing so that it become slower on FPGA because the dedicated carry chains available in modern FPGAs which are significantly faster than FPGA's routing fabric. However, compressors are implemented using dedicated carry chains as discussed in the previous sections it was first shown by Parandeh-Afshar et al. [7] in 2008 that a significant delay improvement can be obtained by using compressor trees on FPGAs by using the concept so called Generalized Parallel Counters (GPCs). The Multi-Operand Adder using GPCs provide a better utilization of the look-up tables (LUTs). They achieved delay reductions of about 30% while having a slight resource overhead of 5%. However, the design of the compressor tree is much more complex compared to the simple classic algorithms from Dadda [18] or Bickerstaff [21]. They provided a heuristic [7] as well as an exact integer linear programming (ILP) method [20].

In 2015, Burhan Khurshid et al. [22], implemented Generalized Parallel Counter (GPC) on Look up Tables. The Generalized Parallel Counters (GPCs) are used in constructing high speed compressor trees along with specialized fast carry chain in existing methods. The fast carry chain is eliminated from the previous existing GPC structure and has focused on achieving efficient mapping of GPCs on FPGAs by using only general Look-up table (LUT) fabric. The resulting structures are purely combinational and cannot be efficiently pipelined to achieve the potential FPGA performance. So the delay cannot be optimized for large number of operands.

In 2018 Martin Kumm et al. [25] was developed "Advanced compressor Tree Synthesis for FPGA" in which it proposed to combine Improved Generalized Parallel Counters and Integer Linear Programming to optimize the delay and resource utilization. The improved GPC is a combination of GPC for column compression and a 4:2 row compressor. This gives a better result in terms of delay and resource utilization. Therefore many approaches for Multi-Operand Adder were proposed in literature on Column compressor for counting one's in a column of bits, Generalized Parallel Counters (GPCs) also called multicolumn counters (different weighted column bits), which are also mapped with LUT's and some row compressor i.e 4:2 (four binary numbers reduced to two binary numbers) and optimization algorithms (Integer Linear Programming) for compressors.

CONCLUSIONS

For adding large number of operands, the Multi-Operand Adder using carry save arithmetic require more delay and complex hardware. Carry save addition is a row wise addition. To optimize area and delay column wise addition i.e compressors is an alternative approach. These compressors are generalized as Generalized Parallel Counters (GPC's) to add multiple operands in parallel. But choosing required number of GPC's and optimizing these GPC's is an overhead. Many optimization algorithms were combined with GPC's for better performance. And also these GPC's are combined with FPGA carry chain logic for efficient implementation on FPGA devices. Some of the techniques are combination of row compressors and mapping of GPC's on Look Up Tables in FPGA with optimization algorithms. In the recent techniques Distributed Arithmetic is adopted for implementing multi-Operand Addition in Filters where small distributed memory elements are used to store pre-computed values and achieving required value with additional hardware. These memory based implementations are well suited for both ASIC as well as FPGA. In future, Artificial Intelligence (AI) will become necessary for most the applications in the modern word. The AI requires a large number of calculations, mappings with less time as well as with smaller circuit chips. Memory based computing will become a choice for deep learning and Machine learning in AI.

References

[1] S. Yu and E. E. Swartzlander, "DCT implementation with distributed arithmetic", IEEE Transactions on Computers, vol. 50, no. 9, pp. 985–991, Sept. 2001.
[2] T.-S. Chang, C. Chen, and C.-W. Jen, "New distributed arithmetic algorithm and its application to IDCT," IEE Proceedings Circuits, Devices and Systems, vol. 146, no. 4, pp. 159–163, Aug. 1999.
[3] T.-S. Chang and C.-W. Jen, "Hardware-efficient implementations for discrete function transforms using LUT-based FPGAs," IEE Proceedings Circuits, Devices and Systems, vol.146, no. 6, pp. 309–315, Nov. 1999.
[4] F. de Dinechin, H. D. Nguyen and B. Pasca, Pipelined FPGA Adders, LIP Research Report no. ensl-00475780, Apr. 2010.
[5] J. Hormigo, M. Ortiz, F. Quiles, F. J. Jaime, J. Villalba and E.L. Zapata, Efficient Implementation of Carry-Save Adders in FPGAs, 20th IEEE international Conference on Application-Specific Systems, Architectures and Processors, pp. 207–210, Jul. 2009.
[6] P. M. Martinez, V. Javier, and B. Eduardo, On the design of FPGA-based Multioperand Pipeline Adders, XII Design of Circuits and Integrated System Conference, 1997.
[7] H. Parandeh-Afshar, P. Brisk, and P. Ienne, "Efficient Synthesis of Compressor Trees on FPGAs," in Asia and South Pacific Design Automation Conference (ASPDAC). IEEE, 2008, pp. 138–143.
[8] Xilinx Inc., Virtex-6 User Guide, 2009, http://www.xilinx.com/.
[9] S. Xing and W. H. Yu, FPGA Adders: Performance Evaluation and Optimal Design, IEEE Design and Test of Computers, vol. 15, no. 1, pp. 24–29, Jan.- Mar. 1998.
[10] R. D. Kenney and M. J. Schulte, "High-Speed Multioperand Decimal Adders", IEEE Transactions on Computers, vol. 54, no. 8, pp. 953-963, Aug. 2005.
[11] J. Villalba, J. Hormigo, J. M. Prades and E. L. Zapata, "On–line Multioperand Addition Based on On–line Full Adders*", in Proc. Int. Conf. on Application-Specific Systems, Architecture Processors (ASAP'05), pp. 322-327, 2005
[12] M. Ortiz, F. Quiles, J. Hormigo, F. J. Jaime, J. Villalba, and E. L. Zapata, "Efficient Implementation of Carry-Save Adders in FPGAs," in IEEE International Conference on Application-specific Systems Architectures and Processors (ASAP), 2009, pp. 207–210.
[13] W. Kamp, A. Bainbridge-Smith, and M. Hayes, "Efficient Implementation of Fast Redundant Number Adders for Long Word- Lengths in FPGAs," in 2009 International Conference on Field- Programmable Technology (FPT). IEEE, 2009, pp. 239–246.
[14] J. Hormigo, J. Villalba, and E. L. Zapata, "Multioperand Redundant Adders on FPGAs," submitted to IEEE Transactions on Computers, vol. 62, no. 10, pp. 2013– 2025, 2013.
[15] S. D. Thabah; M. Sonowal and P. Saha ,"EXPERIMENTAL STUDIES ON MULTI-OPERAND ADDERS", INTERNATIONAL JOURNAL ON SMART SENSING AND INTELLIGENT SYSTEMS VOL. 10, NO. 2, JUNE 2017
[16] S. Singh and D. Waxman, "Multiple Operand Addition and Multiplication", IEEE Transactions on Computers, vol. C-22, no. 2, pp. 113-120, Feb. 1973.
[17] C. Wallace, "A Suggestion for a Fast Multiplier," IEEE Transactions on Electronic Computers, no. 1, pp. 14–17, 1964.
[18] L. Dadda, "Some Schemes For Parallel Multipliers," Alta Frequenza, vol. 45, no. 5, pp. 349–356, 1965.

[19] A. Omondi and B. Premkumar, Residue Number Systems: Theory and Implementation. Imperial College Press, 2007.
[20] A. R. Meo, "Arithmetic Networks and Their Minimization Using a New Line of Elementary Units," submitted to IEEE Transactions on Computers and currently under review, vol. C-24, no. 3, pp. 258–280, 1975.
[21] K.A.C. Bickerstaff, M. Schulte, and E.E. Swartzlander, "Reduced area multipliers," in Application-Specific Array Processors, 1993
[22] Suhas B. Shirol, S. Ramakrishna and Rajashekar B. Shettar, "Design and Implementation of Adders and Multiplier in FPGA Using ChipScope: A Performance Improvement", Information and Communication Technology for Competitive Strategies pp 11-19, 31 August 2018
[23] Duncan J. M. Moss , David Boland, and Philip H. W. Leong, "A Two-Speed, Radix-4, Serial–Parallel Multiplier", IEEE TRANSACTIONS ON VERY LARGE SCALE INTEGRATION (VLSI) SYSTEMS, (Volume: 27 , Issue: 4 , April 2019) Page no. 769 – 777.
[24] Martin Kumm and Johannes Kappauf." Advanced Compressor Tree Synthesis for FPGAs", IEEE Transactions on Computers (Volume: 67 , Issue: 8 , Aug. 1 2018).

ACTA TECHNICA CORVINIENSIS – Bulletin of Engineering
ISSN: 2067-3809

[1.]Suresh Kumar GOVINDARAJAN, [2.]Abhishek KUMAR

DARCY BASED PERMEABILITY IN A PETROLEUM RESERVOIR BEFORE AND AFTER WATER-FLOODING: WHAT DOES IT DEPEND ON?

[1-2.]Reservoir Simulation Laboratory, Petroleum Engineering Programme, Department of Ocean Engineering, Indian Institute of Technology – Madras, Chennai, INDIA

Abstract: A sound knowledge on the estimation of reservoir permeability becomes fundamental for a precise prediction of production forecasts. The problem becomes further complex for multi-phase fluid flow as observed in a petroleum reservoir. Thus, estimating the magnitude of effective/relative permeability remains very challenging in the context of multi-phase fluid flow. Even in a relatively homogeneous sandstone reservoir, the concept of relative/effective permeability becomes very complex. In the present paper, an attempt has been made in order to discuss the sensitive factors that alter the magnitude of effective/relative permeabilities in a petroleum reservoir between the transition period namely 'at the end of primary recovery' and "during water-flooding'. It has been proposed that the 'pressure' in addition to rock and fluid properties will dictate the resulting effective/relative permeability even in the absence of considering the geo-mechanical aspects of the reservoir. The study is further extended to consider the concept of effective/relative permeabilities in a fractured reservoir. It is proposed that the intensity of the coupling between fracture and rock-matrix will significantly influence the resulting effective/relative permeabilities of oil and water within the fracture and rock-matrix, while the fracture relative permeability will become a complex non-linear function of water-saturation.
Keywords: Effective permeability; Relative permeability; Petroleum reservoir; Fracture; Rock-matrix

INTRODUCTION

Permeability along with porosity forms the fundamental reservoir unit. In reality, the magnitude of single-phase absolute permeability has been characterized by log-normal distribution as against the normal distribution meant for porosity. The extended version of Darcy's law that describes the multi-phase fluid flow through a porous medium is given in equations (1) and (2) for liquids and gases respectively.

$$\text{Darcy flux} = (\text{Volumetric flow rate} / \text{Area}) = (1/\text{Dynamic viscosity})\ (\text{Absolute permeability} \times \text{Relative permeability})\ (\text{Pressure gradient}) \quad (1)$$

$$\text{Darcy flux} = (\text{Volumetric flow rate @ mean pressure} / \text{Area}) = (1/\text{Dynamic viscosity})\ (\text{Absolute permeability} \times \text{Relative permeability})\ (\text{Pressure gradient}) \quad (2)$$

For gases, the absolute permeability calculated using Darcy's extension will be larger than the actual absolute permeability and for such cases, slip factor comes into the picture, which is associated with the Klinkenberg effect. The slip factor may be obtained from the values of gas permeability and the reciprocal of average pressure. Relative permeabilities can be generally estimated from Corey curves for a relatively homogeneous porous medium.

The purpose of the present work is to analyze whether the relative/effective permeability of a given geological formation (in a petroleum reservoir) remains constant during primary and secondary recovery or not. If there is a variation in the magnitude of relative/effective permeabilities between primary and secondary recovery, then, what exactly quantifies the resulting permeability. The present work does not the geo-mechanical aspects of a petroleum reservoir. The work is also extended to understand the complexities associated with the estimation of effective/relative permeabilities of a fractured reservoir.

PERMEABILITY IN A PETROLEUM RESERVOIR

A petroleum reservoir represents a geological formation that is completely/fully saturated with the multi-phase fluids that include hydrocarbons (oil and/or gas) along with the formation water [1]. In addition, a petroleum reservoir is supposed to store as well as transmit these hydrocarbons under the confined conditions using the natural energy available within the reservoir (primary hydrocarbon recovery). It should be clearly noted that the reservoir becomes incapable of transmitting significant quantities of oil and/or gas at the end of primary oil recovery, despite, still having significant storage of residual hydrocarbons. Thus, at the end of the primary recovery, a petroleum reservoir replicates a geological formation that is similar to an impervious formation (like clay, having significant storage in the absence of significant transmissivity/ permeability/hydraulic-conductivity). In other words, the relative permeability to oil/gas and water at the end of primary recovery is nearly zero/insignificant; and hence, a secondary recovery method (water/gas flooding) and/or a tertiary recovery method (thermal/chemical/microbial EOR) is applied in order to extract the residual/left hydrocarbons, where the relative permeability, and in turn, the mobility; and subsequently, the production of the concerned multi-phase fluids (oil & gas) gets enhanced. At this point, it is interesting to note that the term 'intrinsic permeability' (or single-phase

'absolute permeability') is a function of rock property alone; and it does not depend on fluid properties at all (unlike 'hydraulic conductivity'). Thus, since, 'intrinsic permeability' is a function of 'rock property' alone, we will not be able to bring in the concept of "hydraulic gradient' (for single-phase fluid flow) or 'pressure gradient' (for multi-phase fluid flow) into the picture. However, it can be clearly understood that the magnitude of 'pressure gradient' becomes insignificant or the same tends to approach zero; and hence, the fluid (oil or gas) ceases to flow within the reservoir; and subsequently, there is no fluid flow towards the production well at the end of primary recovery. Now, the depleted pressure of the reservoir is enhanced 'externally' (and not naturally) by means of secondary recovery (water or gas flooding) technique. By external injection of water and/or gas, the relative/effective permeability of the reservoir fluids is increased; and this results in an improved oil/gas production. And, this sequence of events clearly tells us that the 'effective/relative permeability' associated with the oil, gas and water flow of a petroleum reservoir has indirectly become a function of 'reservoir pressure' as well in addition to its dependence on rock and fluid properties. Strictly speaking, 'intrinsic permeability' is no more a function of fluid for Darcy's law to be valid. On top of it, in a typical petroleum reservoir, the 'relative/effective permeability' becomes a function of 'reservoir pressure'.

DEPENDENCE OF PERMEABILITY

Permeability in a petroleum reservoir has several complexities; and as a result, quantifying permeability has become more and more approximated without solid fundamental theory. In this paper, the author has made an attempt to raise some of the fundamental queries that would help to better understand the dependence of permeability in a typical petroleum reservoir.

(a) Whether the single-phase 'absolute permeability' of the same reservoir has undergone a significant transformation during the periods between 'the end of primary recovery' and 'during secondary/tertiary recovery'?
(b) Whether the pore geometry of the reservoir gets restructured; and in turn, the nature of the 'connected interstices' gets modified during this transition period?
(c) What exactly caused the changes in the magnitude of the relative permeabilities of oil, gas, and water, during the periods between 'the end of primary recovery' and 'during secondary/tertiary recovery'?
(d) Whether Darcy's law accommodates such changes in permeability resulting from the factors that are beyond 'the continuity of the fluid migration by means of well-connected pores'? If so, under what conditions?
(e) If the 'relative/effective permeability' becomes a function of 'pressure'; what does it pertain to? Is it Oil pressure or Gas pressure or Water pressure or Average Reservoir Pressure? If it is 'Average Reservoir Pressure', then, how will it be feasible to provide a link/upscaling between local-scale oil/gas/water pressure to the Darcy-scale 'average reservoir pressure'?
(f) For Darcy's law to be valid, the fluid flow within the reservoir should be essentially 'horizontal'. Under such conditions, the one-dimensional fluid flow essentially indicates the ability of the reservoir to transmit oil, water and/or gas through its entire thickness called the 'reservoir transmissivity'. For a one-dimensional problem, the 'entire thickness' of the reservoir becomes 'a single point' on a single line. If so, how come, the 'permeability' associated with a 'petroleum reservoir' becomes a function of different 'fluids' as well?
(g) The storativity of a petroleum reservoir provides the correlation between the changes in the quantity of oil, water and/or gas stored within the reservoir and its associated changes in the elevations of the 'piezometric surface'. The storativity of a petroleum reservoir should represent the volume of the pore fluids (oil, water and/or gas) released from or added to a vertical column of a reservoir of unit horizontal cross-section, per unit of decline or rise of the piezometric head. However, in a petroleum reservoir, during water flooding, there will be an addition of water only in the absence of adding oil and/or gas. If so, how exactly, can we quantify the concept of 'storativity' associated with an oil reservoir? Further, whether 'storativity' has any correlation with the 'permeability' during the transition period? Because, it should be clearly noted that the storativity of a petroleum reservoir is caused by the compressibility of oil, water and/or gas; and also, by the elastic properties of the bulk reservoir.

PERMEABILITY IN A FRACTURED CARBONATE RESERVOIR

Fluid flow through a fractured reservoir is modelled using multiple continuum as the fundamental entities associated with a fractured reservoir namely fracture and rock-matrix have completely varying reservoir properties. In other words, the concept of the single continuum cannot be applied for a fractured reservoir as it violates the fundamental principle of calculus, which says that the spatial distribution of primary dependent variables and parameters (constant/ varying coefficients) should vary smooth and continuous. However, in a fractured reservoir, the porosity and permeability vary by orders of magnitude at the interface between high-permeable

fracture and low-permeable rock-matrix. And, for this reason, a fractured reservoir is generally modelled using a dual continuum approach, where fracture and rock-matrix are treated as separate continuum, while a coupling term at the fracture-matrix interface ensures the continuity of the fluid mass fluxes ([2-32]). On the other hand, deducing the average permeability value for the entire reservoir as a function fracture and rock-matrix permeability would not be correct; and thus, the concept of Equivalent Porous Medium (EPM) should be handled with utmost care, even for a single-phase fluid flow. Now, for multi-phase fluid flow in a fractured carbonate reservoir, the concept of relative/effective permeability becomes far more complex for the following reasons:

(a) For an oil-water system, any fractured reservoir has the following permeabilities: fracture-permeability; matrix-permeability; effective-permeability of the bulk reservoir; effective-permeability of oil in the matrix; effective-permeability of water in the matrix; effective-permeability of oil in fracture; and effective-permeability of water in fracture. It is not easy to determine the magnitude of all these permeability values. On top of it, how exactly to compute the value of interfacial tension and the maximum capillary pressure for this oil-water system? Since, the recovery factor in a fractured reservoir depends on the magnitude of effective-permeabilities of both fracture and matrix, the estimation of these permeability values deserves special attention.

(b) Estimating the ratio between the effective permeabilities of water and oil against the water saturation remains completely different when the fractured reservoir is treated either as a single or multi-continuum. On top of it, the extent of weathering of rocks, the fracture density, the fracture spacing, the fracture orientation, the fracture length dictates the resultant ratio between the effective permeabilities of water and oil as well as the water saturation. In the absence of all these data, characterizing multiphase fluid flow using the concept of effective/relative permeability would remain highly approximate.

(c) Considering the influence of saturation endpoints within a fracture gets seriously affected by the fracture wall geometry; and hence, the fracture relative permeability becomes a complex non-linear function of water-saturation.

(d) Based on the thickness of the fracture aperture, the rate of fluid mass transfer, i.e., the intensity of coupling between fracture and matrix will vary. For example, when the thickness of the fracture aperture is closer to 10 microns, the intensity of coupling will be very high, while for a 1000 micron and greater aperture thickness, the intensity of coupling between fracture and matrix will be very low. Thus, the intensity of the coupling between the high-permeable fracture and low-permeable rock-matrix significantly influences the resulting effective permeabilities of oil and water within the fracture and rock-matrix.

CONCLUSIONS

The following conclusions have been drawn from the present study.

1. There is no clarity in defining the term 'permeability' associated with a typical petroleum reservoir as in petroleum engineering, neither the term 'intrinsic permeability' nor the term 'hydraulic conductivity' is used.
2. Permeability associated with a petroleum reservoir seems to depend on 'reservoir pressure' as well in addition to the rock and fluid properties during the transition period between 'the end of primary recovery' and 'during secondary/tertiary recovery'.
3. It is concluded that the magnitude of storativity before and after water flooding may be completely different as the storativity of a petroleum reservoir is caused by the compressibilities of oil, water and/or gas, along with the elastic properties of the bulk reservoir. This variation in storativity values before and after water flooding may indirectly influence the resulting reservoir permeability.
4. It is concluded that the estimation of effective permeabilities of oil and water in high-permeable fracture and the low-permeable matrix also depend on the extent of weathering of rocks, the fracture density, the fracture spacing, the fracture orientation, and the fracture length.

References

[1] Bear J. (1972). Dynamics of fluids in porous media. American Elsevier Publishers, New York

[2] Ghassemi, A., and G. Suresh Kumar. (2007) "Changes in fracture aperture and fluid pressure due to thermal stress and silica dissolution/precipitation induced by heat extraction from subsurface rocks". Geothermics, v. 36(2), pp. 115-140

[3] Natarajan, N., and G. Suresh Kumar. (2010) "Radionuclide and colloid co transport in a coupled fracture-skin-matrix system". Colloids and Surfaces A: Physicochemical and Engineering Aspects, vol. 370(1-3), pp. 49-57

[4] Natarajan, N., and G. Suresh Kumar. (2011) "Numerical Modeling of Bacteria Facilitated Contaminant Transport in Fractured Porous Media". Colloids and Surfaces A: Physicochemical and Engineering Aspects, vol. 387(1-3), pp. 104-112

[5] Natarajan. N., and G. Suresh Kumar. (2012). "Effect of Fracture-Skin on Virus Transport in Fractured Porous Media". Geoscience Frontiers, vol. 3(6), pp. 893-900

[6] Natarajan. N., and G. Suresh Kumar. (2014). "Lower order spatial moments for colloidal transport in a

fracture-matrix coupled system". ISH Journal of Hydraulic Engineering, vol. 20(2), pp. 200-211
[7] Natarajan, N., and G. Suresh Kumar. (2015). Numerical Modeling and Spatial Moment Analysis of Solute Transport with Langmuir Sorption in a Fracture Matrix Coupled System. ISH Journal of Hydraulic Engineering, vol. 21(1)., pp. 28-41
[8] Natarajan, N., and G. Suresh Kumar. (2016). "Spatial Moment Analysis of Solute Transport with Langmuir Sorption in a Fracture-Skin-Matrix Coupled System". Journal of King Saud University: Engineering Sciences
[9] Nikhil, B, L., and G. Suresh Kumar. (2015). "Effect of Non-Linear Sorption on Multispecies Radionuclide Transport in Fracture-Matrix System with Variable Fracture Aperture: A Numerical Study". ISH Journal of Hydraulic Engineering, vol. 21(3), pp. 242-254
[10] Nikhil, B, L., and G. Suresh Kumar. (2017). "Effect of Random Fracture Aperture on the Transport of Colloids in a Coupled Fracture-Matrix System". Geosciences Journal, vol. 21(1), pp. 55-69
[11] Rakesh T V., and G. Suresh Kumar. (2016). "Numerical Modeling on the Sensitivity of Directional Dependent Interface Heat Transfer on Thermal Transport in a Coupled Fracture-Matrix System". Geosciences Journal, vol. 20(5)., pp. 639-647
[12] Renu, V. and Suresh Kumar, G. (2012). "Numerical Modeling and Spatial Moment Analysis of Solute Mobility and Spreading in a Coupled Fracture-Skin-Matrix System". Geotechnical and Geological Engineering, vol. 30(6), pp. 1289-1302
[13] Renu, V., and G Suresh Kumar. (2014). "Temporal Moment Analysis of Solute Transport in a Coupled Fracture-Skin-Matrix System" Sadhana – Academy proceedings in Engineering Sciences, vol. 39(2), pp. 487-509
[14] Renu, V., and G Suresh Kumar. (2016). "Temporal Moment Analysis of Multi-Species Radionuclide Transport in a Coupled Fracture-Skin-Matrix System with a Variable Fracture Aperture". Environmental Modeling and Assessment, vol. 21(4)., pp. 547 – 562
[15] Renu V., and Suresh Kumar G. (2017). Benzene Dissolution and Transport in a Saturated Sinusoidal Fracture with non-uniform Flow: Numerical Investigation and Sensitivity Analysis. Environmental Processes, vol. 4(3)., pp. 587-601
[16] Renu V., and G. Suresh Kumar. (2018). "Mathematical Modeling on Mobility and Spreading of BTEX in a Discretely Fractured Aquifer System under the Coupled Effect of Dissolution, Sorption, and Biodegradation". Transport in Porous Media, vol. 123(2), pp. 421-452
[17] Renu Valsala and G. Suresh Kumar. (2019). "Co-colloidal BTEX and Microbial transport in a Saturated Porous System: Numerical Modeling and Sensitivity Analysis". Transport in Porous Media, vol. 127(2), pp. 269-294
[18] Sekhar M., and G. Suresh Kumar. (2006) "Modeling Transport of Linearly Sorbing Solutes in a Single Fracture: Asymptotic Behavior of Solute Velocity and Dispersivity". Geotechnical and Geological Engineering– Vol. 24(1), pp. 183-201
[19] Sekhar M., G. Suresh Kumar and D Mishra. (2006) "Numerical Modeling and Analysis of Solute Velocity and Macrodispersion for Linearly and Nonlinearly Sorbing Solutes in a Single Fracture with Matrix Diffusion". Journal of Hydrologic Engineering (ASCE), v. 11(4), pp. 319-328
[20] Suresh Kumar. G., M. Sekhar., and D. Misra (2006) "Time Dependent Dispersivity Behavior of Non-Reactive Solutes in a System of Parallel Fractures". Hydrology and Earth System Sciences Discussions, vol. 3(3), pp. 895-923.
[21] Suresh Kumar. G. (2008) "Effect of Sorption Intensities on Dispersivity and Macro-dispersion Coefficient in a Single Fracture with Matrix Diffusion". Hydrogeology Journal, 16(2), pp. 235-249
[22] Suresh Kumar. G. (2009) "Influence of Sorption Intensity on Solute Mobility in a Fractured Formation". Journal of Environmental Engineering (ASCE), 135(1), pp. 1-7
[23] Suresh Kumar, G. (2014). "Mathematical Modeling of Groundwater Flow and Solute Transport in a Saturated Fractured Rock using Dual-Porosity Approach". Journal of Hydrologic Engineering (ASCE), vol. 19(12)., pp. 04014033-1 – 04014033-8
[24] Suresh Kumar, G. (2014). "Mathematical Modeling of Groundwater Flow and Solute Transport in a Saturated Fractured Rock using Dual-Porosity Approach". Journal of Hydrologic Engineering (ASCE), vol. 19(12)., pp. 04014033-1 – 04014033-8
[25] Suresh Kumar, G. (2015). "Subsurface Transport of Nuclear Wastes in the Indian Subcontinent". ISH Journal of Hydraulic Engineering, vol. 21(2), pp. 162-176
[26] Suresh Kumar G. (2016). "Modeling Fluid Flow through Fractured Reservoirs: Is it different from Conventional Classical Porous Medium?", Current Science, vol. 110(4)., pp. 695-701
[27] Suresh Kumar G and T V Rakesh. (2015). "Numerical Modeling of Reactive Solute Transport in a Single Fracture with Matrix Diffusion under Complex Boundary Condition". ISH Journal of Hydraulic Engineering, vol. 21(2), pp. 125-141
[28] Suresh Kumar G., and T. V. Rakesh. (2018). "Numerical Modeling of Hyperbolic Dominant Transient Fluid Flow in Saturated Fractured Rocks using Darcian Approach". Groundwater for Sustainable Development, vol. 7., pp. 56-72
[29] Suresh Kumar. G., and A. Ghassemi. (2005) "Numerical Modeling of Non-Isothermal Quartz Dissolution/Precipitation in a Coupled Fracture-Matrix System". Geothermics, v. 34(4), pp. 411-439
[30] Suresh Kumar G., and M. Sekhar. (2005) "Spatial Moment Analysis for Transport of Nonreactive Solutes in a Fracture-Matrix System". Journal of Hydrologic Engineering (ASCE), v. 10(3), pp. 192-199
[31] Suresh Kumar G., and A. Ghassemi. (2006) "Spatial Moment Analysis for One-Dimensional Nonisothermal Quartz Transport and Dissolution/Precipitation in a Fracture-Matrix System". Journal of Hydrologic Engineering (ASCE), v. 11(4), pp. 338-346
[32] Suresh Kumar, G., M. Sekhar and D Mishra. (2008) "Time dependent dispersivity of linearly sorbing solutes in a single fracture with matrix diffusion". Journal of Hydrologic Engineering (ASCE), 13(4), pp. 250-257

[1.]Adewale George ADENIYI, [1.]Joshua O. IGHALO,
[1.]Samson Akorede ADEOYE, [1.]Damilola Edwards ABDULAZEEZ

NUMERICAL INVESTIGATION OF THE EFFECTS OF TEMPERATURE AND BIOMASS DENSITY ON THE PRODUCTS EVOLUTION FROM WOOD PYROLYSIS

[1.]Chemical Engineering Department, Faculty of Engineering and Technology, University of Ilorin, Ilorin, NIGERIA

Abstract: Interest in wood and other biomass as a source of renewable energy has been on the rise as it will help reduce the current reliance on fossil fuels. The aim of this study was to utilize Python 3 programming language in computing the numerical solutions to the differential equations using Euler's method for evaluating the effects of biomass density and system temperature on product evolution and yields during pyrolysis. It was observed that the rate of biomass degradation and product evolution is more rapid at higher temperatures. The final concentration of char decreased as the instantaneous temperature increased. At higher temperatures, gaseous products evolve at a higher rate and exist at a higher proportion in equilibrium. It was also observed that biomass density does not have a significant effect on the rate of the biomass degradation and the nature of the product evolution but biomass with higher density gives more char yield than those with lower densities.
Keywords: biomass pyrolysis; numerical solution; python; density

INTRODUCTION

Interest in biomass as a source of renewable energy has been on the rise as it will help reduce the current reliance on fossil fuels. Also the negative environmental impact of fossil fuels use will consequently be ameliorated. Biomass is identified as natural high-molecular organic substances of lignocellulosic structure (Fu, Hu, Xiang, et al., 2009). Even the largest coal consuming country in the world; China, is now turning towards greener energy sources (Fu et al., 2010). The fraction of the biomass energy consumed in developing countries is between 40% to 50% since these countries have large areas for agriculture (Gani & Naruse, 2007). Biomass from agricultural residues is recognized as one of the most promising sources of renewable energy because of their availability, cheap price and abundance (Fu, Hu, Sun, et al., 2009).

The products of the pyrolysis process are oil/tar, synthesis gas and char. Biomass consists of mainly three components; hemicellulose, cellulose and lignin (Qu, Guo, Shen, Xiao, & Zhao, 2011). They possess very different thermal behaviours (Wang, Zhou, Liang, Song, & Zhang, 2015). The pyrolysis products may be considered to be from the overall conversion of the main components hence, the possibility of predicting the pyrolysis product distribution according to the component proportion in a biomass. Simplifying reaction sequences and overall reaction kinetics for biomass pyrolysis has been proposed and studied over the years (Prakash & Karunanithi, 2008). For numerous biomass samples, kinetics and reaction sequence has been exhaustively examined (Gavin, Stuart, & Emilio, 2016). Pious O. Okekunle and Adeoye (2016) undertook a generic numerical modelling for biomass aimed at studying thermo-physical property effects on product yield. The use of python for kinetic modelling of wood pyrolysis degradation and product evolution is unreported in open literature.

This study aims on taking a step further by utilizing a numerical modelling technique (Euler's method) and Python 3 programming language (on Python v2.7 software) to elucidate the effect of temperature and wood density on the pyrolysis products evolution. It is modelling cum property-effect studies. The approach will encompass the generation of differential governing equations to describe the wood pyrolysis process and these includes solid mass conservation equations, mass conservation equations for gas and tar, energy equation and total pressure equation. Furthermore, Python 3 programming language will be used in computing the numerical solutions to the differential equations using an appropriate computational technique (Euler's method). Graphical plots will be developed and analysed to show the effects of biomass density and system temperature on product evolution and yields during pyrolysis.

METHODOLOGY

— Pyrolysis Mechanism and Kinetics

Pyrolysis is mathematically described through a system of coupled equations. The basic equations are those of chemical kinetics, heat transfer and mass transfer. The pyrolysis mechanism adopted for this research was developed by Chan (1983) and shown in Figure 1. In this mechanism, biomass decomposes via three competing reactions into gas, charcoal and tar. The secondary reaction takes place in the gas/vapour-phase within the pores of the charcoal. Consecutively the tar is converted by two secondary reactions into secondary gases and charcoal. The rate

of the reaction is proportional with the concentration of the tar vapours.

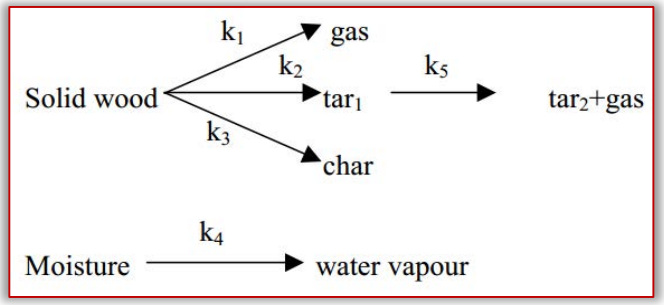

Figure 1. Pyrolysis mechanism by Chan (1983)

For each of the reactions in figure 1, the kinetic constants are presented in table 1. The constants are for the Arrhenius equation given as equation 1

$$k_i = A_i \exp\left(-\frac{E_i}{RT}\right) \quad (1)$$

The values of the pre-exponential factor and activation energy are shown in Figure 1.

Table 1. Kinetic Constants used by Chan (1983)

	Reaction	A_i (sec^{-1})	E_i (kJ/mol)
1	Wood → Gas	1.3×10^8	140
2	Wood → $(Tar)_1$	2×10^8	133
3	Wood → Char	1.08×10^7	121
4	Moisture → Water Vapour	5.13×10^6	87.9
5	$(Tar)_1$ → $(Tar)_2$ +Gas	1.48×10^6	144

— Development of Governing Equations

The governing equations used to describe the processes that occurred during pyrolysis of biomass consist of the solid mass conservation equations, mass conservation equations for gas and tar, energy equation and total pressure equation.

» Solid Mass Conservation Equation

Mass balance equation for each of the reaction yielding char, tar and gas

$$\frac{\partial \rho_{sw}}{\partial t} = -(K_1 + K_2 + K_3)\rho_{sw} \quad (2)$$

Char mass balance

$$\frac{\partial \rho_c}{\partial t} = K_3\, \rho_{sw} \quad (3)$$

» Mass Conservation Equations for Gas, Tar, Water Vapour and Moisture

Mass equations for the inert gas used (Nitrogen) Using two-dimensional cylindrical coordinate system from the equation of continuity

$$N_2: \quad \frac{\partial(\varepsilon\rho_{N_2})}{\partial t} + \frac{\partial(\rho_{N_2}U)}{\partial z} + \frac{1}{r}\frac{\partial(r\rho_{N_2}V)}{\partial r} = S_{N_2} \quad (4)$$

NB: θ direction is zero.

The source term, $S_{N_2} = 0$

$$N_2: \quad \frac{\partial(\varepsilon\rho_{N_2})}{\partial t} + \frac{\partial(\rho_{N_2}U)}{\partial z} + \frac{1}{r}\frac{\partial(r\rho_{N_2}V)}{\partial r} = 0 \quad (5)$$

Mass equation for the gas produced

$$\text{gas:} \quad \frac{\partial(\varepsilon\rho_g)}{\partial t} + \frac{\partial(\rho_g U)}{\partial z} + \frac{1}{r}\frac{\partial(r\rho_g V)}{\partial r} = S_g \quad (6)$$

where $S_g = K_1\rho_{sw} + \varepsilon K_5\rho_{t_1}$

Mass equation for the water vapour produced water vapour:

$$\frac{\partial(\varepsilon\rho_w)}{\partial t} + \frac{\partial(\rho_w U)}{\partial z} + \frac{1}{r}\frac{\partial(r\rho_w V)}{\partial r} = S_w \quad 7)$$

where $S_w = K_4\rho_m$

Mass equation for the tar_1 and tar_2 produced tar_1:

$$\frac{\partial(\varepsilon\rho_{t_1})}{\partial t} + \frac{\partial(\rho_{t_1} U)}{\partial z} + \frac{1}{r}\frac{\partial(r\rho_{t_1} V)}{\partial r} = S_{t_1} \quad (8)$$

where $S_{t_1} = K_2\rho_{sw} - \varepsilon K_5\rho_{t_1}$

$$tar_2: \quad \frac{\partial(\varepsilon\rho_{t_2})}{\partial t} + \frac{\partial(\rho_{t_2} U)}{\partial z} + \frac{1}{r}\frac{\partial(r\rho_{t_2} V)}{\partial r} = S_{t_2} \quad (9)$$

where $S_{t_2} = \varepsilon K_5\rho_{t_1}$

Mass equation for the moisture produced moisture:

$$\frac{\partial(\varepsilon\rho_m)}{\partial t} + \frac{\partial(\rho_m U)}{\partial z} + \frac{1}{r}\frac{\partial(r\rho_m V)}{\partial r} = S_m \quad (10)$$

where $S_m = -K_4\rho_m$

Intra-particle tar and gas transport velocity

Using Darcy's Law

$$U = \frac{-B}{\mu}\left(\frac{\partial \rho}{\partial z}\right) \quad (11)$$

$$V = \frac{-B}{\mu}\left(\frac{\partial \rho}{\partial r}\right) \quad (12)$$

where μ is the viscosity, ε is the porosity

$$\varepsilon = 1 - \frac{\rho_{sw,sum}}{\rho_{sw,o}}\left(1 - \varepsilon_{sw,0}\right) \quad (13)$$

where $\varepsilon_{sw,0}$ = initial porosity of wood, $\rho_{sw,sum}$ = sum of wood density and $\rho_{sw,o}$ = initial wood density. The permeability B of the wood biomass:

$$B = (1 - \eta)\, B_{sw} + \eta B_c \quad (14)$$

where η = degree of pyrolysis

$$\eta = 1 - \frac{\rho_{sw} + \rho_c}{\rho_{sw,o}} \quad (15)$$

— Solution Procedure

The numerical methods listed above are to be programmed to create simple and efficient python codes that output the numerical solutions at the required degree of accuracy, arrays (vectors and matrices) are created and manipulated using 'Numpy' and the plotting functions of 'matplotlib' are used to present the results graphically. The necessary tools and libraries needed to carry out the analysis effectively were Python 3 programming language (on Python v2.7 software), SciPy (mathematical solvers), NumPy (n-dimensional array package), Matplotlib (comprehensive plotting), Pandas (data structures and analysis), iPython (interactive console) and Spyder (a Python IDE similar to Matlab).

RESULTS AND DISCUSSION

— Effect of Temperature

Considering the quantity of data generated from the numerical study, it is very important to carefully present the characteristic features of the concentration profiles of various species resulting from the pyrolysis process.

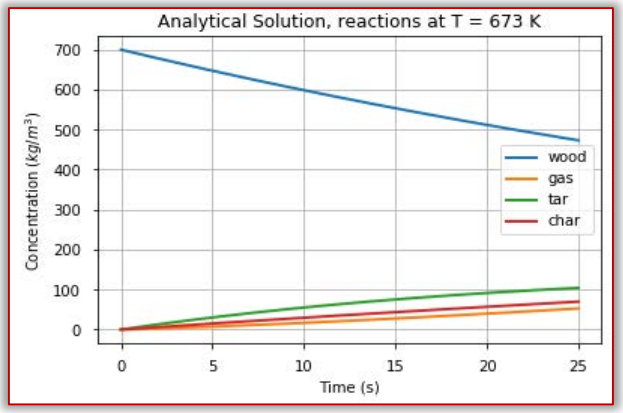

(a)

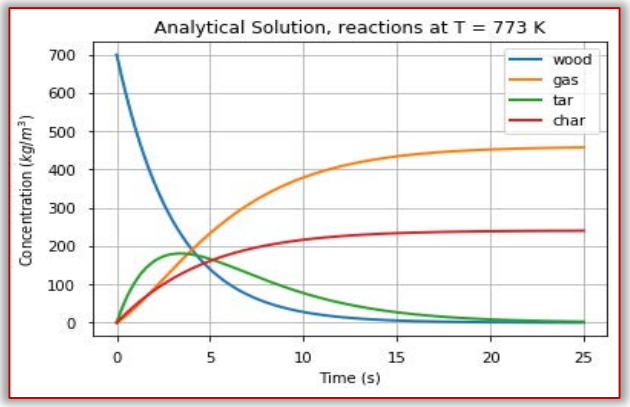

(b)

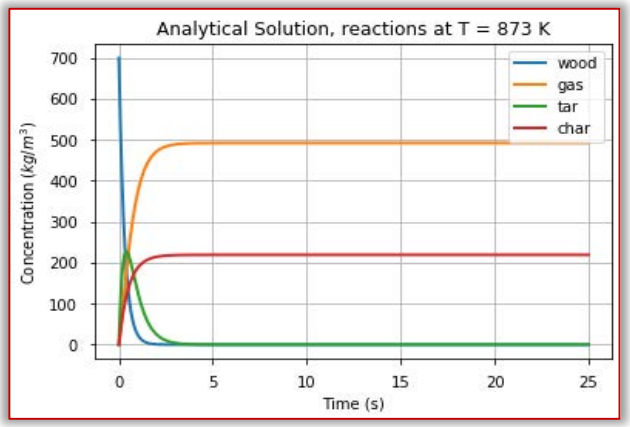

(c)

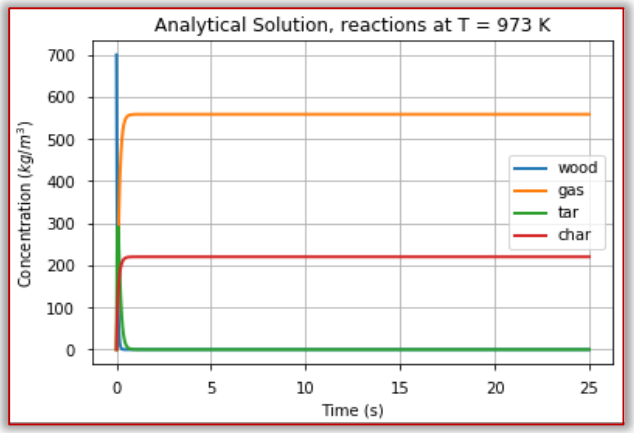

(d)

Figure 2(a-d). Biomass and product species concentration profiles with time sample density of 700kg/m³ and temperature of (a) 673 K (b) 773 K (c) 873 K (d) 973 K

Figures 2 shows the species concentration profiles for wood pyrolysis process. As shown in the figures, the initial temperature being high enough to initiate the process leads to the almost immediate decomposition of biomass.

Figure 2a, 2b, 2c and 2d shows product evolution and biomass concentration loss at an instantaneous temperature of 673K, 773K, 873K and 973K respectively. This biomass decomposition reaction resulted in the formation of gas, tar and intermediate solid. As the temperature increased, the tar and intermediate solid formed further participated in some secondary reactions, characterized by decrease in the concentration of the two species, resulting in the production of more gas and char. The process was terminated when biomass concentration had become so low that no significant decomposition reaction took place any more.

It can be observed that the rate of biomass degradation and product evolution is more rapid at higher temperatures. This was due to the fact that as the instantaneous temperature increased, the rate of chemical reaction was accelerated, resulting in a speedy completion of the pyrolysis process. Furthermore, within the 25 seconds consideration time, concentration equilibrium was not achieved for 673K instantaneous temperature. The equilibrium was almost immediately achieved at the higher end of the temperature considered. At higher temperatures, gaseous products evolve at a higher rate and exist at a higher proportion in equilibrium. Other process modelling techniques (thermodynamic approach) have made similar observations albeit for banana residues (Ighalo & Adeniyi, 2019) and rice husk (Adeniyi, Odetoye, Titiloye, & Ighalo, 2019).

The summation of the final concentration of initial biomass, tar, gas, intermediate solid and char is always the same. This is based on the conservation of mass concept to physical system. It can be observed from Figure 2 that the final concentration of char decreased as the instantaneous temperature increased. This is attributable to the fact that increase in instantaneous temperature favours the yield of fluid phase (tar and gas) products during primary pyrolysis (Adeniyi et al., 2019) and also facilitated secondary reactions. The decrease in the final concentration of the intermediate solid with increasing instantaneous temperature is also attributable to this reason. The final concentration of gas appeared to be inconsistent as instantaneous temperature increased because secondary reactions, which led to more gas yield, depend on both residence time and temperature, and the extent of these reactions is based on a trade-off between the two factors.

— Effect of Biomass Density

Figures 3 show the effect of biomass density on the pyrolysis product evolution.

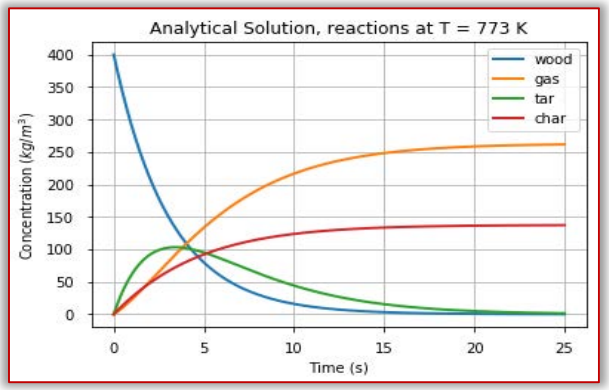

(a)

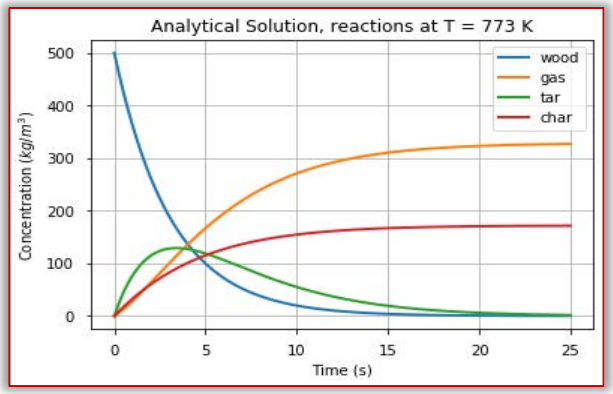

(b)

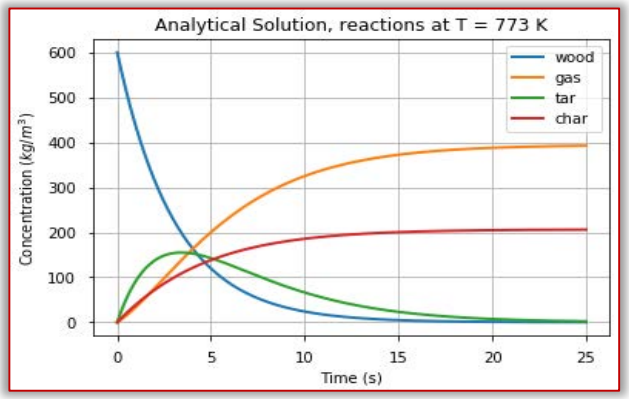

(c)

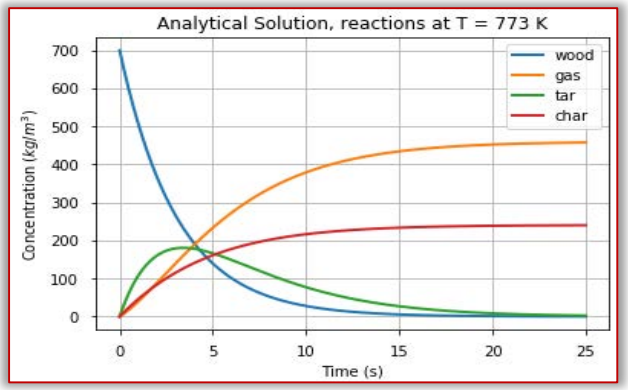

(d)

Figure 3(a-d). Biomass and product species concentration profiles with time at 773 K and sample density of (a) 400 kg/m³ (b) 500 kg/m³ (c) 600 kg/m³ (d) 700 kg/m³

It is observed that biomass density does not have a significant effect on the rate of the biomass degradation and the nature of the product evolution. Although the profiles were similar for all samples considered, the peaks and the final values of the product species concentration profiles, the extent of secondary reactions and the time required for the completion of the pyrolysis process were different for different biomass densities. Wood with higher density gives more char yield than those with lower densities. This is in agreement with the observation of Pious O Okekunle, Akogun, Alagbe, and Osinuga (2015) for hard and soft wood pyrolysis.

CONCLUSION

In this study, Python 3 programming language was successfully used in computing the numerical solutions to the differential equations using Euler's method for evaluating the effects of biomass density and system temperature on product evolution and yields during pyrolysis. It was observed that the rate of biomass degradation and product evolution is more rapid at higher temperatures. This was due to the fact that as the instantaneous temperature increased, the rate of chemical reaction was accelerated, resulting in a speedy completion of the pyrolysis process. The final concentration of char decreased as the instantaneous temperature increased. At higher temperatures, gaseous products evolve at a higher rate and exist at a higher proportion in equilibrium. It was also observed that biomass density does not have a significant effect on the rate of the biomass degradation and the nature of the product evolution. Wood with higher density gives more char yield than those with lower densities.

Acknowledgement

The authors would love to duly acknowledge the input of the process simulation unit of the department of chemical engineering, university of Ilorin, Nigeria. No official funding or grant was received for this research.

References

[1] Adeniyi, A. G., Odetoye, T. E., Titiloye, J., & Ighalo, J. O. (2019). A Thermodynamic Study Of Rice Husk (Oryza Sativa) Pyrolysis. European Journal of Sustainable Development Research, 3(4)

[2] Chan, W. C. R. (1983). Analysis of chemical and physical processes during the pyrolysis of large biomass pellets. (PhD), University of Washington, Seattle, WA.

[3] Fu, P., Hu, S., Sun, L., Xiang, J., Yang, T., Zhang, A., & Zhang, J. (2009). Structural evolution of maize stalk/char particles during pyrolysis. Bioresource Technology, 100(20), 4877-4883.

[4] Fu, P., Hu, S., Xiang, J., Li, P., Huang, D., Jiang, L., . . . Zhang, J. (2010). FTIR study of pyrolysis products evolving from typical agricultural residues. Journal of Analytical and Applied Pyrolysis, 88(2), 117-123.

[5] Fu, P., Hu, S., Xiang, J., Sun, L., Li, P., Zhang, J., & Zheng, C. (2009). Pyrolysis of maize stalk on the

characterization of chars formed under different devolatilization conditions. Energy & Fuels, 23(9), 4605-4611
[6] Gani, A., & Naruse, I. (2007). Effect of cellulose and lignin content on pyrolysis and combustion characteristics for several types of biomass. Renewable Energy, 32(4), 649-661
[7] Gavin, W., Stuart, D., & Emilio, R. (2016). Modeling the impact of biomass particle residence time on fast pyrolysis yield and composition. Paper presented at the AIChE Annual Meeting, San Francisco.
[8] Ighalo, J. O., & Adeniyi, A. G. (2019). Thermodynamic modelling and temperature sensitivity analysis of banana (Musa spp.) waste pyrolysis. SN Applied Sciences, 1(9)
[9] Okekunle, P. O., & Adeoye, O. O. (2016). Numerical investigation of the effects of some selected thermo-physical properties on products evolution and yields during biomass pyrolysis. Biofuels
[10] Okekunle, P. O., Akogun, T. O., Alagbe, G. O., & Osinuga, M. A. (2015). Experimental Investigation of the Effect of Reactor Temperature on Soft and Hardwood Pyrolysis Characteristics in a Fixed-Bed Reactor. Journal of Natural Sciences Research, 5(10).
[11] Prakash, N., & Karunanithi, T. (2008). Kinetic modeling in biomass pyrolysis–a review. Journal of Applied Sciences Research, 4(12), 1627-1636.
[12] Qu, T., Guo, W., Shen, L., Xiao, J., & Zhao, K. (2011). Experimental Study of Biomass Pyrolysis Based on Three Major Components: Hemicellulose, Cellulose, and Lignin. Industrial & Engineering Chemistry Research, 50, 10424–10433
[13] Wang, X., Zhou, W., Liang, G., Song, D., & Zhang, X. (2015). Characteristics of maize biochar with different pyrolysis temperatures and its effects on organic carbon, nitrogen and enzymatic activities after addition to fluvo-aquic soil. Science of The Total Environment, 538, 137-144.

ACTA TECHNICA CORVINIENSIS – Bulletin of Engineering
ISSN: 2067-3809

Fascicule 2
[April – June]
tome XIII
[2020]

ACTA Technica CORVINIENSIS
BULLETIN OF ENGINEERING

ACTA TECHNICA CORVINIENSIS – Bulletin of Engineering
ISSN: 2067-3809

http://acta.fih.upt.ro

[1.]Muhanned AL-RAWI, [2.]Muaayed AL-RAWI

SYSTEM DESIGN OF CELL PHONE DETECTOR

[1.]Ibb University, Ibb, YEMEN,
[2.]Al-Mustansiriya University, Bagdad, IRAQ

Abstract: Cell phones are widely used in the world. While people have to be connected to one another, there are situations or places where there usage is to be prohibited either due to security reasons or it may cause health hazards. Cell phone detection has been on investigation for a long time. There are techniques which have been formulated or proposed on how cell phones can be detected. Most of them use the features such as audio system, radio frequency (RF) system and common materials of the phones and try to look into how they can be used as basis to detect mobile phones. This paper utilizes the RF system of the cell phone as the feature to be used to detect its presence. A circuit that detects signals of the range 0.9GHz to 3GHz is used to detect a cell phone when in use. When the signal is detected, a light emitting diode (LED) blinks to indicate the usage of a cell phone within a radius of 1.5metres.
Keywords: design; implementation; cell phone detector

INTRODUCTION

Cell phones have become an integral part of people's lives. They are not only used for communication via short messaging service (SMS), calls, emails and internet but advanced applications such as remote health monitoring systems and security systems have been integrated with mobile phones[1,2].

The recent years have seen rapid advancements in the value of addition applications in mobile phones such as high definition cameras and high speed internet connectivity. Despite the advantages enjoyed by these advancements in mobile technology, there are threats that have been posed by their usage. Company data mining has been a big threat in the industry where employees are able to access sensitive company information and share with the competitors. This led to the development of cell phone jammers where signal reception is completely blocked when you enter the premises. Despite personal privacy invaded by the usage of such devices, this could not put to end the vice since mobile phones could be connected to the computer and information transferred and sent when the employee is out of the company premises. Criminal activities and attempted escape incidences have been organized by inmates in correctional institutions through the use of mobile phones in such facilities. The most common incidence is when people were conned by inmates who impersonated promoters and required winners to send money as fees to facilitate the award of prizes. Life support machines are also sensitive to the use of mobile phones. The use of mobile phones in such a facility leads to adverse repercussions to the life of persons whose lives depend on the proper functionality of the machines. Other places are aeroplanes, petrol stations, conference halls, examination halls, worship centers, etc., where the use of mobile phones can either lead to failure of sensitive machines or is a nuisance[3,4,5].

It is therefore a reality that mobile usage in some places must be prohibited. Due to the privacy laws that limit the use of cell phone jammers, cell phone detectors must be designed and installed so that in case a person gets in with a phone into such places, they can be notified and either told to switch them off or take them outside. The effectiveness of cell phone detectors is that they continually scan for the presence and usage of the cell phone and sound an alarm to notify the user or security personnel [6].

DESIGN METHODOLOGY

Among the detection techniques, the RF spectrum approach is selected for implementation. The choice of this selection is based on the ease of implementation due to readily availability of the discrete components required in the local market. The block diagram of the design is shown in Figure1 below. Based on the block diagram of Figure1, the circuit design of each block is designed and the final circuit integrated together. The subsequent sections explain the detail and design of each block diagram.

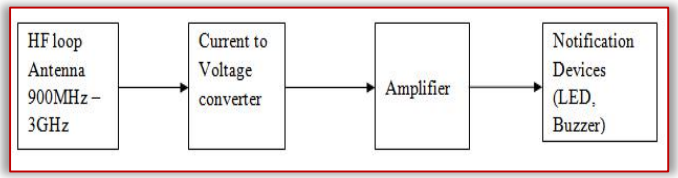

Figure 1. Block diagram

—High frequency loop antenna

The frequency to be detected is 0.9 Gigahertz to 3 Gigahertz. Passive components suffer from parasitic effects at this high frequency. In ordinary radio frequency antenna design, LC components tuned at desired frequency are used. However, at this frequency the components behave as lumped R, L and C and as transmission lines and antenna. In the loop antenna design at this frequency, the parasitic effects of these elements are used.

The loop antenna consists of a 0.22uF ceramic capacitor with it leads fixed at 18mm long and 8mm

wide. These dimensions provide an area sufficient to capture the frequency required. Hence, it is a loop antenna. When there is no signal detected, the capacitor charges and stores energy. When a field created by the presence of a mobile phone is detected, the energy balance in the capacitor is perturbed. A displacement current is injected into the capacitor leads generating a magnetic field hence inductance in the leads. The inductance together with the capacitance acts as a transmission line that transmits the current to the current to voltage converter.

— Current to voltage converter

The current to voltage converter shown in Figure2 consists of a CA3130E operational amplifier. It has a MOSFET input stage and a CMOS output stage. The input stage provides a very high input impedance and low input current (typical 5pA at 15V). Since the loop antenna generates very small current, this makes this type of operational amplifier suitable for this application. Furthermore, it is a single power supply operational amplifier. Therefore, it gives no hard work generating a negative biasing voltage as a dual voltage operational amplifier. The CMOS stage provides an output swing to about 10mV of the supply voltage.

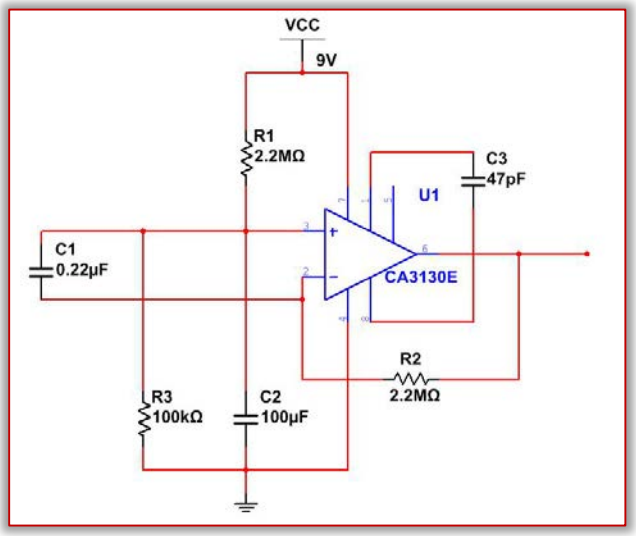

Figure 2. Current to voltage converter

The operational amplifier is connected as a current to voltage converter and has a voltage comparator. The comparator consists of R1 and R3 connected on the non-inverting terminal. These two resistors responsible for setting V_{ref} at 0.52V using voltage divider formula.

From Figure 2, the 0.22µF capacitor which acts as a loop antenna is connected across the non-inverting and inverting terminals of the operational amplifier. The capacitor stores energy and in the absence of a mobile phone, both the positive and negative terminals receive the same voltage, that is equal to V_{ref}, hence the output of the operational amplifier is low.

When a mobile phone is radiating and its frequency is sensed by capacitor C1, the balance between the inverting and non-inverting terminals of the operational amplifier is perturbed. The current is transmitted to the non-inverting terminal and a voltage is sensed at the output. The 100uF electrolytic capacitor (C2) connected to the non-inverting terminal ensures stability of the terminal and fast output swing. The capacitor charges during operation and to bring it back to stable condition, the 100K resistor (R3) provides a discharge path.

The feedback resistor is not for amplification but provides feedback to the inverting terminal such that when the output goes high, the state is also fed back to the inverting terminal making it high. However, since the frequency of the radiation from the mobile phone is pulsating, the sensing capacitor C1 (loop) oscillates hence the output.

— Amplifier

Since the voltage at the output is small, it needs to be amplified in order to drive the notification devices (LED or sound buzzer). At standby mode of the cell phone, the voltage output from the current to voltage converter can be as low as 10mV. Therefore an amplifier that has little or no offsets voltage level is required. The best amplifier is a two stage transistor based as shown in Figure3. An op-amp based would suffer from offset voltages hence not effective in this design. With a low voltage of this order, it is hard to eliminate the effects of noise due to the sensitive tuning of the amplifier.

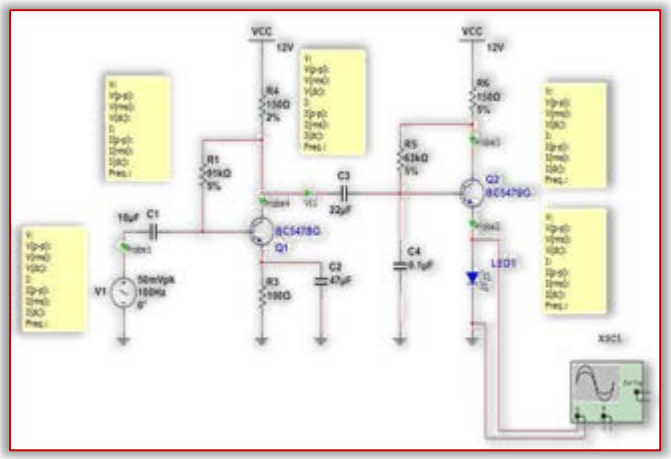

Figure 3. Amplifier

The 10µF input coupling capacitor blocks any dc voltages at the input. The biasing used is the collector-feedback bias. The advantage of this bias design in RF operation is that it provides temperature stabilization such that as the temperature increases, the transistor starts to conduct more current from emitter to collector.

Since the base resistor is directly connected to the collector, any rise in collector current (Ic) will permit more voltage to drop across the collector resistor. This

will force less voltage to be dropped across the base resistor hence base current (I_B) decreases and consequently Ic.
The bypass capacitor at the emitter bypasses the RF signal around the emitter resistor to avoid excessive RF gain degeneration in the circuit.
C4 (0.1μF) is connected between the base and emitter of the transistor in the final stage to ensure that it provides fast switching of the transistor.
The final stage which is the notification stage is integrated with the amplifier. The chosen notification in the design is an LED. The LED is connected to the emitter of the last transistor of the final amplification stage. The operating point of the voltage at the emitter is held at about 3.0V to ensure that a small variation of the voltage due to voltage swing from the current to voltage converter would make the LED to blink.

— Complete circuit

The complete circuit for the cell phone detector is shown in Figure 4. The 22pF capacitors are connected to the antenna side. The antenna is to make sure the detector receives the optimum level of the signal from the phone.

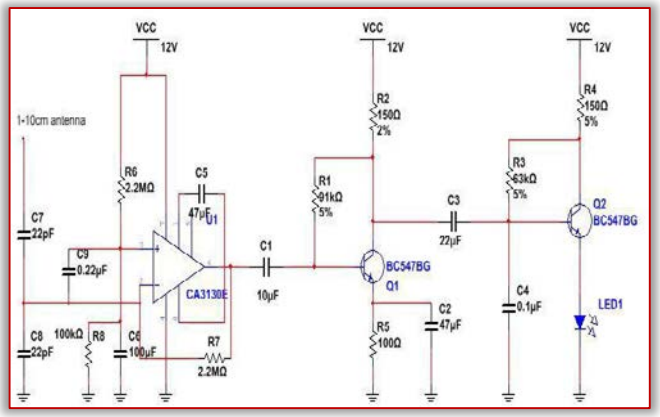

Figure 4. Complete detector circuit

RESULTS

— Simulation results

The loop antenna designed in this paper is not subjected to simulation environment due to the limitation of the software at the design operating frequency of the detector. Most soft-wares are limited to 100MHz operating frequency. Beyond this point, the software overloads the central process unit(CPU) hence no real time results can be obtained. Furthermore, at the very high frequency operation expected, the parasitic effects of the passive elements will not be depicted in the software environment hence real-time operation of the detector could not be obtained by simulation.
The amplifier is simulated, in place of the current to voltage converter, a signal generator is used. The amplifier is simulated at 50mV pk voltage and the voltage waveforms at the LED monitored.
With the swinging of the voltage at the output, the LED is found to be blinking. Therefore it is expected that upon connection of the detector and current to voltage converter to the amplification stage, the LED would blink as expected in these simulation results as shown in Figure 5.

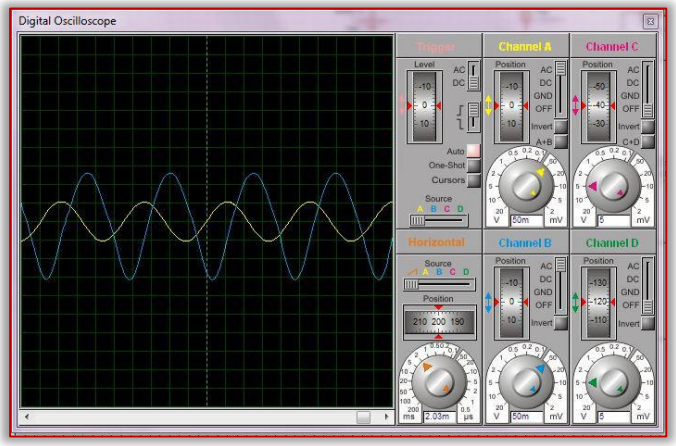

Figure 5. Output simulation results

— Practical results

The practical results obtained from the detector before and after a cell phone is adjacent to the detector are shown in Figure 6 and Figure 7. Figure 6 shows the detector output when cell phone is not in use, while, Figure 7 shows the detector output when cell phone is in use.

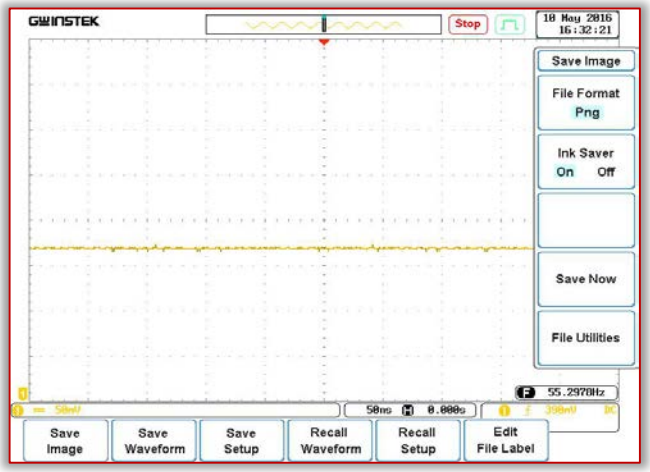

Figure 6. Detector output when cell phone is not in use

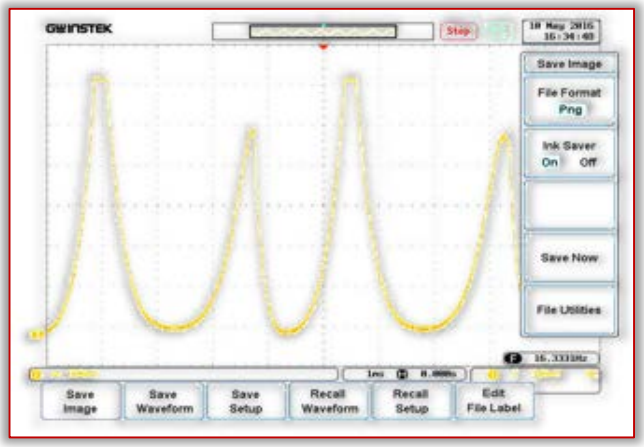

Figure 7. Detector output when cell phone is in use

At the output of the cell phone detector circuit, an LED is used. The practical waveform obtained is shown in Figure8. This output waveform makes the LED to blink indicating that a cell phone is in use.

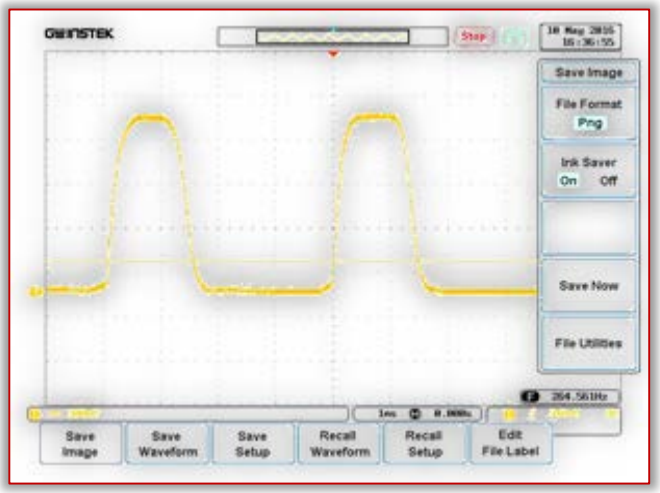

Figure 8. Output of LED

Upon completion, the user is allowed to install new devices in the system. This includes bedroom light, sitting room light, A DVD player radio system and a gate. Each of these devices are then assigned operating commands shown in the command table 1. When the system is fully initialized, the user exited graphics thereafter activating speech operating mode for the system as shown in Figure 8.

CONCLUSIONS

The results in this paper show that the cell phone detector worked sufficiently. The detector could detect the signal in the frequency range of 0.9GHz to 3.0 GHz, thus a cell phone that is in use. This phone usage was indicated by the blinking of the LED. When a cell phone is on standby mode, it keeps a radio silence therefore cannot be detected using this cell phone detector. This detector can therefore be used to track the usage of a cell phone in an examination room where a buzzer usage will be too loud and disturb the examiners.

References

[1] C. Mbaocha, "Design and implementation of intelligent mobile phone detector", Academic Research International, Vol 3, No 1, 2012.
[2] K. Mohan, "Novel mobile detector sensing alarming and reporting system", ARPN Journal of Science and Technology, Vol.2, No.1, 2012.
[3] T. Deshpande and N. Jadhav, "Active cell phone detection and display using Atmega-88 microcontroller", International Journal of Research in Engineering & Technology, Vol. 3, Issue 8, 2015.
[4] O. Oke and A. Falohun, "The design and implementation of a mobile phone detector device with a frequency jamming feature", International Journal of Computer Applications, Vol.143, No.1, 2016.
[5] H. Verma, "Intelligent cell phone detector system at 4g bands of frequencies", IOSR Journal of Electronics and Communication Engineering, Vol.12, Issue 2, PP. 55-59, 2017.
[6] C. Ramya, and S. Reeva, "Mobile phone detector using OP-AMP", International Journal of Innovative Research in Science, Engineering and Technology, Vol.7, Special Issue 1, 2018.

ACTA TECHNICA CORVINIENSIS – Bulletin of Engineering
ISSN: 2067-3809

[1.]Amar KALYANE, [2.]R.J. PATIL

EXPERIMENTAL INVESTIGATION OF BLACK COTTON SOIL BY LIME AND FLY-ASH STABILIZATION

[1.]Department of Civil Engineering, Navsahyadri Education Society's & Group of Institutes, Pune, INDIA
[2.]Department of Mechanical Engineering, Navsahyadri Education Society's & Group of Institutes, Pune, INDIA

Abstract: Black cotton soil is widely distributed in India, Maharashtra is mainly covering with black cotton soil. Black cotton soil is having high swelling and shrinkage character in nature. Because of this heavily loaded structure like dam, bridge etc are severely damaged. Its stabilization is required to mainly improve the Soil properties. In this paper Black cotton soil mainly stabilized using Fly ash and Lime. Combination of Fly ash and Lime proves to be very effective and cheaper method of stabilization. This paper also describes that if we add the admixture in Black cotton soil we can improve the strength of soil as well as Stabilize the soil. Stabilized Black cotton soil shows less swelling of soil and increases in OMC of soil. Results of MDD, LL, PL all indicates that Combination Fly ash and Lime are stabilized at 5% is better than the Lime and Fly ash of 5%, 10%, 15%.
Keywords: Black Cotton Soil, Soil Stabilization, Fly Ash, Lime

INTRODUCTION

The study is being carried out mainly in Bhatgar dam, Pune. An experimental investigation is made to find the soil condition and conduct the lab test to find soil properties. For stabilization Lime and Fly ash are used in different proportion. For lightly loaded structure swelling of soil will be more under any load. As a result there is a settlement of structure and differential movements, resulting into damage to foundation.

Fly ash: Fly ash is a by-product from burning pulverized coal in electric power generating plants. As the fused material rises, it cools and solidifies into spherical glassy particles is fly ash. Fly ash is collected from the exhaust gases by electrostatic precipitators or bag filters.

Lime: It is a white powder and composed primarily of oxides and hydroxide, or "slaked" with water. Lime is used in large quantities as building and engineering materials, lime is derived from rocks and minerals typically limestone or chalk.

LITERATURE REVIEW

≡ Kaniraj S R, Havanagi V G: In this paper, Rajghat fly ash from Delhi, India and Baumineral fly ash near Bochum, Germany, were mixed with the locally available soils silt and Yamuna sand withRajghat fly ash and Rhine sand with Baumineral fly ash in different proportions. Cement, varying from 3–9% was added to stabilize the fly ash-soil mixtures. Cylindrical samples were prepared at optimum moisture content and maximum dry density and were cured for different duration. Unconfined compression tests were conducted on these samples. Correlations for unconfined compressive strength and secant modulus as functions of curing time, fly ash content, and cement content have been established. Correlations for water content as functions of curing time and cement content have also been established [1].

≡ Cokca E: In this study, high-calcium and low-calcium class C fly ashes from the Soma and Tuncbilek thermal power plants, respectively, in Turkey, were used for stabilization of an expansive soil. Lime and cement were added to the expansive soil at 0–8% to establish baseline values. Soma fly ash and Tuncbilek fly ash were added to the expansive soil at 0–25%. Test specimens were subjected to chemical composition, grain size distribution, consistency limits, and free swell tests. Specimens with fly ash were cured for 7 days and 28 days, after which they were subjected to odometer free swell tests. Based on the favorable results obtained, it can be concluded that the expansive soil can be successfully stabilized by fly ashes [2].

≡ Amer Ali Al-Rawas, Ramzi Taha, John D. Nelson, Thamer Beit Al-Shab, Hilal Al-Siyabi: This paper investigates the effectiveness of using cement bypass dust, copper slag, granulated blast furnace slag, and slag-cement in reducing the swelling potential and plasticity of expansive soils. The soil used in this study was brought from Al-Khod (a town located in Northern Oman) where structural damage was observed. [3].

≡ Bell, F.G: Clay soil can be stabilized by the addition of a small percentage, by weight, of lime, that is, it enhances many of the engineering properties of the soil. This produces an improved construction material and so the technique has been used for many construction purposes, notably in highway, railroad and airport construction to improve subgrades and sub-bases. Generally the amount of lime needed to modify a clay soil varies from 1 to 3 per cent, whilst that required for cementation varies from 2 to 8 percent [4].

≡ Karthik S, Ashokkumar E, Gowtham P, Elango G, Gokul D, Thangaraj S: The objective of this study was to evaluate the effect of Fly Ash derived from combustion of sub-bituminous coal at electric power plants in stabilization of soft fine-grained red soils. California bearing ratio (CBR) and other strength property tests were conducted on soil. The soil is in range of plasticity, with plasticity indices ranging between 25 and 30. Tests were conducted on soils and soil–Fly Ash mixtures prepared at optimum water content of 9% .Addition of Fly Ash resulted in appreciable increases in the CBR of the soil. For water contents 9% wet of optimum, CBRs of the soils are found in varying percentage such that 3,5,6and 9.We will found optimum CBR value of the soil is 6%.Increment of CBR value is used to reduce the thickness of the pavement. And increasing the bearing capacity of soil [5].

≡ Amu, O.O., Fajobi, A.B. and Oke B.O: This research was meant to study the effect of Eggshell Powder (ESP) on the stabilizing potential of lime on an expansive clay soil. Tests were carried out to determine the optimal quantity of lime and the optimal percentage of lime-ESP combination; the optimal quantity of lime was gradually replaced with suitable amount of eggshell powder. The lime stabilized and lime-ESP stabilized mixtures were subjected to engineering tests. The optimal percentage of lime-ESP combination was attained at a 4% ESP + 3% lime, which served as a control. Results of the Maximum Dry Density (MDD), California Bearing Ratio (CBR), unconfined compression test and Undrained triaxial shear strength test all indicated that lime stabilization at 7% is better than the combination of 4% ESP + 3% lime [6].

≡ Muntohar, A.S. and Hantoro, G: When geotechnical engineers are faced with clayey soils, the engineering properties of those soils may need to be improved to make them suitable for construction. Waste materials such as fly ash or pozzolanic materials have been used for soil improvement. Recent research, based on pozzolanic activity, found that rice husk ash was a potential material to be utilized for soil improvement. The effects of the engineering properties of clayey soils when blended with lime and rice husk ash are the focus of this paper [7].

≡ Phani Kumar, B.R and Sharma, S.R.: This note presents a study of the efficacy of fly ash as an additive in improving the engineering characteristics of expansive soils. An experimental program has evaluated the effect of the fly ash content on the free swell index, swell potential, swelling pressure, plasticity, compaction, strength, and hydraulic conductivity characteristics of expansive soil. The plasticity, hydraulic conductivity and swelling properties of the blends decreased and the dry unit weight and strength increased with an increase in fly ash content. The resistance to penetration of the blends increased significantly with an increase in fly ash content for a given water content. Excellent correlation was obtained between the measured and predicted undrained shear strengths [8].

≡ Rajan, B.H. and Subrahmanyam, N.: Problems associated with the use of black cotton soil in India are usually caused by swelling and shrinkage on the absorption or depletion of moisture. The stabilization of the soil is therefore of importance and ways of overcoming the shrinkage and swelling characteristics are considered. Stabilizers such as cement and lime have been widely used to counteract these problems although to achieve greater economy. It was found that the 28-day shear strength with such an admixture in the proportion 1:4.5 indicated that almost 50% savings in lime could be made with such an admixture compared with soil treated with only 12% lime [9].

OBJECTIVE

—to study the properties of soil when stabilized with lime and fly ash in certain proportion

—to analyze the characteristic of fly ash and lime

—to improve the engineering properties of soil

—to determine the effect of lime and fly ash used as stabilizing material in Black cotton soil.

MATERIALS & METHODOLOGY

≡ Black Cotton Soil

≡ Fly ash

≡ Lime

Table 1. Properties of Black Cotton Soil

Properties	Results
Specific Gravity	2.71
Liquid Limit (WL)	47%
Plastic Limit (WP)	17%
Optimum Moisture Content	15%
Maximum Dry Density	1.658 g/cc
Unconfined Compressive Strength (qu)	84.12 kN/m²
Cohesion (Cu)	42.06 kN/m²

Methodology provides in detail on the basis of which experiments are carried out. The soil was collected from the Bhatgar dam in Bhor. The soil was air dried and the lumps in the soil is crushed.Then it is compacted or powdered so that the soil can pass through 425-micron sieve.

Preliminary tests were conducted on the materials as per I.S. Standards and specifications. Where the black cotton soil was initially tested for its physical and engineering properties. Fly ash and lime are varied accordingly with percentage to evaluate the characteristics of strength variation.

The main aim of the methodology is to:

- To evaluate strength characteristic of Black cotton soil with different percentage of fly ash and lime with varying proportion.
- To improve the properties of the Black cotton soil by adding admixtures.
- To determine the effect of Fly ash, Lime as stabilizing agents on Black cotton soil.

EXPERIMENTAL WORK

Following laboratory tests have been carried out as per I.S.2720. The test was carried out on both natural soil and stabilized soil with fly ash and lime.
Tests conducted on Black Cotton soil:

— Liquid Limit

Liquid limit is defined as the moisture content at which soil begins to behave as a liquid material and begins to flow. The importance of the liquid limit test is to classify soils. Different soils have varying liquid limits. Also, once must use the plastic limit to determine its plasticity index.

Figure 1. Determining the plasticity index

— Plastic limit

Plastic limit is defined as the percentage of moisture content and expressed as a percentage of the percentage of the oven dried soil at which the soil can be rolled into the threads one-eighth inch in a diameter without the soil breaking into pieces. This is also the moisture content of a solid at which a soil changes from a plastic state to a semisolid state.

— Standard and proctor test

Compaction is the process of densification of soil mass by reducing air voids under dynamic loading. This test is conducted in order to find out the optimum moisture content and maximum dry density of the soil.

Figure 2. Determining the compaction

— Unconfined compression test

The unconfined compression test is used to measure the shearing resistance of cohesive soils which may be undisturbed or remolded specimens. The shear strength of the expansive soil and the soil additive mixes were obtained by the unconfined compression tests performed according to IS.2720 part-10, 1991. An axial load is applied using either strain-control or stress-control condition.
The unconfined compressive strength (UCS) is the maximum axial compressive stress that a right-cylindrical sample of material can withstand under unconfined conditions—the confining stress is zero. It is also known as the *uniaxial compressive strength* of a material because the application of compressive stress is only along one axis—the longitudinal axis—of the sample

Figure 3. Determining the UCS

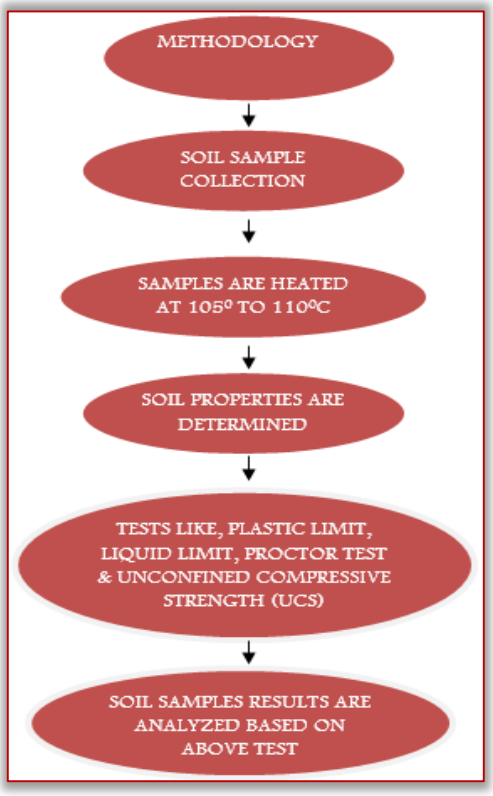

Figure 4. Methodology

EXPERIMENTAL DESIGN

The proportion of Black cotton soil is determined and then the soil is stabilized with varying proportion of lime and fly ash.

1. Black cotton soil + 5% fly ash
2. Black cotton soil + 10% fly ash
3. Black cotton soil + 15% fly ash
4. Black cotton soil +5% Lime + 5% fly ash
5. Black cotton soil +5% Lime+10% fly ash
6. Black cotton soil +5% Lime+15% fly ash

RESULTS

The soil samples have been investigated Geotechnical laboratory in our college for various Engineering properties. The results of the various routine tests and strength characteristics of soils found during investigations have already been mentioned above.

Table 2. Test on Black Cotton Soil

Sr.No.	Name of Test		Result
1	Liquid Limit		54.01
2	Plastic Limit		32.04
3	Compaction	OMC	14 %
		MDD	1.68 gm/cc
4	UCS		110Kn/m²

Table 3. Test on Black Cotton Soil with Different % of Fly ash.

Sr. No.	Name of Test		Results 5%	10%	15%
1	Liquid Limit		52	48	47
2	Plastic Limit		31	30	28
3	Compaction	OMC	15	15.5	16.5
		MDD	1.72	1.74	1.82
4	UCS		112	115	117

Table 4. Test on Black Cotton Soil for Combination of Lime and Fly ash

Sr No.	Name of Test		Results 5% L + 5% F	5% L + 10% F	5%L + 15% F
1	Liquid Limit		50	48	45
2	Plastic Limit		40	37	34
3	Compaction	OMC	17	16.7	16.9
		MDD	1.67	1.65	1.63
4	UCS		121	123	127

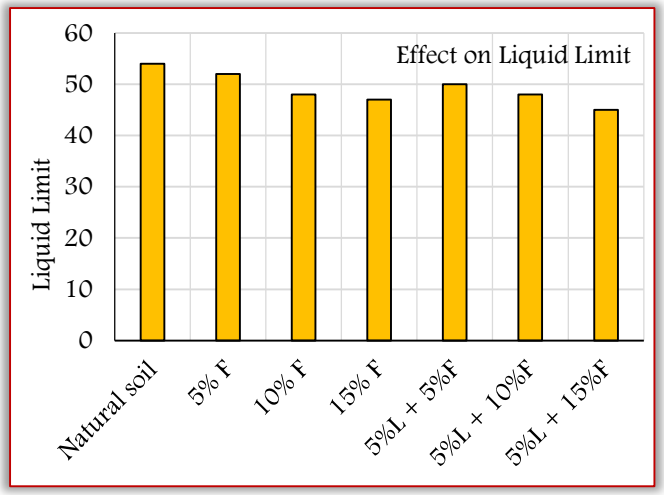

Figure 5. Comparison for liquid limit for natural soil, Fly ash and Lime Mixtures.

— Liquid limit

From the above Figure it shows that the liquid limit of natural Black Cotton Soil is 54.01 and it is declined with % increase in the fly ash content from 5% to 15% along with 5% Lime as constant.

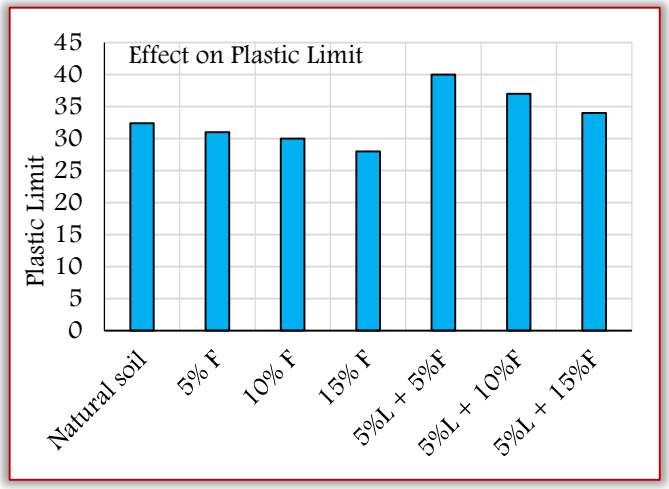

Figure 6. Comparison for Plastic Limit for natural soil, Fly ash and Lime Mixtures

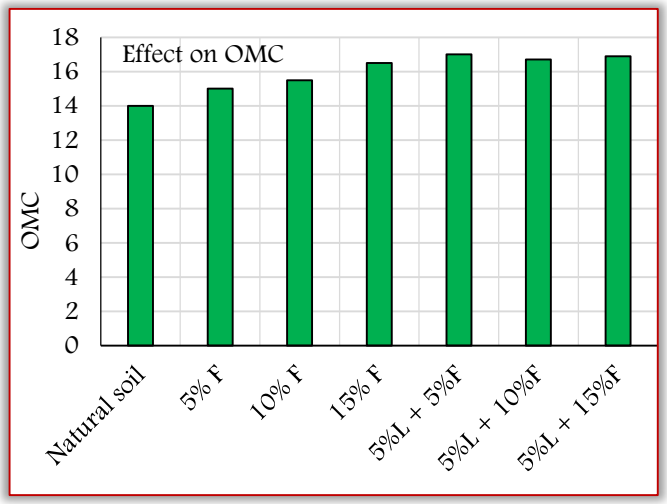

Figure 7. Comparison for Optimum Moisture Content for natural soil, Fly ash and Lime Mixtures

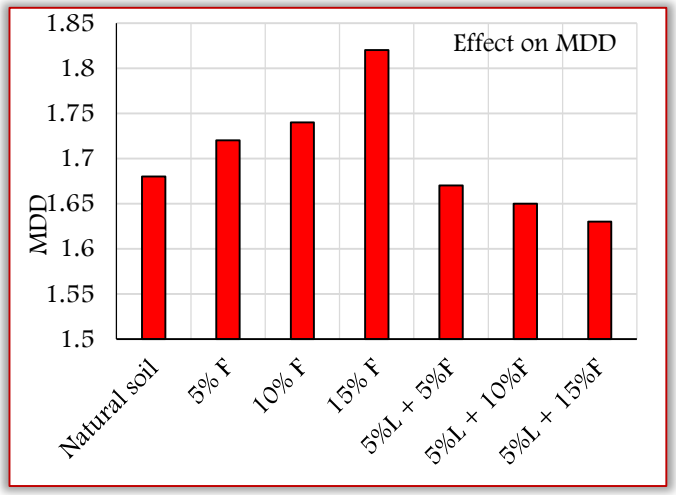

Figure 8. Comparison for Maximum Dry Density for natural soil, Fly ash and Lime Mixtures

— **Plastic limit**

With 15% of fly ash resulted the maximum decrement of 28% in the plastic limit of Black Cotton soil. With the 5% lime combined with 5% fly ash, there was an increase in plastic limit by 40% Black cotton soil.

— **Standard Proctor Test**

The readings for different Percentage are as below: With the varying Constant % of Lime and Varying % of fly ash for the calculation of Maximum dry density and Optimum moisture content. It has been found that with the increase in percentage fly ash there is an increase in Maximum dry density values where as there is considerable reduction in optimum moisture content for the given soil.

Combination of fly ash and Lime showed a consistent decrease in the maximum dry density (MDD) and increase in optimum moisture content (OMC).

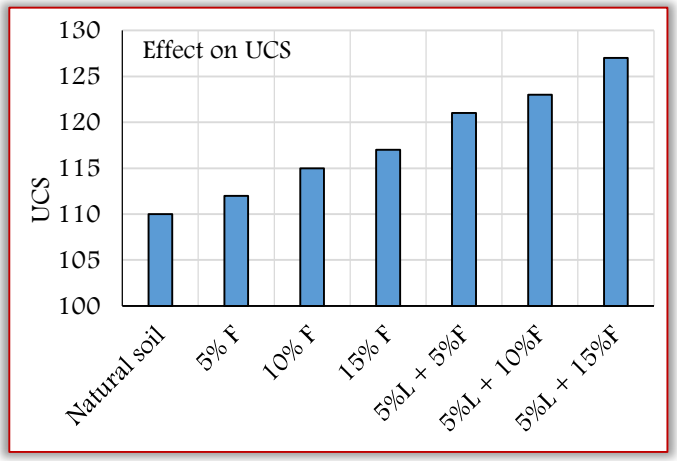

Figure 9. Comparison for Unconfined Compression strength for natural soil, Fly ash and Lime Mixtures

— **Unconfined compression test**

Natural Black Cotton Soil has 110Kn/m². With 5% of fly ash, the UCC value has increased by 112Kn/m²and further increment occurred with more percentage of fly ash added. When the lime was combined with fly ash, UCC value increased 121 on 5% of lime and 5% fly ash. The maximum UCC of the Black Cotton soil gained by 5% Lime and 15% Fly ash.

CONCLUSIONS

— With the use of Fly Ash and Lime in Black Cotton Soil near BHATGHAR Dam, there is a great change in Index properties. It further leads towards stabilization of soil. With the help of this stabilization of soil, which also leads to reduction in swell & shrink behaviour of BC soil

— When Lime and Fly ash are mixed with Black cotton soil. Plastic limit increases by mixing Lime and Liquid Limit decreases by mixing fly ash.

— As the amount of fly ash & lime increases there is reduction in Maximum dry density and increases in the OMC.

— It can be concluded that fly ash can be used in the civil Engineering Construction and it became more effective when mixed with 5%.

— UCS increases with increase in Fly ash it is observed from the UCS test the utilization of fly ash and in combination of fly ash and lime, the shear strength can be modified. Hence, stability is achieved.

— It can be concluded that the lime & fly ash are used in different proportion with the Black cotton soil is an effective method to tackle the problem of shrinkage, swelling and settlement.

SCOPE FOR FURTHER INVESTIGATION

— Natural soil has been stabilized with fly ash and lime. Percentage of mixing these stabilizing materials should be extended to get the optimum strength of soil.

— To avoid the erosion in the basins and life loss, stabilization by lime and fly ash can be done.

— Construction of foundation in marshy lands.

References

[1] Kaniraj S R, Havanagi V G. Compressive Strength of Cement Stabilized Fly Ash-soil Mixtures.*Cement and Concrete Res.*, 1999, 29(5): 673–677

[2] Cokca E. Use of Class C Fly Ashes for the Stabilization of an Expansive Soil,*Journal of Geotechnical and Geoenvironmental Engineering*, 2001, 127(7): 568–573

[3] Amer Ali Al-Rawas, Ramzi Taha, John D. Nelson, Thamer Beit Al-Shab, Hilal Al-Siyabi: A comparative evaluation of various additives used in the stabilization of expansive soils. Geotech Test. J. **25**(2), 199–209 (2002)

[4] Bell, F.G.: Lime stabilization of clay soils. Bull. Int. Assoc. Eng. Geol. **39**, 67 (1989)

[5] Karthik. S, Ashokkumar. E, Gowtham. P, Elango. G, Gokul. D, Thangaraj. S: Soil Stabilization By Using Fly Ash. Journal of Mechanical and Civil Engineering (IOSR-JMCE).e-ISSN: 2278-1684,p-ISSN: 2320-334X, Volume 10, Issue 6 (Jan. 2014)

[6] Amu, O.O., Fajobi, A.B., Oke, B.O. (2005) - Effect of eggshell powder on the stabilizing potential of Lime on an expansive clay soil. Journal of Applied Sciences, Vol. 5 (8), pp. 1474-1478.

[7] Muntohar, A.S. and Hantoro, G. (2000) - Influence of Rice Husk Ash and lime on engineering properties of a clayey sub grade. Electronic Journal of Geotechnical engineering, Vol.5

[8] Phani Kumar, B. R, and Sharma, S.R. (2004) - Effect of Fly Ash on Engineering Properties of Expansive Soils. J. Geotech. And Geoenvir. Engg. ASCE Vol. 130(7), pp. 764-767.

[9] Rajan, B.H., and Subrahmanyam, N. (1982)-Research on Rice husk ash for stabilizing Black cotton soil. Highway research bulletin, No.17, pp. 61-74.

[10] Satyanarayana, P.V.V, Rama Rao, R., and Krishna Rao, C.V. (2004) - Utilization of lime fly ash stabilized expansive soil in road side embankments. Proceedings of Indian Geotechnical Conference, Warangal, pp. 465-467.

[11] Sharma, A.K., Sivapullah, P.V. (2016) - Swelling behaviour of expansive soil treated with Fly Ash-GGBS based binder. Geomechanics and Geoengineering,
[12] Turker, D. and Cokca, E. (2004) - Stabilization of an Expansive Soil with Fly Ash and Sand. Proceedings of 6th International conference on Advances in Civil Engineering ACE2004, Istanbul, Turkey, pp.1613-1622.
[13] Sharma, S.R., Phani Kumar, B.R., and Rao, B.V. (2008) -Engineering behaviour of a remoulded expansive clay blended with lime, calcium chloride and Rice-husk ash. Journal of Materials in Civil Engineering, ASCE, Vol.20 (8), pp. 509-515.
[14] IS: 2720 (Part 5)-1985 "Code of practice for Determination of Liquid and Plastic Limit".
[15] IS: 2720 (Part 29) -1975 "Code of practise for Standard proctor test".
[16] K.R. Arora "Soil Mechanics and Foundation Engineering"

ACTA TECHNICA CORVINIENSIS – Bulletin of Engineering
ISSN: 2067-3809

[1.]S. PRAVEEN KUMAR, [2.]K. NARASIMHA RAO, [3.]Y. KRISHNA MOHAN

STUDY AND ANALYSIS OF THE OFFSET MHO CHARACTERISTICS FOR THE LOSS OF EXCITATION PROTECTION OF AN ALTERNATOR

[1-2.]Department of Electrical and Electronics Engineering, Gayatri Vidya Parishad College of Engineering, INDIA
[3.] Visakhapatnam Steel Plant- RINL, Andhra Pradesh, INDIA

Abstract: Loss of Excitation threatens the generator and power system stability. Several criteria have been proposed for loss of excitation detection and some of them are field under voltage/current criterion, impedance criterion, reverse reactive power criterion etc. Among them impedance boundary of steady state stability limit (SSSL) is widely used. But this criterion is sensitive to the variation of output active power of synchronous generator and may mal-operate in external faults, power swings and other non-LOE condition. In this study a Novel adaptive protection criterion with an offset mho element based on SSSL is used to distinguish LOE from non-LOE condition. This adaptive criterion could automatically adapt to the system operating modes and correctly operate in LOE condition. The impedance boundary circle of the steady state stability limit can adaptively fit for operating modes. The simulation results show that the adaptive impedance criterion is better for reliable protection against LOE and non-LOE condition.
Keywords: Adaptive criterion, External faults, Generator protection, Loss of Excitation (LOE), Power swings, Synchronous generator, Steady state stability limit

INTRODUCTION

In power generating plants Loss of Excitation (LOE)is a critical fault condition caused due to the accidental tripping of a field breaker, AVR system failure, field open short circuit (flashover of the slip rings), or even generator protection mis-operation. With the development of power system network Loss of Excitation protection of synchronous generators is becoming more and more important for the reliability of the system [1].

Generator may completely or partly lose its field excitation. Complete loss of excitation means the generator field voltage is reduced to zero. The partial loss of excitation means only part of field winding is excited by the voltage. Loss of Excitation causes the generator to absorb large amount of reactive power from the grid. This condition causes the machine speed to go above the synchronous speed, and the machine starts operating like an induction generator. So, the machine draws a large amount of reactive power from the power system [2][3].

Generator may fail to have its field supply due to various causes. Generally, the generator may completely or partially lose its excitation depending upon the cause. Some of the reasons for occurring of the loss of excitation condition are,

- Field winding open circuit.
- Field winding short circuit.
- Flash over occur at brushes or slip rings.
- Loss of supply to the main exciter.
- Accidental field breaker tripping.
- AVR control circuit failure.

LOE PROTECTION BASED ON IMPEDANCE METHODS

Mho distance relays are widely used within the industry to provide high – speed LOE detection. Currently, the most accepted methods for LOE protection are the Berdy and Two zone positive Offset approaches. Both are impedance – based methods with a negative offset Mho and Two zone positive offset Mho with directional unit supervision [4][5].

—Berdy or negative offset Mho relay characteristics:

Negative Mho offset relay is a single-phase single element high speed distance relay. It is arranged to operate from the voltage between two phases, and the difference between the currents of the two phases, at the terminals of the generator to be protected. The operating characteristic plotted on an R-X diagram.

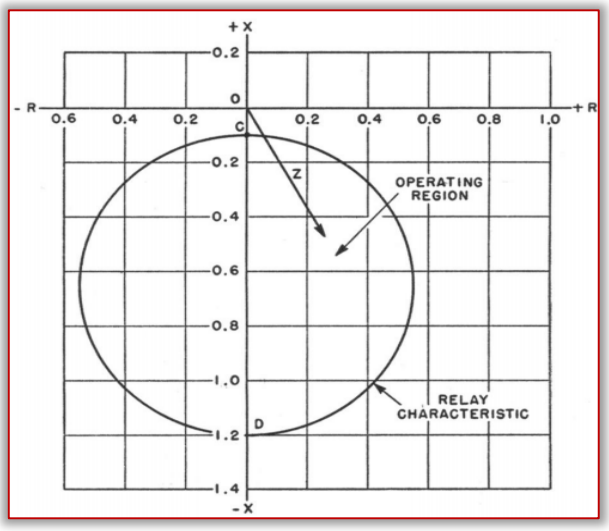

Figure 1. Operating characteristics of negative offset Mho relay

The centre of the circle is on the –X axis. The Offset is approximately equal to half of the direct – axis transient reactance of the generator and diameter is approximately its direct -–axis synchronous reactance. The relay will operate to close its contacts for any impedance vector such as Z, which terminates within the circular operating characteristic shown in figure 1[6].

—Two zone positive Mho offset with directional unit:

Two zone positive offset contains two circle zones shown in figure 2. One is outer circle called as zone-2 and the inner circle is called as zone-1. Zone-2 reach diameter is equal to 110% of direct axis reactance (X_d) plus system reactance (Xs) with an offset which is equal to the system reactance (Xs). Generally, the system reactance (Xs) is considered as both the transformer reactance (X_t) plus transmission line system reactance. But in this proposed scheme only transmission line reactance (Xs) is considered and the transformer reactance is neglected. Here the system reactance (Xs) is referred as the transformer reactance (X_t) [7].

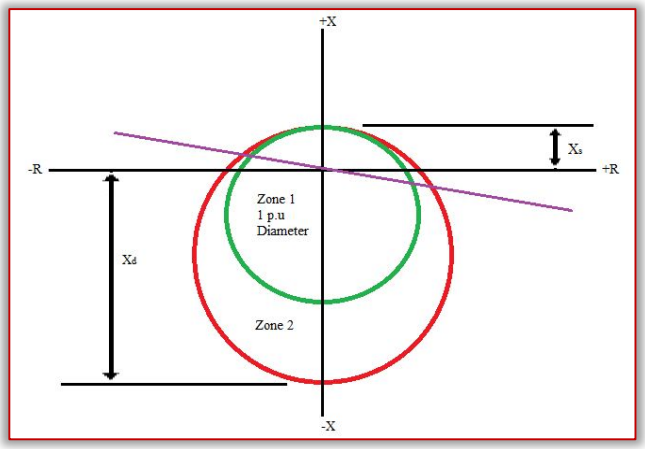

Figure 2. Two positive offset mho relay characteristics

STEADY STATE STABILITY LIMIT CIRCLE

The Impedance boundary criterion of steady state stability limit is commonly used for the detection of the Loss of Excitation (LOE). It is analyzed in a single-machine infinite bus system, as shown in the fig 3[1][6][8].

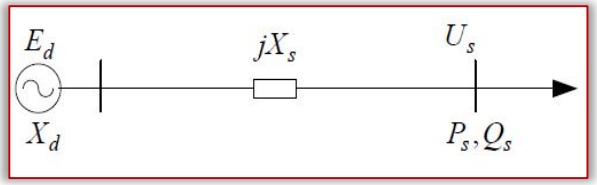

Figure 3. Single Machine Infinite Bus System

As the system shown in Figure 3, the active and reactive power of the synchronous generator can be expressed as follows:

$$P_s = \frac{U_s E_d}{X_d + X_s}$$

$$Q_s = \frac{-U_s^{\,2}}{X_d + X_s}$$

where, X_d is the synchronous reactance of a non-salient pole generator; E_d is the inner electric potential of the generator; X_s is the connecting system reactance; U_s is the voltage of infinite-bus system; P_s, Q_s is active and reactive power output to the system.

Then the impedance boundary of SSSL at the generator terminal is:

$$Z_{G.cr} = \frac{V_s^{\,2}}{P_s - jQ_s} + jX_s$$

$$Z_{G.cr} = \frac{-j(X_d - X_s)}{2} + j\frac{(X_d + X_s)}{2} e^{j2\varphi})$$

where, $\varphi_s = \arctan\frac{Q_{s,cr}}{P} = \arctan\left[\frac{-U_s^{\,2}}{(X_d + X_s)P}\right]$

ADAPTIVE PROTECTION CRITERION FOR LOSS OF EXCITATION PROTECTION

From the beginning of Loss of Excitation to the boundary of Steady State Stability Limit (SSSL) and in normal operating conditions, slip is approximately equal to zero, and the excitation voltage U_L is equal to the electrical potential, E_d in per unit value.

Then the impedance boundary circle shown in Figure4 is as follows:

$$Z_{G.cr} = -j\frac{U_{lb}}{2P_s}\left(1 - e^{j2\varphi}\right) + jX_s$$

$$= \frac{-jU_{lb}}{2P_s} + j\frac{U_{lb}}{2P_s} e^{j2\varphi_s} + jX_s$$

From the above equations the center, $C=\left[0, \frac{-jU_{lb}}{2P_s}\right]$ and the radius will be as shown below, $r = \frac{U_{lb}}{2P_s}$,

Where U_{lb} and X_s are the impedance boundary circle settings of the adaptive protection criterion.

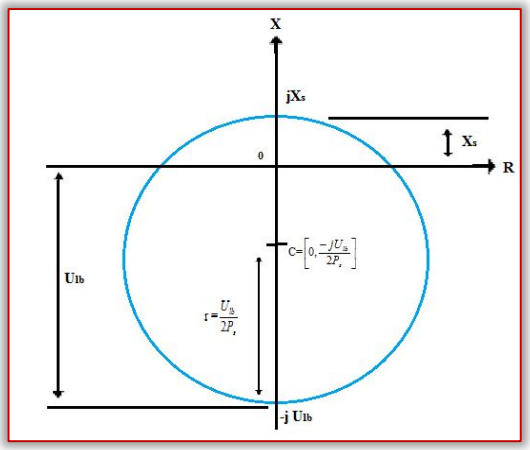

Figure 4. The Impedance boundary circle of adaptive protection criterion

To develop a complete protection scheme, some methods to resolve the problems like external fault, power swings etc.

≡ Method 1: External fault can be resolved by adding negative sequence current blocking unit for ground or arcing ground faults, and directional unit for symmetrical faults. A time delay unit can also resist external fault well.

≡ Method 2: Power swing, time delay could be adopted to prevent mal-operation.

According to all the analysis above, a LOE protection scheme based on the adaptive criterion could be presented as shown in Figure 5.

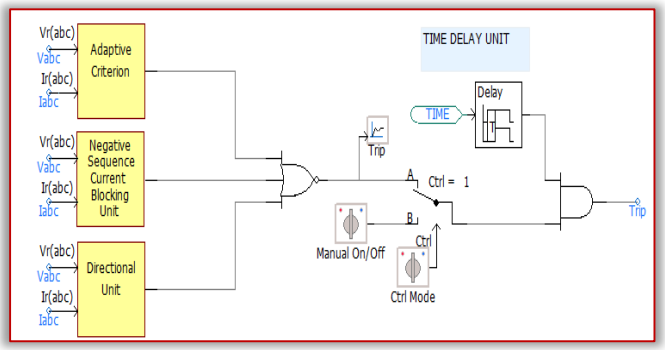

Figure 5. Adaptive LOE protection scheme logic diagram

PROPOSED ALGORITHM ON PSCAD

The PSCAD model of test power system model is developed. Loss of Excitation is obtained by applying timed logic field voltage tripper. Protection algorithm is developed using Frequency Fourier Transform (FFT) blocks. These FFT blocks extract the phase voltages and the phase currents. The phase voltages and currents are converted into Positive, Negative and Zero sequence voltages and currents respectively by sequence filter blocks is in Figure 6.

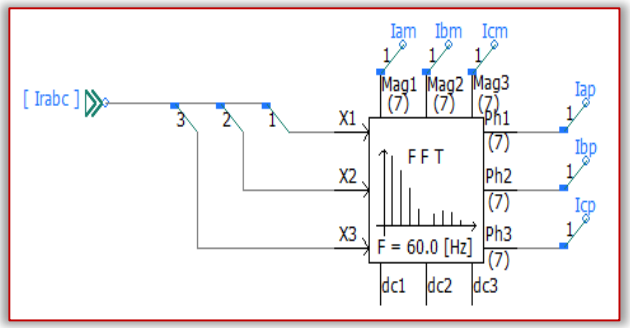

Figure 6(a). Frequency Fourier Transform (FFT) blocks for phase currents

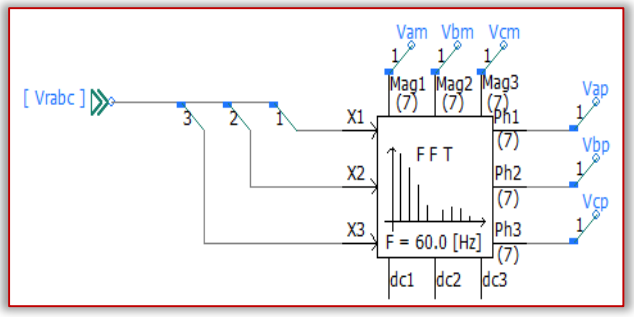

Figure 6(b). Frequency Fourier Transform (FFT) blocks for phase voltage

From the direct axis reactance and transient reactance parameters of the test system synchronous generator, the Zone1 and Zone 2 circles radius and origins are calculated. These calculations are done using the subsystems shown in Figure 7. These values are given to the Offset mho relay block and time delay block introduce to set relay intentional time delay for each zone. Finally, these two zones of relays are connected by OR gate and output of this gate create a relay trip signal.

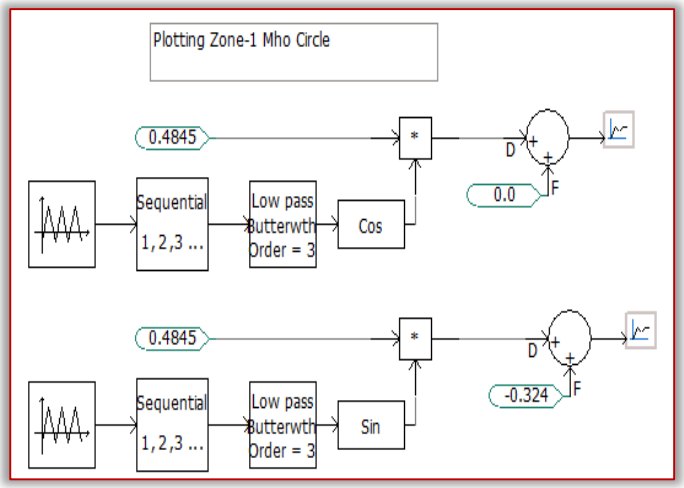

Figure 7(a). Algorithm to plot zone1 Mho circle

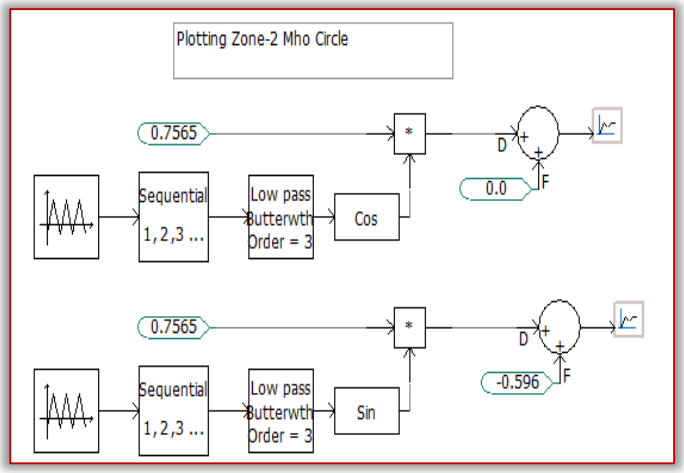

Figure 7. Algorithm to plot zone2 Mho circle

SIMULATION RESULTS OF THE ADAPTIVE LOE PROTECTION CRITERION

The simulation results were shown for the two different cases

—LOE (During field fault condition)

From the Figures 8 and 9, it can be observed that in the case of without adaptive protection criterion the impedances trajectories took more time to enter in the impedance circles.

During light load condition even, trajectory didn't enter into the impedance circle. But with the case of adaptive protection criterion follows the change of the generator load, impedance trajectories took shorter time to enter into the circles to reliably trip rather than the traditional impedance criterion.

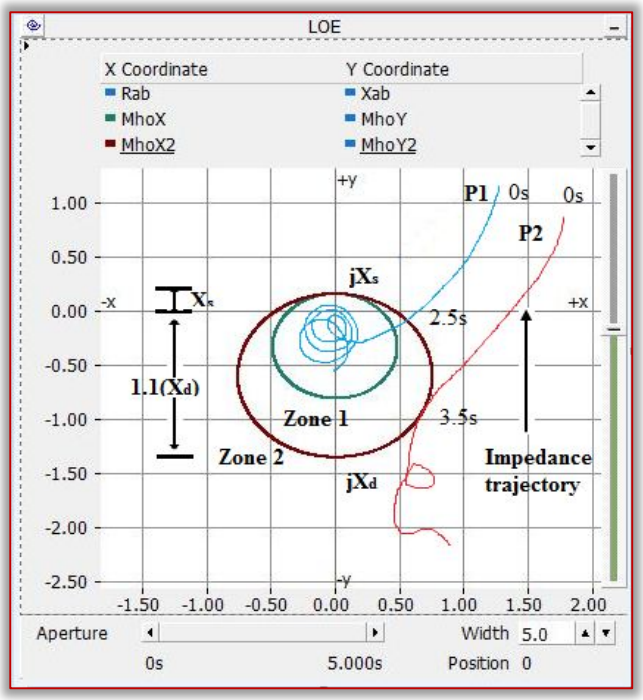

Figure 8 Impedance boundary circles and trajectory of LOE without adaptive protection criterion in R-X plane.

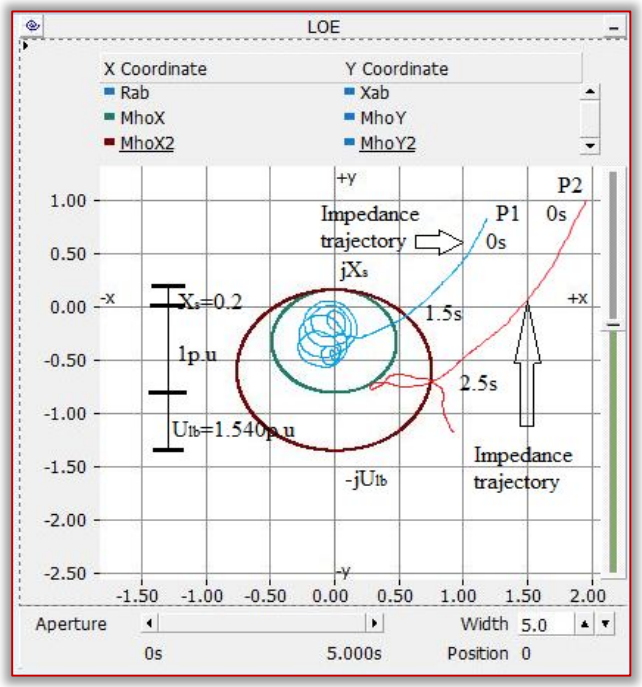

Figure 9. Impedance boundary circles and trajectory of LOE with adaptive protection criterion in R-X plane.

—Non-LOE (External fault condition)

From the Figures 10 and 11, it can be observed that with adaptive protection criterion, the simulation results under single phase ground fault are verified the effectiveness of the blocking methods mentioned above.

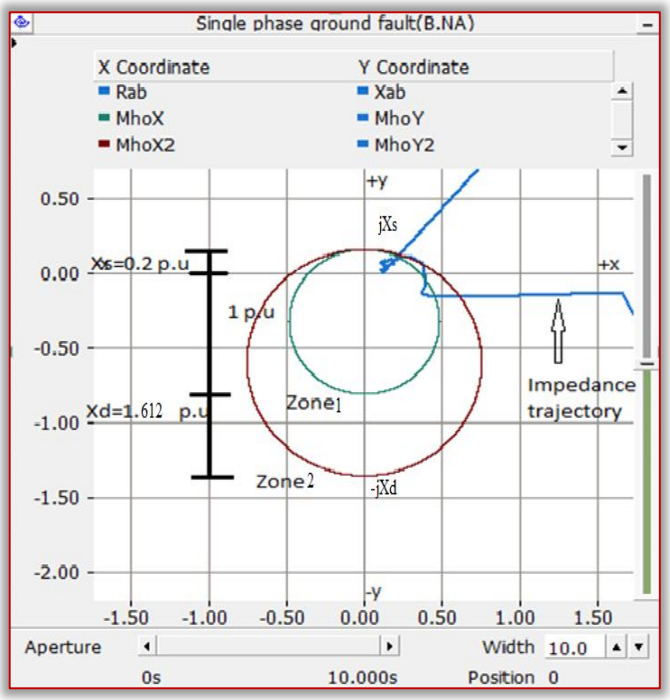

Figure 10. Impedance boundary circles and trajectory of single-phase ground fault without adaptive protection criterion in R-X plane

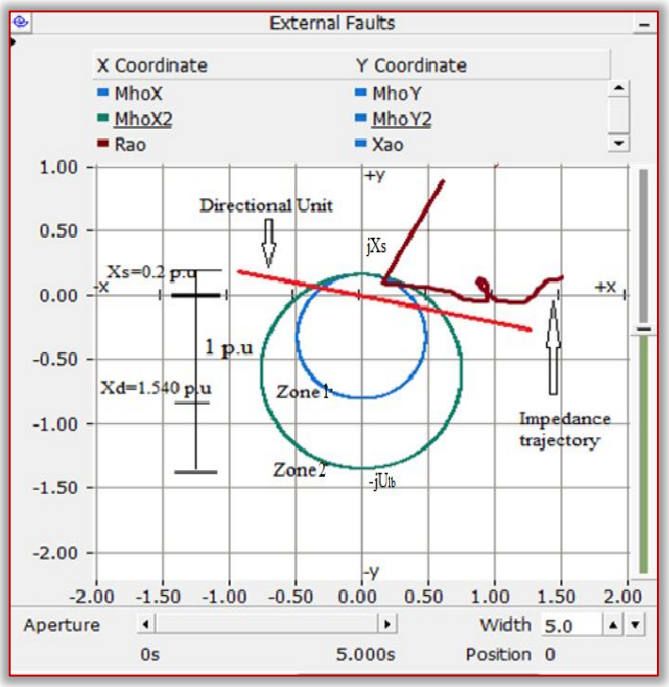

Figure 11. Impedance boundary circles and trajectory of single-phase ground fault with adaptive protection criterion in R-X plane.

For the external faults the impedance trajectory is much faster than LOE, in order to avoid this the negative sequence current unit and directional and a time delay is used.

From the Figures 12 and 13, it can be concluded that the simulation results under the three-phase ground fault is verified with and without adaptive protection criterion and verified the effectiveness of the blocking methods.

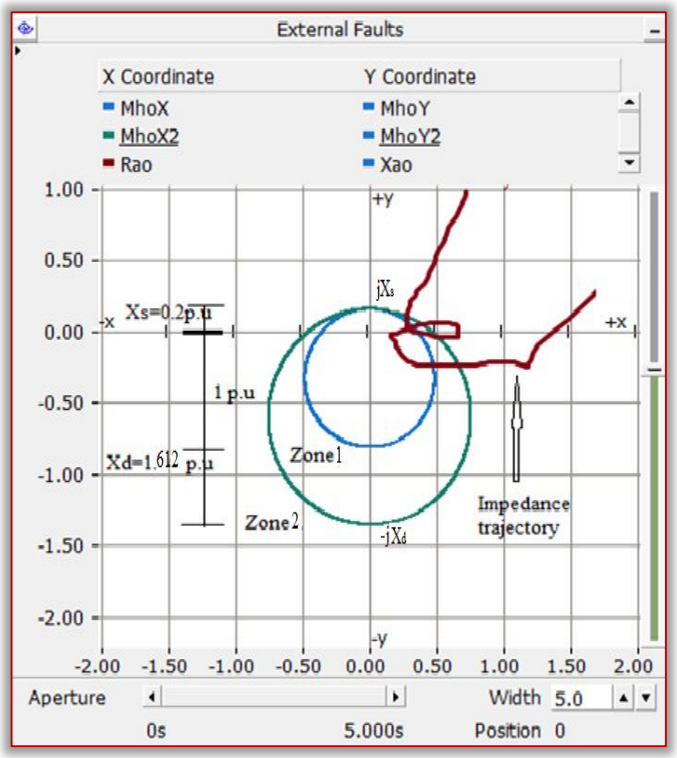

Figure 12. Impedance boundary circles and trajectory of three phase ground fault without adaptive protection criterion in R-X plane

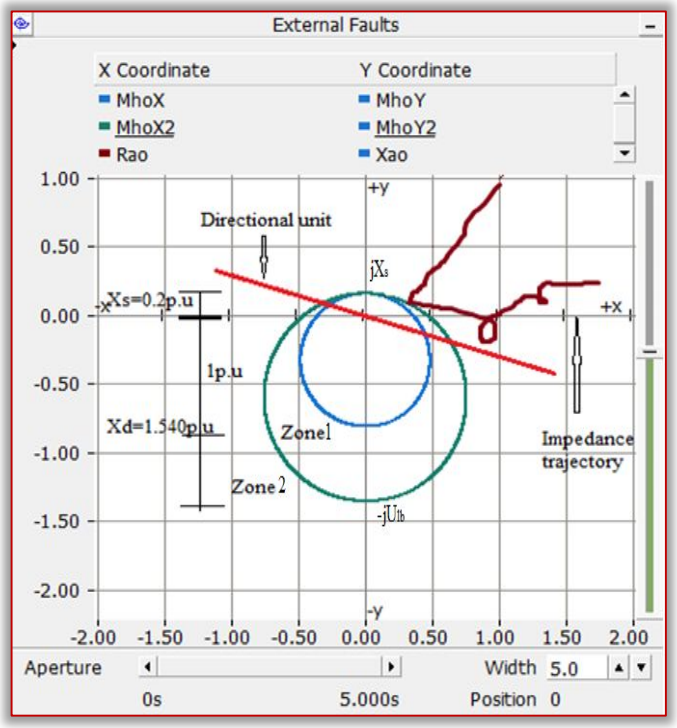

Figure 13. Impedance boundary circles and trajectory of three phase ground fault with adaptive protection criterion in R-X plane

The impedance trajectory of the three-phase fault is blocked by the blocking units like negative sequence current blocking unit and directional unit and time delay unit to resist the impedance trajectory, not to enter into the circles. This is how the relay mal operation is overcome during the non-LOE condition. By this the effectiveness of the relay will improve to operate at the different operating modes at different fault conditions, and reliability of the power system is improved.

CONCLUSIONS

It is observed that the traditional impedance boundary criterion scheme fails to differentiate the LOE and non-LOE condition, but with the Adaptive protection scheme, it is able to detect and mitigate the mal-operation of relays during non-LOE conditions. Not only that, the traditional impedance scheme takes more time to give the trip initiation, when compared with the adaptive protection criterion with the positive offset mho element.

- With the help of Adaptive criterion, the reliability of the system at different operating conditions is improved and reduce mal-operation of LOE protection.
- Mal operation over the external faults is avoided by adding negative sequence current blocking unit and directional unit, which improved the reliability of the protection scheme.

References

[1] Ya-dong Liu ; Zeng-ping Wang ; Tao Zheng ; Li-ming Tu ; Yi Su ; Zhao-qiang Wu, "A Novel Adaptive Loss of Excitation Protection Criterion Based on Steady State Stability Limit", IEEE PES Asia-Pacific Power and Energy Engineering Conference (APPEEC)" 2013

[2] D. Reimert. "Protective Relaying for power generation systems", Boca Raton: CRC Press, 2006, pp. 321-355.

[3] Charles J. Mozina, Michael Reichard "Coordination of Generator Protection with Generator Excitation Control and Generator Capability", IEEE Power Engineering Society General Meeting, 2007

[4] Z.P.Shi, J.P.Wang, Z.Gajic, C.Sao, M. Ghandari, "The Comparison and Analysis for Loss of Excitation Protection Schemes in Generator Protection", Conference paper, 2014.

[5] Nitish Kumar D, R.Nagaraja, H.P.Kincha, "A comprehensive Protection Scheme for Generator Loss of Excitation, IEEE conference, 2014.

[6] Berdy, J. "Loss of Excitation Protection for Modern Synchronous Generators," IEEE Trans., PAS, 1975, 94, pp. 1457-1463.

[7] C. R. Mason. "A New Loss of Excitation Relay for Synchronous Generators," AIEE Trans., Vol. 68, pt. II, pp. 1240-1245, 1949.

[8] Amini, M., Davarpanah, M., Sanaye-Pasand, M: "A Novel Approach to Detect the Synchronous Generator Loss of Excitation", IEEE Trans. Power Deliv., 2015, 30, (3), pp. 1429 –1438.

[9] IEEE PES, "IEEE Guide for AC Generator Protection", IEEEStd-2005.

[10] Adriano P. de Morais, Ghendy Cardoso, Jr., and L. Mariotto, "An Innovative Loss-of-Excitation

Protection Based on the Fuzzy Inference Mechanism", IEEE Transactions On Power Delivery, Vol. 25, No. 4, 2010.
[11] Avijit Maity, Kesab Bhattacharya, Amar Nath Sanyal, "Asynchronous Operation of Synchronous Generators under Field Failure". Conference paper, 2012.
[12] Yao Siwang, Wang Weijian, Luo Ling, Gui Lin, Qiu Arui, "Discussion on Setting Calculation of Loss-Of-Excitation Protection for Large Turbogenerator", conference paper 2010.
[13] BHEL Generator Manual, BHEL AVR Manual, MICOM Relay Manual.

ACTA TECHNICA CORVINIENSIS – Bulletin of Engineering
ISSN: 2067-3809

[1.]Andrei Mihai BACIU, [2.]Imre KISS

REVIEW ON THE POST–CONSUMER PLASTIC WASTE RECYCLING PRACTICES AND USE THEIR PRODUCTS INTO SEVERAL INDUSTRIAL APPLICATIONS

[1.]University Politehnica Timisoara, Faculty of Engineering Hunedoara, Center for Research in Advanced Materials & Technologies, Hunedoara, ROMANIA
[2.]University Politehnica Timisoara, Faculty of Engineering Hunedoara, Department of Engineering & Management, Hunedoara, ROMANIA

Abstract: The global plastic production has increased immensely during the last decades and the plastics have become an essential part of our modern lifestyle. This has contributed greatly to the increasing quantity of plastic–related waste. Numerous plastic waste materials are generated both from production and from the population, plus a few other special waste streams, such as packaging. The increasing awareness about the environment has tremendously contributed to the concerns related with disposal of the generated wastes. Reuse of waste and recycled plastic materials in several application as an environmental friendly by–products has drawn attention of researchers in recent times, and a large number of studies reporting new developments in this area. This paper presents a conceptual overview related to the plastic products categories (easily recyclable and rarely recyclable plastics), plastic materials recycling (mechanical recycling, chemical mechanical recycling and energy recovery), and recycling of the post–consumer plastic waste. Also, the paper presents the most important applications of the recycled plastic materials.
Keywords: plastic waste, types of plastic, waste hierarchy, post–consumer waste, recycling & reuse of plastics

INTRODUCTIVE NOTES

Plastics, also called polymeric materials, allow the obtaining in large manufacturing series of different sizes product, rigid or flexible, transparent or coloured. The plastic products are characterized by the diversity of processing processes, under the conditions of a high productivity compared to the traditional materials.[1–6] Most polymers have low densities, around 1 g/cm3 (polypropylene is 0.90 g/cm3, polycarbonate is 1.2 g/cm3, polyethylene varying from as low as 0.912 g/cm3 to as high as 0.975 g/cm3), compared to traditional materials (7.8 g/cm3 for steel, 2.7 g/cm3 for aluminium and 2.54 g/cm3 for glass), which ensures light products with satisfactory qualities especially in the field of consumer goods.[1–6] To the obvious qualities, noted above, the advantages conferred by the pleasing appearance and colouring or by the resistance to corrosion are not infrequently added. The combined action of the above advantages often determines the preferential use of plastics, being light, strong and resource–efficient.[1–9]

The needs of a modern society, which stimulated the intensive development of the plastic's production, determined the consecration of activities directly or indirectly related to their production, use and strictly management.[1–12] The consumption of plastic materials is increasing worldwide, with dozens of types of plastics being known. Of these, several types are used in the manufacture of packaging, other types in manufacturing of several consumer goods, in automotive related industry, in construction industry etc.[2–7,13–16]

Most of the world's plastic production, however, is transformed into polluting waste.[1–17] Every year, large quantities of waste are generated both from production and from the population, plus a few other special waste streams, such as packaging.[1–12] The plastic packaging reaches the first to the garbage dump (Figure 1) or to the collection centres.[2,4–7,12–16] Annually, over 8 million tonnes of plastic of all categories end up in the environment and then in the oceans.[1–18]

Figure 1. Large quantities of plastic waste

Due to the wide variety of plastic waste as well as their increasing quantities, their collection, recycling and processing has become an acute problem lately.[1–18] Thus, large quantities of waste occupy large areas of land, and the respective wastes are highly resistant to natural degradation factors.[3–5,11,13–16] Given that the volume of waste deposited in landfills needs to be stabilized or reduced, increasing the volume of

waste highlights the importance of ensuring new waste treatment capacities (recycling, reuse, co–incineration, etc.).[1–18]

Of the most harmful polymers, we mention the category of thermoplastic materials, which include polystyrene (PS), polycarbonate (PC), polyamides (PA) and polyvinyl chloride (PVC) or those found in packaging (container body, bags), such as polyethylene terephthalate (PET), polyethylene (PE) – low density polyethylene (LDPE) and high density polyethylene (HDPE) – and polypropylene (PP).[1,4,5,14]

The share of packaging waste (which also includes plastic packaging, Figure 2) from the total municipal solid waste generated has increased significantly in recent years, following the increasing trend of the quantities of packaging placed on the market.[1,3,7,11] Some statistics say that packaging waste accounts for up to 15–20% of the municipal waste stream, and polyethylene terephthalate (PET) waste accounts for about 3–5% of this quantity.[1–17]

Figure 2. Plastic packaging products

The wide range of different plastics with different properties and applications makes the collection and sorting of plastics much more complex than for most other basic materials such as metals, paper or glass.[4,5,7–11] In some cases, it can work reasonably well, e.g. in the collection and recycling of PET bottles. In other cases, there are no set systems – such polystyrene (PS) and polyvinyl chloride (PVC) from construction – or the existing system is simply not working well enough.[4–9] Globally only 9% of plastic ever produced has been recycled, whilst 79% can now be found in landfills, dumps or the environment and 12% has been incinerated (Figure 3). Plastics are all around us, a large part is incinerated or much of its value is lost once a plastic object has been used just once. Almost 50% of the plastic waste generated globally was single–use packaging.[17,18]

Figure 3. Globally plastic waste recycled, landfilled and incinerated

The rate of plastic production has grown faster than that of any other material.[3,5,17,18] Researchers estimate that about 60% of that plastic has ended up in either a landfill or the natural environment.[3,7,9,17,18] We need to slow the flow of plastic at its source, but we also need to improve the way we manage plastic waste, because a lot of it ends up in the environment.[1–18] By efficiently managing plastic waste (including the packaging waste), the amount of waste that is deposited at landfills is significantly reduced. Also, the recovery of plastics from post–consumer waste can lead to the saving of crude oil (basic raw material) and some of the energy used in manufacturing processes.[2,9,11,13–18]

The world is already struggling with its plastic waste and recycling issues. Therefore, the recycling of post–consumer plastic waste is increasingly promoted as the means to achieving circular economy. It converts plastic waste into a secondary material that can be fed back into the system, for use in the same or new products, with similar or lower functionality.[1–37] However, this is not so simple. The wide variety of polymers currently used is a major obstacle to the recycling of all plastics.

RECYCLING PACKAGING MATERIALS

The environmental aspects of the use of packaging are of great importance.[17–24,26–37] For a particular packaged product, the most appropriate approach must be chosen, which can be described as follows:[2,5–11,16–37]

- the volume and mass of the packaging must be minimized and redesigned the current packaging size to optimize it for space, maintaining the required levels of safety, hygiene and acceptability for the packaged product and its user;
- the packages must be manufactured in such a way as to allow reuse according to the rules in force;
- the packages must be manufactured in such a way as to allow the recovery of materials, energy recovery or composting, in accordance with the norms in force.

The most effective way to reduce waste is to not create it in the first place. Making a new product requires a lot of materials and energy – raw materials must be extracted from the earth, and the product must be fabricated then transported to wherever it will be sold.[4,5,7–11] As a result, reduction and reuse are the most effective ways you can save natural resources, protect the environment and save money.
Specific measures regarding the prevention and / or reduction of the quantities of waste resulting from each container and packaging products production and use can be achieved by implementing policies and practices such as:

- efficient management of materials destined to packaging (paper and corrugated paperboard, glass, steel, aluminum, plastics, wood, and small amounts of other materials);
- reducing packaging quantities through new packaging solutions and strategies;
- efficient management of all packaging waste.

Basically, there is no ideal ecological solution for packaging, being only a multitude of measures that can be taken.[16–24] One of them is recycling, processing of empty packaging, so that it is brought to their original form or a similar model. Some materials are very suitable for recycling. Others, although theoretically are recyclable, they require complicated procedures and technologies.
Some packaging materials are not suitable for recycling. Because of this, other storage methods must be found for them, not just garbage pits. One solution might be burning, but some materials become very polluting in this process. Landfill process has several disadvantages such as wastes have great volumes, decrease of the areas in which the wastes are stored, high cost and contamination of water and soil. Due to these reasons, the process of landfill should be preferred in a situation when the process of recycling cannot be performed.[19,25–27]

Figure 4. The waste hierarchy

REDUCTION (Figure 4) is the first and most important step in material efficiency practices and the prevention of packaging waste formation.[2,6–9,12–16,19–11] It is the essential element of this problem, because it involves the actions of eliminating or reducing the toxicity of the materials before they reach the landfill. The reduction of raw materials includes the following actions:

- reducing the use of non–recyclable materials;
- replacing available materials and products with reusable materials and products;
- reducing the amount of generated waste;
- increasing the efficiency of the use of all packaging destined materials.

REUSING (Figure 4) is the next step in the efficiency of materials and in the prevention of waste formation. The actual reuse preserves the original structures of the material. In fact, the reusing is the practice of using a product, whether for its original purpose (conventional reusing) or to fulfil a different function (creative reusing or repurposing).[12,21]
RECYCLING (Figure 4) is the third step of this hierarchy, which involves converting the waste into a raw material for re–manufacturing. By replacing natural materials with recycled natural resources, natural resources and energy are conserved. In fact, by transforming waste into usable resources, recycling offers a way of managing waste by reducing pollution, conserving energy and developing more competitive manufacturing industries.[12,21–37]
RECYCLING differs from REUSE in that it transform wastes into new raw materials which are then used to make new product, as opposed to reusing the intact waste. As this extra processing requires energy, and therefore, REUSE is environmentally preferable to RECYCLING.[12,21]
Over the last decades, the plastic fraction of plastic waste is treat by incineration or landfilling, although the recycling is possible, their mechanical properties making them adequate to produce constructive components like bricks, synthetic coarse aggregates for concrete or armouring fiber for a concrete mixture in building materials sector.[27] Thus, plastic fraction of waste could be used to develop novel recycled materials.[19–37]

PLASTIC PRODUCTS CATEGORIES

Today the plastic materials are produced from fossil based chemicals that are put together into long fibers, molecular chains. Currently, petrochemical plastics such as polyethylene terephthalate (PET), polyvinyl chloride (PVC), polyethylene (PE), polypropylene (PP), polystyrene (PS) and polyamide (PA) have a relatively low cost and a good cost, mechanical performance, such as breaking resistance, ensures heat tightness, etc. Given that the accumulation of large quantities of these materials in the environment has serious and irreversible ecological consequences, the current global approaches are focused on the use of efficient recycling strategies and practices.[19–37]

Figure 5. Plastic products categories
PET/PETE, plastic products of category # 1; HDPE, category # 2 plastic products; V or PVC, plastic products of category # 3; LPDE, plastic products of category # 4; PP, plastic products of category # 5; PS, plastic products of category # 6; OTHERS, plastic products of category # 7

Of the 7 types of plastic (Figure 5) we meet on the market, each is composed of different substances that must be treated individually. The first step to knowing how to recycle or reuse plastic is to easily identify the waste category:

— Polyethylene Terephthalate (PET, plastic products of category # 1) is one of the most used types of plastic and is found in most colourless or colour water and soft drinks bottles or other containers used for consumer goods. It is intended for single use only. It is a lightweight, durable and easily recyclable material that can be transformed into polyester fibres or foil. In the recycling process, the plastic is crushed into flakes which are then reprocessed to create new products. PET must be recycled, but not reused (Figure 6).

— High Density Polyethylene (HDPE, category # 2 plastic products) is a rigid type of plastic from which detergent canisters are produced, is the most frequently recycled type of plastic and is considered among the least dangerous plastic forms. HDPE products are reusable and recyclable (Figure 6).

— Polyvinyl Chloride (PVC, plastic products of category # 3) is a soft and flexible type of plastic used for food packaging or for the production of plastic products. PVC is cheap, durable, easy to handle, but it is a major threat to the environment as it is very difficult to reuse, difficult to recycle and requires high costs in the recovery process. PVC products are not recyclable, and many of them are not reusable (Figure 8).

— Low Density Polyethylene (LPDE, plastic products of category # 4) is a type of plastic often found in heat–insulating packaging, in shopping bags, but also in some clothes and furniture items. This type of plastic is considered to be less toxic than others, but it is not normally recycled that LDPE recycling products are not very resistant. LDPE products are reusable, but not usually recyclable (Figure 7).

— Polypropylene (PP, plastic products of category # 5) is a type of hard and light plastic that has excellent qualities of heat resistance. It is used for packing food, for making the bottle caps. PP products are considered safe for any reuse, but their recycling is done only under certain conditions (Figure 7).

— Polystyrene (PS, plastic products of category # 6) is a cheap, lightweight plastic with a wide variety of uses: from disposable products to building materials. It is one of the most used plastics, found in expanded, extruded or foam forms. PS products should be avoided where possible, as their recycling is quite difficult (Figure 8).

— The plastic products of category # 7 are made from a combination of the other types of plastics or from less commonly used plastics (such as PC–polycarbonate or unlabelled plastic) and are difficult to recycle because they do not fall into a fixed category. These plastic products are not recommended for reuse (Figure 8).

Packaging containers (PET–polyethylene terephthalate) and their caps (PP–polypropylene) are among the most polluting plastic articles found in nature, analysing the quantities of waste they produce, as well as the existing recovery options. The management modalities (according to the waste hierarchy) are multiple such as reuse, recycling, reuse as raw material, incineration or final storage. Although most thermoplastic polymers can be recycled, recycling PET containers is much more practical.

Figure 6. Always recyclable plastics

Figure 7. Sometimes recyclable plastics

Figure 8. Rarely recyclable plastics

Polyethylene terephthalate (PET, category # 1 plastic products) appears in waste from the packaging of non–alcoholic or soft drinks, water (flat or carbonated) or beer. Containers for bottles stained with liquid detergent, cosmetics or shampoo are high density polyethylene products (HDPE, plastic products of category # 2). The caps of these containers are made of polypropylene (PP, plastic products of category # 5). They are not suitable for reuse (although they are reused), but they are easily recyclable in many products.

Figure 9. Easily recyclable plastics

All these plastic products (categories # 1, 2, 4 and 5, Figure 9) although they could be recycled, do not always reach the collection system. However, according to numerous researches, there are alternatives.[19–37]

PLASTIC MATERIALS RECYCLING

Household refuse and industrial disposal of plastic materials is a major environmental concern.[15] Because of legal requirements, which have been enforced to protect the environment, there is a pressing need to develop methods to recycle plastic waste.

RECYCLING (Figure 10) is an important key factor to get plastics into a circular economy, as we above–mentioned. Plastics recycling is the process of waste plastic reprocessing into useful by–products.[19–37] Since the majority of plastic materials are non–biodegradable, the recycling actions are an important part of global efforts to reduce plastic in the waste stream.[1–37] Mechanical recycling has emerged as the most economical, as well as the most energetic and ecologically efficient option. (Figure 10)

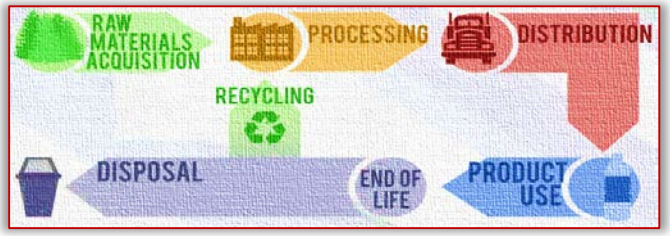

Figure 10. Recycling into a circular economy – a concept

Energy recovery is a valuable alternative for plastics–rich waste fractions that cannot be sustainably recycled.[16] Some plastics cannot be recycled in an eco–efficient manner. For these plastics, energy recovery (Figure 11) is the most resource–efficient solution available when compared to landfilling.[16]

Therefore, there are two major ways to recycle plastic products, including the packaging plastics:

- MECHANICAL RECYCLING, where the plastic is washed, ground into flakes and melted, and
- CHEMICAL RECYCLING, where the plastic is broken down into basic components.

MECHANICAL RECYCLING where the plastics are sorted, grinded, washed and then reused in the production to partly or fully replace virgin polymers.[13–16,19] Key requirements for successful mechanical recycling are large, homogenous streams with constant and even quality. To achieve this, the design of the packaging is very important for recycling and waste management with collection of sorted waste at the households to avoid contamination (Figure 11).

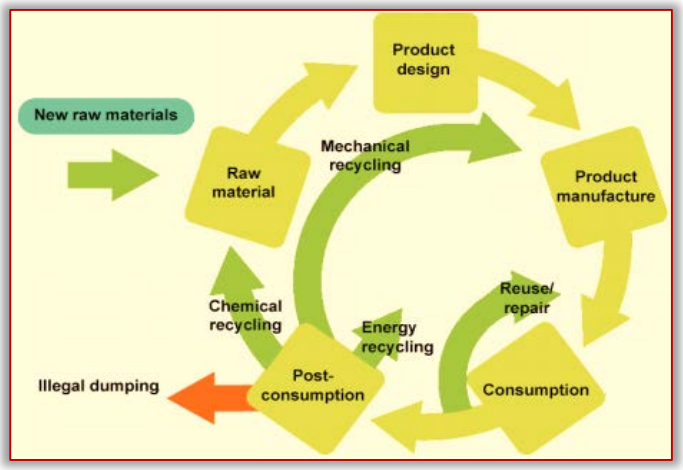

Figure 11. Recycling and reuse of plastics [13]

CHEMICAL RECYCLING (Figure 11) is a complementary technology, that can help diverting from landfill certain plastic waste which cannot be sustainably recycled by mechanical recycling.[16] Examples of suitable streams for feedstock recycling include laminated and composite plastics, low quality mixed plastics streams and contaminated plastics. Chemical recycling (or feedstock recycling) is much less developed to industrial scale and means a process where the polymers are degraded back to monomers to be used as raw material to produce new polymers.[16] In fact, processes as gasification and pyrolysis break down plastic waste to produce synthesis gas (syngas) as well as other liquid and semi–liquid products.[16]

MECHANICAL RECYCLING of plastics refers to the processing of plastics waste into secondary raw material or products without significantly changing the chemical structure of the material.[16] Before recycling, most plastic products are sorted according to their resin type, resin identification code or are separated by color before they are recycled. After sorting, for mechanical recycling the plastic recyclables are then shredded. These shredded fragments then undergo processes to eliminate

impurities like paper labels. This sorted plastics are melted and often extruded into the form of pellets which are then used to manufacture other by–products.[16]

Analysis has shown that 84% of the plastic packaging waste originates from polyolefins and polyethylene terephthalate (PET).[25] The polyolefin group comprises polyethylene (PE) and polypropylene (PP) polymers. PET is the most recycled plastic packaging material and today the PET bottle recycling is the only true circular stream in large scale where post–consumer packaging becomes packaging again in recycled bottle to new bottle or bottle–to–new by–product applications.

PVC is a universal polymer which can be processed into a wide variety of short–life or long–life products.[26] As a result of increasing consumption of PVC–made products in recent years, the quantity of used PVC items entering the waste stream is gradually increased. Currently, there is a considerable public concern about the problem of plastic wastes, from which PVC has not escaped and the material or energy recycling may be a suitable way to overcome this problem.[26]

The scrap of polycarbonate – PC can be used in several civil engineering applications as addition in cementitious materials, as an aggregate to prepare concrete mixtures or as a substitute for sand in cement mortars.[28–30] Thus, polycarbonate aggregates can provide good energy absorbing materials which are especially interesting in structures subjected to dynamic or impact efforts. Also, the scrap of polycarbonate can be used in several road and urban applications as partial substitution of natural coarse or fine ingredients in a bituminous mix.[33–37]

When different types of plastics are melted together, which cause structural weakness in the resulting material, meaning that polymer blends are useful in only limited applications. Plastic solid waste, such as polypropylene (PP) and polyethylene (PE), is creating new challenges, which in today's scenario are major research concerns. The two most widely manufactured plastics, polypropylene (PP) and polyethylene (PE) – low density polyethylene (LDPE), high density polyethylene (HDPE) – and polypropylene (PP) and polyethylene terephthalate (PET), behave this way, which limits their utility for recycling.

How plastic waste is processed remains extremely variable from country to country, and recycling remains considerably under–used.[4–8,10–14] Yet recycling is the best solution for processing plastic waste because it limits environmental impact and generates significant socio–economic gains. However, at every stage of the plastic life cycle, there remain a large number of impediments to the development of recycling.[14]

APPLICATIONS

There is low utilisation of plastic waste and only a fraction of plastic materials go back into production processes through reuse and recycling practices, despite of their recycling potential.[2–6,10–11] Now, an important plastic fraction of waste is treat by incineration or landfilling, although the recycling is possible, their mechanical properties making them adequate to produce new by–products.[2–6,10–11] The use of waste products in several industrial applications not only makes it economical, but also helps in reducing disposal problems.[2–6,10–11] One such waste is plastic, which could be used in various applications and new by–products. However, efforts have also been made to explore its use in several application, several of them being below presented:

- The main application in this sense is the polyethylene terephthalate (PET) bottle recycling. In the recycling industry, this is referred to as "post–consumer PET". In this sense, the collected post–consumer PET containers are sorted into different color fractions and they are washed and flaked (or flaked and then washed). This sorted post–consumer PET waste is crushed, chopped into different size flakes, pressed into bales, and offered for reusing (Figure 12). PET flakes are used as raw material for a range of products that would otherwise be made of polyester.

Figure 12. PET waste and crushed PET flakes

Figure 13. Recycling PET waste into polyester fibres

- One use for this PET flakes is to create polyester fibres (a base material for production of clothing, pillows, carpets, bags etc.). The

recycled PET thread or yarn (Figure 13) can be used either alone or together with other fibers to create a very wide variety of fabrics;

— Other major outlets for recycled PET are new containers (bottles and food or non–food–contact packages);

Figure 14. Recycling PET waste into new bottles

(a)

(b)

Figure 15. Armed concrete blocks (a) and floor tiles (b)

— Also, the PET products can be easily used in the construction sector, as reinforcement in armed concrete blocks or paving slabs, for consolidation their structure or as substitute of sand and gravel sorts from the aggregate;

— High–density polyethylene (HDPE) is a commonly recycled plastic, being easily extruded or injection molded and turned into brand new pipe. Often it is typically downcycled into plastic lumber or and other durable products like detergent or shampoo bottles;

— LDPE is not often recycled but can be recycled into lumber, landscaping ties or floor tile;

— PP (polypropylene), found in some containers and medicine bottles or caps, is gradually becoming more accepted by recyclers and offered for reusing for plastic lumber or custom–made products;

— Several plastic products are recovered from the waste stream, are not landfilled or burned, and successfully recycled into much larger products for industrial applications such as plastic composite railroad ties (Figure 16) or used as rain resistant recycled plastic (aggregate, bitumen or asphalt);

— Most polystyrene products are not recycled, altrough their scrap can easily be added to products such as insulation sheets for construction applications, metal casting operations or for producing insulating concrete forms;

Figure 16. Plastic composite railroad ties

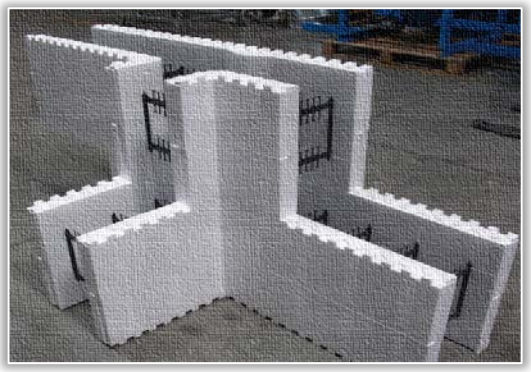

Figure 17. Insulating concrete forms

— Recycled plastic lumber (RPL) is a wood–like material made from recycled plastics that aims to diminish the environmental pollution resulting from plastic wastes. This material is used in different kinds of nonstructural and structural applications. Recently, the recycled plastic lumber (Figure 18) has been proposed as a suitable material to develop structural walls that comprise the seismic resistant system of housings;

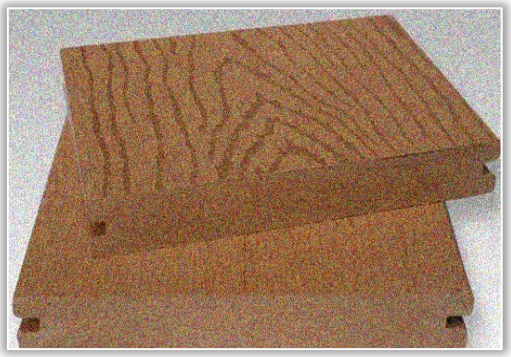

Figure 18. Recycled plastic lumber

— Plastic pipe producers are forced by various initiatives to increase the content of recycled material in their products. The performance of the recycled material is worse than the performance of the virgin material, but it would be theoretically possible to use the recycled material in pressure applications as a part of multilayer pipes.

— Commingled, mixed or contaminated plastic materials – including some material groups such as thermosets or mixed plastics which were labeled as un–recyclable – can all be used as feed stock, and,

therefore, composite products can be produced of 100% waste plastics. Developping a non–traditional (but patented) processes, virtually any plastic waste can be economically recycled into useful composites for nearly endless recycled content product applications.[38] The main advantage is that materials need no separation, cleaning, or pre–processing other than size reduction into chips or flakes. This allows heavy, solid, and durable recycled content products to be produced economically without concern for material cost.

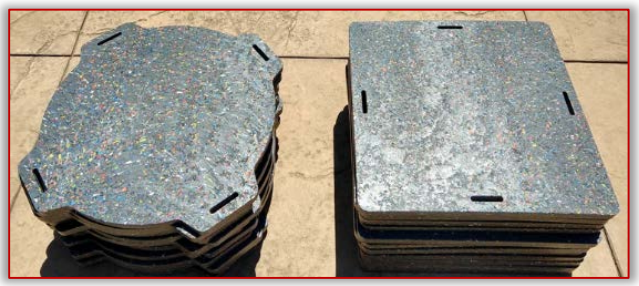

Figure 19. Composite products from 100% waste plastics (commingled, or mixed plastic materials) [38]

CONCLUSIONS

A large variety of materials fall into the category of plastics. These versatile materials have found their way into almost every aspect of daily life. Often described as durable materials they unfortunately spend the majority of their long life in a landfill.

The building and construction industry has a key role to play in sustainability of the built environment by promoting plastics recycling, a large percentage of plastics being recycled into extended–lifetime construction products (building blocks, roof tiles, insulation, panels etc.). Other areas include paving bricks production and roads or bridge construction. Also, recycled waste plastics have been found to replace aggregates in road construction and landscape.

One of the advantages of products made from recycled plastic is the cost of manufacturing cheaper than those made from virgin raw materials. The benefits of using recycled plastic are:

- disposal of the quantities of waste deposited in garbage dumps or collected systematically, and
- saving the energy quantities needed to produce raw materials for various industries.

Increased recycling will reduce the need for fossil feedstock but due to downgrading of plastics in the use and recycling phases there will be a continued need for virgin material. Therefore, contributing to the conservation and reuse of existing resources is more than a good civic policy, it is an imperative.

The efficiency of the materials and the prevention of the formation of waste imposes a more cyclical approach than the typical linear one, for the processing and use of resources. The world is heading for an era of natural resource conservation, of which recycling is an integral part. Without recycling, the circuit of materials in nature would become a series of events without a logical resolution. Any useful materials would become dispensable and would not be retained as a possible resource. The use of already processed materials implies substantial energy savings compared to the use of raw materials, and the by–products are less polluting than the raw materials.

According to the environmental legislation it is necessary to save natural resources, to reduce the management costs and to apply effective solutions to diminish the impact on the environment, by recovering waste. Currently, unused waste is mostly stored, although if we could use waste as a valuable resource. In this context, unused waste is also a potential loss.

The application of recycled wastes inevitably lead to develop green construction materials. Therefore, promoting the sustainable and affordable development of green concrete and mixtures by incorporating different plastic wastes in the road construction and building materials industries can solve partly, of course, the impasses of degradation of natural restricted aggregate resources as well as contaminations of environment, due to landfilling.

References

[1] MacArthur, E., Beyond plastic waste (2017) 843–843
[2] European Commission, A European Strategy for Plastics in a Circular Economy, Brussels (2018)
[3] Geyer, R., Jambeck, J.R., Law, K.L., Production, use, and fate of all plastics ever made. Science advances, 3(7), (2017) e1700782
[4] Merrington, A.. Recycling of plastics, in Applied plastics engineering handbook William Andrew Publishing (2017) 167–189
[5] Scheirs, J., Polymer recycling: science, technology and applications, Vol. 132, New York: Wiley (1998)
[6] Allwood, J.M., Squaring the circular economy: the role of recycling within a hierarchy of material management strategies. In Handbook of recycling (2014) 445–477
[7] Hopewell, J., Dvorak, R., Kosior, E. Plastics recycling: challenges and opportunities. Philosophical Transactions of the Royal Society B: Biological Sciences, 364(1526), (2009) 2115–2126
[8] Lazarevic, D., Aoustin, E., Buclet, N., Brandt, N., Plastic waste management in context of a European recycling society: Comparing results and uncertainties in a life cycle perspective. Resources, Conservation & Recycling, 55(2) (2010) 246–259
[9] Gharfalkar, M., Court, R., Campbell, C., Ali, Z., Hillier, G., Analysis of waste hierarchy in the European waste directive 2008/98/EC. Waste management, 3 (2015) 305–313
[10] Shen, H., Pugh, R.J., Forsberg, E., A review of plastics waste recycling and the flotation of plastics, Resources, Conservation and Recycling, 27(3) (1999) 285–286

[11] Mwanza, B.G., Mbohwa, C., Drivers to sustainable plastic solid waste recycling: a review. Procedia Manufacturing, 8, (2017) 649–656.
[12] Huysman, S., De Schaepmeester, J., Ragaert, K., Dewulf, J., De Meester, S., Performance indicators for a circular economy: A case study on post–industrial plastic waste. Resources, Conservation and Recycling, 120 (2017) 46–54
[13] STEPS – Annual Report 2016–17, Plastic waste – A Challenge for the entire value chain, (STEPS) Sustainable Plastics and Transition Pathways (2017)
[14] d'Ambrières, W., Plastics recycling worldwide: current overview and desirable changes, Field ACTions Science Reports (FACTS), Special Issue 19: Reinventing Plastics (2019) 12–21
[15] Maris, J., Bourdon S., Brossard J–M, Cauret, L., Fontaine, L., Montembault, V., Mechanical recycling: Compatibilization of mixed thermoplastic wastes, Polymer Degradation and Stability, Vol. 147 (2018) 245–266
[16] Plastics Europe: Recycling and energy recovery – Zero plastics to landfill (2020), https://www.plasticseurope.org/
[17] UNEP, Single–use plastics – A roadmap for sustainability, United Nations Environment Programme, 2018
[18] UNEP, The state of plastics – World Environment Day Outlook, United Nations Environment Programme, 2018
[19] Ragaert, K., Delva, L., Geem, K., Mechanical and chemical recycling of solid plastic waste, Waste Management, 69 (2017) 24–58
[20] Tam, V.W., Tam, C.M., A review on the viable technology for construction waste recycling. Resources, conservation and recycling, 47(3) (2006) 209–221
[21] Brems, A., Baeyens, J., Dewil, R., Recycling and recovery of post–consumer plastic solid waste in a European context. Thermal Science, 16(3) (2012) 669–685
[22] Singh, N., Hui, D., Singh, R., Ahuja, I. P. S., Feo, L., Fraternali, F., Recycling of plastic solid waste: A state of art review and future applications. Composites Part B: Engineering, 115 (2017) 409–422
[23] Malik, N., Kumar, P., Shrivastava, S., Ghosh, S. B., An overview on PET waste recycling for application in packaging. International Journal of Plastics Technology, 21(1) (2017) 1–24
[24] Jankauskaite, V., Recycled polyethylene terephthalate waste for different application solutions. Environmental Research, Engineering and Management, 72(1) (2016) 5–7
[25] Jinghua, W., Recycling of polyolefin plastics waste. China Plastics Industry, 33(1) (2005) 40–45
[26] Sadat, M., Gholam, S., Bakhshandeh, R., Recycling of PVC wastes, Polymer Degradation and Stability, 96(4) (2011) 404–415
[27] Buekens, A., Yang, J., Recycling of WEEE plastics: a review, Journal of Material Cycles and Waste Management, 16(3), (2014) 415–434
[28] Rebeiz, K.S., Craft, A.P., Plastic waste management in construction: technological and institutional issues. Resources, conservation and recycling, 15(3–4) (1995) 245–257
[29] Rebeiz, K.S., Fowler, D.W., Paul, D.R., Recycling plastics in polymer concrete systems for engineering applications. Polymer–Plastics Technology and Engineering, 30(8) (1991) 809–825
[30] Saikia, N., De Brito, J., Use of plastic waste as aggregate in cement mortar and concrete preparation: a review, Construction and Building Materials, 34 (2012) 385–401
[31] Siddique, R., Khatib, J., Kaur, I., Use of recycled plastic in concrete: A review. Waste management, 28(10), (2008) 1835–1852
[32] Chavan, M.A, Use of plastic waste in flexible pavements, International Journal of Application or Innovation in Engineering and Management, 2(4) (2013) 540–552
[33] Hassani, A., Ganjidoust, H., Maghanaki, A.A., Use of plastic waste (poly–ethylene terephthalate) in asphalt concrete mixture as aggregate replacement. Waste Management & Research, 23(4) (2005) 322–327
[34] Mathew, P., Varghese, S., Paul, T., Varghese, E. Recycled plastics as coarse aggregate for structural concrete. International Journal of Innovative Research in Science, Engineering and Technology, 2(3), (2013) 687–690
[35] Louie, M.L., Sustainable solutions for railroad trackwork. In Urban Public Transportation Systems (2013) 338–346
[36] Krishnaswamy, P., Lampo, R., Recycled–plastic lumber standards: From waste plastics to markets for plastic–lumber bridges. Standardization News, 2 (2001)
[37] Najafi, S.K., Use of recycled plastics in wood plastic composites–A review. Waste management, 33(9) (2013) 1898–1905
[38] Commingled plastic recycling and molding, http://goodinnovation.com

ACTA TECHNICA CORVINIENSIS – Bulletin of Engineering
ISSN: 2067-3809

Fascicule 2
[April – June]
tome XIII
[2020]

ACTA Technica CORVINIENSIS
BULLETIN OF ENGINEERING

ACTA TECHNICA CORVINIENSIS – Bulletin of Engineering
ISSN: 2067-3809

http://acta.fih.upt.ro

[1.]Adewale George ADENIYI, [2.]Joshua O. IGHALO

COMPUTER-AIDED MODELLING OF THE PYROLYSIS OF RUBBER SAW DUST (*Hevea Brasiliensis*) USING ASPEN PLUS

[1,2.]Chemical Engineering Department, University of Ilorin, NIGERIA

Abstract: Lignocellulosic biomass such as rubber (*Hevea brasiliensis*) saw dust is an energy-rich waste material that is readily available at local timber industries across Nigeria which can be sourced at very low or no cost. A steady-state sequential-modular simulation model was designed using ASPEN Plus V8.8 to evaluate the technical feasibility of applying pyrolysis technology for the recovery of energy from the biomass. The key pyrolysis parameters, such as the reaction temperature, pressure, flow rate and feeding rate were incorporated, and the product yields and properties was investigated and validated. The pyrolysis reactor was modelled by a combination of the RYIELD reactor and RGIBBS reactor. The model simulated the pyrolysis at 500^{0}C and 1 atm to obtain a liquid yield of 58.9%. The Char and synthesis gas yield from the process were 18.7% and 22.4% respectively.
Keywords: Modelling, Rubber (*Hevea brasiliensis*) Saw Dust, Pyrolysis, Aspen Plus

INTRODUCTION

Forest and agricultural waste is a source of interest as an energy source. As a world average, about 15% of primary energy consumption is supplied from biomass and this figure rises to more than 35% when considering only developing countries (Cordero, Marquez, Rodriguez-Mirasol, & Rodriguez, 2001). Biomass is recognised as the third largest primary energy source in the world (Gani & Naruse, 2007). Lignocellulosic biomass such as rubber (*Hevea brasiliensis*) saw dust is a waste material that is readily available at local timber industries across Nigeria. It has a very rich carbon content and can be sourced at very low or no cost. Thermochemical processes are widely used for biomass conversion and energy recovery. These processes includes combustion, gasification, liquefaction, hydrogenation and pyrolysis (Goyal, Seal, & Saxena, 2008).

The products from the pyrolysis process are char, oil and gases and their distribution and composition are mainly dependent on temperature, heating rate and pressure (Di Blasi, Signorelli, Di Russo, & Rea, 1999). Fast pyrolysis can produce very good pyrolysis oil yields and contains up to 70% of the energy of the biomass feed (French & Czernik, 2010). However, certain bio-oil characteristics significantly hinder its widespread application. These properties include low heating value, incomplete volatility and acidity (French & Czernik, 2010). These undesirable properties of pyrolysis oil are as a result of an uncharacteristically high proportion of different classes of oxygenated organic compounds. Removing oxygen is thus necessary to reform the oil into an accepted and economically attractive fuel.

Fast pyrolysis for energy recovery has been carried out on numerous wood samples under different conditions to obtain good liquid yield (Prakash & Karunanithi, 2008), (Heo et al., 2010), (Gani & Naruse, 2007), (B. Peters & Bruch, 2003). Goyal et al. (2008) in their extensive review presented pyrolysis products yield for an assortment of cellulosic and Lignocellulosic biomass samples. Sawdust samples that have been pyrolysed and reported includes Hinoki saw dust (Gani & Naruse, 2007), teak saw dust (Ismadji, Sudaryanto, Hartono, Setiawan, & Ayucitra, 2005), waste furniture saw dust (Heo et al., 2010), *Larix Leptolepis* saw dust (Park, Kim, Lee, & Lee, 2010), Pine saw dust (Oasmaa, Solantausta, Arpiainen, Kuoppala, & Sipilä, 2009) (Carlson, Cheng, Jae, & Huber, 2011), Red Oak and Sweet Gum saw dusts (Zhang, Toghiani, Mohan, Pittman, & Toghiani, 2007) and Douglas Fir saw dust (Ren et al., 2012).

Extensive work has been done to understand biomass pyrolysis in terms of kinetics and reaction sequence (Gavin, Stuart, & Emilio, 2016), (Srivastava & Jalan, 1996a, 1996b), (Alves & Figueiredo, 1989). Modelling and simulation of biomass pyrolysis (and gasification) using ASPEN Plus in particular (Yan & Zhang, 1999), (Tan & Zhong, 2010), (Samson, Shaharin, & Suzana, 2011), (Ramzan, Ashraf, Naveed, & Malik, 2011), (Abdelouahed et al., 2012), (J. F. Peters, Iribarren, & Dufour, 2013), (Ward, Rasul, & Bhuiya, 2014), (Onarheim, Solantausta, & Lehto, 2014) and other software in general (Zhang et al., 2007) have been explored.

Fast pyrolysis is a high temperature process in which biomass is rapidly heated an inert environment. Heating rate is somewhere about 300^0 C/min (Goyal et al., 2008). The biomass then vaporizes and condenses to a dark brown liquid known as pyrolysis oil. It has been observed that maximum yield of oil is obtained with high heating rates, at reaction temperatures around 500^{0}C and short vapor residence times so as to minimize secondary reactions (Ward et al., 2014).

In the present study, simulation modelling of the pyrolysis rubber (*Hevea brasiliensis*) sawdust was

carried out with ASPEN Plus V8.8 to evaluate the technical feasibility of applying this technology to rubber sawdust. The key pyrolysis parameters, such as the reaction temperature, pressure, flow rate and feeding rate were incorporated, and the product yields and properties was investigated and validated.

METHODOLOGY

— Model component specification

In ASPEN Plus V8.8 the components are classified into major classes. In this research work, three component classes have been used: conventional components, non-conventional components and solids. In the global settings of the simulation, the stream class is set to MIXCINC as there are conventional and non-conventional solids alongside the conventional components. Particle size distribution will not be considered under this selection. Non-conventional components are not chemical components and they do not have a molecular formula. Instead, in Aspen Plus V8.8 they are specified by empirical factors representing their elemental composition. Enthalpy and density are the only properties calculated for non-conventional components and it is done by empirical correlations. The specific property methods for enthalpy and density for rubber wood were chosen as HCOALGEN method and DGOALIGT method respectively, which is based on ultimate analyses and proximate analyses. Rubber (*Hevea brasiliensis*) saw dust is a non-conventional material which is modelled in the ASPEN Plus by the proximate and ultimate analysis using the data in Table 1.

Table 1: Proximate and Ultimate Analysis of Rubber (*Hevea brasiliensis*) saw dust (Srinivasakannan & Bakar, 2004).

Proximate analysis (wt% wet basis)	
Moisture	6.20%
Fixed Carbon	23.38%
Volatile Matter	69.68%
Ash	0.74%
Ultimate analysis (wt% moisture free)	
Carbon	43.98%
Hydrogen	8.04%
Sulphur	0.45%
Oxygen	47.53%
Nitrogen	Nil

The conventional components added to the simulation include saturated aliphatic hydrocarbons $C_1 - C_{20}$. Nitrogen, Hydrogen Sulphide, some aromatic compounds and elemental carbon were the other components added to the simulation. Hydrogen Sulphide gas was added to the simulation to help account for the sulphur content of the biomass.

For the estimate the physical properties of the conventional components in the simulation, the Peng-Robinson with Boston-Mathias alpha function equation of state (PR-BM) was used. Alpha is a temperature dependent parameter that improves the pure component vapor pressure correlation at very high temperatures (Altayeb, 2015). For this reason, PR-BM is suitable for the pyrolysis process since relatively high temperatures are involved.

— Reactor Model Description

The pyrolysis reactor was modelled in the simulation by two stages. The reactor was modelled by a combination of the RYIELD reactor and the RGIBBS reactor. The RYIELD (yield) reactor converts the dry non-conventional feedstock to conventional components. The RGIBBS (Gibbs) reactor calculates the final component distribution and phase equilibrium through the minimization of Gibbs free energy.

The Gibbs reactor in ASPEN Plus does not require a specified reaction stoichiometry. This reactor is suitable in simulating different types of chemical reactions amongst which is combustion, gasification and pyrolysis. Separation of the char from the vapour in the product stream is modelled by a cyclone. Reduction of product vapour temperature to induce condensation of liquid products is modelled by a heater set to ambient conditions.

Table 2: ASPEN Plus unit operations model description

ASPEN Plus ID	Block ID	Description
RYIELD	DECOMPOS	Conversion of non-conventional material (rubber saw dust) to conventional components
RGIBBS	PYRO	Calculation of the composition of the products through the minimisation of Gibbs free energy
SSPLIT	SEP1	Separation of the char from the product vapour by specifying split ratio
HEATER	CONDENSR	Condensation of the vapour products to give oil and non-condensable gases
FLASH2	SEP1	Separation of pyrolysis oil from non-condensable gases.

The following assumptions are considered in the simulation to reduce complexity. However, care was taken to prevent oversimplification of the model.

- ≡ The pyrolysis simulation model prepared with Aspen PLUS V8.8 is a steady-state isothermal model.
- ≡ All sulphur is represented as Hydrogen sulphide and char is assumed to be composed of elemental carbon alone.
- ≡ All elements take part in the chemical reaction except ash which is considered as inert.

— Process Model Description

A steady-state sequential-modular simulation model was designed using ASPEN Plus V8.8. Sequencing generally connotes designating the order of performance of tasks to assure optimal utilisation of available inputs (Licker, 2003). In ASPEN PLUS it connotes a sequential block-by-block calculation method where the results of one block serve as the basis for the next.

The simulation ambient temperature and pressure were specified as 25°C and 1 atm respectively. The saw dust (10kg/hr) and Nitrogen gas (0.1kmol/hr) was fed into the pyrolysis reactor block at ambient conditions. The Nitrogen helps to provide an inert environment in the reactor. The first rector block converts the sawdust into conventional chemical components. The second reactor block predicts the final product distribution vis the minimisation of Gibbs free energy. The Nitrogen gas is specified as an inert in the Gibbs reactor.

The temperature and pressure of the reactor system is taken as the temperature and pressure of the final reactor block and they were specified at 500°C and atmospheric pressure. The process flow diagram (PFD) of the simulation is presented in Figure 1.

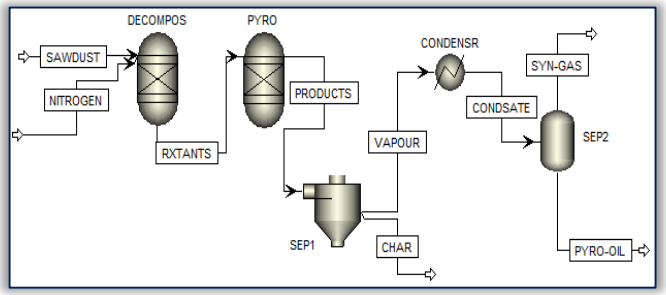

Figure 1: The process flow diagram (PFD) of the simulation

The cyclone is used to separate the char from the vapour products. The vapours are then condensed to ambient temperature before the final separation of the non-condensable gases from the oil. Due to the nitrogen gas present in the synthesis gas stream, actual synthesis gas amount will be estimated by subtracting the Nitrogen gas flowrate fed into the system from the overall gas flowrate.

RESULTS AND DISCUSSION

The results of the products yield at feed rate of 100kg/hr and 500°C pyrolysis temperature from the simulation are presented in Table 3.

Table 3: Results of Product Yields

Product	Yield (wt%)
Pyrolysis oil	58.90%
Char	18.70%
Synthesis Gas	22.40%

The results show a good yield of pyrolysis oil with respect to the other products. The synthesis gas and char was composed of light hydrocarbons and elemental carbon respectively. The pyrolysis oil was composed of the other hydrocarbons and aromatics. Considering the technical and economic feasibility, rubber (*Hevea brasiliensis*) saw dust produces as good an oil yield as most other lignocellulosic feedstock available.

Pyrolysis of wood saw dust in general has been proved possible (Gani & Naruse, 2007; Heo et al., 2010; Ismadji et al., 2005; Oasmaa et al., 2009; Park et al., 2010) (Carlson et al., 2011; Ren et al., 2012; Zhang et al., 2007) and rubber (*Hevea brasiliensis*) saw dust is not be an exception. Financial/economic feasibility of biomass pyrolysis is still not as positive as expected. Wood pyrolysis is majorly justifiable from the standpoint of energy recovery from waste biomass and also that of environmental consideration. The oil itself still lacks full backing in the world market as it is generally considered as acidic and unstable (Perry H. Robert & Don, 1999).

Experimental data of the product composition from a pyrolysis process and the oil yield was used to validate the simulation model (Goyal et al., 2008). The product yield is fairly in line with experimental results for wood pyrolysis. There is a considerable difference between the simulation results and the experimental data with respect to product composition. Due to the extent of diversity of the components of pyrolytic oil, it is difficult to accurately quantify all of them.

The simulation model failed to evaluate the composition of the higher alkanes $C_{10} - C_{20}$, and the concentrations of the other components are significantly varied from literature information. The reason behind these discrepancies is due to the Gibbs model calculating product compositions by minimizing Gibbs free energy as observed by other researchers (Altayeb, 2015).

In order to be able to obtain fairly accurate and reliable results consistent with the literature, a kinetic model based on reaction mechanisms needs to be established to predict the pyrolysis products with respect to biomass composition and operating factors. Considering that pyrolysis reactions stoichiometric relationships are still currently estimations, it is still quite difficult to obtain fully accurate results from the method.

CONCLUSION

A steady-state sequential-modular simulation model was designed using ASPEN Plus V8.8 to evaluate the technical feasibility of applying pyrolysis technology to rubber (*Hevea brasiliensis*) sawdust. The pyrolysis reactor was modelled by a combination of the RYIELD reactor and RGIBBS reactor.

The model simulated the pyrolysis at 500°C and 1 atm to obtain a liquid yield of 58.9%. The Char and synthesis gas yield from the process were 18.7% and 22.4% respectively.

The model showed correlation with literature in terms of product yield but not in terms of product composition. Discrepancies in compositional values were pinpointed on the inadequacy of the calculation technique utilised by the RGIBBS reactor.

References

[1] Abdelouahed, L., Authier, O., Mauviel, G., Corriou, J.-P., Verdier, G., & Dufour, A. (2012). Detailed modeling of biomass gasification in dual fluidized bed reactors under Aspen Plus. Energy & Fuels, 26(6), 3840-3855.
[2] Altayeb, R. K. (2015). Liquid Fuel Production From Pyrolysis Of Waste Tires: Process Simulation, Exergetic Analysis, And Life Cycle Assessment. (Master of Science in Chemical Engineering Masters Thesis), American University of Sharjah, Sharjah, United Arab Emirates.
[3] Alves, S., & Figueiredo, J. (1989). A model for pyrolysis of wet wood. Chemical engineering science, 44(12), 2861-2869.
[4] Carlson, T. R., Cheng, Y.-T., Jae, J., & Huber, G. W. (2011). Production of green aromatics and olefins by catalytic fast pyrolysis of wood sawdust. Energy & Environmental Science, 4(1), 145-161.
[5] Cordero, T., Marquez, F., Rodriguez-Mirasol, J., & Rodriguez, J. (2001). Predicting heating values of lignocellulosics and carbonaceous materials from proximate analysis. Fuel, 80(11), 1567-1571.
[6] Di Blasi, C., Signorelli, G., Di Russo, C., & Rea, G. (1999). Product distribution from pyrolysis of wood and agricultural residues. Industrial & Engineering Chemistry Research, 38(6), 2216-2224.
[7] French, R., & Czernik, S. (2010). Catalytic pyrolysis of biomass for biofuels production. Fuel Processing Technology, 91(1), 25-32.
[8] Gani, A., & Naruse, I. (2007). Effect of cellulose and lignin content on pyrolysis and combustion characteristics for several types of biomass. Renewable Energy, 32(4), 649-661.
[9] Gavin, W., Stuart, D., & Emilio, R. (2016). Modeling the impact of biomass particle residence time on fast pyrolysis yield and composition. Paper presented at the AIChE Annual Meeting, San Francisco.
[10] Goyal, H., Seal, D., & Saxena, R. (2008). Bio-fuels from thermochemical conversion of renewable resources: a review. Renewable and sustainable energy reviews, 12(2), 504-517.
[11] Heo, H. S., Park, H. J., Park, Y.-K., Ryu, C., Suh, D. J., Suh, Y.-W., . . . Kim, S.-S. (2010). Bio-oil production from fast pyrolysis of waste furniture sawdust in a fluidized bed. Bioresource technology, 101(1), S91-S96.
[12] Ismadji, S., Sudaryanto, Y., Hartono, S., Setiawan, L., & Ayucitra, A. (2005). Activated carbon from char obtained from vacuum pyrolysis of teak sawdust: pore structure development and characterization. Bioresource technology, 96(12), 1364-1369.
[13] Licker, D. M. (2003). Dictionary of Engineering (2nd ed.). Chicago: Mc-Graw Hill Publishers.
[14] Oasmaa, A., Solantausta, Y., Arpiainen, V., Kuoppala, E., & Sipilä, K. (2009). Fast pyrolysis bio-oils from wood and agricultural residues. Energy & Fuels, 24(2), 1380-1388.
[15] Onarheim, K., Solantausta, Y., & Lehto, J. (2014). Process simulation development of fast pyrolysis of wood using aspen plus. Energy & Fuels, 29(1), 205-217.
[16] Park, D. K., Kim, S. D., Lee, S. H., & Lee, J. G. (2010). Co-pyrolysis characteristics of sawdust and coal blend in TGA and a fixed bed reactor. Bioresource technology, 101(15), 6151-6156.
[17] Perry H. Robert, & Don, G. W. (1999). Perry's Chemical Engineers' Handbook (7th ed.): McGraw-Hill companies Inc.
[18] Peters, B., & Bruch, C. (2003). Drying and pyrolysis of wood particles: experiments and simulation. Journal of Analytical and Applied Pyrolysis, 70(2), 233-250.
[19] Peters, J. F., Iribarren, D., & Dufour, J. (2013). Predictive pyrolysis process modelling in Aspen Plus. Paper presented at the 21st Eur biomass conf exhib.
[20] Prakash, N., & Karunanithi, T. (2008). Kinetic modeling in biomass pyrolysis–a review. Journal of Applied Sciences Research, 4(12), 1627-1636.
[21] Ramzan, N., Ashraf, A., Naveed, S., & Malik, A. (2011). Simulation of hybrid biomass gasification using Aspen plus: A comparative performance analysis for food, municipal solid and poultry waste. Biomass and bioenergy, 35(9), 3962-3969.
[22] Ren, S., Lei, H., Wang, L., Bu, Q., Chen, S., Wu, J., Ruan, R. (2012). Biofuel production and kinetics analysis for microwave pyrolysis of Douglas fir sawdust pellet. Journal of Analytical and Applied Pyrolysis, 94, 163-169.
[23] Samson, M. A., Shaharin, A. S., & Suzana, Y. (2011). A simulation study of downdraft gasification of oil-palm fronds using ASPEN PLUS. Journal of Applied Sciences, 11(11), 1913-1920.
[24] Srinivasakannan, C., & Bakar, M. Z. A. (2004). Production of activated carbon from rubber wood sawdust. Biomass and bioenergy, 27(1), 89-96.
[25] Srivastava, V., & Jalan, R. (1996a). Development of mathematical model for prediction of concentration in the pyrolysis of biomass material.
[26] Srivastava, V., & Jalan, R. (1996b). Prediction of concentration in the pyrolysis of biomass material—II. Energy conversion and Management, 37(4), 473-483.
[27] Tan, W., & Zhong, Q. (2010). Simulation of hydrogen production in biomass gasifier by ASPEN PLUS. Paper presented at the Power and Energy Engineering Conference (APPEEC), 2010 Asia-Pacific.
[28] Ward, J., Rasul, M. G., & Bhuiya, M. M. K. (2014). Energy recovery from biomass by fast pyrolysis. Procedia Engineering 90, 90, 669-674.
[29] Yan, H., & Zhang, D. (1999). Modeling of a low temperature pyrolysis process using ASPEN PLUS. Asia-Pacific Journal of Chemical Engineering, 7(5-6), 577-591.
[30] Zhang, J., Toghiani, H., Mohan, D., Pittman, C. U., & Toghiani, R. K. (2007). Product analysis and thermodynamic simulations from the pyrolysis of several biomass feedstocks. Energy & Fuels, 21(4), 2373-2385.

ACTA TECHNICA CORVINIENSIS – Bulletin of Engineering
ISSN: 2067-3809

[1.]G.K. GIRISHA, [2.]S.L. PINJARE

IMPLEMENTATION OF NOVEL ALGORITHM FOR AUDITORY COMPENSATION IN HEARING AIDS USING STFT

[1,2.]Nitte Meenakshi Institute of Technology, Bangalore, INDIA

Abstract: Audiogram is the graphic record drawn from the results of hearing tests with an audiometer, which charts the threshold of hearing at various frequencies against sound intensity in decibels. This paper presents the work on auditory compensation (also known as audiogram equalizer) implemented with the help of Short Time Fourier Transform (STFT) algorithm. For humans normal hearing ranges from -10dB to 15dB, although 0dB from 250Hz to 8 kHz is reckoned as the average normal hearing. An audiogram is obtained to determine the frequency range the listener is audibly challenged to. STFT algorithm is employed to determine the frequency range of audio signal which is to be selectively amplified as per the audiogram. The present work uses verilog language to implement STFT algorithm. The entire system is developed on Zynq Evaluation and Development Board (Zedboard) using Vivado.
Keywords: Audiogram, STFT, Zedboard

INTRODUCTION

Hearing is one of the important senses which alert us to danger that sometimes may be out of our visual range. Sound is produced upon vibration or back and forth movement. Audio or sound is merely quick movement of air molecules which are caused by vibrations caused by such actions. The human ear is of three parts: inner ear, middle ear and outer ear. The pinnae are structured to gather sounds from different directions and funnel them into the ear canal. The sound waves are then conveyed onto the middle ear and then the inner ear. Hearing loss or hearing impairment can be partial or total inability to hear, caused by the interruption of audio signals at either or multiple sections of the ear. Certain factors including genetics, aging, infections, exposure to noise, trauma, birth conditions and medications or toxins can invoke hearing loss. Hearing impairment is categorized into: conductive hearing loss, sensorineural hearing loss (SNHL) and mixed hearing loss. Conductive hearing loss is caused by the impediment in conveying the sound in its mechanical form through the middle cavity to the inner ear. Sensorineural hearing loss is due to nerve-related hearing loss. Mixed hearing loss is a combination of the two.

Although there is a wide range of options to treat hearing impairment, hearing aid is one such option in high demand. Hearing aids are sound-amplifying devices designed to increase audibility. Most of the hearing aids cognate similar components such as microphone, amplifier circuitry, miniature loudspeakers and batteries to power the device. Based on the technology used, hearing aids are classified into: Analog and Digital (DSP) hearing aid. Analog hearing aids operate by amplifying continuous audio waves. Digital hearing aids come with the similar features of programmable analog hearing aid, but convert the audio signal to digital signal to yield an exact replica of each signal rather than entirely amplifying the signal.

Digital hearing aid alike analog hearing aid, has a microphone to convert the analog audio signals to digital form, a microprocessor to amplify and process the digital signal and a miniature loudspeaker to convey audio directly to the ear canal. The signal processing is executed by the microprocessor in real time taking into account of individual user preferences.

Researchers have so far been implementing audiogram equalizer using filter banks for processing audio signal. An array of filters known as analysis filter bank are used to divide the audio signal to different channels based on frequencies. Then an array of amplifier with specific gain is used to amplify signals in each channel. FIR/IIR filters have been used for implementing filter banks. Filter number and the implementation architectures have a significant impact on system performances, such as computation complexity, area, throughput, and power consumption.

Certain signals are confined by the filters based on their frequency values, therefore the filter component values must be selected effectively else required frequencies may be accidently filtered out. Digital sequences have smaller signal bandwidth when compared to analog sequences, which puts signal processing time in a significant position among the factors effecting device performance. FFT algorithm operates at a faster pace and since all signals are considered for evaluation no frequency is filtered out, sanctity of the signal is preserved.

This paper shows the implementation of auditory compensation block by selective amplification of audio signal on Zedboard. Zynq-7000 processor is used to perform the processing and amplification of the signal. Zedboard has two 12-bit (each) analog to digital converters (ADC) and an in-built Codec –

ADAU1761 for analog to digital conversion and audio interfacing with the processor respectively.

AUDITORY COMPENSATION

Auditory compensation is the hearing aid's primary functionality to compensate the loss in the hearing level of a patient by amplifying the audio signals depending on the frequency band. The amount of amplification required for an individual is determined by the Audiometry test performed by audiologist.

Each user may have different requirements as per their audiogram results. The audiogram equalizer is one such algorithm which can be used to customize the hearing aid operation. An individual may have attenuated audibility at a particular frequency range, the STFT algorithm is implemented in this paper to identify the frequency range to be processed and then amplified.

— STFT algorithm

STFT also referred to as Short-term Fourier transform is employed to determine the frequency and phase content of a signal over a period of time. The incoming long term audio signal is divided to short terms of equal length and Fourier transform is computed on each of these shorter segments [1].

The discrete STFT is a time-localized spectral transformation based on the discrete Fourier transform (DFT). The DFT coefficients X(k) of a discrete time signal x(t) composed of T samples are calculated according to

$$X(k) = \sum_{t=0}^{T-1} \left(x(t) e^{-j\frac{2\pi}{T}kt} \right), k = 0, .., T-1$$

where k is frequency. The DFT is a frequency localized transformation, the analog frequencies equivalent to normalized frequency are fixed and given by

$$f_k = \frac{k f_s}{T}$$

where k = 0,1,2,3.....T-1 and f_s is sampling frequency. The samples of the speech signal are real numbers which makes the DFT to be symmetric.

The STFT can be viewed as a two-dimensional transformation (i.e. frequency and time) which is calculated by splitting the input signal into segments using a sliding time-limited window and then calculating the DFT of each of the segments.

Considering a discrete time input signal, it is segmented into frames according to

$$x_i(r) = w(r)\, x(r + iD), \quad r = 0, \ldots, R-1$$

where $x_i(r)$ is the windowed i-th frame, r is a local time index, R is the window length, and D is the hop size which represents the number of samples that the sliding window moves between two consecutive frames.

The window lengths of the signal may vary from 8, 16, 32 and so on, and the audio frequency is equally divided among these channels. The frequency range to which the audio signal belongs is determined by the position of maximum magnitude of the complex Fourier sequence.

— Audio Amplification

Audio amplification is the process of making a small signal bigger by a particular factor without affecting other features of the same. An amplifier which amplifies audio of all frequencies by a same factor is called linear amplifier. In this paper a non-linear amplification method is employed, as the user may require different audio intensity at different frequencies. The user has to undergo an audiogram test to determine his hearing attenuation at various frequencies at both his left and right ear. As per the audiogram result the hearing aid can be configured to amplify the signal to a gain preferred by the user. Each channel represents a particular frequency range and as per the user audiogram result.

METHODOLOGY

The figure 1 presents the novel auditory compensation algorithm using STFT algorithm implemented. The audio signal picked up from the microphone are then converted to digital signals using ADC. The continuous audio signal is divided into smaller segments and STFT is performed on each of these segments. The STFT block finds the FFT of the signal. The FFT implementation is carried out using butterfly method. After FFT calculations, the Max-Bin block calculates the magnitude of each bin of FFT and results with the index of the bin which has got the maximum magnitude. The index represents the frequency of the audio signal. The amplifier block is used to amplify the real time audio signal based on the frequency determined and the amplification requirement data taken from audiogram to compensate the hearing loss of the patient [2].

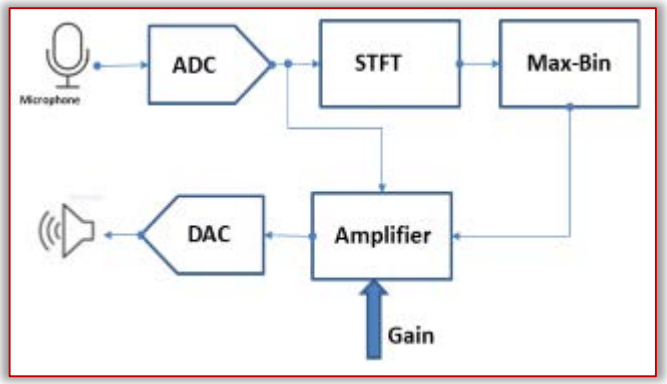

Figure 1: Block diagram of STFT algorithm for Auditory Compensation

IMPLEMENTATION

All the blocks of figure 1 have been implemented using the tool Vivado and the hardware platform being Zynq evaluation and development board. Figure 2 represents the schematic of the algorithm implemented.

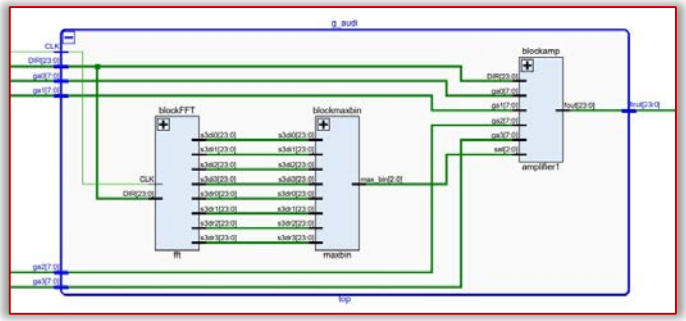

Figure 2: Schematic of the Algorithm Implementation.

ADAU1761 codec of Zedboard was utilized to accept audio signal through line in channel. GPIO -1 is the audio input and GPIO-0 is the processed output. Figure 3 is the complete schematic including codec and algorithm.

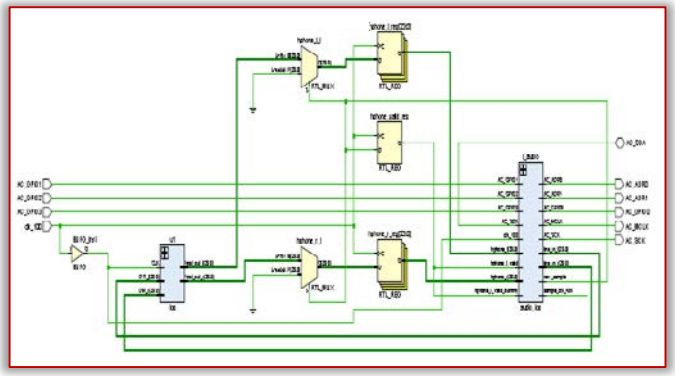

Figure 3: Complete Schematic including Codec and Algorithm

RESULTS

The proposed algorithm in this paper has been successfully implemented and derived of satisfactory results.

Implementation of this project involved utilization of certain device resources such as LUT (look up table), FF(Flip-flops), IO (I/O pads), BRAM (Block RAM), MMCM (Mixed-mode Clock manager) etc. Utilization of the resources post synthesis and implementation can be seen in the figure 4.

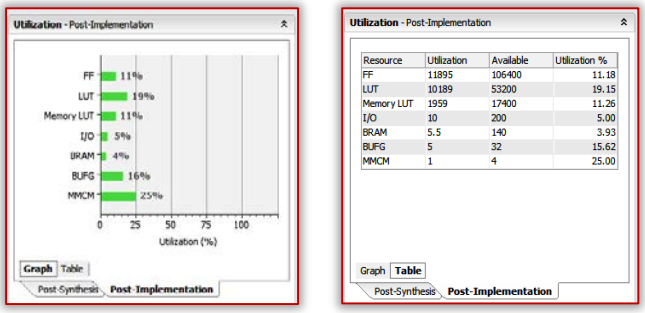

Figure 4: Post implementation resource utilization report

Implementation setup includes a Zed Board, Digital storage oscilloscope, microphone and speakers as shown in figure 5. The audio signal of different frequencies were fed as input and the amplified output were observed with the set gain factor.

Figure 5: Implementation Setup

CONCLUSIONS

The advantages of the novel approach implemented in the work over the filter bank approach are:

- In the novel approach the problem of reconstructing the signal does not exist. Whereas perfect reconstruction of the speech signal is a challenging task in the filter bank approach as the signal is divided into different channels.
- The resolution in frequency depends on the length N of the STFT whereas in filter bank approach we need to have an additional filter for every channel. The novel approach solves the problem of Signal Distortion due to filters in filter bank approach.

The proposed algorithm in this paper has been successfully implemented and derived of satisfactory results.

References

[1] Chong K. S, Gwee B H, Chang J S, A 16-channel low-power non-uniform spaced filter bank core for digital hearing aids. Circuits and Systems II: Express Briefs, IEEE Transactions on, vol. 53, pp. 853-857, September 2006.

[2] Nielsen L. S, Sparso J, Designing asynchronous circuits for low power: An IFIR filter bank for a digital hearing aid. Proceedings of the IEEE, vol. 87, pp. 268-281, February 1999.

[3] Li M, McAllister H. G, Black N. D, et al, Wavelet-based nonlinear AGC method for hearing aid loudness compensation. IEEE Proceedings-Vision, Image and Signal Processing, vol. 147, pp. 502-507, June 2000

[4] Vikrant N. P, Krishna Y, Rajashekhar B, et al. Critical-band based compression—an insight into the future of digital hearing aids, Audio, Language and Image Processing, ICALIP 2008. International Conference on. IEEE, pp. 1620-1623, 2008.

[5] S Hamid Nawab, Thomas F. Quatieri, "Signal Reconstruction from Short-Time Fourier Transform magnitude", IEEE transactions on acoustics, speech, and signal processing, vol. assp-31, no. 4, August 1983

[6] Martin Krawczyk and Timo Gerkmann, "STFT Phase Reconstruction in Voiced Speech for an Improved Single-Channel Speech Enhancement", IEEE transactions on audio, speech, and language processing, vol. 22, no. 12, December 2014

[7] D. W. Griffin and J. S. Lim, "Signal estimation from modified short-time Fourier transform," IEEE Trans. Acoust., Speech, Signal Process., vol. 32, no. 2, pp. 236–243, Apr. 1984
[8] Y. Ephraim and D. Malah, "Speech enhancement using a minimum mean-square error short-time spectral amplitude estimator," IEEE Trans. Acoust., Speech, Signal Process., vol. 32, no. 6, pp. 1109–1121, Dec,1984
[9] R.Crochiere, "A weighted overlap-add method of short-time Fourier analysis/ syntesis" IEEE Transform modified. Acoust, Speech, Signal Process, vol ASSP-28,no.2, Apr.1980
[10] Wang Qing-yun, Zhao Li, Zhao Li-ye, Zou Cai-rong, A Multichannel Loudness Compensation Method for Digital Hearing Aids, Journal of Electronics & Information Technology, vol. 31, April 2009.
[11] Y. Lian and Y. Wei, "A Computationally Efficient Non-Uniform FIR Digital Filter Bank for Hearing Aid," IEEE Trans. on Circuits and Systems, vol. 52, December, 2005.
[12] Ching-Ta Lu and Hsiao-Chuan Wang, "Speech enhancement using robust weighting factors for critical-band-wavelet-packet transform," IEEE International Conference on Acoustics, Speech, and Signal Processing, vol. 1, May 2004.

ACTA TECHNICA CORVINIENSIS – Bulletin of Engineering
ISSN: 2067-3809

[1.]Mustefa JIBRIL, [2.]Tesfabirhan SHOGA

COMPARISON OF H∞ AND μ-SYNTHESIS CONTROL DESIGN FOR QUARTER CAR ACTIVE SUSPENSION SYSTEM USING SIMULINK

[1.]Dire Dawa Institute of Technology, DireDawa, ETHIOPIA
[2.]Jimma Institute of Technology, Jimma, ETHIOPIA

Abstract: In order to improve the road handling and passenger comfort of a vehicle, suspension system is provided. An active suspension system is considered to be better than passive suspension system. In this paper, a linear quarter car active suspension system is designed, which subjected to different road disturbances. Since parametric uncertainty in the spring, damper and actuator has been considered, therefore robust control is used. H∞ and μ–synthesis controllers are used to improve the ride comfort and road handling ability of the car as well as to check the robust stability and performance of the system. In H∞ design, we design a controller for passenger comfort purpose and to keep the suspension deflection small and to reduce the road disturbance to suspension deflection. For the μ–synthesis design, we design a controller with hydraulic actuator and uncertainty model. We design a MATLAB/SIMULINK model for the active suspension system with the H∞ and μ–synthesis controllers and we made test using four road disturbance inputs (bump, random, sine pavement and slope) for suspension deflection, body acceleration and body travel for passive, active suspension with controller and active suspension without controller. Finally we compare the H∞ and μ–synthesis controllers with a Simulink model for suspension deflection, body acceleration and body travel simulation and the result shows that both designs give good performance but H∞ controller has superior performance as compared to μ–synthesis controller.

Keywords: Quarter Car Active Suspension System, H∞ Controller, μ–Synthesis Controller, Robust Performance, Robust Stability

INTRODUCTION

At present, the world's leading automotive companies and research institutions have invested considerable human and material resources to develop a cost-effective vehicle suspension system, in order to be widely used in the vehicle. The main aim of suspension system is to isolate a vehicle body from road irregularities in order to maximize passenger ride comfort and retain continuous road wheel contact in order to provide road holding. Many studies have shown that the vibrations caused by irregular road surfaces have an energy draining effect on drivers, affecting their physical and mental health [1]. Demands for better ride comfort and controllability of road vehicles like passenger cars has motivated to develop new type of suspension systems like active and semi active suspension systems. These electronically controlled suspension systems can potentially improve the ride comfort as well as the road handling of the vehicle. An active suspension system has the capability to adjust itself continuously to changing road conditions. By changing its character to respond to varying road conditions, active suspension offers superior handling, road feel, responsiveness and safety.

An active suspension system has the ability to continuously adjust to changing road conditions. By changing its character to respond to different road conditions, the active suspension offers superior handling, road feel, responsiveness and safety.

Active suspension systems dynamically respond to changes in the road profile because of their ability to supply energy that can be used to produce relative motion between the body and wheel. Typically, the active suspension systems include sensors to measure suspension variables such as body velocity, suspension displacement, and wheel velocity and wheel and body acceleration. An active suspension is one in which the passive components are augmented by actuators that supply additional forces. These additional forces are determined by a feedback control law using data from sensors attached to the vehicle.

The existing active suspension system is inefficient if there are changes in parameter of the system or of actuator, then controlling the suspension system becomes a big problem. Therefore H∞ and μ–synthesis control technique are used. H∞ and μ–synthesis control effectively suppresses the vehicle vibrations in the sensitive frequency range of the human body. The desired robust performance and robust stability are achieved in the closed loop system for a quarter vehicle model in the presence of structured uncertainties.

REVIEW ON DIFFERENT CONTROL METHODS OF CAR ACTIVE SUSPENSION SYSTEM

Vivek Kumar Maurya and Narinder Singh Bhangal [2] presented optimal control of vehicle active suspension system. A linear model of active suspension system has been developed since it contains all the basic parameters of its performance body deflection,

suspension deflection and body acceleration. Two control techniques PID and LQR are used to suppress the vibrations of the system. A comparison between passive and active suspension system using PID and LQR control technique with road disturbance as input has been made.

Michiel Haemers et al. [3] presented a proportional-integral state-feedback controller optimization for a full-car active suspension setup using a genetic algorithm. In his work, an optimal control for a full-car electromechanical active suspension was presented. Therefore, a scaled-down lab setup model of this full-car active suspension was established, capable of emulating a car driving over a road surface with a much simpler approach in comparison with a classical full-car setup. A kinematic analysis is performed to assure system behavior which matches typical full-car dynamics. A state-space model was deducted, in order to accurately simulate the behavior of a car driving over an actual road profile, in agreement with the ISO 8608 norm. The active suspension control makes use of a Multiple-Input-Multiple- Output (MIMO) state-feedback controller with proportional and integral actions. The optimal controller tuning parameters are determined using a Genetic Algorithm, with respect to actuator constraints and without the need of any further manual re-tuning.

Ahmed A. Abougarair and Muawia M. A. Mahmoud [6] have introduced the design and simulation of optimal controller for quarter car active suspension system. In their work, the Proportional Derivative (PD), Linear Quadratic Control (LQR) and Fuzzy logic tune PD controllers' techniques implemented to the active suspensions system for a quarter car model. The comparison between these controllers by means of the reduction of body displacement trajectory under influence two road profiles and variation of body mass.

J. Marzbanrad and N. Zahabi [7] have presented H ∞ active control of a vehicle suspension system exited by harmonic and random roads. In their work they proposes a controller based upon H ∞ control approach in order to improve the vehicle performance under two different road profiles. In their study, there are two control targets that they are car body travel and suspension deflection. In fact, H ∞ controller is responsible for minimizing the infinity norm of two subsystems. The first one is from car body travel to road disturbance and second is from suspension deflection to road disturbance. These two control targets must be improved by a logical control input that is determined by H ∞ control approach. In order to improve the performance of the quarter–car, weighting functions are also defined. Disturbance that is the system input is considered as two types of road profiles, harmonic and random. The results show that the H ∞ controller is able to improve the quarter–car performance for both roads. In addition, the sensitivity analysis is done to show that the active suspension system is able to work when sprung mass changes as may be occurred when passengers added.

Shital M. Pawar and A.A. Panchwadkar [8] presents estimation of state variables of active suspension system using kalman filter. In their work, active suspension systems use an actuator which is governed by the control strategy using an ECU. Most of the literature focuses on feedback control of active suspension systems. Their study aims to make use of an algorithm which predicts the states of the suspension systems in response to the road input using Kalman filter and control the suspension travel between the sprung and unsprung masses of the suspension. The Kalman filter is used as the observer which will observe the system states and predict the next states of the plant model. A linear Quadratic Regulator (LQR) and a Linear Quadratic Gaussian (LQG) control strategy was used to control the required force to minimize the suspension travel. The suspension system model was prepared in Matlab™/Simulink and simulated. Comparison of the estimation errors in open loop (passive suspension), the LQR control and LQG control using Kalman filter was made to study the effectiveness of the new control strategy.

The gap of this study is there is no design of MATLAB/Simulink model for the active suspension system with H ∞ and μ - synthesis controllers in the presence of uncertainty. No comparison has been made between H ∞ and μ - synthesis in the tests of suspension deflection, body acceleration and body travel using random, sine pavement and slope road disturbances for passive, active suspension with H ∞ and μ - synthesis controller and active suspension without controller and no comparison has been made based on impulse, step, Nichols, NY Quist and Bode magnitude response of the active suspension system with H ∞ and μ - synthesis controllers in the presence of uncertainty.

MATHEMATICAL MODELS

— Passive Suspension System Mathematical Model

Vibration control system design should start with the establishment of mathematical model of the system, and then determine the design requirements, and formal description of it. And then select one or several design methods to design the control system, and further attached to simulation or model experiments to identify the control system is designed to meet the performance requirements. Therefore, the establishment of the mathematical models of the system is a prerequisite for the entire control designs and control system design is closely related to the control system quality evaluation model.

As with other engineering control system, a mathematical model of the suspension control system refers to the formal model, for short the mathematical model. Such models typically rely on the dynamic principle to be derived or through some of the system dynamics test. Then it experiences mathematical simulation and optimization, or statistical approach. The key to create a system of mathematical models is to provide a description of the model form and determine its parameters.

In vibration control area, there are three kinds of models most popular to describe the form, the state space description, transfer function description and weight function description. In accordance with the implementation of continuous control and discrete control of different characteristics, they are each divided into a time continuous and time discrete mathematical description.

The automotive is a complex vibration system, should simplify based on the analysis of the problem. Simplification of motor vehicles there are several ways, but according to the convenience of the study, in this paper we simplify it into a system model as shown in Figure 1 below:

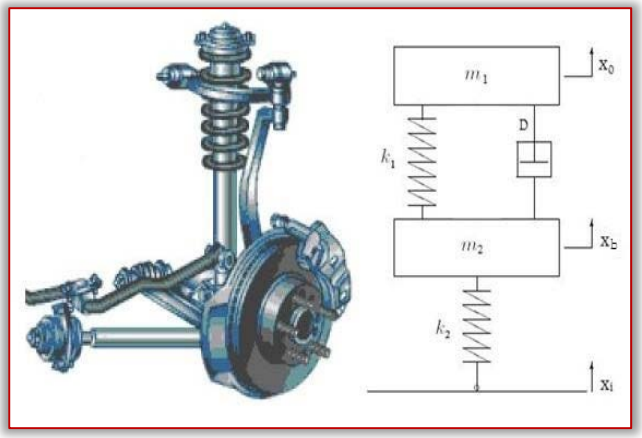

Figure 1. Quarter Model of Passive suspension system

Figure 1 shows a quarter vehicle model of the passive suspension system. The sprung mass m_1 represents the vehicle body, and the unsprung mass m_2 is an assembly of the axle and wheel. The tire is assured to contact the surface of the road when the vehicle is traveling, and is modeled as a linear spring with stiffness k_2. The linear damper, whose average damping coefficient is D, and the linear spring, whose average stiffness coefficient is k_1, consist of the passive component of the suspension system. The state variables x_0 (t) and x_b (t) are the vertical displacements of the sprung and unsprung masses, respectively, and x_i (t) is the vertical road profile.

This is a vehicle body and wheel dual-mass vibration system model. From this model, we can analyze the vehicle suspension system dynamics and establish two degrees of freedom motion differential equations. Their equilibrium position is the origin of coordinates; we can get the equations as follow (1) and (2).

$$m_1 \ddot{x}_0(t) + D\left[\dot{x}_0(t) - \dot{x}_b(t)\right] + k_1\left[x_0(t) - x_b(t)\right] = 0 \qquad (1)$$

$$m_2 \ddot{x}_b(t) - D\left[\dot{x}_0(t) - \dot{x}_b(t)\right] + k_1\left[x_b(t) - x_0(t)\right] + k_2\left[x_b(t) - x_i(t)\right] = 0 \qquad (2)$$

Letting

$$W = x_0 - x_b$$

where: W-Suspension Deflection; X_i-Road Disturbance

If we make a Laplace transformation to the above equation, we can get equation (3):

$$\frac{W}{X_i} = \frac{M_1 K_2}{M_1 M_2 s^2 + (M_2 + K_2) Ds + (M_2 K_1 + M_1 K_1 + M_2 K_2 + K_1 K_2)} \qquad (3)$$

Table 1: Parameters of quarter vehicle model

Model parameters	Symbol	Symbol Values
Vehicle body mass	m 1	300 Kg
Wheel assembly mass	m 2	40 Kg
Suspension stiffness	k 1	15,000 N/m
Tire stiffness	k 2	150,000 N/m
Suspension damping	D	1000 N-s/m

The passive suspension system P_{C1} (s) transfer function is

$$P_{C1}(s) = \frac{4.5\times10^9}{12000s^2 + 1.5\times10^8 s + 2.261\times10^9}$$

— Active Suspension System Mathematical Model

The mathematical model and the simulation made by the following sections are only discussing the amount of force created by the active suspension. Active suspensions allow the designer to balance these objectives using a feedback-controller hydraulic actuator which is driven by a motor between the chassis and wheel assembly. The force U applied between the body and wheel assembly is controlled by feedback and represents the active component of the suspension system.

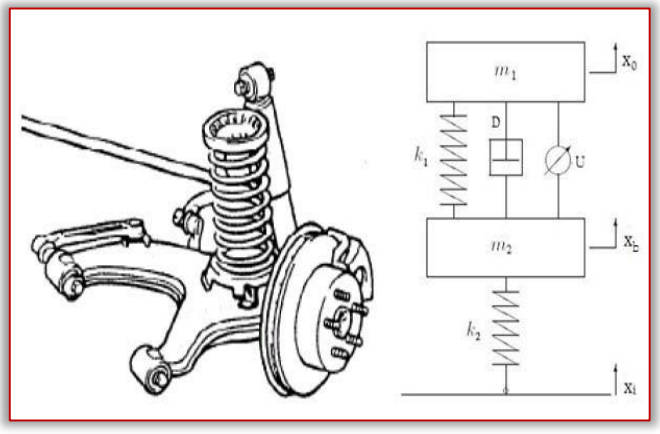

Figure 2. Quarter Model of active suspension system with actuating force (u) between sprung and unsprung mass.

Figure 2 shows a vehicle quarter model of active suspension system. The mass m 1 (in kilograms) represents the car chassis (body) and the mass m 2 (in kilograms) represents the wheel assembly.

The spring K 1 and damper D represent the passive spring and shock absorber placed between the car body and the wheel assembly. The spring K 2 models the compressibility of the pneumatic tire. The variables x 0 , x b and x i (all in meters) are the body travel, wheel travel, and road disturbance, respectively. The actuator force f s (in KiloNewtons) applied between the body and wheel assembly is controlled by feedback and represents the active component of the suspension system.

From this model, we can analyze the vehicle suspension system dynamics as a linear system model and establish two degrees of freedom motion differential equations will be as follow:

$$m_1\ddot{x}_0(t)+D\left[\dot{x}_0(t)-\dot{x}_2(t)\right]+k_1\left[x_0(t)-x_2(t)\right]=u$$

$$m_2\ddot{x}_2(t)-D\left[\dot{x}_0(t)-\dot{x}_2(t)\right]+k_1\left[x_2(t)-x_0(t)\right]+k_2\left[x_2(t)-x_1(t)\right]=-u$$

We can set:

$$x_1=x_2(t), x_2=x_0(t), x_3=\dot{x}_2(t), x_4=\dot{x}_0(t)$$

The system state space equation can be express as:

$$\frac{dX}{dt}=AX+BU$$

In this equation, state variable matrixes are:

$$X=\begin{pmatrix}x_1 & x_2 & x_3 & x_4\end{pmatrix}^T$$

Constant matrixes A and B are shown as below:

$$A=\begin{pmatrix}0 & 0 & 1 & 0\\ 0 & 0 & 0 & 1\\ -\frac{k_1+k_2}{m_2} & \frac{k_1}{m_2} & -\frac{D}{m_2} & \frac{D}{m_2}\\ \frac{k_1}{m_1} & -\frac{k_1}{m_1} & \frac{D}{m_1} & -\frac{D}{m_1}\end{pmatrix}$$

$$B=\begin{pmatrix}0 & 0\\ 0 & 0\\ \frac{k_2}{m_2} & \frac{1}{m_2}\\ 0 & -\frac{1}{m_1}\end{pmatrix}$$

The system input variable matrix will be:

$$U=\begin{pmatrix}x_1(t) & u\end{pmatrix}^T$$

The vehicle suspension system output matrix equation will be:

$$Y=CX+DU$$

In above equation, the output variable matrix Y will be:

$$Y=\begin{pmatrix}k_2\left[x_1(t)-x_2(t)\right] & \ddot{x}_0(t) & x_0(t)\end{pmatrix}$$

Y will also express as the following equation:

$$Y=\begin{pmatrix}k_2\left[x_1(t)-x_2(t)\right] & \ddot{x}_0(t) & x_0(t)\end{pmatrix}$$

Constant matrixes C and D will be shown as below:

$$C=\begin{pmatrix}-k_2 & 0 & 0 & 0\\ \frac{k_1}{m_1} & -\frac{k_1}{m_1} & \frac{D}{m_1} & -\frac{D}{m_1}\\ 0 & 1 & 0 & 0\end{pmatrix}$$

$$D=\begin{pmatrix}k_2 & 0\\ 0 & -\frac{1}{m_1}\\ 0 & 0\end{pmatrix}$$

ROAD PROFILES

Four types of road disturbance input signal will be used to simulate different kinds of road condition. They are bump input signal, sine pavement input signal, random input signal and slope road input signal. These inputs are the prerequisite to simulate the vehicle suspension system, and they should be accurately reflecting the real road condition when a vehicle drives on the road. Precise signal is crucial to the result of the simulation. We assume the vehicle is a linear system.

—Bump Road Disturbance:

Bump input signal is a basic input to research the suspension system. It simulated a very intense force for a very short time, such as a vehicle drive through a speed hump. This road disturbance has a maximum height of 10 cm as shown in Figure 3.

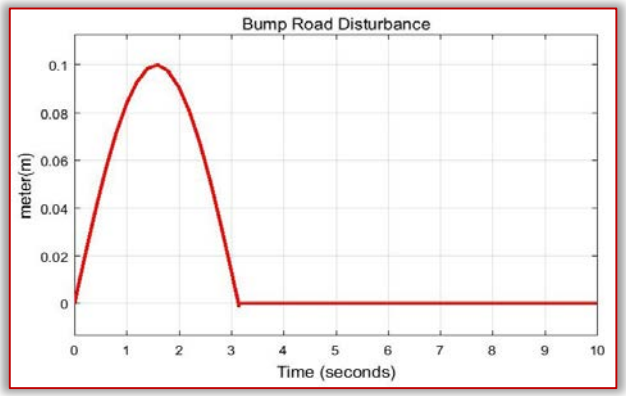

Figure 3. Bump road disturbance

—Random Road Disturbance:

Numerous researches show that it is necessary to test a car to a random road disturbance to check the spring and damper respond quickly and correctly.

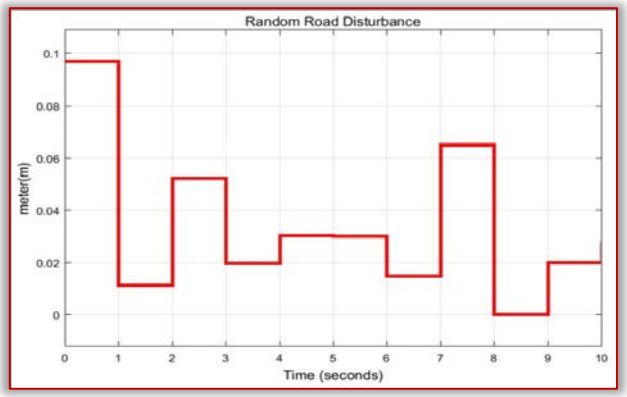

Figure 4. Random road disturbance

The random road disturbance has a maximum height of 10 cm and minimum height of 0 cm as shown in Figure 4.

— Sine Pavement Road Disturbance:

Sine wave input signal can be used to simulate periodic pavement fluctuations. It can test the vehicle suspension system elastic resilience ability while the car experiences a periodic wave pavement. Sine input pavement test is made by every automotive industries before a new vehicle drives on road. The sine pavement road disturbance has a height of -10 cm to 10 cm as shown in Figure 5.

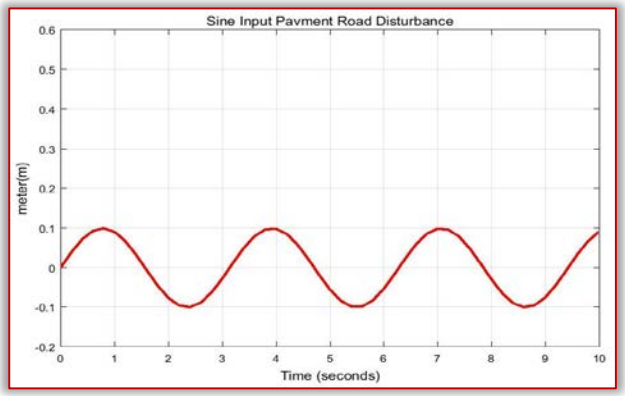

Figure 5. Sine Input pavement road disturbance

— Slope Road Disturbance:

The suspension performance is tested using slope road disturbance by checking the degree of elevation of the road that the suspension handle. The proposed slope road disturbance is 45^0 degree elevated as shown in Figure 6.

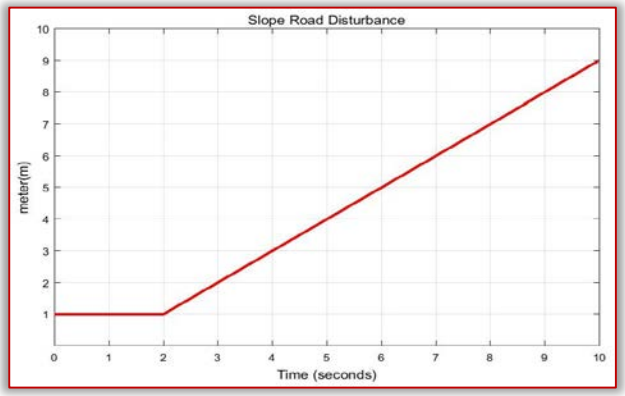

Figure 6. Slope road disturbance

THE PROPOSED H ∞ CONTROL DESIGN

The design of active suspension system to provide passenger comfort and road handling is developed using H ∞ controller design. The main aim of the controller design is to minimize suspension deflection, body acceleration and body travel of the system. H ∞ synthesis is the method used to design the proposed controller by achieving the performance objective via minimizing the weighted transfer function norm. The H infinity interconnected design for active suspension system is shown in Figure 7.

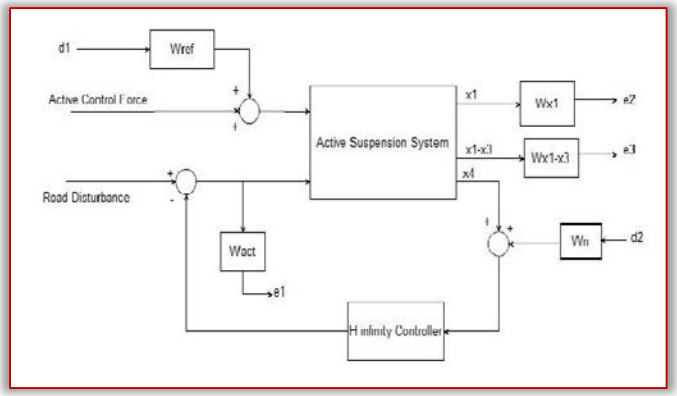

Figure 7. H ∞ system interconnected block diagram

There are two purposes for the weighted functions norm: for a given norm, there will be a direct comparison for different performance objectives and they are used for knowing the frequency information incorporated into the analysis. The output or feedback signal y is

$$y = (x\,4 + d2 * Wn) * H\infty \text{ Controller}$$

The controller's acts on the y signal to produce the road disturbance signal. The W_n block modelled the sensor noise in the channel. W_n is given a sensor noise of 0.05 m.

$$W_n = 0.05$$

W_n is used to model the noise of the displacement sensor. The magnitude of the active control force is scaled using the weight W_{ref}. Let us assume the maximum control force is 0.1Newton which means

$$W_{ref} = 0.1$$

The weighting function W_{act} is used to limit the magnitude and frequency content of the input road disturbance signal. Choosing

$$W_{act} = \frac{80}{11}\frac{s+60}{s+600}$$

— H infinity Controller Design G_{c1} (s):

W_{x1} and W_{x1-x3} are used to keep the car deflection and the suspension deflection small over the desired range. The car body deflection W_{x1} is given as

$$W_{x1} = \frac{508.1}{s+56.55}$$

The suspension deflection is used via weighting function

W_{x1-x3}. The weighting function is given as

$$W_{x1-x3} = \frac{15}{0.2s+1}$$

— The Proposed μ-Synthesis Control Design

In the active suspension system, μ-synthesis design included the hydraulic actuator dynamics. In order to account for the difference between the actuator model and the actual actuator dynamics, we used a first order model of the actuator dynamics as well as an uncertainty model. The μ-synthesis interconnection block diagram for active suspension system is shown in Figure 8.

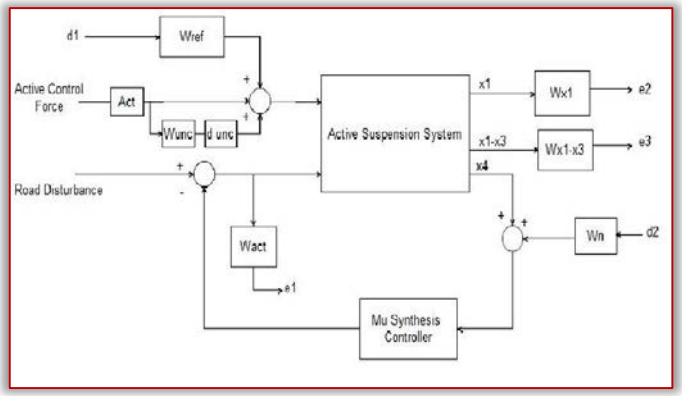

Figure 8. μ-synthesis interconnection block diagram

—µ-Synthesis Controller Design S_{c1} (s):

The nominal model for the hydraulic actuator is

$$HYD_{act} = \frac{1}{\frac{1}{50}s + 1}$$

We describe the actuator model error as a set of possible models using a weighting function because the actuator model itself is uncertain. The model uncertainty is represented by weight W_{unc} which corresponds to the frequency variation of the model uncertainty and the uncertain LTI dynamics object 4_{unc} which is Unc=Uncertain LTI dynamics "*unc*" with 1 outputs, 1 inputs, and gain less than 1.

$$W_{unc} = \frac{0.03s + 0.15}{0.001667s + 1}$$

The uncertain actuator model represents the model of the hydraulic actuator used for control. A μ-synthesis controller is synthesized using D-K iteration. The D-K iteration method is an approximation to synthesis that attempts to synthesize the controller. There is two control input the road disturbance signal and the active control force. There are three measurement output signals, the suspension deflection, car body acceleration and car body travel.

RESULT AND DISCUSSION

—Simulation of the Proposed Controllers

In this subsection we simulate passive suspension system, active suspension system with G_{C1} (*s*) controller, active suspension system with S_{C1} (*s*) controller and active suspension system without controller for suspension deflection, body acceleration and body travel using bump, random, sine pavement and slope road disturbances.

» Simulation of a Bump Road Disturbance:

The Simulink model for a bump input road disturbance and active control force input is shown in Figure 9. In this Simulink model, we simulate passive suspension system, active suspension system with G_{C1} (*s*) controller, active suspension system with S_{C1} (*s*) controller and active suspension system without controller for suspension deflection, body acceleration and body travel. Here in this Simulink we assign d1 and d2 as a random signal with amplitude of 0.001 and period of 10 seconds and there are three error signals named e1, e2 and e3 and there are three active control force for the active suspension with controller and without controller with a step function input.

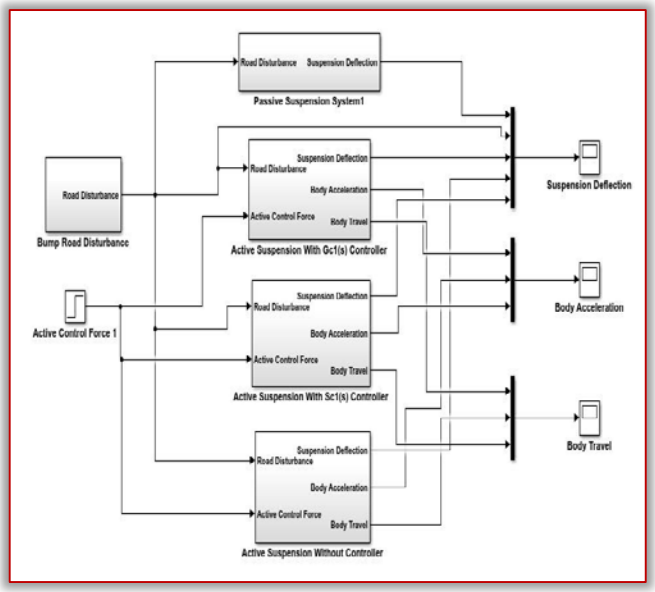

Figure 9. Simulink model of a Bump road disturbance

The suspension deflection, body acceleration and body travel simulation output is shown in Figure 10, Figure 11 and Figure 12 respectively for a bump road disturbance and active control force inputs.

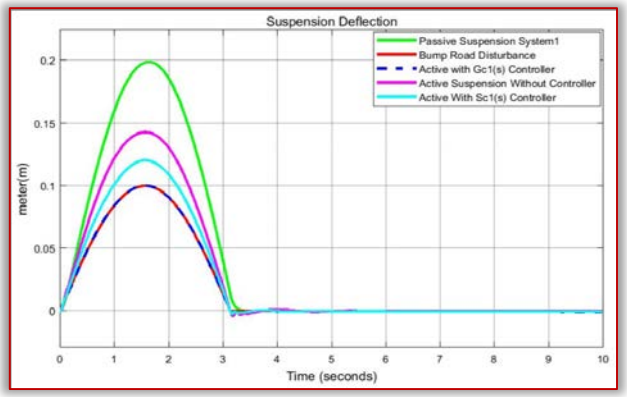

Figure 10. Suspension deflection for Bump road disturbance

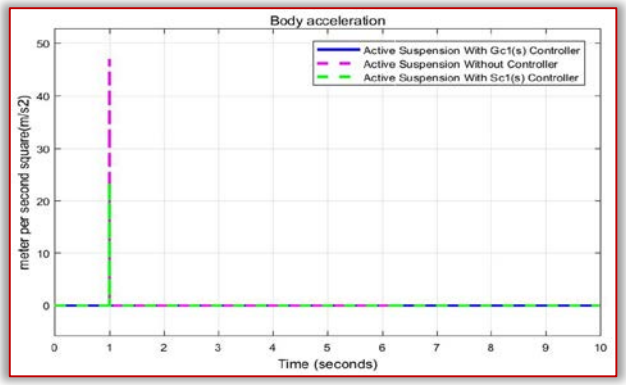

Figure 11. Body acceleration for Bump road disturbance

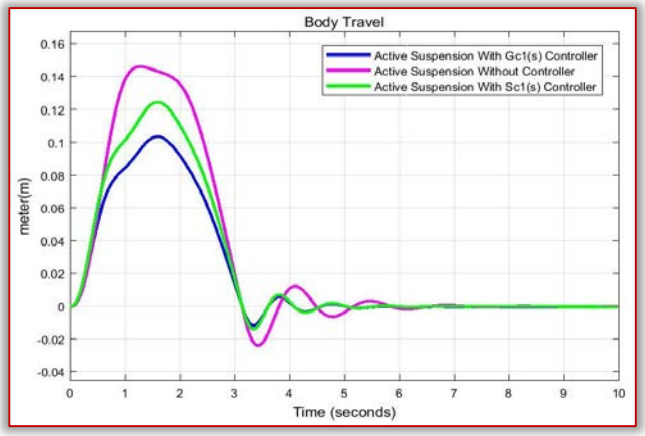

Figure 12. Body travel for Bump road disturbance

» **Simulation of a Random Road Disturbance:**

The Simulink model for a random road disturbance and active control force inputs is shown in Figure 13.The suspension deflection, body acceleration and body travel simulation is shown in Figure 14, Figure 15 and Figure 16 respectively.

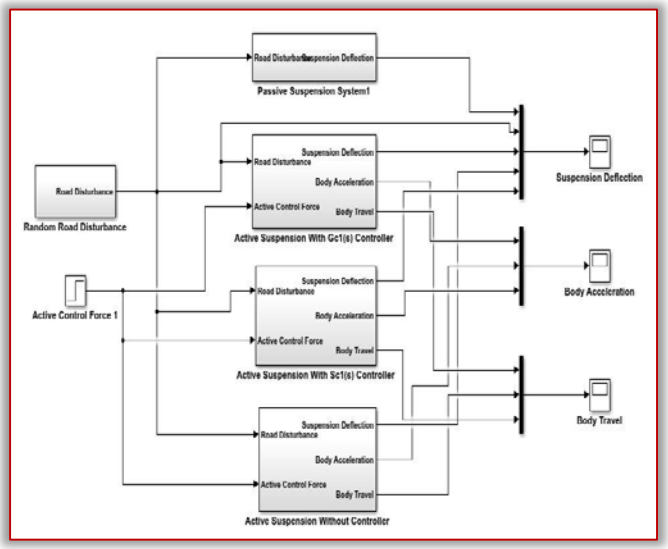

Figure 13. Simulink model for a Random road disturbance

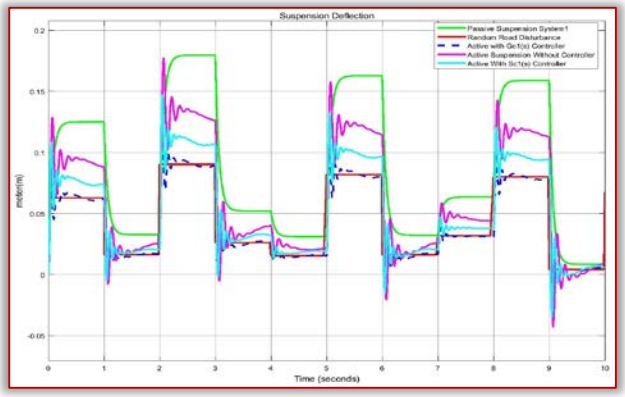

Figure14.Suspension deflection for Random road disturbance

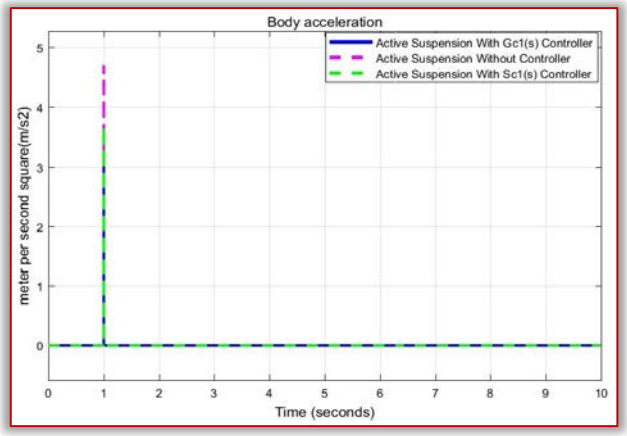

Figure 15. Body acceleration for Random road disturbance

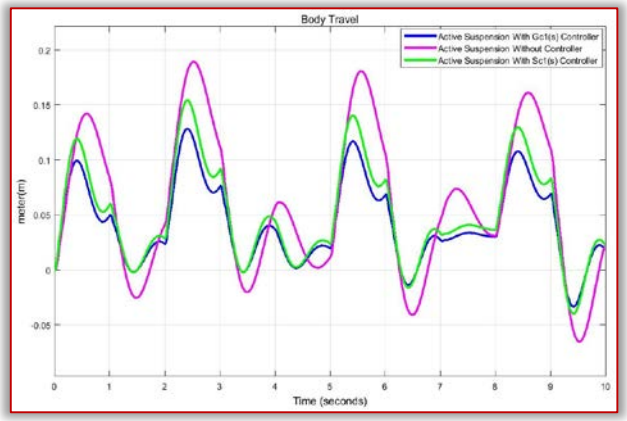

Figure 16. Body travel for Random road disturbance

» **Simulation of a Sine Input Pavement Road Disturbance:**

The Simulink model for a sine input pavement road disturbance and active control force inputs is shown in Figure 17. The suspension deflection, body acceleration and body travel simulation is shown in Figure 18, Figure 19 and Figure 20 respectively.

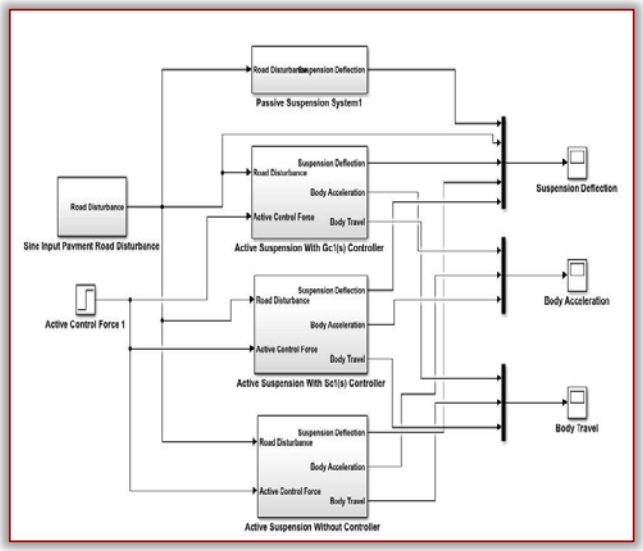

Figure 17. Simulink model for a Sine input pavement road disturbance

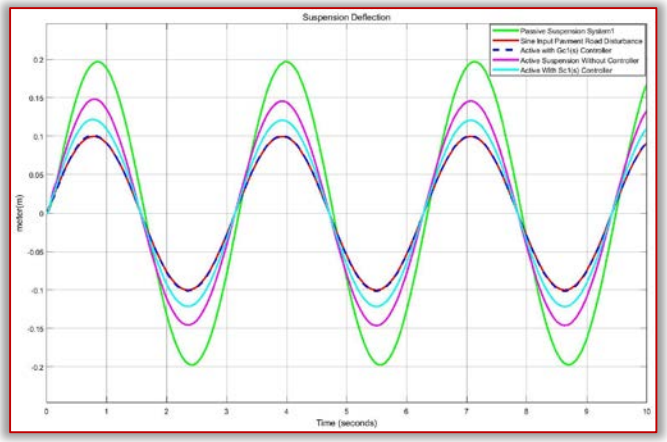

Figure 18. Suspension deflection for Sine input pavement road disturbance

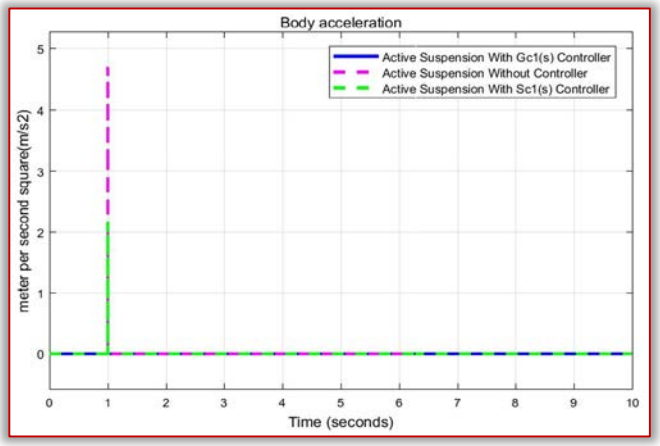

Figure 19. Body acceleration for Sine input pavement road disturbance

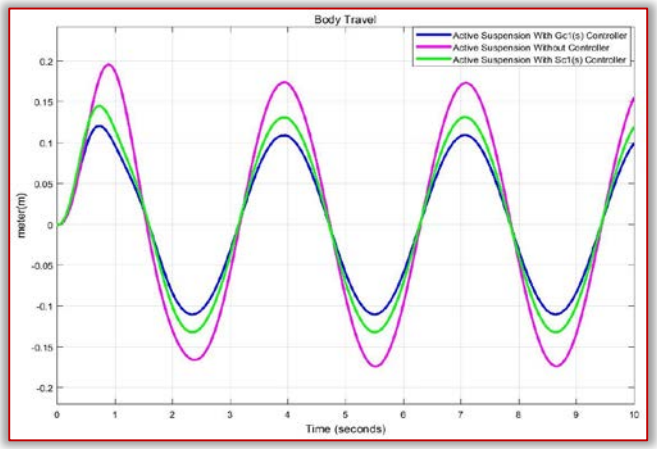

Figure 20. Body travel for Sine input pavement road disturbance

» **Simulation of a Slope Road Disturbance:**

The Simulink model for a slope road disturbance and active control force inputs is shown in Figure 21.The suspension deflection, body acceleration and body travel simulation is shown in Figure 22, Figure 23 and Figure 24 respectively.

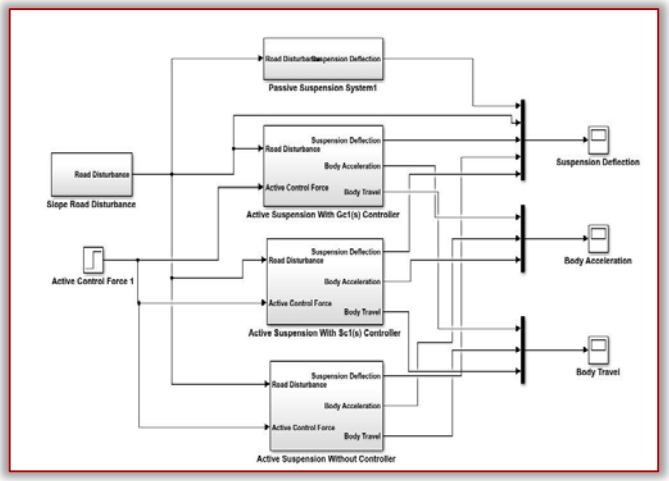

Figure 21. Simulink model for a Slope road disturbance

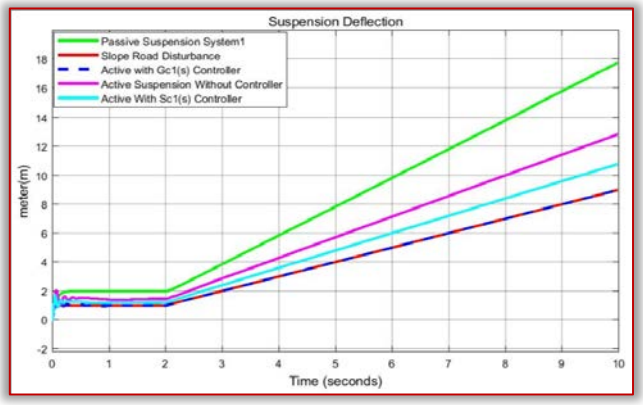

Figure 22. Suspension deflection for Slope road disturbance

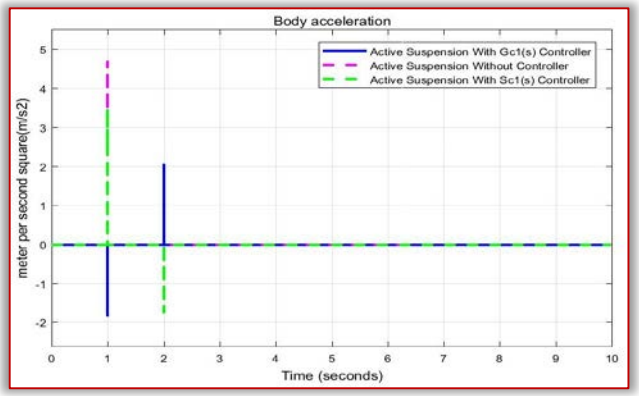

Figure 23. Body acceleration for Slope road disturbance

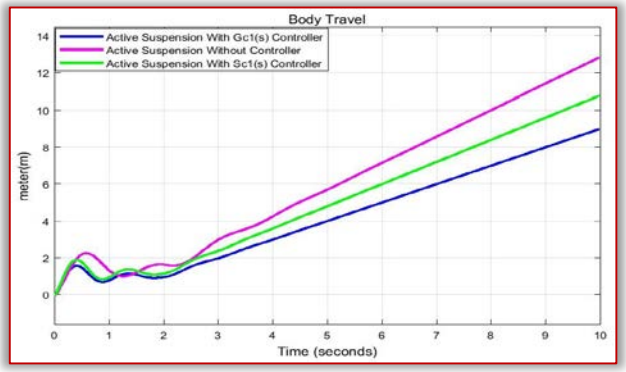

Figure 24. Body travel for Slope road disturbance

— Comparison of Active Suspension System With H∞ $G_{C1}(s)$ and μ–Synthesis $S_{C1}(s)$ Controllers

Here in this section, we compare active suspension system with $H\infty$ controller ($G_{C1}(s)$) and μ–synthesis controller ($S_{C1}(s)$) for suspension deflection, body acceleration and body travel with bump, random, sine and slope road disturbances.

» Comparison for Bump Road Disturbance:

In the suspension deflection simulation as shown in Figure 10, the active suspension system with $S_{C1}(s)$ controller strokes are larger than the road surface wave amplitude while the active suspension system with $G_{C1}(s)$ controller strokes fits the road surface wave amplitude. In the body acceleration as shown in Figure 11, the acceleration is effectively reduced in the active suspension system with $G_{C1}(s)$ controller. In the body travel as shown in Figure 12, the vertical distance that the body travels is effectively reduced in the active suspension system with $G_{C1}(s)$ controller. The reduction in overshoot value is shown in Table 2.

Table 2 Reduction in overshoot value for bump road disturbance

Parameters	S_{C1} (s)	G_{C1} (s)	% in Reduction
Suspension Deflection	0.13 m	0.1 m	23.08 %
Body Acceleration	$24\frac{m}{s^2}$	$5\frac{m}{s^2}$	79.2 %
Body Travel	0.13m	0.11 m	15.38 %

» Comparison for Random Road Disturbance:

In the suspension deflection simulation as shown in Figure 14, the active suspension system with $S_{C1}(s)$ controller strokes have a larger amplitude than the active suspension system with $G_{C1}(s)$ controller. In the body acceleration as shown in Figure 15, the acceleration is effective reduced in the active suspension system with $G_{C1}(s)$ controller. In the body travel as shown in Figure 16, the vertical distance that the body travels is effectively reduced in the active suspension system with $G_{C1}(s)$ controller. The reduction in overshoot value is shown in Table 3.

Table 3 Reduction in overshoot value for random road disturbance

Parameters	S_{C1} (s)	G_{C1} (s)	% in Reduction
Suspension Deflection	0.18 m	0.13 m	27.78 %
Body Acceleration	$3.7\frac{m}{s^2}$	$3\frac{m}{s^2}$	19 %
Body Travel	0.16 m	0.13 m	18.75

» Comparison for Sine Pavement Road Disturbance:

In the suspension deflection simulation as shown in Figure 18, the active suspension system with $S_{C1}(s)$ controller strokes are larger than the road surface wave amplitude while the active suspension system with $G_{C1}(s)$ controller strokes fits the road surface wave amplitude. In the body acceleration as shown in Figure 19, the acceleration is effectively reduced in the active suspension system with $G_{C1}(s)$ controller. In the body travel as shown in Figure 20, the vertical distance that the body travels has a large amplitude in the active suspension system with $S_{C1}(s)$ controller and is effectively reduced in the active suspension system with $G_{C1}(s)$ controller. The reduction in overshoot value is shown in Table 4.

Table 4 Reduction in overshoot value for sine pavement road disturbance

Parameters	S_{C1} (s)	G_{C1} (s)	% in Reduction
Suspension Deflection	0.13 m	0.1 m	23.08 %
Body Acceleration	$2.\frac{m}{s^2}$	$2.\frac{m}{s^2}$	4.56 %
Body Travel	0.14 m	0.12 m	14.3 %

» Comparison for Slope Road Disturbance:

In the suspension deflection simulation as shown in Figure 22, the active suspension system with $S_{C1}(s)$ controller slopes are larger than the road surface wave amplitude while the active suspension system with $G_{C1}(s)$ controller slope fits the road surface wave amplitude. In the body acceleration as shown in Figure 23, the acceleration is effectively reduced in the active suspension system with $G_{C1}(s)$ controller. In the body travel as shown in Figure 24, the body travels has a large slope and vibration in the active suspension system with $S_{C1}(s)$ controller and is effectively aligned with small vibration in the active suspension system with $G_{C1}(s)$ controller. The reduction in overshoot value is shown in Table 5.

Table 5 Reduction in overshoot value for slope road disturbance

Parameters	S_{C1} (s)	G_{C1} (s)	% in Reduction
Suspension Deflection	51.3^0	45^0	12.3 %
Body Acceleration	$3.5\frac{m}{s^2}$	$2\frac{m}{s^2}$	43 %
Body Travel	51.3^0	45^0	12.3 %

CONCLUSION

In this paper, H ∞ controller and μ - synthesis controllers are successfully designed using MATLAB/SIMULINK for quarter car active suspension system. We design a Simulink model that represents the active suspension system with H ∞ controller, μ - synthesis controller, without controller and passive suspension system and tasted with bump, sine input pavement, random and slope road disturbances for suspension deflection, body acceleration and body travel. We compared the active suspension system with H ∞ controller and μ - synthesis controller for the three parameters and we

analyze the percentage reduction in overshoot of the two controllers.

The simulation results shows that the active suspension system with H ∞ controller is capable of stabilizing the suspension system very effectively than the active suspension system with μ - synthesis controller for suspension deflection, body acceleration and body travel parameters with the four road input disturbances. The system with H ∞ controller has a percentage reduction in overshoot than a system with μ - synthesis controller.

We conclude that an active suspension system with H ∞ controller has the best performance with the different tests we made on the system and it achieves the passenger comfort and road handling criteria that it needed to make the active suspension system is the best suspension system.

Acknowledgments

First and formost, I would like to express my deepest thanks and gratitude to Dr.Parashante and Mr.Tesfabirhan for their invaluable advices, encouragement, continuous guidance and caring support during my journal preparation.

Last but not least, I am always indebted to my brother, Taha Jibril, my sister, Nejat Jibril and my family members for their endless support and love throughout these years. They gave me additional motivation and determination during my journal preparation.

References

[1] Nasir, Ahmed and Al-awad "Genetic Algorithm Control of Model Reduction Passive Quarter Car Suspension System" I.J. Modern Education and Computer Science, 2019.

[2] Vivek Kumar Maurya and Narinder Singh Bhangal "Optimal Control of Vehicle Active Suspension System" Journal of Automation and Control Engineering Vol. 6, No. 1, 2018.

[3] Michiel Haemers "Proportional-Integral State-Feedback Controller Optimization for a Full-Car Active Suspension Setup using a Genetic Algorithm" The 3rd IFAC Conference on Advances in Proportional Integral-Derivative Control, Ghent, Belgium, 2018.

[4] Vinayak S. Dixit and Sachin C. Borse "SemiactiveSsuspensionSsystem Design for QuarterCcar Model and itsAanalysis with Passive Suspension Model" International Journal of Engineering Sciences & Research Technology, 2017

[5] Yakubu G.1, Adisa A. B., "Simulation and Analysis of Active Damping System for Vibration Control", American Journal of Engineering Research, Vol. 6, Issue 11, 2017.

[6] Ahmed A. Abougarair and Muawia M. A. Mahmoud "Design and Simulation Optimal Controller for Quarter Car Active Suspension System" 1st Conference of Industrial Technology (CIT2017), 2017.

[7] J. Marzbanrad and N. Zahabi "H∞ Active Control of a Vehicle Suspension System Exited by Harmonic and Random Roads" Journal of Mechanics and Mechanical Engineering Vol. 21, No. 1 pp 171–180, 2017.

[8] Shital M. Pawar and A.A. Panchwadkar "Estimation of State Variables of Active Suspension System using Kalman Filter" International Journal of Current Engineering and Technology E-ISSN 2277 – 4106 , P-ISSN 2347 – 5161,Vol.7, No.2, 2017.

[9] Libin Li and Qiang Li "Vibration Analysis Based on Full Multi Body Model for a Commercial Vehicle Syspension System"ISPRA'07 Proceeding of the 6th WSEAS International, 2016.

[10] Narinder Singh"Robust Control of Vehicle Active Suspension System" International Journal of Control and Automation Vol. 9, No. 4 (2016), pp. 149-160, 2016.

[11] Panshuo Li, James Lam, Kie Chung Cheung "Experimental Investigation of Active Disturbance Rejection Control for Vehicle Suspension Design"International Journal of Theoretical and Applied Mechanics Volume 1, 2016.

[12] Ahmed S Ali, Gamal A.Jaber, Nouby M Ghazaly, "H∞ Control of Active Suspension System for a Quarter Car Model", International Journal of Vehicle Structures and Systems Vol.8, No.1, 2016.

[13] M. P. Nagarkar and G. J. Vikhe Patil "Multi-Objective Optimization of LQR Control Quarter Car Suspension System using Genetic Algorithm" FME Transactions, 44, 187-196, 2016.

ACTA TECHNICA CORVINIENSIS – Bulletin of Engineering
ISSN: 2067-3809

[1.]Ghanendra KUMAR, [2.]Chakresh KUMAR

PERFORMANCE ANALYSIS OF CROSSTALK INDUCED OPTICAL COMMUNICATION SYSTEM

[1.]Department of Electronics and Communication Engineering, National Institute of Technology, New Delhi, INDIA
[2.]University School of Information, Communication & Technology, Guru Gobind Singh Indraprastha University, New Delhi, INDIA

Abstract: Cross-phase Modulation and self-phase modulation has some effect on two analog channels propagating in the optical fiber. The motivation behind this work is to compute these effects by studying the interaction between two channels and modulating the components of two channels. Crosstalk between two channels depends on wavelength spacing, sub-carrier frequency and optical power. Crosstalk due to cross-phase modulation depends on channel spacing and dispersion in fiber. The power of the crosstalk created by the received radio frequency and the two channels are calculated in direct identification. Formulations for phase modulation and amplitude are analyzed with the help of SPM and XPM. In this approach, it is assumed that there is no distortion in the pump channel therefore this method computes distortions due to Self-phase modulation, cross-phase modulation and dispersion in both channels.
Keywords: Cross-phase Modulation (XPM), Pump, Self- Phase Modulation (SPM), Probe, Crosstalk, Amplitude Modulation, Phase Modulation

INTRODUCTION

When a number of signals are multiple into a single optical fiber by using different wavelength, an optical effect which is non-linear in nature takes place. In this effect, one wavelength of signal affects the phase of some other wavelength of light due to the kerr effect. This is known as Cross-phase modulation (XPM). This effect is huge and harmful in nature in the presence of dispersion. Probe channel is the channel in which phase modulation is transferred by XPM and similarly pump channel is the channel in which intensity modulation is transferred.

Intensity modulation which is transferred from the pump to probe is calculated in terms of crosstalk. Mathematically, it is the ratio of power of the received radio frequency in probe channel to received radio frequency power in the pump channel in decibels. [1-5]

Crosstalk in optical fiber arises because of the Kerr effect. Therefore, it is necessary to reduce it by using some techniques. These techniques have been used successfully to reduce this interaction between channels. The dispersion-managed system is a system in which a technique is used to reduce the dispersion introduced in the optical fiber, generally, a dispersion slope compensator is used. In these types of dispersion-managed systems, a large difference between group velocity is achieved between two channels which reduce the nonlinearity in phase rotation in a probe over many periods of amplitude modulation [6-8].

In the past work, it is difficult to calculate crosstalk I analog fiber links. In previous work, some expression for crosstalk has been presented. However, in previous researches, it is assumed that there is no distortion in the pump channel during transmission. But it is necessary to take the distortion in the account to compute crosstalk accurately for large frequency in modulation for dispersion-managed systems on which we are working in this work.

One of the techniques to calculate the crosstalk for any system is by using the Schrödinger equation. But, in this paper there is an assumption that modulation depth (modulation index) and the ratio of modulation frequency to the spacing between two channels are very small, therefore, contributing to a linear system of ordinary differential equation. So, crosstalk can be determined by solving differential equations. The linearization helps us in getting characteristics of XPM in dispersion-managed systems [9-10].

ANALYSIS

Let D (z) be the dispersion dependent on z-axis, and our electric field is E that is normalized in order that $|E|^2$ has power units, C is fiber's coefficient that are non-linear & L (z) is the Z dependent loss/gain. So, our equation is

$$\frac{\delta E}{\delta Z} = \frac{j}{2} D(z) \frac{\delta^2 E}{\delta t^2} + jC|E|^2 - \frac{1}{2} L(z) E$$

Let us analyses our equation taking Z varying dispersive and non-linear coefficients by making the transformation

$$q(z,t) = E(z,t) e^{[\frac{1}{2}\int_0^z L(z')dz']}$$

which yields

$$\frac{\delta q}{\delta Z} = \frac{j}{2} D(z) \frac{\delta^2 q}{\delta t^2} + jF(z) q|q|^2 \qquad (1)$$

where,

$$F(z) = Ce^{[-\int_0^Z L(z')dz']}$$

In our equation (1) we have not included the RAMAN effect since in this paper our main goal is to observe the Kerr effects at larger modulation frequency (>2GHz) and also we know that RAMAN effect plays

vital role in lower frequency region only (<2GHz). That's why we haven't counted RAMAN Effect in our equation. Let the signal consists of two adequately separated wavelength channels. Here the term adequately separated implies that demultiplexer doesn't produce any crosstalk in between them. So, the crosstalk (our main focus) comes only from the interaction during the propagation that is non-linear. So,we can write

$$Q`(z,t) = P(z,t) + Q(z,t)e^{(j\Delta\omega t)} \quad (2)$$

Here $\Delta\omega$ is the difference in frequency or spacing between the two channels. Since each channel P and Q are well separated so we can write separate equations for the wavelength channel

$$\frac{\delta P}{\delta Z} = \frac{j}{2}D(z)\frac{\delta^2 P}{\delta t^2} + jF(z)(|P|^2 + 2|Q|^2)P$$

$$\frac{\delta Q}{\delta Z} = \frac{j}{2}D(z)\left\{\frac{\delta^2 Q}{\delta t^2} + 2j\Delta\omega\frac{\delta Q}{\delta t} - \Delta\omega^2 Q\right\} + jF(z)(2|P|^2 + |Q|^2)Q$$

We obtained this equation by putting $q = P + Qe^{j\Delta\omega t}$ into equation (1) and setting $e^{j\Delta\omega t} = 1$. Now, Our main interest is only a small number of radio frequency tones in transmission. We know that RF tones produce electric fields. So the electric field decomposing in our RF tone is obvious. So, let's the decomposition are

$$P(z,t) = \sum_{k=-\infty}^{\infty}\overline{P}k(z)e^{(jk\beta t)}$$

$$Q(z,t) = \sum_{k=-\infty}^{\infty}\overline{Q}k(z)e^{(jk\beta[t-\Delta\omega g(z)])}$$

where $g(z) = \int_0^z D(z')dz'$

Since, Q is $\Delta\omega$ apart from P so decomposition in fourier domain for Q contains the group velocity that is dependent on dispersion that is directly related to the P channel.

CHANNEL'S FOURIER EVOLUTION

We know that in the transmission of either phase modulation or amplitude modulation in the optical field there are three tones in each channel. Two weak sidebands corresponding to modulation and one strong tone that corresponds to the optical carrier. Let's us introduce here an expansion that is a perturbation expansion (a theory in which we conclude an approximate solution to a problem by taking an exact solution to a similar problem) of each channel, which is given as

$$\begin{Bmatrix}\overline{P}K\\ \overline{Q}K\end{Bmatrix} = \begin{Bmatrix}\overline{P}\,0,K\\ \overline{Q}\,0,K\end{Bmatrix} + m\begin{Bmatrix}\overline{P}\,1,K\\ \overline{Q}\,1,K\end{Bmatrix} + O(m^2)$$

Here M is the modulation depth. Our main objective is to make the interaction between channels in linear to the optical carrier. So, let us lower the modulation depth m. Due to small modulation we also need to get derived

Area improvement. So, taking those requirements in mind we assume that $\overline{P}0$ & $\overline{Q}0$ are of unity order and $\overline{P}(+\text{-}1)$ & $\overline{Q}(+\text{-}1)$ are of Mth order , and all other Fourier components of the channels are of order 2^{nd} order of M or higher. In order to handle the highest interaction between the leading order and optical carrier of the two channels, we should assume that there is no modulation in both channels. So, our intersection equals.

$$\frac{\delta P1,0}{\delta Z} = jF(z)(|P1,0|^3 + 2|Q1,0|^3)P1,0$$

$$\frac{\delta Q1,0}{\delta Z} = -\frac{j}{2}D(z)\Delta\omega^3 Q1,0 + jF(z)(2|P1,0|^3 + |Q1,0|^3)Q1,0$$

By using these equations, we yielded explicit solutions

$P1,0(z) = P1,0(0)e^{j(P1+2P2)n(z)}$

where,

$n(z) = \int_0^z F(z')dz'$

$P1 = |P1,0(0)|^3$ and

$P2 = |Q1,0(0)|^3$

We assume that there was no loss of generality.

$$So, P1,0(0) = (P1)^{0.5}$$

and

$$Q1,0(0) = (P2)^{0.5}.$$

Next, let us solve for $P1,\pm1$ and $Q1,\pm1$ by considering the higher order in distortion expansion, O (m), we obtained four equations that are coupled for $P1,\pm1$ and $Q1,\pm1$.

Let us change the variables which simplifies the equations significantly.

$$y1(z) = P1,1\ (z)e^{j\varphi1(z)}$$

$$y2(z) = P'1,-1\ (z)e^{j\varphi2(z)}$$

$$y3(z) = Q1,1\ (z)e^{j\varphi3(z)}$$

$$y4(z) = Q'1,-1\ (z)e^{j\varphi4(z)}$$

when we choose these substitution

$$\varphi1\ (z) = -(P1 + 2P2)n(z) + \Omega\frac{\Delta\omega}{2}g(z)$$

$$\varphi2\ (z) = (P1 + 2P2)n(z) + \Omega\frac{\Delta\omega}{2}g(z)$$

$$\varphi3\ (z) = -(2P1 + P2)n(z) + \frac{1}{2}(\Delta\omega^2 - \Omega\Delta\omega)g(z)$$

$$\varphi4\ (z) = (2P1 + P2)n(z) - \frac{1}{2}(\Delta\omega^2 + \Omega\Delta\omega)g(z)$$

Since, we have changed the variables so we get

$$\frac{dy}{dz} = j\left[\frac{1}{2}D(z)\Omega A + F(z)B\right]y(z) \quad (3)$$

where $Y`(z) = (Y`1, Y`2, Y`3, Y`4)^T$ and here we have taken A and B as constant square matrices of order 4, that are given below

$$A = \begin{pmatrix}-\beta+\Delta\omega & 0 & 0 & 0\\ 0 & \beta+\Delta\omega & 0 & 1\\ 1 & 0 & -\beta-\Delta\omega & 0\\ 0 & 1 & 0 & \beta-\Delta\omega\end{pmatrix}$$

and

$$B = \begin{pmatrix}P1 & P1 & 2(P1P2)^{0.7} & 2(P1P2)^{0.7}\\ -P1 & -P1 & -2(P1P2)^{0.7} & -2(P1P2)^{0.7}\\ 2(P1P2)^{0.7} & 2(P1P2)^{0.7} & P2 & P2\\ 2(P1P2)^{0.7} & 2(P1P2)^{0.7} & -P2 & -P2\end{pmatrix}$$

Here we can see that equation 3 is an ordinary differential equation that is a linear system that is also homogeneous. Since these equations are fourth order

ODEs so its solution i.e., quantitative evaluation is far rapid and it will be very useful in parametric studies of the system. Also here in equation (3) there are two explicit terms which separate the effect of power dispersion and fluctuation in the variable coefficients D (z) and F (z).

COMPUTING CROSSTALK BETWEEN SIMPLE WIRES

Crosstalk is the coupling of energy from one wire to other wire when both are parallel to each other and carrying some signal. Coupling of energy takes place through mutual induction and mutual capacitance between two wires.

Due to the mutual induction, current will induce in each wire opposite to the signal current. It is known as Lenz's law. Due to the mutual capacitance, some signal current will pass through this capacitor and producing some error.

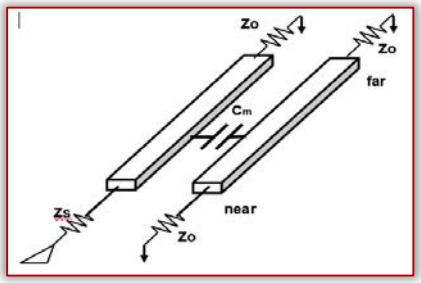

Figure 1. Mutual Capacitance

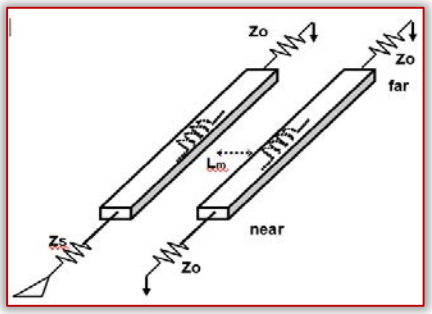

Figure 2. Mutual Inductance

L AND C MATRIX

L and C matrix are the transmission matrices which are to evaluate electrical characteristics and help us to compute crosstalk.

L matrix is known as the Inductance matrix and it is shown in figure 3. C matrix is known as Capacitance matrix and it is shown in figure 4.

$$\begin{bmatrix} L_{11} & L_{12} & \dots & L_{1N} \\ L_{21} & L_{22} & & \\ & & & \\ L_{N1} & & & L_{NN} \end{bmatrix}$$

Figure 3. Inductance matrix

$$\begin{bmatrix} C_{11} & C_{12} & \dots & C_{1N} \\ C_{21} & C_{22} & & \\ & & & \\ C_{N1} & & & C_{NN} \end{bmatrix}$$

Figure 4. Capacitance matrix

In the L matrix L_{11} L_{22} etc. are the self-inductance of line per unit length where L_{xy} is the mutual inductance between line x and line y. In the C matrix C_{11} C_{22} etc. are the self-capacitance of line per unit length and C_{xy} is the mutual capacitance.

With the help of L and C matrices, the crosstalk voltages of the end and far-end can be easily found. Quotes for near end and far end crosstalk amplitude can be written as below:

$$V_{near} = \frac{V_{input}}{4}\left[\frac{L_{12}}{L_{11}} + \frac{C_{12}}{C_{11}}\right] \quad (4)$$

$$V_{far} = \frac{V_{input}(X\sqrt{LC})}{2T_{rise}}\left(\frac{L_{12}}{L_{11}} - \frac{C_{12}}{C_{11}}\right) \quad (5)$$

Where V_{input} is input voltage, X is the length of line and L and C is the values of inductor and capacitor.

COMPUTING CROSSTALK-DIRECT DETECTION

Direct optical transmission systems are characterized by their capability to do "direct detection". It is used by systems which have 10GB/s or lower speed. I a direct detection receiver, the photodetector is sensitive to changes in receiving signal optical power, it cannot extract or get the information of phase or frequency from optical carrier (4).

Crosstalk can be calculated in optical direct transmission at some distance. Therefore, crosstalk is defined as:

$$\text{Crosstalk}(\Omega) = 1010 \log_{10} \frac{\text{RF power of signal 1}}{\text{RF power of signal 2}} \quad (6)$$

Where signal 1 is in probe channel and signal 2 is in the pump channel.

Radio frequency spectrum analyzer is similar to an oscilloscope, but it displays the signal in frequency domain i.e. signals versus frequency. This is helpful to test RF circuits and to get the RF power. Therefore, RF analyzer gives power of the radio frequency that considers probe channel and pump channel by squaring the amplitude and the complex Fourier component of acquired photocurrent in the analyzer of the above channel. The relation between radio frequency power and the optical field is:

$$\text{RF power}(\beta) = R\left|\frac{K}{T}\int_0^T |\mu(z,t)|^2 e^{i\beta t} dt\right|^2 \quad (7)$$

where the radio frequency spectrum analyzer that consider the load resistance and denoted by R, photodetector's responsivity by K and $T = \frac{2\pi}{\beta}$ denotes the time duration of the radio frequency oscillation.

These expressions are used to calculate RF power for probe and pump channel. By using equations 6(a) and 6(b) and above equation for u channel, the RF power is calculated as:

$$\text{Radio frequency power of } \mu(\beta) = RRK^2[(|\tilde{\mu}_{-1}|^2 + |\tilde{\mu}_1|^2)|\tilde{\mu}_0|^2 + |\tilde{\mu}_0|^2|\tilde{\mu}_1|^*|\tilde{\mu}_{-1}|^* + |\tilde{\mu}_0|^2\tilde{\mu}_1\tilde{\mu}_{-1}]$$

Similarly, the same expression is for v channel. Finally, RF power of u and v channel is described as:

$$\text{RF power of u } (\Omega) = RK^2m^2P_1|y_1(z) + y_2(z)|^2$$

$$\text{RF power of v}(\Omega) = RK^2m^2P_2|y_3(z) + y_4(z)|^2$$

With the help of the previous two expressions, crosstalk can be calculated by the assumption that v channel is pump channel and u channel is probe channel as:

$$\text{Crosstalk}(\Omega) = 10\log_{10}\left[\frac{|w_1(z)+w_2(z)|^2}{|w_3(z)+w_4(z)|^2}\right]$$

AM AND PM MODE EVOLUTION

Above discussions shows that phase modulation mode of a channel affected by amplitude modulation and phase modulation mode of the same channel and amplitude modulation mode of another channel. But, the amplitude modulation mode affected by the modulation technques that are amplitude and phase modulation of the same channel only. Due to dispersion, amplitude modulation in one channel transfers to phase modulation in another channel and phase modulation in one channel transforms to amplitude modulation in the same channel.

Therefore, crosstalk in direct detection assuming pump and probe channel as a v channel and μ channel respectively is given as:

$$\text{Crosstalk}(\Omega) = 10\log_{10}\left[\frac{P_1|A_u(z)|^2}{P_2|A_v(z)|^2}\right] \quad (8)$$

In direct detection, Crosstalk is zero when AM mode of probe channel is zero and crosstalk is infinity when AM mode of pump channel is zero. It means that direct detection receiver cannot extract information about the phase of the pump channel. When AM mode vanishes, the modulation exists as PM mode. So, A system cannot be designed to work on the frequency at which crosstalk is infinity.

RESULTS

Equations for near-end and far-end voltage:

$$V_{near} = \frac{V_{input}}{4}\left[\frac{L_{12}}{L_{11}} + \frac{C_{12}}{C_{11}}\right]$$

$$V_{far} = \frac{V_{input}(X\sqrt{LC})}{2T_{rise}}\left(\frac{L_{12}}{L_{11}} - \frac{C_{12}}{C_{11}}\right)$$

For the two wires the parameters required to calculate the crosstalk are input voltage,self-inductance between wire L_{11}, self-capacitance between wires C_{11}, mutual inductance L_{12}, mutual capacitance C_{12}. From MATLAB software the distance between wires is 1m and the radius of each wire is 0.1m. The input voltage is 1V and length of the each wire is 2inches and the T_{rise}=100ps.

The L and C matrices given by MATLAB is:

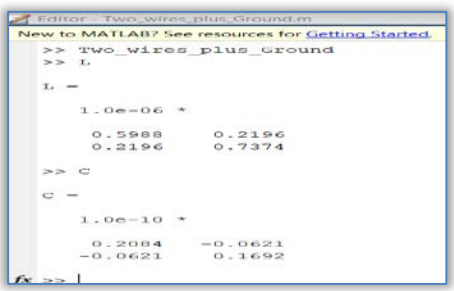

From above The crossstalk voltage is 0.017V at the far and at the end is the crosstalk voltage is 0.004V

CONCLUSION

The work is performed to determine crosstalk induced by cross-phase modulation (XPM) in analog fiber link by solving an ordinary differential equation. Crosstalk between two wires is also calculated with the help of inductance and capacitance matrix. Then, near and far end crosstalk voltages are analyzed. Optical fiber converts Am to PM when direct detection is used. When distortion in the pump channel has neglected the results varies from practical answers where distortion is taken into account tells that distortion in the pump channel cannot be neglected.

References

[1] P.-L. Luo, J. Hu, Y. Feng, L.-B. Wang, and J.-T. Shy, "Doppler-free intermodulated fluorescence spectroscopy of 4He 23P–31,3D transitions at 5 88 nm with a 1-W compact laser system," Appl. Phys. B, Lasers Opt., vol. 120, no. 2, pp. 279–284, 2015.

[2] J. W. Nicholson et al., "Raman fiber laser with 81 W output power at 1480 nm," Opt. Lett., vol. 35, no. 18, pp. 3069–3071, 2010.

[3] V. R. Supradeepa and J. W. Nicholson, "Power scaling of high-efficiency 1.5 μm cascaded Raman fiber lasers," Opt. Lett., vol. 38, no. 14, pp. 2538–2541, 2013.

[4] J. E. Heebner et al., "High brightness, quantum-defect-limited conversion efficiency in cladding-pumped Raman fiber amplifiers and oscillators," Opt. Express, vol. 18, no. 14, pp. 14705–14716, Jul. 2010.

[5] J. Nilsson, J. Ji, C. A. Codemard, and J. K. Sahu, "Design, performance, and limitations of fibers for cladding-pumped Raman lasers," Opt. Fiber Technol., vol. 16, no. 6, pp. 428–441, 2010.

[6] J. Ji, C. A. Codemard, and J. Nilsson, "Analysis of spectral bendloss filtering in a cladding-pumped W-type fiber Raman amplifier," J. Lightw. Technol., vol. 28, no. 15, pp. 2179–2186, 2010.

[7] L. Zhang et al., "Kilowatt ytterbium-Raman fiber laser," Opt. Express, vol. 22, no. 15, pp. 18483–18489, 2014.

[8] H. Zhang, R. Tao, P. Zhou, X. Wang, and X. Xu, "1.5-kW Yb-Raman combined nonlinear fiber amplifier at 1120 nm," IEEE Photon. Technol. Lett., vol. 27, no. 6, pp. 628–630, 2015.

[9] T. H. Runcorn, R. T. Murray, E. J. R. Kelleher, S. V. Popov, and J. R. Taylor, "Duration-tunable picosecond source at 560 nm with watt-level average power," Opt. Lett., vol. 40, no. 13, pp. 3085–3088, 2015.

[10] C. E. Max et al., "Image improvement from a sodium-layer laser guide star adaptive optics system," Science, vol. 277, no. 5332, pp. 1649–1652, 1997

ACTA TECHNICA CORVINIENSIS – Bulletin of Engineering
ISSN: 2067-3809

[1.]Iqbal SINGH, [2.]Salil BHARANY

COMPARATIVE STUDIES OF VARIOUS TECHNIQUES FOR IMAGE COMPRESSION ALGORITHM

[1.]CS&A Department, A.S.B.A.S.J.S. Memorial College Bela, Ropar, INDIA
[2.]Guru Nanak Dev University, Amritsar, INDIA

Abstract: With the increase of modern communications technology, there is a great need of data compression so that it will allocate less storage. This book provides an overview of compression–level principles, classes of compressions, various algorithm of compression. Well, compression of image is a solution to problems relating to digital image transmission and digital data storage. Image compression includes programs such as remote satellite viewing, television broadcasting and other long distance communications. Image storage is required for satellite images, medical images, documents and pictures. Image compression is essential for these types of applications.With the help of this article we will able to know the best method of selecting popular image compression algorithms based on criteria like Wavelet, JPEG / DCT, VQ, and Fractal Methods. Pros and cons of these compression algorithms are also being discussed .With a limited bandwidth the best way to utilize digital images effectively is make a need of compression techniques. Image compression is a technique for reconstructing the image in such a way that the quality of the original image is not effected.

Keywords: Image compression techniques, DCT, JPEG, VQ, Fractal, Wavelet, Genetic algorithm, Lossless and Lossy image Compression, Run Length encoding, Transform Coding

INTRODUCTION

As growing of media communication and video on demand is desired, image data compression has received an increasing interest. The primary purpose of image compression is to gain the low transmission speed and to have the high image quality of the expanded image. Image compression are used all fields of media communication such as multimedia, medical image recognition, digital image processing.The basic video compression technique is based on gray compression and color compression .Basically images which we take from camera are in analog form and to process, transmit it we have to convert it to digital format .Image is 2–D array of pixels. Basic image compression different from compression of digital data. We can use the compression algorithm for data compression, but the output is less than the optimal result. By removing some additional data we can achieve Compression. The two main components of compression are to eliminate redundancy and minimize irrelevance eliminating Redundancy aims to eliminate duplication of source signals (images / videos). Removing the part of signal which is not noticed by the receivers is considered as irrelevant like (HVS) which is called as reducing the irrelevance.

Uncompressed images load large files in storage media and takes a long time to transfer from one device to another .So if we want to transfer or save the digital image, we have to first compress it for faster transfer rate and use less space which increases the importance of compression.

PERFORMANCE PARAMETERS

There are various parameters present which are used to measure the performance of different compression algorithm. Most important performance parameters of image compression are given below:

a) Peak signal to noise ratio (PSNR): It is one of the most important performance parameter in image processing. Is been calculated by the peak error present between the original image and the compressed image. Higher PSNR is always preferred as it leads better quality of image.
b) Compression ratio: CR is a proportion of the size of the image compressed to the size of the original image. The compression ratio should be as high as possible for better compression.

Compressed ratio = uncompressed size/ compressed size

c) Mean square error: Mean Square Error (MSE) is the difference between original and compressed images. MSE should be as small as possible

TYPES OF COMPRESSION

Compression of images can be lossy or loslesss. Compression without losing weight is used for archival purposes and often for medical, painting, comic. This is because you lossy the compression method, especially when used, with little bit rates introduced with compression artifacts [1]. Higher compression ratio can be obtained if error is usually encountered that is difficult to detect, allowed between the expanded image and the original image. It is a loss of compression. In many cases it is not necessary or would like to create the original image without errors.

For example, if there are some disruptions, the error caused by the noise will be significantly reduced by some denoising methods. In this case, a small number of errors that are suggested by lossy compression might be optimal. Another use of lossy compression is the ability to send images online quickly over internet as we all know that the original file need more storage as compared to zip compressed file but it is also not true to compress image repeatedly lead to smallest in fact it usually lead to increase in size.

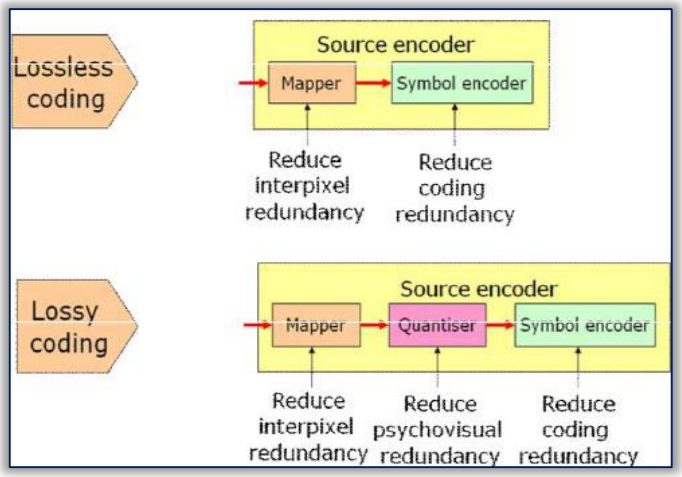

Figure 1. Image compression Model

IMAGE COMPRESSION STANDARD

During the past two decades, a range of compression methods have been developed to address main challenges faced by digital imaging. These compression methods can be classified broadly as Lossy Compression Methods and Lossless Compression Methods.

— Lossy Compression methods

Basically, almost all lossy compressors (Figure 2) are three–step algorithms, each of which is corresponding with three abbreviations of redundancy mentioned above.

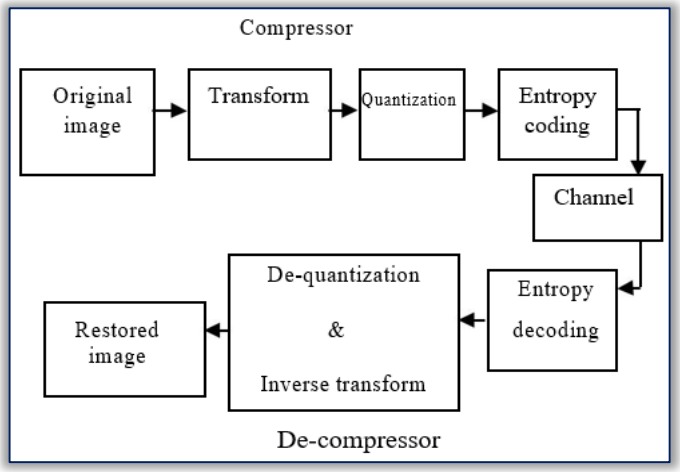

Figure 2. Lossy image compression

In the first stage a change is done to eliminate the inter–pixel redundancy to group information competently. Then psycho–visual redundancy is removed by a quantizer as to symbolize the collected information with as few bits as achievable. The quantized bits converted to a resource to get some extra compression from the coding redundancy.

» Quantization

Quantization is one by one, which replaces a set of values with a single value. Scalar and vector quantization are two significant types of quantization. SQ (scalar quantization) performs differently than creating a map for each value. VQ (Vectors) replaces each pixel block with a vector index in a codebook near the input vector by using a few closeness dimensions. Decoders get only the indexes and find the equivalent vector in the code book.

Shannon debuted for the first time that VQ would end at a lower bit rate than SQ. But VQ has to deal with due to short of generality codebook ought to be taught on some set of initial images. As a result, the bit rate and distortion [20] is being affected by the plan of the codebook. Riskin and. Al. Offer VQ design with variable–rate VQ and apply it to MR picture. Cosman and. Al. Use similar compression methods of CT and MR scans [1].

» Transform Coding

Transform Encoding becomes a common method for compressing lossy pictures. It uses a reversible and linear transformation to gainsay the real image into a set of coefficients in the transformed region. Then coefficients are measured and decoded gradually in the transformed region.

Numerous changes had done in some programs. The discrete KLT (Karhunen–Loeve transform), who's base is hotelling transformation which is best as it has packing properties but not able to make it practical. The DFT (discrete Fourier transform) and DCT (discrete cosine transform) are most accurate for energy packing efficiency of the KLT while DCT is most used transformation because of the DCT coefficients uses two timeless storage space.

» Block Transform Coding

To reduce the calculation, correlation of pixels inside a small blocks that divide the image is exploited by the block transform coding. As a result, each blog goes through the task like altered, quantized and independently encoded. Square of 8x8–pixel block and DCT block is used in the ISO JPEG (Joint Photographic Expert Group) to create an international standard for compression of images which is further followed by Huffman or the arithmetic code,. The disadvantage of this approach is that the blocking (or tiling) artifacts can be seen by rising the compaction ratio.

As the acceptance of the JPEG standard, the algorithm has been the topic of great research. Collins studied the effects of a 10:1 lossy image compression method based on JPEG, with alterations to reduce the blocking

artifacts are reduced. Baskurt used an algorithm analogous to JPEG to compress mammograms with a bit rate as low as 0.27 bpp (bits per pixel) while retaining recognition ability of pathologies by radiologists. Kostas uses JPEG, which can process 12–bit images and quantization tables for compression of x–ray of the chest and mammograms.
Furthermore, the ISO JPEG commission is at the present developing a replacement of still–image compression referred to as JPEG–2000 for delivery to the marketplace by the tale of year 2000. The new JPEG–2000 commonplace relies upon wavelet decompositions put together with lots powerful quantization and secret writing methods like embedded quantization and context–based arithmetic. It offers the possibility of obtaining numerous advantages over the obtained JPEG standard.Compression efficiency at low bit rates is being improved .Performance improvements include improved compression at low bit rates for large images, while new features consist of multi–resolution representations, scalability and integrated bit stream design, lossless progression, ROI (region of interest and an enriched file format [3].

— Lossless Compression Methods

The lossless compressing machine (Figure 3) is generally a two–step algorithm. The first step changes the real image to another format, which reduces the pixel redundancy. In The second coding redundancy is done by the use of an entropy encoder. Ideal inverse of lossless compressor is the lossless decompressor [8].

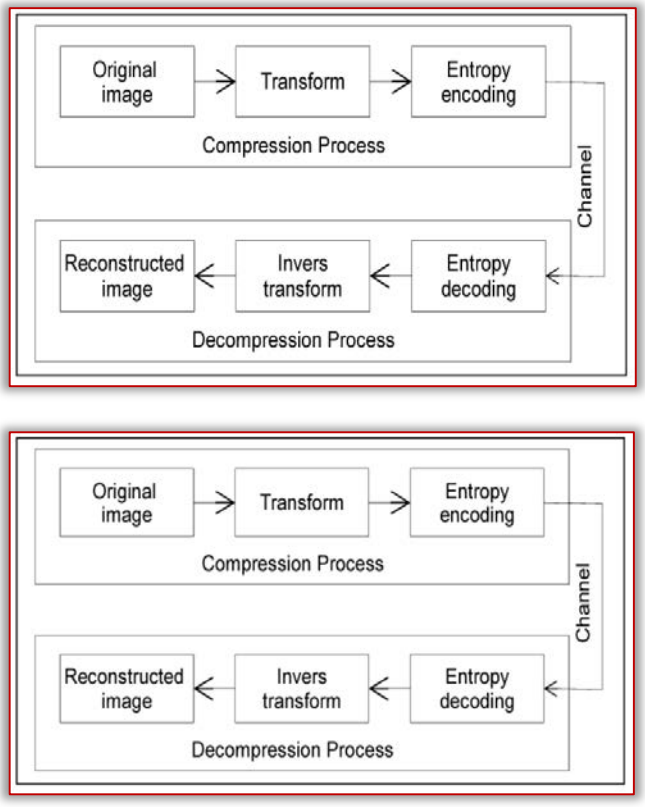

Figure 3: Lossless image compression

» Run length coding

Run length coding replaces data by a (length, value) duo, where "value" is the recurring value and "length" is the quantity of repetitions. This method is especially winning in compressing bi–level images since the happening of a long run of a value is unusual in usual gray–scale images. A resolution to this is to decay the gray–scale image into bit planes and compress individual bit–plane separately. Efficient run–length coding technique is one of the variations of run length coding [7].

» Lossless Predictive Coding

Lossless predictive coding by using adjacent pixel values for prediction the value of other pixel. As a result, each pixel is encoded with a forecast error a little more than its actual value. In general, errors are much smaller than the actual value, so less bits are needed to store them.
DPCM (differential pulse code modulation) is a predictive coding based lossless image compression scheme. It is too the base for lossless JPEG compression. A variation of the lossless predictive coding is the adaptive prediction that divides the image into blocks and calculates the prediction coefficients separately for every block to attain high prediction performance. It can to be combined with other scheme to get a hybrid coding algorithm with superior performance.
DPCM (differential pulse code modulation) based on predictive coding is lossless image compression method. well it is the basic of JPEG compression without loss of data adaptive prediction is variant of predictive coding without any kind of loss of data that divides the image into blocks and calculate the prediction coefficients independently so that each block have high prediction performance. It can also be combined with another scheme to achieve a hybrid coding algorithm with superior performance.

» Multi–resolution Coding

HINT (hierarchical interpolation) is based on sub sampling is a multi–resolution digital coder. In the beginning a low resolution version of the actual image and then the pixel values are interpolates to produce superior resolutions. The error between values between low–resolution image and the error values is recorded together with the first low –quality image. Compression is achieved because both the low quality image and the error value can be saved with a bits smaller than the actual image Algorithms with better results.
The Laplacian Pyramid is a compressed method for multi resolution designed by Bert and Adelson. It subsequently creates a low resolution of the real image by choosing so the number of pixels is reduced by factors of 2 on each scale. The difference between the subsequent solutions with the lowest resolution

image is saved and used to recover the actual image. But it cannot achieve a higher compression ratio, because the amount of data is refined by 4/3 of the actual image size.

In general, images are reversed in a set of set of dissimilar resolution sub–images in multi resolution coding.. Usually it reduces entropy. Some types of tree kind representation can be worn to get more compression rate by exploiting using tree structure of the Multi–resolution Method.

VARIOUS COMPRESSION METHODS

—JPEG Uploading an image based on DCT.

Image Compression in JPEG / DCT has become a new standard. JPEG is designed to compress the full–color image or grayscale image of a natural realistic set. To take benefits from this system, without any kind of overlapping 8x8 blocks are created as by dividing the image. For each block, separate Cosmetic Change (DCT) is applied to every block as to convert the degree of gray pixel into the spatial domain to coefficient of the frequency domain [3]. According to the quantization tables provided by the JPEG standard. The coefficients are normalized to different scales, which has some psychological evidence. The quantitative coefficients have been redesigned to further to compress by a lossless coding such as Huffman coding. Quantization process only leads to information loss. For all images that are not suitable 8x8 standard quantization table is set by The JPEG standard. To obtain better coding quality for different images by the same compression using the quantization DCT method can be used instead of the standard quantum table [2].

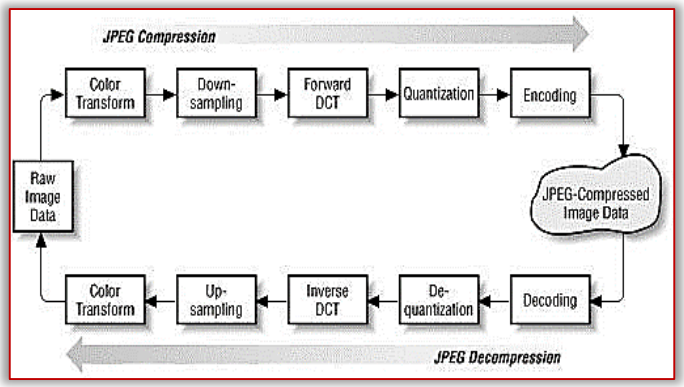

Figure 4. JPEG/DCT compression

—Wavelets

Wavelets are functions that determine the gaps and the mean values of zero. The main idea behind wavelet transform to represents any random function (t), as a superposition of a set of wavelet or basis functions. These basic functions or baby waves are derived from the model of the mother vector, called the iodine by dilations The Discrete Wavelet Transform of a finite length signal x(n) have N components, for example, is expressed by an N x N matrix . Despite all the advantages of the DCT–based JPEG compression plan is that it is very simple approach, and performance is quite good and availability of special purpose hardware for deploying.

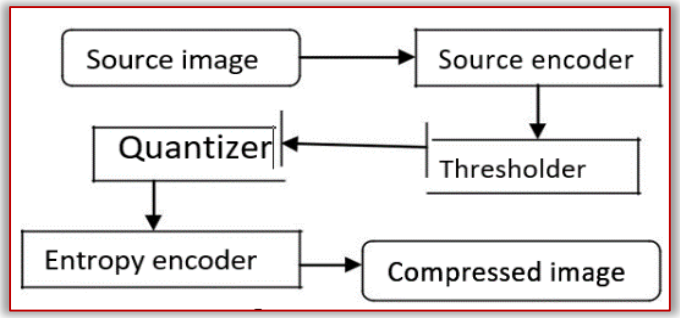

Figure 5. Compression plan

—Vector quantization

Vector quantization are signal processing techniques that allow the model of the probability density function of the distribution of prototype vectors. Basically it Works by values which are been encoded from the multi–dimensional vector to the set of values from the discrete subspace of the low size .The data is compressed easily as The low space vector requires less space Because of the density properties corresponding to the amount of vectors, compressed data errors that are inversely proportional to their density [6].

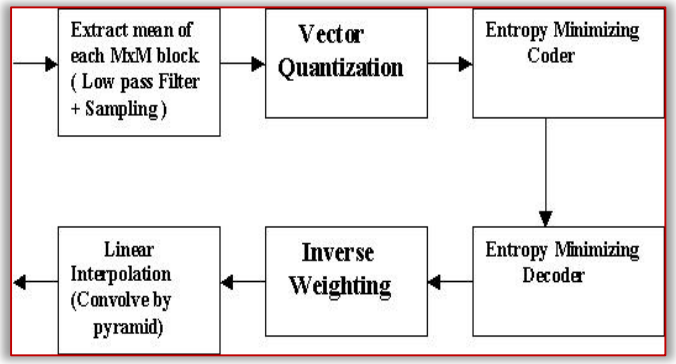

Figure 6. Vector quantization compression

—Fractal conversion

Fractal conversion is a compression method in digital images, which is lossy and based on fractals. This approach is best suited for texture and natural images, depending on the fact that part of the image is always similar to the other parts of the image.

In The Fractal algorithm parts are converted to mathematical statements, that we call the fractal code that are further useful for encoding images. There is a very interesting and important feature that we call the resolution–independent decoding property.

In this using decoding we can enlarge an encoded image having smaller size so that compression ratio may increase exponentially.

— **Genetic Algorithms** (GAs)

Genetic Algorithms (GAs) are methods that take after the standards of normal determination and regular hereditary genetics code, that have turned out to be extremely proficient scanning for approximations to worldwide optima in vast and complex spaces in moderately brief time.Genetic Algorithms (GA) is a procedure that follows the principles of natural selection and the natural code of nature that have proved to be most effective in jointly exploring global optimism in large and complex complexity over the short term.

The basic components of GAs are:

- genetic operators (mating and mutation)
- an appropriate representation of the problem that is to be solved
- a fitness function
- an initialization procedure

With these basic GA compounds, the procedure is as follows. Start with the beginning procedure to create the first population Members of the majority of the people are string of symbolic symbols (chromosomes) that provide solution of the unsolved problem need to be addressed. Each member of this generation is evaluated and depending on their ability is determined to be selected for reproduction. Using this probability, the genetic operator chooses some people.

Figure 7: Original image

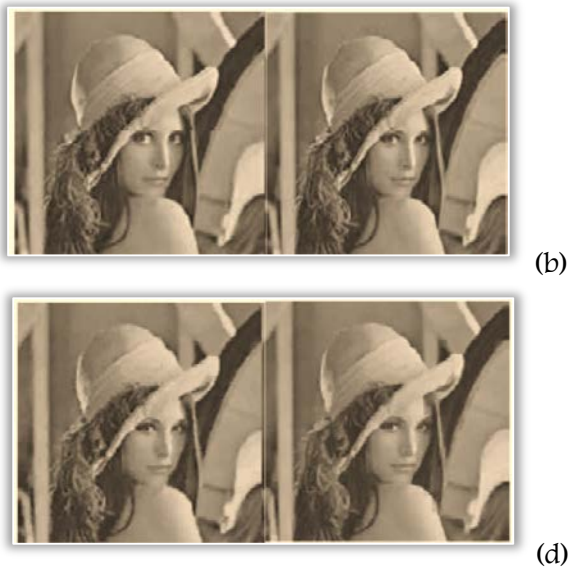

(a) (b) (c) (d)

Figure 8: Decoded image of Lena (a) Wavelet; (b) JPEG; (c) VQ; (d) Fractal Algorithm

New people are bought by practicing these operators. The contact operator chooses two members and integrates their respective chromosomes to produce offspring. The mutation operator selects a member of the population and changes some part of its chromosomes. The elements of the populations with the worst fitness measure are replaced by the new individuals compression on original using different compression algorithm.

LITERATURE REVIEW

- S.N Raj – *A Set of Partitioning in Hierarchical Trees Algorithm for Image Compression*. This method [5] provides high quality of images which use SPIHT with the best PSNR value and is the best method for transferring the image. In this work, SPIHT is compared to the DCT, DWT algorithm. Different images are accepted as inputs in the name, size of quality are compared with PSNR and MSE values. Before and after compression for each and every picture value it is been calculated. This demonstrates that SPIHT is more efficient and effective than existing algorithms, which means that it can compress and restore the original image without affecting the source and quality of the image. Future scope are machine learning methods and artificial intelligence are used to compress images and compare them with SPIHT algorithms.
- In 2010, Jau Ji Shen et al demonstrated *The Technique of Compressing Images Based on Vector* [6]. In this paper, the encoding of differences between the original and the compressed image has already been adjusted and then restored to a compressed VQ version. The results of this experiment show that even though the process required to provide additional data, it can improve the quality of the Vector quantized compressed image, and is further correlated with the map of the difference in compression loss to lossless compression.
- *New Algorithm for Compression of Images Using Modified Filter Banks* by Gaurav Sharma and K.G.Kirar [7]. This research describes new algorithms for compressing images with modified wavelet filter–bank using Kaiser window, and this technique is used with many test images. It provides a highly compressed scheme without affecting image quality. From the results, the compression technique suggested good results compared to previous works.
- Suresh Yerva et al *Introduced Methods to Compress Lossless Images Using a New Concept of Folding*. In 2011 [8]. In this method, column folding followed by row folding is applied iteratively on the image till the image size reduces to a smaller pre–defined value this method is compared to the lossless compression algorithm, and the result shows the comparison between

different methods. Data folding method is a simple image compression technique that offers good performance and simplicity of calculation, lower than the SPIHT technique for lossless compression.

A Wavelet Based Biomedical Image Compression ROI Coding by Pooja Sharma and Dr. Rekha vig [9]. This article uses the DCT and DWT method for medical images. For this method to be more effective, ROI extraction is performed. The experimental work showed that the information could be extracted, and then the segmentation was carried out to protect the information. Using DCT and DWT, the loss of information is minimized. The results show that previous compression was high when information was lost. Chances of information lost is reduced using PSNR and MSE values.

New Image Compression Method Called Five Modular Methods by Firas A. Jassim. In this method, they convert each pixel value to a multi–dimensional 8x8 layout into multiple of 5 for each RGB array [13]. Then, the value is divided by 5 to get a new value, which is known as the bit length for each pixel, and uses less space to store than the original values which is 8 bits. This article demonstrates the potential of FMM compression technology. The advantage of this approach is that it provides best compression using a high PSNR although it has low CR (compression ratio). This method is ideal for 2–level black and white medical images, in which pixel are presented using one byte that is 8 bit .According to the recommendation, the method for the Variable Module (X) MM can be created where X can be any number in further research.

Image Compression technique Utilizing reference Points Coding with Threshold Values. In 2012, Yi–Fei Tan, et al exhibits a procedure which uses the reference points coding with limit esteems for picture compression. This paper gives the possibility of a picture compression technique which can be utilized to perform both lossy and lossless compression [12]. A threshold is related in the compression procedure, by shifting this edge esteems, distinctive compression proportions can be accomplished and if we set the threshold value to zero then lossless compression can be performed .quality of the decompressed image can be calculated during the process of compression. When the threshold value of a parameter assumes positive values, lossy pressure can be accomplished. Additionally study can likewise be performed to decide the ideal limit esteem T.

COMPARESION BETWEEN COMPRESSION TECHNIQUES

There are given a comparison between image compression techniques. These techniques have some advantages and disadvantages which consider in table.

Tabel 1. Comparison between image compression techniques

Method	Advantages	Disadvantages
Wavelet	a)High compression ratio b)state-of-the art c)low encoding complexity d)it produces no blocking artifacts	a)Coefficient quantization b)bit allocation c)less efficient
JPEG/DCT	a)current standard b) high quality and small degree of compression c)comparatively fast with others methods	a)Coefficient quantization b)bit allocation
VQ	a)Simple decoder b)no coefficient quantization	a)slow codebook generation b)small bpp
Fractal	a)good mathematical encoding frame b)resolution free decoding	a)slow encoding
Genetic algorithm	a)capable of handling complexity and irregular solution spaces b)robust technique	a)repeated fitness function evaluation for complex problem b)not more efficient

CONCLUSION

Fundamental idea of picture compression and different technologies utilized are talked about in this paper. All the picture compression methods are helpful in their related zones and consistently new compression procedure is creating which gives better compression ratio.

We have additionally examined favorable circumstances and parameters of some lossy image compression systems. This survey paper additionally gives the thought regarding different image composes and execution parameter of image compression. Basically Quality of image, amount of compression and speed of compression are the major factor on which compression is totally dependent.

References

[1] Adams CN, Cosman PC, Fajardo L, Gray RM, Ikeda D, Olshen RA, Williams M. Evaluating quality and utility of digital mammograms and lossy compressed digital mammograms. In: Proc Workshop on Digital Mammography. Amsterdam: Elsevier, 1996: 169–76.

[2] Antonini A, Barlaud M, Mathieu P, Daubechies I. Image coding using wavelet transform. IEEE Trans. on Image Processing. 1992; 1(2): 205–20.

[3] Beylkin G, Coifman R, Rokhlin V. Fast wavelet transforms and numerical algorithms. Comm. Pure Appl. Math. 1991; 44: 141–83.

[4] Cohen A, Daubechies I, Vial P. Wavelets on the interval and fast wavelet transforms. Appl. Comput. Harm. Anal. 1993; 1:54–82.
[5] S. Nirmal Raj, "SPIHT: A Set Partitioning in Hierarchical Trees Algorithm for Image Compression "Contemporary Engineering Sciences, Vol. 8, 2015, no. 6, 263–270 HIKARI Ltd, www.m–hikari.com.
[6] Jau–Ji Shen and Hsiu–Chuan Huang, An Adaptive Image Compression Method Based on Vector Quantization, IEEE, pp. 377–381, 2010.
[7] Gaurav Sharma and K.G.Kirar, "A novel image compression algorithm using modified filter bank", International Journal of Current Engineering and Technology
[8] Suresh Yerva, Smita Nair and Krishnan Kutty, Lossless Image Compression based on Data Folding, IEEE, pp. 999–1004, 2011.
[9] Pooja Sharma and Rekha Vig, "A wavelet based biomedical image compression ROI coding", International Journal of Computer Science and Mobile Computing, vol.4, Issue.5, May 2015, ISSN: 2320–088X
[10] Ranju Yadav and Prof. Anuj Bhargava,"Review of Image Compression Methods" International Journal of Advanced Engineering, Management and Science vol.1 Issue 6, 2015
[11] S. Srikanth and Sukadev Meher, Compression Efficiency for Combining Different Embedded Image Compression Techniques with Huffman Encoding, IEEE, pp. 816–820, 2013.
[12] Firas A. Jassim and Hind E. Qassim, "Five Modulus Method for Image Compression" SIPIJ Vol.3, No.5, pp. 19–28, 2012
[13] Amit S. Tajne and Pravin S. Kulkarni, "Medical images compression using hybrid technique.
[14] John Miano; "Compressed image file formats: JPEG, PNG, GIL, XBM, BMP", 2000, page 23.
[15] Yi–Fei Tan and Wooi–Nee Tan, Image Compression Technique Utilizing Reference Points Coding with Threshold Values, IEEE, pp. 74–77, 2012.
[16] A.S. Ragab, Abdalla S.A. Mohmed, M.S. Hamid, "Efficiency of Analytical Transforms for Image Compression" 15th National Radio Science Conference, Feb.24–26, 1998, Cairo– Egypt.
[17] Varsha. C.K and R. Manoharan, "Application of hybrid technique in medical image compression based on SVM and clustering method" International Journal of Research in Aeronautical and Mechanical Engineering, Vol.3, Issue 2015
[18] Woods, R. C. 2008. "Digital Image processing. New Delhi" Pearson Pentice Hall, Third Edition, Low price edition, 1–904.
[19] Yi–Fei Tan and Wooi–Nee Tan, Image Compression technique Utilizing reference Points Coding with Threshold Values, IEEE pp.74–77,2012
[20] D. Singh, S. K. Ranade, "Comparative Analysis of Transform based Lossy Image Compression Techniques" International Journal of Engineering Research and Applications (IJERA) , Vol. 2, Issue 5, pp.1736–1741, 2012

ACTA TECHNICA CORVINIENSIS – Bulletin of Engineering
ISSN: 2067-3809

Fascicule 2
[April – June]
tome XIII
[2020]

ACTA Technica CORVINIENSIS
BULLETIN OF ENGINEERING

ACTA TECHNICA CORVINIENSIS – Bulletin of Engineering
ISSN: 2067-3809

http://acta.fih.upt.ro

[1.]Vasile George CIOATĂ, [1.]Vasile ALEXA, [2.]Bogdan Dorel CIOROAGĂ

PARAMETRIC DESIGN OF LINEAR HYDRAULIC MOTORS

[1.]University Politehnica Timişoara, Faculty of Engineering Hunedoara, Hunedoara, ROMANIA
[2.]ASSA ABLOY Entrance Systems Production Romania S.R.L, Hunedoara, ROMANIA

Abstract: This paper deals with issues regarding the possibility of automation of 3D models used in design processes. The examples of methods and tools used in the computer-aided design process are highlighted using the 3D model of a double-acting. The purpose of the paper is to present a possibility worth considering for the optimization of time required for design processes. The paper presents both theoretical aspects and results from the practice of building the 3D model needed to describe the methods and tools through which the design process was done.
Keywords: parameters, configuration, 3D model, design, automation

INTRODUCTION

Due to the increasingly fast rhythm of technology evolution, industry and design departments are forced to reduce the time required to manage current day-to-day problems to make room for new market requirements. Modern computer-aided design methods open new horizons in the sense of optimizing the work done for product development and design [1,2,6,7].

The paper highlights the possibility of automating the 3D model of an assembly representing a linear hydraulic motor with double action. This automation consists of a different approach, in terms of the design process, compared to the design made through clearly defined 3D models.

To achieve this automation will need a set of algorithms, constraints, input data and limitations of this data set as operating limits for generating new configurations of our product.

The concept of configuration will be a very common one in the paper, due to the fact that by automating the virtual model of the product it will be defined through the configuration resulting from the processing of input data.

Finally, this whole design process driven automatically has the role of optimizing design times and simulating different product configurations, in order to choose an optimal configuration.

THEORETICAL ASPECTS REGARDING THE AUTOMATION OF 3D MODEL DESIGN

In order for the design activity to take place, it is necessary to have a design theme, which provides us with the main input data that outlines the product. Based on these input data, a standard product configuration is established, which serves as a reference base for the allocation in the areas where it is necessary within the 3D model of the main parameters, which will subsequently generate new product configurations.

These parameters are generated by a configurator that processes the input data taken from the design theme, through algorithms that can contain both logical and mathematical functions.

Keeping records of parameters is recommended to be done through coding systems that give them the possibility to be easily identified and to have a unique character.

The main characteristics of the parameters are:

- name or code;
- the value it indicates
- unit of measurement

Configurators are the ones who manage the situation of the parameters, they can be incorporated into the 3D model or they can be external files. The structure of these configurators varies depending on the needs or limitations imposed by certain programs in which they run or interact with. The general structure of such a configurator tool is:

- user interface, the place where the input data is entered;
- the data processor, where the data processing takes place;
- the exported database, where the parameters intended for export to the 3D model are located.

The 3D model of the product is usually a final assembly that consists of components such as parts and subassemblies. These parts are connected to each other by through of assembly constraints. The pieces are always modeled starting from the sketching environment, after which the development of 3D geometric shapes takes place using specific commands (extrude, revolver, sweep, loft, etc.) and, subsequently, editing using tools provided by the software used.

Considering all this, we can list a series of steps necessary to build an automatic 3D model:

- Step 1 – Define the product by creating the standard 3D model;
- Step 2 – Identify the configuration range;
- Step 3 – Establishing the areas that will be defined by the variable parameters;

≡ Step 4 – Establishing the algorithms necessary to obtain the values of the variable parameters;
≡ Step 5 – Defining the configurator structure, creating it;
≡ Step 6 – Import the parameters into the 3D model;
≡ Step 7 – Linking the parameters in the preset areas;
≡ Step 8 – Test the 3D model.

The structure of the 3D model must be flexible in terms of adaptation to new configurations, areas must be foreseen where geometric interference or open loops may occur (in particular, such problems occur in the sketching environment). Problems can occur in the assembly environment in the area of geometric constraints, due to the disappearance of some references due to the transition from one configuration to another. To avoid these situations, it is recommended to avoid complicated geometries and to adopt technical solutions that require as few areas as possible defined by variable parameters.

A problem very common seen in practice, during the definition of algorithms for calculating variable parameters, due to the large number of parameters that are dependent on each other may occur, at some point, blockages in defining the functions required for the next parameters. This problem is caused by trying to define a parameter based on another parameter that can include the first on in its algorithm.

Coding the specific parts of a certain product configuration can often be difficult due to the fact that the part can have a large number of variable parameters, a large number being considered over two parameters. If all those components are used only in the current configuration, the problem is simplified by the fact that they may contain in the part number an area assigned to identify the configuration to which it belongs.

In case the respective parts can be found and configured to result other products, the problem of coding the configuration of the respective part appears, which must consider all possible configuration variants – if they are known – or have an algorithm for generating an extension of the base code called a variant, taking into consideration the variation of the parameters that shape the configuration of the component. The most difficult part is to describe the value of parameters of a certain number of digits in a space reserved within the variant that has a predefined and limited number of characters, which in most cases is insufficient when the component has more than two such parameters.

3D MODEL OF A DOUBLE ACTION LINEAR HYDRAULIC ENGINE

In the case of linear hydraulic motors, the input data taken from the design themes are generally the same for most of those constructive-functional types of these products. This generality is due to the fact that linear hydraulic motors, regardless of their constructive structure or their functionality, always have in common both the same functional parameters (developed force, pressure, flow, stroke, piston travel speed) and most parts that compose them (rods, piston, gaskets, caps).

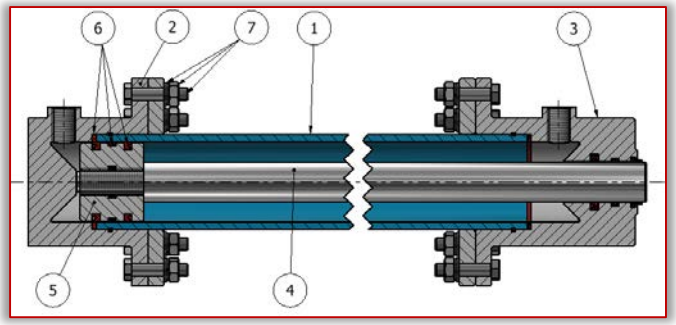

Figure 1 - Longitudinal section by standard 3D model - linear hydraulic motor with double action

The common elements mentioned before of this type of product facilitate and at the same time justify the application of a design method using automated 3D models.

The constructive solution of the standard 3D model is shown in figure 1, where it can be seen that the hydraulic motor is composed of a cylindrical tube (1) which at both ends is sealed by two caps, one clogged (2) and one pierced (3) to facilitate the passage of the rod (4), which is driven by the piston (5) flowing through the cylindrical tube. The sealing of this system is performed with the help of sealing elements (6) which are marked with red color in the section from the image. With (7) we noted the assembly elements of screw, washer and nuts.

The input data, made up of the functional parameters for the automation of the 3D model for the presented example, are:

≡ the stroke;
≡ nominal pressure;
≡ nominal pushing force;
≡ nominal flow;
≡ rod / inner diameter ratio.

The configuration limits considered for the design of the different configurations of the 3D model through which the linear hydraulic motor with double action is represented are:

≡ Piston stroke, between 300 - 2000 mm;
≡ Nominal operating pressure, between 50 - 500 bar;
≡ Nominal pushing force, between 9.8 - 883 kN;
≡ Nominal flow supplied by the pump, between 2.5 - 215 l / min;
≡ Piston diameter, between 50 -150 mm.

Due to the fact that the rods and covers can be of several types of dimensions, the configuration process and the possibility of choosing them will be taken into

consideration, being available the following possibilities to enter configuration data in this respect:

≡ rod type (TT): smooth cylindrical, threaded cylindrical, fork, eye bolt;

≡ support type (TR): simple cylindrical, cylindrical with flanges, eye bolt.

Regarding the type of rod, this in turn has the possibility to configure the geometric characteristics of the end area where the interaction of the linear hydraulic motor with other external systems takes place.

The configurator is created in an Excel file, consisting of 3 spreadsheets with distinct functions. The first spreadsheet is the register of parameters intended for export, the second spreadsheet functions as an interface for entering configuration data, and the third spreadsheet has the basic role of processing input data.

Figure 2 shows the structure of the interface page, which shows the configuration data entry fields on the left, and on the right side of the interface is a table with configuration limits that shows the minimum and maximum accepted for configuration for each field.

Configurator

Input data				
	Stroke	400	mm	
	Nominal pressure (P)	500	bar	
	Nominal pushing force (F)	880	kN	
	Nominal flow (Q)	50	l/min	
	Inner diameter rod ratio	1/2	ul	
	Rod extension (ET)	20	mm	
	Rod type (TT)	Cilindric neted	-	
	Threaded rod length (LF)	30	mm	Validated
	Metric threaded rods (MTF)	40	mm	Validated
	Fork hole (GF)	32	mm	Validated
	Opening fork (DF)	35	mm	Validated
	Rod eye diameter (OT)	30	mm	Validated
	Support type (TR)	Simple cylindrical	-	
	General model	Da	-	

Configuration limits					
Stroke	maximum	2000	mm	Validated
	minimum	300		
Nominal pressure (P)	maximum	500	bar	Validated
	minimum	50		
Nominal pushing force (F)	maximum	883	kN	Validated
	minimum	9.8		
Nominal flow (Q)	maximum	215	l/min	Validated
	minimum	2.5		
Rod extension (ET)	maximum	80	mm	Validated
	minimum	0		
Piston diameter (Dic)	maxim	150	mm	Validated
	minimum	50		
	Actual	150		

Figure 2 - Configuration interface, 3D model configurator

Next to each data entry field is placed a warning cell regarding the framing of the data entered within the preset limits. If the data entered is within the preset limits, the message "Validated" is displayed in the cell, when all these fields have this message, it means that the chosen configuration is possible and no problems will occur in the 3D model.

It can be seen that the last field in the configuration interface is called "General Model" it has two configuration possibilities:

≡ "Yes" - If you want to generate the standard 3D model;

≡ "No" - If you want to obtain the configuration generated by entering the configuration data from this interface.

Figure 3 shows a collage with possible product configurations, obtained from the export of the parameters processed by the excel configuration file.

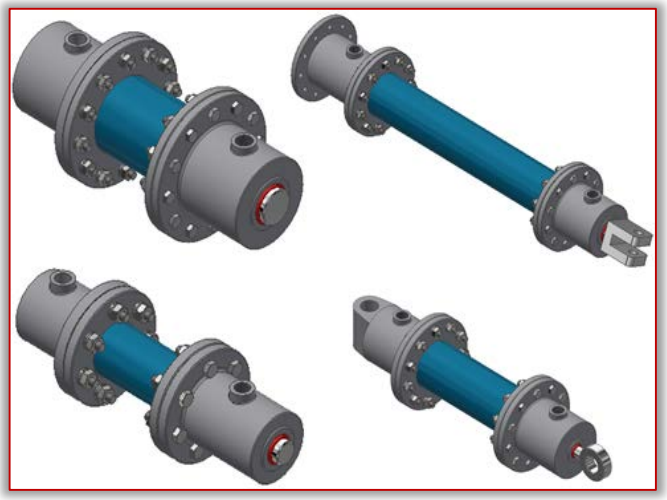

Figure 3 – Adaptations of the automatic 3D model to different configurations

If we analyze figure 3 it can be seen that the differences that appear between the configurations presented are not only dimensional in nature, there are substitutions of certain parts such as the clogged cover that is used as a fixed or articulated support and the rod that can be of 4 types. These replacement parts are possible with the "iLogic" feature implemented in the Autodesk Inventor software in which the 3D model was built.

Through the iLogic function, the 3D model can be programmed in order to obtain part substitutions by assigning values to certain parameters that have a command role in this regard. An example of programming to control a part replacement is shown in Figure 4.

The parameter under the code name Z1_F1_F_003 can take values from 1 to 3 depending on the settings set in the configurator for choosing the type of support.

From the represented code it can be seen that while the control parameter has the value 1 the 3D model

will display the part 0002-0001: 1 from the assembly environment of the 3D model and the other parts will be suppressed.

```
If Z1_F1_F_003=1 Then
Component.IsActive("0002-0001:1")=True
Component.IsActive("0002-0002:1")=False
Component.IsActive("0002-0003:1")=False
End If
If Z1_F1_F_003=2 Then
Component.IsActive("0002-0001:1")=False
Component.IsActive("0002-0002:1")=True
Component.IsActive("0002-0003:1")=False
End If
If Z1_F1_F_003=3 Then
Component.IsActive("0002-0001:1")=False
Component.IsActive("0002-0002:1")=False
Component.IsActive("0002-0003:1")=True
End If
```

Figure 4 – Example of programming

It is important to note that all these parts must be constrained by a part that cannot be replaced to avoid that the dimensional constraints in the assembly medium lose their references to the possible substitution of the part considered the basis of the constraint.

CONCLUSION

It can be concluded that this design method is successfully applicable for products whose configuration ranges are known and within some limits of the input data from the design theme. The main advantage of this method is that a 3D model of the product can be generated in a short time, which is often required especially in offers made to customers as a preliminary project. All this without generating other design costs. The method is easy to use even for a non-specialist after the launching in use the 3D model by specialized personnel, due to the fact that it is based on entering input data into a form-type structure.

This method it can be in the future a starting point for the introduction of artificial intelligence in mechanical design departments, replacing the current designer with a simple form for entering data by the beneficiary.

References

[1] Cioată, V. G., Miklos, I. Z, Proiectare asistată de calculator cu Autodesk Inventor, Ed. Mirton, Timişoara, 2009

[2] Cioroagă B. D., Proiectarea prin intermediul modelelor 3D configurabile, Simpozion Ştiinţific Studenţesc HD-50-STUD, 15-16 mai, Facultatea de Inginerie Hunedoara, Romania, 2020

[3] Stăncescu C., Proiectare parametrică şi adaptivă cu Inventor, Ed. Fast, Bucureşti, 2014

[4] Tickoo, Sham, s.a., Autodesk Inventor 2008 for Designers, CADCIM Technologies, 2008

[5] Saxena, A., s.a., Computer Aided Engineering Design, Springer, 2005

[6] Cioată, V. G., Computer aided design of clamping mechanisms with articulated arms, ANNALS of F.E.H. - International Journal of Engineering, 2007, 5(3), 157-161

[7] Cioată, V. G., Kiss, I., Dynamic analysis and parametric optimisation of the connecting rod using Autodesk Inventor, Machine Design, 2017, 9(1), 29-34

[8] http://www.autodesk.com

ACTA TECHNICA CORVINIENSIS – Bulletin of Engineering
ISSN: 2067-3809

[1.]Olaolu George FADUGBA

APPLICATION OF MULTIVARIATE DATA ANALYSIS IN THE INTERPRETATION OF GEOTECHNICAL INDEX PARAMETERS – A CASE STUDY OF THE FEDERAL UNIVERSITY OF TECHNOLOGY AKURE, ONDO STATE

[1.]Department of Civil Engineering, The Federal University of Technology, Akure, NIGERIA

Abstract: Geotechnical investigation has evolved from the traditional methods of interpretation to more reliable and improved methods, where their as been an increasing implementation to predictive analysis for the interpretation of geotechnical investigation data and to gain decision making information from these data. The presented work looks into the application of multivariate data analysis for the interpretation of geotechnical index parameters. Uncertainty in geotechnical engineering was discussed, its causes and the use of reliable–based design to achieve a stable design. Data of One hundred and eighty nine soil samples was collected from seven different locations in the Federal University of technology, Akure, and this was what was used for the development of the model. The multivariate data analysis method used for this work was the multiple linear regression method. This method involves a single metric dependent variable that are related to two or more metric independent variables. The objective of multiple linear regression analysis is to predict the changes in the dependent variable in response to changes in the independent variables. This objective is most often achieved through the statistical rule of least squares. Because this research is interested in predicting an amount and size of dependent variable, multiple linear regression method is used. It is a statistical technique that is basically used to analyze the relationship between a single dependent variable and several independent variables.
Keywords: index properties, uncertainty, reliable–based design, multivariate data analysis, multiple linear regressions

INTRODUCTION

Geotechnical engineering over the years has been proven to be very important and critical in construction and civil engineering, because, every structure constructed in one way or the other has a direct or indirect contact with the soil as foundation, and geotechnical engineering deals with the investigation and analysis of the soil. But there has been a need for adequate and reliable geotechnical characterization of the soil because of the much uncertainties involved with geotechnical investigations.

Evaluation of the uncertainties in geotechnical design parameters provides the foundation for reliability–based design (RBD). For example, Baecher and Ladd (1997), Phoon and Kulhawy (1999), Müller (2013) and Mašín (2015) have presented methodologies on how to evaluate uncertainties from a single test procedure. In most cases, the design parameter and associated uncertainty are evaluated using more than one investigation method, which includes both in–situ and laboratory measurements. As such, it is highly beneficial to combine (i.e., cross–validate) data from different types of investigation method to reduce the uncertainty in the design parameter.

Multivariate analysis according to bioimpedance and bioelectricity basics 2015, can be said to be set of operation procedures used for analysis of data sets that consists of more than one variable, and the techniques are especially valuable when working with correlated variables. Olkin et al., 2001 conceptualized multivariate analysis traditionally as the statistical study of experiments in which numerous measurement are made on each experimental unit and for which the relationship among multivariate measurements and their structure are important to the experiment's understanding.

Multivariate analysis is an important tool in data management and it has been widely used in managing and interpreting various data like geochemical characterization of groundwater and soil science. Thus, the use of multivariate methods requires large data sets and therefore its application in geotechnical engineering is not frequently used, since even for large construction projects the number of laboratory analyses usually provides only a relatively limited amount of data in statistical terms. At the same time, it has been known to some extent that data analyses are useful tools in geotechnical engineering. More recent studies have demonstrated the applicability of multivariate data analyses in various fields of engineering geology such as rock engineering soil liquefaction, landslide susceptibility analyses and even in investigating the correlation between clay mineralogy and shear strength of soils. (Kovacs et al., 2015).

LITERATURE REVIEW

— Reliability–based design in geotechnical uncertainties

Reliability–based designs can be simply and best explained as statistical approaches to provide stable and reliable design. Considering the large number of uncertainty involved and associated with geotechnical investigation, reliability–based designs are needed for cost effective and reliable site

investigation (Anders et al., 2017). Reliability designs aims at assessing to what extent uniformity, consistency and stability can be achieved in design. Failure probability and reliability index are used to quantify the reliability of a design. The lower the failure probability the higher the reliability index, the more reliable a design is. To fully adhere the scope of geotechnical site–investigation with the reliability of a construction, the uncertainty related to inherent variability of soil (aleatory uncertainty) must be accompanied by the epistemic uncertainties related to the method of soil characterization, which is typically divided into measurement error, statistical uncertainty and transformation uncertainty (Prästings et al. 2016; Ching et al. 2014; Ching et al. 2016). A major approach to a reliable based design is the multivariate approach, which was considered in this research.

— Multivariate data analysis

Multivariate data analysis (MVDA) describes the practice of using mathematical and statistical tools to extract information from data tables where each observation contains a large number of variables. In such cases, the desired information lies in the correlation structure between variables, this often leads to erroneous results when tested independently. Multivariate data analysis by means of projection methods is able to analyze data where challenges such as multidimensionality of the data set, multicollinearity, missing data and variation introduced by deviating factors such as experimental error.(Darren et al, 2014)

The increasing use of multivariate data analysis (MVDA) in both basic research and applied scientific fields has enabled the diagnostic evaluation of parameter interactions that were previously undefined. Therefore univariate or bivariate analysis is often inefficient resulting in misleading conclusions (Kourti, 2004). Key information in such cases lies in the correlation structure between variables and can lead to spurious results when tested independently.

MATERIALS AND METHOD

The type of data used were secondary data from previous subsoil investigation conducted in FUTA, the data comprised of various index parameters extracted from the subsoil investigation of these selected places: New 1000 capacity multipurpose hall, the new postgraduate school, the new staff, block of classroom A and B, and the indoor sports hall. Only a few selected index parameters where used, and they are: the depth, the natural moisture content (NMC), specific gravity (Gs), average pocket penetrometer value (kPa), cohesion c, and Atterberg limits LL – Liquid Limit, PL – Plastic Limit, PI – Plasticity Index, LS – Linear Shrinkage.

The area used for the research is The Federal University of Technology, Akure. FUTA, located in Akure, the capital city of Ondo state. About 250m north of highway 364 (Ilesa–Owo Expressway), southwestern Nigeria. The campus falls within latitudes 7°17'03"N – 7°19'06"N and longitudes 5°07'02"E – 5°09'05"E

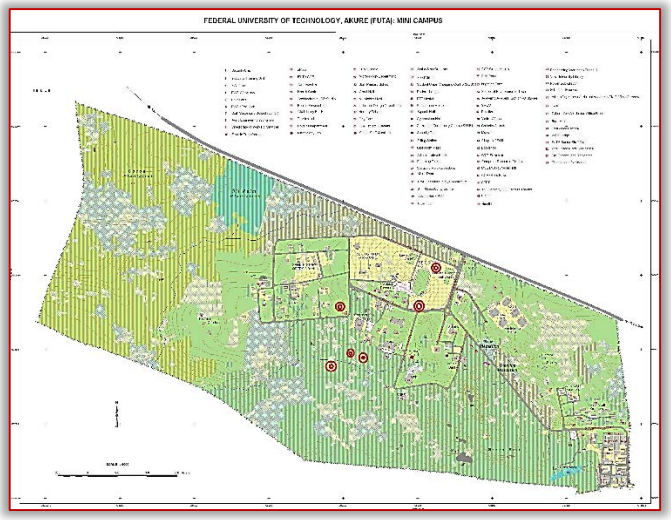

Figure 1. Map of Study Area

RESULT AND DISCUSSION

To evaluate the geotechnical parameters and to generate the regression model by identifying the combinations of the inputs ad their linearization, the MATLAB software was used. To analyze the random relationship that exists between the variables, a matrix correlation was used. The correlation coefficient (R) and its square, the coefficient of determination (R^2) describe the linear connection. The correlation is strong, when $|R| \geq 0.7$ and weak, when $|R| \leq 0.5$.

The models were developed taking Average Pocket Penetrometer value as the dependent variable while other parameters were considered as independent variables. The following abbreviations were used in the tables.

Table 1. Summary of Correlation Adequacy Check.

Location	Degree of freedom	Coefficient of determination (R^2)	F–Statistic	P–Value
Block of Classrooms Block A	15	0.597	2.221	0.136
Block of Classrooms Block B	19	0.164	0.335	0.922
Indoor Sports Hall	23	0.314	1.046	0.439
New 1000 Capacity Multipurpose Hall	23	0.429	2.131	0.103
New Staff Offices	17	0.266	0.663	0.682
New Postgraduate School	18	0.255	0.741	0.626

Natural Moisture Content (NMC), Specific gravity (SG), Cohesion (C), Average Pocket Penetrometer Value (APPV), Liquid Limit (LL), Plastic Limit (PL), Plasticity Index (PI) and Liquid shrinkage (LS). The models try to predict the desired Average Pocket Penetrometer for a given set of data.

For data evaluation, it is important that no missing data occur in the matrix. The samples with missing data points were not used in the analyses.

The data provided required computerized statistical analysis to determine any meaningful correlations between the variables and to establish relevant predictive models. In this study, the statistical analyses performed include:

- descriptive statistics (mean, standard deviation, etc. of each variable),
- linear and nonlinear regression analyses between all variables, and
- multivariant analyses between selected variables.

The statistical runs included F–tests and the use of correlation coefficients before drawing inferences. Six functions were fitted using the data at various data collection points. The main objective is to extract, in a condensed form, the largest possible information contained in the data, whether related to links between variables or between individuals (tests).

In order to determine the overall significance of the regression tests, the F–test was also performed. The coefficient of multiple determination, R^2, provides an overall measure of the adequacy of the equation to predict. If the line is a good estimator of the data, this coefficient will be near unity. Based on the correlation model generated only the data obtained from the block of classrooms showed a strong correlation of the model with R^2 value of 0.597, however, it doesn't show a measure of statistical significance because probability of F–values is greater than 0.05 significance level and the regression can therefore be considered as insignificant. This could possibly be attributed to the lack of sufficient data collected or lack of cohesion in the test data provided.

The Pearson Correlation table obtained from the data analysis was also studied with an aim to understand several correlation that may exist between the independent variables: The Pearson Correlation table shows a weak negative correlation between specific gravity and Atterberg limit values. Also a relatively strong positive correlation between cohesion and APPV. Further as observed from the analysis, the Pearson Table suggests a moderately strong positive correlation between the natural moisture content and the Atterberg tests and rightfully so since Atterberg tests are measures of the critical water contents of a fine–grained soil

The model generated from the multivariate analysis indicates a significant negative linear relationship between cohesion and Average pocket penetrometer value. Also it shows a negative correlation for natural moisture content

A plot of the parameters against each other allowed the following observations to be made: the natural moisture content has a positive correlation with the depth as a 60% deduction in soil depth yielded a 27% decrease in Natural Moisture Content, but the cohesion has a weak positive non–significant correlation with the depth, that is as a 50% depth decrease results in an average 6% increase in cohesion values. This, thereby confirms the findings of Netra R et al., 2015 that cohesion strongly depends on the bonding of fine–grained particles and some physical properties of the soil such as moisture content, that that an increasing soil moisture content reduces the cohesion and thus shear strength.

Table 2. Summary of Models

LOCATION	MODEL EQUATIONS
Block of Classrooms Block A	APPV = –210.271 – 1.000NMC + 40.184SG + 0.162C + 2.408PL – 0.342PI + 3.170LS
Block of Classrooms Block B	APPV = –1647.996 – 3.774NMC – 480.083SG – 0.106C + 4.247LL – 1.014PL + 0.285PI – 0.223LS
Indoor Sports Hall	APPV = –47.766 – 2.939NMC + 110.409SG + 0.020C – 93.514LL + 95.018PL + 97.911PI + 2.752LS
New 1000 Capacity Multipurpose Hall	APPV = 56.037 – 1.951NMC + 144.498SG – 0.027C + 2.796PL + 2.100PI + 1.754LS
New Staff Offices	APPV = –963.077 – 2.521NMC – 248.606SG – 0.387C + 9.745PL + 5.387PI – 14.728LS
New Postgraduate School	APPV = –777.925 – 2.291NMC – 189.916SG – 0.191C + 9.363PL + 5.330PI – 15.133LS

CONCLUSIONS

From the study, the following conclusions were drawn:

- There is a strong correlation between the index properties and the APPV of the soil.
- The cohesion value is an essential soil property for foundation design. However, it can't be measured as accurately from the linear regression models provided as it shows a negative correlation with the soils Atterberg limit.
- The Average Pocket Penetrometer Value and the Cohesion value are closely correlated, both being important in foundation design problems and as such, appropriate means should be devised to measure or estimate their values.
- The application of multivariate analysis in geotechnical engineering designs offers a reliable guide and solution to the interpretation of

geotechnical index parameters, problems and geotechnical uncertainty

References

[1] Prästings A, (2016). Aspects on probabilistic approach to design: from uncertainties in pre–investigation to final design Licentiate Thesis.
[2] Baecher, G., Ladd, C., (1997). Formal observational approach to staged loading. Transportation Research Record: Journal of the Transportation Research Board, 1582, pp.49–52.
[3] Baecher, G.B. Christian, T. (2003). Reliability and statistics in geotechnical engineering. Wiley
[4] Bradák B., Kovács J. (2014). Quaternary surface processes indicated by the magnetic fabric of undisturbed, reworked and fine–layered loess in Hungary. Quatern. Int., 319, 76–87.
[5] Christian, J.T., Ladd, C.C., Baecher, G.B. (1994). Reliability applied to slope stability analysis. Journal of Geotechnical Engineering, ASCE: Vol. 120, No. 12, pp. 2180–2207.
[6] Cameron, G. (2002). Uncertainty, reliability and risk in geotechnical engineering. Proc. of the British Geotechnical Association: 7th Young Geotechnical Engineers Symposium – Diversity in Geotechnics, Dundee, pp. 19–20.
[7] Contreras, L.F, Ruest, M. (2016), unconventional methods to treat geotechnical uncertainty in slope design, Australian center for Geomechanics.
[8] Dalu T., Richoux N.B., Froneman P.W., (2014). Using multivariate analysis and stable isotopes to assess the effects of substrate type on phytobenthos communities. Journal of the International Society of Limnology, Inland Waters, 4, 397–412.
[9] Elkateb, T., Chalaturnyk, R., Robertson, P.K. (2003a). An Overview of Soil Heterogeneity: Quantification and Implications on Geotechnical Field Problems, Canadian Geo
[10] Griffiths, D.V., Fenton, G. A., Manoharan, N. (2002). Bearing capacity of rough rigid strip footing on cohesive soil: Probabilistic study. Journal of Geotechnical and Geoenvironmental Engineering, ASCE: Vol. 128, No. 9, pp. 743–755.
[11] Harr, M. E. (1977). Mechanics of particulate media – a probabilistic approach. McGrawHill, New York.
[12] Kovács, J, Bodnár, N., Török, Á. (2016). The application of multivariate data analysis in the interpretation of engineering geological parameters: Journal of Open Geosci.8, 52–61.
[13] Lacasse, S., Nadim, F. (1996). Uncertainties in Characterizing Soil Properties. In Uncertainty in the Geological Environment: From Theory to Practice, Geotechnical Special Publication No. 58, C.D. Shackleford, P.P. Nelson, and M.J.S. Roth (eds.), pp 49–75.
[14] Lumb, P. (1966). The Variability of Natural Soils, Canadian Geotechnical Journal, Vol 3, No. 2, pp. 74–79.
[15] Muller, R., (2013). Probabilistic stability analysis of embankments founded on clay. KTH, Royal Institute of Technology.
[16] Phoon, K.–K., Kulhawy, F.H., (1999). Characterization of geotechnical variability. Canadian Geotechnical Journal, 36, pp.612–624
[17] Phoon, K. K. (1995). Reliability–based design of foundations for transmission line structures. A PhD dissertation submitted to Cornell University.

ACTA TECHNICA CORVINIENSIS – Bulletin of Engineering
ISSN: 2067-3809

[1.]Deepak NANDAL, [2.]Om Prakash SANGWAN, [3.]Nandal VIKAS

A COMPARATIVE STUDY OF POPULATION BASED META-HEURISTIC TECHNIQUES FOR VARIOUS APPLICATIONS IN SOFTWARE TESTING

[1.]Department of Computer Science and Engineering, Guru Jambheshwar University of Science and Technology, Hisar, Haryana, INDIA
[2.]Department of Computer Science and Engineering, Guru Jambheshwar University of Science and Technology, Hisar, Haryana, INDIA
[3.]Electronics and Communications (UIET), Maharishi Dyanand University, Rohtak, Haryana, INDIA

Abstract: Software testing is a process of evaluating the functionality of different software applications intending to find the errors and defects to ensure that the product is error and bug free so that a good quality software product can be achieved. It should also satisfies all the requirements as specified by the vender at the time of finalizing the SRS. This testing process tests the entire software with a sole objective of to produce a quality software. The quality will be compromised if the software product has bugs. The selection of testing data for the same is very crucial. Different population based meta-heuristic techniques are implemented for the automation and optimization of selection of the test data. There are some meta-heuristic techniques that are used in the field of engineering for optimization problems. This paper produces a comparative study of different researches that uses the meta-heuristic techniques in the field of software testing.
Keywords: Software testing, BAT, GA, Particle Swarm optimization, Test cases, Optimization

INTRODUCTION

Software Engineering is solely concerned with the idea of development of software applications to be economical with utmost efficiency as well. It comprises of a number of phases of the software development life cycle and these phases differ from one software development model to another, where software testing is a part of the development cycle that concentrates on producing a quality software product with no errors Mayan et al[1]. Testing part of it covers almost half of the total development cost of the software product[3,4]. So this has been a major field when it comes to the software engineering.

To achieve the main objective that is the quality of the software or error free software, test data generation as well as structural testing has been emerged as a major field of research for many researchers in the last decade and so.

The selection and creation of the test suite is the most crucial part of this phase, when it comes to applying the testing methodologies. As earlier discussed the software testing is a tedious, complex and a very expensive phase when it comes to the software development life cycle. Many modern optimizing techniques for selection of test cases may result in lowering the overall cost of software testing[2, 3].

Software testing gains the vendor's acceptance for the software, which extends the objective of doing software testing to acquire the assurance of quality of the software[5]. The overall cost of finding errors and bugs can be reduced by applied optimizing models such as ANN, ACO, GA and other meta-heuristic approaches, which also helps to meet the target of time deadlines associated with the software development. This research paper has sections, firstly the introduction part which is followed by the introduction of different meta-heuristic techniques such as BAT and PSO which both are populations based search techniques. Next sections discusses the literature review part and the criteria for selection of the above techniques. Last section discusses the observations of the analysis of the related papers of the techniques PSO and BAT followed by the conclusions.

POPULATION BASED META-HEURISTIC TECHNIQUES

The classification of meta-heuristic techniques can be done on the based on the solutions they focuses i.e. single solution and populations based approaches. The population based approaches focuses on improving the multiple candidate solutions where the population characteristics guides the search both local and global search[7, 18]. This paper focuses on two such population based meta-heuristic approaches BAT algorithm and Particle Swarm intelligence algorithm.

— BAT Algorithm

Bat algorithm demonstrates the hunting and routing behavior of the bat[9, 12]. Bat uses echolocation property i.e. identifying the location of any object or prey by the reflecting sound signal from that particular object or prey.

This algorithm assumes the ideal condition for the echolocation of the bat. It includes the automatic adjustment of the sound wavelength transmitted by the bat with respect to emission rate and loudness[8]. The algorithm focuses on both the local search as well as global search.

— Particle Swarm Optimization Algorithm

Particle swarm optimization is inspired from the simulation social behavior related to bird clustering and swarming theory[17]. A swarm can be defined as a structured collection of interacting agents. It focuses straight to the center of the swarm then matches the neighbor's velocity to avoid the collisions. It intelligently combines the self-experience with the social experience.

The agents which are also known as particles that constitute a swarm moving around in the search space looking for the best solution[17]. Each agent adjust its search space according to its own experience and as well as the others[19]. The particle swarm intelligence is one the majorly used population based optimization technique that is applied to various fields of engineering for optimization problems.

ESTIMATION CRITERIA

A process must be followed in order to implement software testing, so that the implementation on software results in finding the bugs effectively. For the same a thorough literature review has been conducted so find out the research gaps of the existing technologies. Major databases which were used to gather the required information and research papers (Table (a)).

This table (a) shows the keywords used for searching the related research papers. Some research questions are observed that analyzes the applications of BAT as well as PSO in the field of software testing. It also shows the number of aspects that are used for evaluating the testing techniques[14, 15, 16, 19, 20, 21]. The (Table (b)) shows the final result.

Table: a Keywords used in searching papers

S. No.	Keywords
1	Meta-heuristic techniques used in software testing
2	Implementation of BAT in Software Testing
3	Implementation of PSO in Software Testing
4	Implementation of BAT and PSO in Software Testing

Table: 2 Analysis of aspects satisfied

Aspects	[3]	[4]	[16]	[20]	[21]	[28]
A1	√	√		√	√	√
A2		√	√	√		
A3		√	√		√	
A4		√		√	√	
A5	√			√	√	√
A6			√		√	
A7		√			√	
Total no of aspects satisfied	2	5	3	4	6	2

≡ A1: Can the model reduces the efforts required for test case generation?

The efforts related to a software development comprises of mainly the person per hour, as the human factor is the most important aspect when it comes to cost of a software product and software testing is a time consuming process. The test case generation is a complex process and to figure out the suitable test suits cases which covers all the desired aspects evenly is even more complicated[22]. So this is an important aspect that must be reduced to lower the cost which is directly dependent on the effort of the software product.

≡ A2: Does the model reduces the testing time?

When it comes to test a software it is clear that it will take an ample amount of the testing team. It is almost not possible to test the entire software with in a given time frame, so testing the unnecessary content should be avoided.

≡ A3: Does the model generated test data automatically?

The test case data are the basis of testing a software and manually selection may be a very time consuming process[24]. So it is the demand of time to generate the test cases automatically by the models.

≡ A4: Does the model focuses on global optimum solution?

There are local search space and as well as global search space, the global optimum solution is most crucial as it finds the optimum solution among the possible solutions. The optimizing algorithm must not only be bidirectional in the local search space, it should also include the global search space as well.

≡ A5: Does the model reduces redundancy?

As discussed in the A1 and A2 that effort, cost and time are most important when it comes to software testing and must be reduced. For the same if the test cases focuses on the remove the redundancy, helps a lot to reduce the effort as well as time consumed[25].

≡ A6: Does the model reduces the cost of software testing?

To reduce the cost is critical to overall development of any system, which is also applied to the field of software engineering as well. Almost 50% of the total cost of software product development goes to software testing itself. If the test cases are selected properly and data redundancy is controlled then cost itself will be reduced.

≡ A7: Does the model reduces the size of test suite?

As the test suite size reduces the effort of the software development decreases, which directly related to the cost as well[26]. Large test suits may increase the chances of data redundancy.

ANALYSIS OF BAT AND PSO

Bat algorithm and particle swarm optimization technique are both population based meta-heuristic approaches, which are here applied to optimization of software testing[26, 27]. The results after implementation of these techniques gives better solutions than other customary techniques. Both the meta-heuristic approaches generates global optimum solution.

Following are some research papers that are analyzed for the study of application of these techniques in the field of software engineering.

— BAT Algorithm

Srivastava et al. [3] suggested a model that examines the performance of BAT algorithm. When this model is applied on UCP and TPA and the estimations have directed to the conclusions that test effort can be optimized by using BAT. The results were compared with those obtained from other existing methods, and it was found that the results are better and closer to the actual effort.

Yazan A. et al. [4] suggested a model that evaluates that the performance for interaction testing. The case study results are promising, especially with the prospect of supporting a high interaction strength. The optimizing of the test suite of the case study is different among traditional strategies, which perform a simple number of processes during generation due to the use of the meta-heuristic algorithm.

Yazan A et al. [8] suggested a model that uses the BAT algorithm and studies the benchmarking of BAT for real-world software systems to show it applicability in real-world test suite generation scenarios. BAT produces competitive test suite sizes compared to its counterparts. BAT was able to achieve 3 of the best test suite sizes.

Srivastava et al. [12] suggested a model that generates a satisfactory test sequence generation in stat-based testing implements BAT algorithm. The results observed are better than existing techniques such as GA , ACO techniques, intelligent water drop & cuckoo search algorithm in terms of optimality & coverage of generated sequences.

Kaur A. et al. [13] suggested a model that combines the BAT and cuckoo search algorithms for selecting test cases. With the objective of reducing the overall cost in regression testing and also reduce the cost of maintenance as well.

Sugave S.R et al. [16] suggested a model for test suite reduction in software testing. This model illustrations that the reduced test suite with the implementation of DIV-TBAT underperforms the entire existing methods when it comes to the test suite reduction problem.

— Particle Swarm Intelligence

Windisch A. et al. [20] suggested a model that applies PSO to software testing. This research paper takes 25 artificial test objects and 13 more complex test objects. The outcomes from the research papers shows that PSO out preforms GAs for most code elements to be covered in terms of effectiveness and efficiency.

Chen X. et al. [21] suggested a model that performs pairwise testing and applies particle swarm optimization. This paper analyze the impact factors of the approach and compare that approach to other well-known approaches. Final empirical results show the effectiveness and efficiency of the approach.

Zhang S. et al. [24] suggested a model based on a hybrid of GA and PSO for automatic test data generation. The model proved effective by a representative test of the "triangle type of discrimination". The experiment shows that the new algorithm has higher performance when the value of Φ is around 20%.

Ai-guo Li et al. [27] suggested a model that is based in PSO for automatic generation of test data. This model show that the approach is more efficient than GA based approach: when the number of particles of PSO is equal to the size of GA, the mean number of iteration of proposed approach is about 1/16 as many as that of GA-based approach.

Zhu X. et al. [28] proposed a model that implements adaptive particle swarm optimizer for test case generation. The outcome illustrations that Adaptive PSO is a better performer but also advanced to the immune genetic algorithm (IGA) as well as outperforms PSO, and has a wide-ranging applications for software testing.

Table 2 displays various research questions represented by A1-A7 alongside the research papers from which these questions were assumed[3, 4, 16, 20, 21, 28]. The tick mark represents the identified aspects which depicts as satisfied by that resultant research paper.

CONCLUSION

The results and applications of BAT algorithm and Particle Swarm Optimization algorithm are presented in this research paper by survey various research papers from different repositories. It is observed that PSO and BAT algorithm both individually as well as combination of both can be used for extensive software testing fields such as test data generations, optimization of test suite, automatic generation of test cases, and minimization of test suite. It is also observed that there are some limitations of both the meta-heuristic algorithms. This research paper provides future guidance to the researchers to use more meta-heuristics in the field of software testing, as well as the combination of the two approaches can be applied that may be considered as a hybrid meta-heuristic approach.

References

[1] Mayan, J.A., Ravi, T.: Test case optimization using hybrid search. In: International Conference on Interdisciplinary Advances in Applied Computing. New York, NY, USA (2014)

[2] B. Jones, H. Sthamer, and D. Eyres. Automatic structural testing using genetic algorithms. Software Engineering Journal, 11(5):299-306, 1996.

[3] Srivastava PR, Bidwai A, Khan A, Rathore K, Sharma R, Yang XS. An empirical study of test effort estimation based on bat algorithm. International Journal of Bio-Inspired Computation. 2014 Jan 1;6(1):57-70.

[4] Kiran A., Haider W., Waseem M., Azam A.F., Maqbool B. "A Comprehensive Investigation of Modern Test

Suite Optimization Trends Tools and Techniques", Access IEEE, vol. 7, pp. 89093-89117, 2019.
[5] Alsariera YA, Majid MA, Zamli KZ. Adopting the bat-inspired algorithm for interaction testing. InThe 8th edition of annual conference for software testing 2015 (Vol. 14).
[6] Nakamura RY, Pereira LA, Costa KA, Rodrigues D, Papa JP, Yang XS. BBA: a binary bat algorithm for feature selection. In2012 25th SIBGRAPI conference on graphics, patterns and images 2012 Aug 22 (pp. 291-297). IEEE.
[7] Biswal S, Barisal AK, Behera A, Prakash T. Optimal power dispatch using BAT algorithm. In2013 International conference on energy efficient technologies for sustainability 2013 Apr 10 (pp. 1018-1023). IEEE.
[8] Sugave SR, Patil SH, Reddy BE. A Cost-Aware Test Suite Minimization Approach Using TAP Measure and Greedy Search Algorithm. International Journal of Intelligent Engineering and Systems. 2017;10(4):60-9.
[9] Alsariera YA, Zamli KZ. A real-world test suite generation using the bat-inspired t-way strategy. InThe 10th Asia Software Testing Conference (SOFTEC2017) 2017 (Vol. 10, pp. 71-79).
[10] De Souza LS, Prudêncio RB, Barros FD. Multi-Objective Test Case Selection: A study of the influence of the Catfish effect on PSO based strategies. InAnais do XV Workshop de Testes e Tolerância a Falhas-WTF 2014 (pp. 3-16).
[11] Wang G, Guo L. A novel hybrid bat algorithm with harmony search for global numerical optimization. Journal of Applied Mathematics. 2013; 2013.
[12] Nachiyappan S, Vimaladevi A, SelvaLakshmi CB. An evolutionary algorithm for regression test suite reduction. In2010 International Conference on Communication and Computational Intelligence (INCOCCI) 2010 Dec 27 (pp. 503-508). IEEE.
[13] Srivastava PR, Pradyot K, Sharma D, Gouthami KP. Favourable test sequence generation in state-based testing using bat algorithm. International Journal of Computer Applications in Technology. 2015; 51(4):334-43.
[14] Kaur A, Agrawal AP. A comparative study of bat and cuckoo search algorithm for regression test case selection. In2017 7th International Conference on Cloud Computing, Data Science & Engineering-Confluence 2017 Jan 12 (pp. 164-170). IEEE.
[15] Lin CT, Tang KW, Kapfhammer GM. Test suite reduction methods that decrease regression testing costs by identifying irreplaceable tests. Information and Software Technology. 2014 Oct 1;56(10):1322-44.
[16] Sugave SR, Patil SH, Reddy BE. A Cost-Aware Test Suite Minimization Approach Using TAP Measure and Greedy Search Algorithm. International Journal of Intelligent Engineering and Systems. 2017;10(4):60-9.
[17] Sugave SR, Patil SH, Reddy BE. DIV-TBAT algorithm for test suite reduction in software testing. IET Software. 2018 Mar 13;12(3):271-9.
[18] Qu X, Cohen MB, Woolf KM. Combinatorial interaction regression testing: A study of test case generation and prioritization. In2007 IEEE International Conference on Software Maintenance 2007 Oct 2 (pp. 255-264). IEEE.
[19] Robinson J, Rahmat-Samii Y. Particle swarm optimization in electromagnetics. IEEE transactions on antennas and propagation. 2004 Apr 5;52(2):397-407.
[20] Tai KC, Lei Y. A test generation strategy for pairwise testing. IEEE transactions on software Engineering. 2002 Aug 7;28(1):109-11.
[21] Windisch A, Wappler S, Wegener J. Applying particle swarm optimization to software testing. InProceedings of the 9th annual conference on Genetic and evolutionary computation 2007 Jul 7 (pp. 1121-1128).
[22] Chen X, Gu Q, Qi J, Chen D. Applying particle swarm optimization to pairwise testing. In2010 IEEE 34th Annual Computer Software and Applications Conference 2010 Jul 19 (pp. 107-116). IEEE.
[23] Windisch A, Wappler S, Wegener J. Applying particle swarm optimization to software testing. InProceedings of the 9th annual conference on Genetic and evolutionary computation 2007 Jul 7 (pp. 1121-1128).
[24] Zhu H, Hall PA, May JH. Software unit test coverage and adequacy. Acm computing surveys (csur). 1997 Dec 1;29(4):366-427.
[25] Zhang S, Zhang Y, Zhou H, He Q. Automatic path test data generation based on GA-PSO. In2010 IEEE International Conference on intelligent computing and intelligent systems 2010 Oct 29 (Vol. 1, pp. 142-146). IEEE.
[26] Bo F. Automated software test data generation based on simulated annealing genetic algorithms [J]. Computer Engineering and Applications. 2005;12.
[27] Ding R, Feng X, Li S, Dong H. Automatic generation of software test data based on hybrid particle swarm genetic algorithm. In2012 IEEE Symposium on Electrical & Electronics Engineering (EEESYM) 2012 Jun 24 (pp. 670-673). IEEE.
[28] Zhang S, Zhang Y, Zhou H, He Q. Automatic path test data generation based on GA-PSO. In2010 IEEE International Conference on intelligent computing and intelligent systems 2010 Oct 29 (Vol. 1, pp. 142-146). IEEE.
[29] Zhu XM, Yang XF. Software test data generation automatically based on improved adaptive particle swarm optimizer. In2010 International Conference on Computational and Information Sciences 2010 Dec 17 (pp. 1300-1303). IEEE

ACTA TECHNICA CORVINIENSIS – Bulletin of Engineering
ISSN: 2067-3809

[1.]Cristian PANDELESCU, [2.]Elisa-Florina PLOPEANU,
[3.]Nicolae CONSTANTIN, [4.]Elena Mădălina VLAD

ANALYSIS OF THE CURRENT SITUATION CONCERNING THE DURATION OF USE AND THE MAIN DEFECTIONS OF THE PUMPING AGGREGATES

[1-4.]University "Politehnica" of Bucharest, ROMANIA

Abstract: The pumping units used in irrigation and for domestic and industrial users are made up of subassemblies made of metallic materials. The normal operating time of the pumping units is dependent on the reliability of the metal parts that make up the unit. In this paper the authors present an analysis of the real defects arising from an industrial operation of the pumping units, presents the presumed causes of the defects, especially of the causes related to the quality of the metallic and non-metallic materials, the reliability of the materials. For each type of defect, the real possibilities of remedying the defects are presented.
Keywords: pumping aggregates, reliability, metallic piece, defected, causes, remedied

INTRODUCTION

The pump-motor units, also called pumping groups, are the basic equipment of a pumping plant. They relate to the upstream suction-intake and downstream discharge, as a whole constituting the hydromechanical equipment of the pumping plant [1, 2].

The characteristic parameters of a pumping group are the unit flow rate, pumping height, speed, pump and motor power, the overall efficiency of the pumping unit.

At pumping installations for irrigation through automated pipes it is sometimes required to install different pumps [2, 3]

Reserve groups will be installed only when the consumption graph has a peak that lasts more than two months.

The groups with vertical pumps are preferred which, being drowned below the minimum suction level, no longer requires priming installations, and the surface of the building is smaller than the horizontal pumps. If electric motors are protected from rain, they can operate outdoors, and the superstructure of the pumping station can be removed.

The hydrophobic (hydro pneumatic reservoir) is frequently used in pumping installations for water supply, in order to compensate between the pumped flow and the required flow, for the automatic control of the installation and for the attenuation of the ram blows in the network.

The capacity of the tank is calculated based on the number of starts allowed per hour, taking into account the heating of the motor and the wear of the contacts of the switch. [4, 5] The number of starts of the pump is maxim when the flow consumed is half the pumped flow.

In order to meet the variation of the required flows, the pumping stations that supply the irrigation systems will have automatic control.

The problem of regulation is difficult, because the irrigation stations are equipped with identical pumps in order to be able to exchange them, for the purpose of balancing the wear, and with a single reserve group, the variation of the flow of the station is in stages, depending on the number of pumps in operation.

Continuous flow regulation requires adjustable speed pumps or adjustable blades [6, 7].

EXPERIMENTS

The normal operating time is the duration of use in which it recovers, from a fiscal point of view, the value that the pumping unit had at the date of commissioning. Consequently, the normal operating life is shorter than the physical life of the respective pumping unit [7, 8].

For each newly purchased pumping unit, the system of year's ranges between a minimum and a maximum value is used, thus being able to choose the normal operating time within these limits. Thus established, the normal operating time of the pumping unit remains unchanged until it has fully recovered its input value or is removed from operation.

If reliability is defined as the ability of a technical system to function flawlessly for a period of time as close to the time prescribed by the designer-builder, the normal operating time of a pumping unit is directly influenced by its actual operating time. The actual operating time is influenced by the complexity and the periodicity of the occurrence of the wear on the parts that form, in our case, a pumping unit. Reliability is the ability of a product to function without fail [9].

Mathematically it is possible to estimate with a certain degree of certainty the behaviour of a product under

certain conditions of use. Reliability is one of the basic components of a product's quality. From a certain point of view, quality can be considered as a "static" trait of satisfying certain conditions at a certain time, while reliability is a quality over time or a "dynamic" trait. From this point of view reliability represents a new dimension of quality, a component over time of quality [10]. This definition contains five fundamental concepts:

—The concept of characteristic

Reliability is therefore a characteristic of a product, which can be determined and characterized, as well as the other technical characteristics (power, speed, etc.) and expressed quantitatively.

Reliability must have the same status as the other technical characteristics: it must be considered starting from conception to design, be properly monitored in manufacturing and be attested by tests or other estimation methods.

—The concept of probability

Reliability is expressed by a probability and has a value between 0 and 1. Being a probability cannot be measured directly as is the case with other physical quantities, but it is determined based on mathematical statistics methods and probability theory. This is still an important obstacle to properly assimilating this feature. Especially for design and design, reliability must be regarded as a basic feature to guide and optimize the constructive solution.

—The concept of function

Reliability implies the satiation of a required function. This implies the correct definition of the function that it must perform. In the case of a simple element, the function means what it has to do, within the assembly of which it is part. In complex products or equipment there may be multiple functions, depending on different states and operating regimes considered explicit or implicit. Reliability refers to all these functions.

—The concept of operating conditions

The concept of operating conditions (environmental use) represents the set of conditions for which the product was designed.

It is observed that in many cases the notion of reliability is not interpreted correctly, especially when the value of reliability is estimated from the perspective of laboratory tests in which the requests are not correlated with those of normal use. Operating conditions directly influence reliability.

An ideal product has the reliability corresponding to the given conditions. Failure to meet certain conditions means that the reliability does not have the desired value. From this, a series of conditions revising which concern the use, and on the other hand the conception and the design.

—The concept of service life

Reliability involves a service life expressed in units of time (hours, days, years, etc.) or a number of cycles, connections, manoeuvres, etc. In conclusion, the duration is expressed in the characteristic units of the respective product.

The correct expression of reliability requires clarification regarding the five concepts listed.

The analysis of the product failure mode is an intuitive analysis, representing a first step in the engineering approach of the product reliability and maintainability field. Without using a special mathematical tool, the analysis of the failure mode can only be performed by specialists in the respective field of expertise. These methods of analysis are standardized. The most used method is the AMDE method (Analysis of failure modes and their effects).

The AMDE method aims to identify defects whose consequences affect the functioning of the product.

The AMDE analysis is based on complete information and documentation activities.

There are four main steps in carrying out the AMDE analysis:

» definition of the system, functions, components and their role;
» establishing the failure mode;
» study of the effects of the failure modes;
» observations, conclusions and recommendations.

The main elaboration stages of the AMDE method are presented in the graph in figure 1.

The definition of the system (equipment) is made according to the standard specifications and specifications.

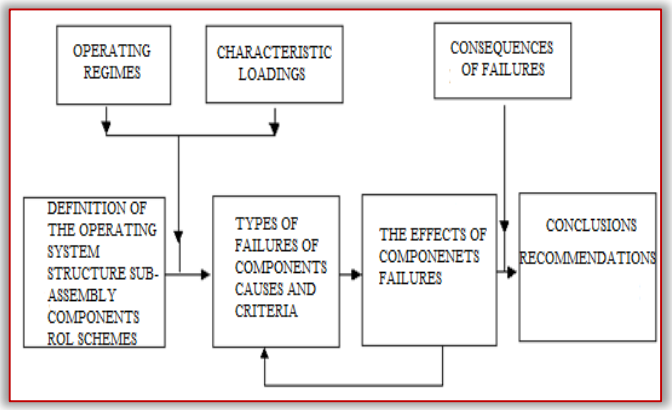

Figure 1. The development stages of the AMDE method

The AMDE method makes a census of all the defects of a system by collecting information from all the possible places where defects were found and the conditions in which they occurred.

Determining the physical mechanism of the failure process is the essential problem of this analysis. The qualitative analysis of the defective process requires a

thorough knowledge of the respective field of specialty.
The potential failure modes can be reduced based on the physical parameters of the component and its functional characteristics. The failure modes are classified in:

» General failure modes, deduced by defining the reliability of the system;
» Specific modes of system failure.

— **Defects of common cause**

A common cause failure is the result of an event that, due to dependencies, simultaneously causes several components to come out of operation (eliminating secondary failures that result from the effects of a primary defect).
Defects in the common cause can cause performance degradation or total system failure and are due to only single sources, such as conception error, human factor error, etc.
These cases fall into the following categories:

» Effects of environmental demands (normal or accidental conditions);
» Design errors;
» Manufacturing defects;
» Mounting and commissioning errors;
» Human errors (during operation and / or maintenance).

Combined measures are used to prevent such defects from occurring. Other preventive measures include: functional diversity, redundancies of different types, physical separations of systems, additional tests.

— **The way of presenting the analysis**

Generally, the analysis is presented in the form of an analysis report containing a specification of the analysed system (subassemblies, component elements, schemes, etc.), functional role, process description, effects, conclusions and observations developed at the level of the requirements and use of the respective material.
This analyser may be included in a general study or may be a technical document in its own right.
The analysis ends with a sub-chapter on observations and conclusions stemming from the findings.
Proposals may also be made to improve the diagnosis of defects, maintenance activities and actions and activities regarding the phase out of operation related to material recovery and environmental protection.

— **Identification of the main types of uses for pumping units**

The main types of uses that appear on the parts and components of a pumping unit, selected as a result of the processing of data from the units in operation are:

» The pump shaft - material from which OL 50 is made.

The wear of the spindles for the semi-duplicate and the spindle wear for the chromed bushes, which can be seen by visual control and by measuring the diameter of the spindle with an external micrometre, after previously removing the bushes from the shaft.
The spindles for used bushes and semi-couplings are reconditioned by electric vibrating spring loading.

» Rotor chamber - material from which it is made – cast iron.
≡ Hydro-abrasive wear of the inner surface of the rotor chamber, is seen by visual control and by measuring the internal diameter of the rotor chamber in the maximum wear area.
≡ Wear or deterioration of the places corresponding to the mounting of the wear rings
» The assembled rotor - material of which it is made of pocket OT-OT 45, pallets 7 NC 180
≡ The wear of the front surfaces of the blades is ascertained by visual control, by checking the profile of the blade with a template after a new blade and by measuring the outer diameter of the rotor.
≡ Wear or damage of threaded holes.
» Stator -material from which it is made-cast iron.
≡ wear inside diameter,
≡ wear of the front surfaces of the pallets,
≡ wear of threaded holes.
» Bearing body (outer, upper or intermediate)
≡ the material from which it is made – cast iron,
≡ wear of the inner surfaces of the bearings in contact with the bearing's bushes
» The bearing - the material from which it is executed - OLT 35 sleeve, rubber lining
≡ wear of the inner surface in contact with the chrome bushing,
≡ wear of the outer surface of the bearing,
» Bush - the material from which it is made - OL 50 or OLT 35.
≡ wear of the outer surface of the bush in rubbing with the rubber bearing
≡ wear of the inner surface of the bush in contact with the pump shaft.

— **Faults in operation with mention especially of those generated by the metallic materials used in the pumping units**

The defects that occur frequently in the operation of the pumping units, the way they are manifested, the effects and the way to remedy them are multiple due to the great diversity of construction types and installations in which the centrifugal pumps are used. Most of the cases are in conjugated fields, so that the analysis to determine the origin of the defect must go through all possible investigations, starting with the

most "at hand" and easier to find, to those that require knowledge and interpretation. complex and specialized in the field of pumping installations and pumps (example: the material of the rotor has chemical and / or mechanical characteristics incompatible with the vehicle environment and / or has not been controlled with penetrating liquids but also due to the suction conditions - NPSH -, non-compliant with those for which the pump was offered).

The interventions carried out for the removal of any kind of defect should not harm the energy balance of the pumping unit.

The corrective measures taken must be thoroughly analyzed (technical - economic calculation in the short, medium and long term) so that the adopted measure does not lead to harmful exploitation from the point of view of energy consumption.

RESULTS AND DISCUSSION

— Faults, causes and remedies

≡ Incomplete open suction valve, due to blocking or heavy operation.

The valves that equip the pumping units can be flat or oval. Regardless of its type, the mechanism of the drawer is composed of a screw and a fixed nut. If the screws in almost all cases are made of steel, the nuts can be either steel, cast iron or bronze. Valve locking is rarely encountered in industrial pumping installations, where their handling also takes place several times during a work shift; in contrast to irrigation or drying facilities, the rest period may be as high as ten - eleven months per year. In this period due to the justified lack of manoeuvres, the materials from which they are manufactured interact, creating a blockage that leads to the failure of the screw-nut mechanism.

Remedy: For this, metallic materials should be chosen for the manufacture of the screw and valve nut, which, after processing by cutting, and thus obtaining a minimum roughness, should not lead to a high self-braking condition of the screw-nut mechanism, which in the absence of frequent periodic manoeuvring, but also of the lack of lubrication, to lead to blockage.

≡ The suction segment of the installation (starting with the suction) and / or the rotor are clogged.

Also, in the irrigation and drying pumping systems, the fluids conveyed are not the cleanest, with all the systems of grids and grills with which the installation is equipped, foreign bodies penetrate which can block the rotor assembly or the elements of first transport of the water.

Remedy: To the extent that a decent manufacturing cost limit is not exceeded, these pump component parts should be made of metals with a high degree of roughness, without prominent edges and corners, thus ensuring a high flow of fluids, as well as a heavier attachment of foreign objects to moving parts.

≡ Air penetration into the suction pipe

Due to the corrosion the suction pipe can be perforated giving rise to holes through which the pump pulls the so-called "false air" situation which leads to the occurrence of amplified vibrations leading to a shock request on the rotor blade, eventually leading to the water column breaking and by default, defrosting the pump.

Remedy: Manufacture of metallic pipes that, with or without improvement, resist corrosion, also taking into account the natural atmospheric conditions, summer-winter to which they are subjected by the nature of the location on the ground.

≡ Formation of air bags or vapours in the suction pipe or in the pump housing

Their appearance can lead to the phenomenon of cavitation, which is very dangerous in the construction of pumping units.

Remedy: Making the component parts of the rotor assembly as well as the rotor chamber and stator of the pump, made of harder metallic material, which does not give way to the destructive effects of the cavitation phenomenon, especially in situations where it occurs frequently.

≡ Air penetration on the sealing of the pump

The sealing of the pump at the shaft side is performed both at the vertical and horizontal pumps with a gland and a graphite asbestos ring. The sealing is carried out in the immediate vicinity of one of the pump bearings generally in the bearing from the drive motor. Due to this constructive positioning near the camp, the existing thermal regime, as well as its value variation, leads, due to the expansion, to an inadequate seal.

Remedy: manufacture of the cable gland and its assembly elements made of metallic material with a lower coefficient of expansion, and a corresponding resistance taking into account that outside the thermal regime the cable gland must also face the vibration system as well as the shocks in the pump shaft.

≡ Insufficient immersion of the vertical pump

Depending on the pumping height, the pump has a certain immersion rating from the design, more specifically a minimum water column above the rotor so that the load of the blades is appropriate. If this condition is not met, the pump enters a vibration regime, which can even lead to so-called junctions that are transmitted as shocks to the rolling bearings of the pump shaft.

Remedy: Respecting the immersion depth is the only solution, because regardless of the hardness of the pump parts, the support of a vibration regime ended with mechanical shocks leads to the safe damage of the pump.

≡ **Deviations from the specifications regarding the manufacturing dimensions of the pump parts**

In the case where the parts are mainly made of steel, at very long lengths (30 m axle pumps) there is an arrow of the material that can be forced in one of the directions to the wrong installation of the pump with the corresponding piping in the recesses of the pumping station. .

Remedy: Use castings as much as possible due to their lower elasticity than steel.

≡ **The game between pair mazes is increased**

Labyrinths or wear rings as other designers call them are the parts that by mounting on the sides of the rotor chamber transform its architecture from the rotor chamber into a spherical chamber and vice versa. These rings are generally made of cast iron, having very large diameters, and very small thicknesses (hence their low strength) and are mounted on the rotor chamber with the help of intercalated screws.

As the spindle grows larger, a larger portion of the rotor flow returns to the suction.

Forced by the installation that requires the flow rate to be retained, the rotor will have to carry an internal flow greater than the flow rate in the case of unused labyrinths. .

Remedy: Manufacture these mazes or wear rings from a more resistant metal material.

≡ **Destruction of the bearings of a pump**

The existing pump bearings are generally of two types of roller bearings having bearings and bushings. Due to the difficulty of securing a closed, watertight and very well lubricated housing, bearings with bearings are used only at horizontal pumps. At vertical pumps with very long lengths the bearings used are composed of:

» a casing made of cast iron or steel to which is subsequently applied a layer of hard chrome with a thickness of 0.1 mm

» a bearing made of steel, in one piece or two half-pieces, on which a layer of rubber with grooved architecture is vulcanized, subjected to a bake at 160°C, for eight hours, in which regime the rubber loses elasticity, becoming brittle, adhering very well to the steel housing.

If, in the case of roller bearings, lubrication is carried out with oils and greases, at bearings and rubber bearings, the lubrication is done with clean water, coming from an auxiliary installation of the pumping station, provided with a well and filter assembly.

Remedy: making the chrome plated bush from a more resistant metallic material that may no longer require chrome plating, or applying a harder and more resistant chrome coating, which can withstand a thermal regime in the absence of the cooling liquid, and which may eventually it does not adhere to the vulcanized rubber on the bearing housing.

≡ **The decalibration of the connection couplings between the axes**

The shafts of long and very long shafts are connected together by means of assembly elements, called couplings which, on the inside, have two diametrically opposed fuses, or multiple grooves, depending on the size of the moment to be transmitted by the propeller motor to the pump rotor. Due to wear over time, these connecting couplings no longer make intimate contact between the ends of the axes, so that the rotational movement is transmitted with shocks from one axis to another. Also due to this wear also appear the beats in the bearing, the eccentric movements inside the bearing, which leads to the destruction of the bearing.

Remedy: making these couplings from harder materials, to achieve the coupling of the axes in the best possible regime, avoiding the occurrence of games between semi-couplings and obviously between axes.

≡ **Destruction of a rotor blade**

In the manufacturing architecture of pump rotors, they can be - closed radial rotor, star rotor, open rotor, closed diagonal rotor, radial shrink rotor, axial rotor with fixed blades, and axial rotor with adjustable blades. In all types of rotors, the penetration of a hard object can cause a blade to break. In addition to leaving the rotor by a blade (in the case of axial blades), or a piece of the rotor (on closed rotors), it leads to its imbalance, the piece detached from it is entrained and during the shortest time it destroys and the other blades or the closing part of the rotor.

Remedy: making rotor blades made of metallic materials to withstand these penetrations, which in conjunction with the overload protection of the pumping unit, lead to the momentary locking of the pump and decoupling from the power supply, thus avoiding damage.

≡ **Breaking the rotor chamber of a pump.**

In correlation with the anomaly from the previous point, we can say that while entering the rotor chamber of a foreign object, besides the rotor blade or sectors, the wall of the rotor chamber is also required. Given that the permissible clearance between the rotor and the rotor chamber is generally at large vertical pumps, about one millimetre, it is understood that the compression stress occurs between the blade and the wall of the rotor chamber.

As the rotor chamber is generally made of cast iron, so with a mechanical resistance lower than that of the pallet, made of steel or stainless steel, the first step that yields is the wall of the rotor chamber.

The malfunction appears as a hole in the rotor chamber, the pump unbalancing due to the fact that the liquid is no longer raised to the discharge area, but is mixed in the suction area.

Remedy: making the rotor chambers of metallic materials that confer a superior resistance to the shocks to which the pump is subjected to the penetration of hard foreign bodies into the rotor chamber.

≡ **Wear on conjugated parts inside a pump**

The appearance of wear on the vast majority of the pump's parts is manifested by detaching a number of layers from the surface of the part, which leads to the reduction of the initial quota. This results in games - in the case of pump bearings; when driving a much smaller volume of fluid - in case of wear of the pump blades and the walls of the rotor chamber, etc.

Remedy: making the parts of a pump made of metallic materials that accept the reconditioning by applying successive layers of metal and which, after the machining by cutting, return to the initial dimensions of the project.

≡ **Corrosion of the pump pipe**

Regardless of whether it is in operation or during a stationary period, submerged or dry, the pump operates in a hostile environment from the point of view of the environmental factors.

Remedy: manufacture of pipes made of metallic materials that accept the adhesion on its surface of insulating elements such as paints, varnishes, rubber or polycarbonate layers to protect the entire structure against corrosion.

CONCLUSIONS

The actual operating life of a pumping unit differs from one area of use to another. Thus, if in the industrial field for a vacuum pump in the MIL family the manufacturer offers a duration of 12 years, and for a vertical pump type DV, AV, Danube, etc., a duration of 20 years, taking into account that their operation it is permanently daily, in agriculture, both in the field of irrigation and drying, the existence of periods of months or years in which they are not started, changes the life span. However, the service life does not extend, because during the stationary period the pump is in the same hostile-corrosive environment (moisture, impurities, snow, etc.). The pumping unit is not dismantled from the installation and protected in a so-called park waiting cold.

From this point of view the durations expressed by the manufacturer are purely informative, of maximum importance being only the warranty period granted, and this is quite small depending on the actual operating conditions.

By analysing the types of defects and centralizing the results, a complete set of information about the operation of the pumping units of different types of construction can be realized.

For each type of defect based on the deviations from a functioning in the real environment of the aggregates, the causes can be determined precisely and based on the previous experience centralized in that complete set of information, the best decision can be made to correct the defects and to extend the duration functioning of the unit in question until its replacement with a new one.

Acknowledgment: The work has been funded by the Operational Programme Human Capital of the Ministry of European Funds, Work-based learning systems through entrepreneur scholarships for doctoral and post-doctoral students through the financial agreement 51668/09.07.2019, SMIS code 124705.

References

[1] Aurel Blidaru - Instalaţii de pompare pentru agricultură - Ed. Ceres Bucureşti 1984
[2] Gheorghe Negru - Instalaţii de pompare şi pompe - Ed. Estfalia Bucureşti 2006
[3] Dumitru Manea - Pompa de căldură - Ed. Tehnică Bucureşti 1982
[4] V.S.E. Volod Radcenco şi alţii - Instalaţii de pompare de căldură - Ed. Tehnică Bucureşti 1985
[5] Ursula Schreier şi alţii - Pompe de căldură -Ed. Casa Oradea 2011
[6] Florea Ştefan şi alţii - Tehnologii de reparare pentru grupuri de pompare - Ed. RMPA 1980
[7] Aversa Manufacturing SRL -Catalog Pompe
[8] S.C. Utilaje, Piese schimb şi servicii S.A. Botoşani- Catalog Pompe
[9] Rada Andrei Cristian, Teza de doctorat „Cercetări privind funcţionareasistemelor hidraulice pentru pomparea apelor din exploatările miniere în vederea îmbunătăţirii eficienţei lor “
[10] Popescu Luminiţa Georgeta, Universitatea “Constantin Brâncuşi” din Târgu Jiu, România, Monitorizarea unui agregat de pompare utilizat pentru evacuarea apelor în cariera Roşia, Analele Universităţii „Constantin Brâncuşi” din Târgu Jiu, Seria Inginerie, Nr. 2/2009, pag.253-261

ACTA TECHNICA CORVINIENSIS – Bulletin of Engineering
ISSN: 2067-3809

[1.]Shweta K. BORSE

A REVIEW: PREDICTING AIR QUALITY USING DIFFERENT TECHNIQUE

[1.]Dept of Computer Engineering, R. H. Sapat College of Engineering, Management Studied and Research, Savitribai Phule Pune University, Nashik, INDIA

Abstract: Nowadays pollution problems are growing in the world. It has become a big issue because it is harmful to health, it causes health problems like asthma, cancer, heart attack and so on. An air impurity is defined on chemicals present in the environment. If a chemical is higher than the target level of chemicals presents in the air, it is known as an air pollutant. Air pollution levels in most of the urban areas have been a matter of serious concern. In forecasting of pollution, the soft computing techniques are used. Besides, machine learning techniques and data mining techniques namely recurrent neural network, Long Short-Term Memory, gated recurrent unit, artificial neural network, support vector machine, fuzzy logic, genetic algorithm is used in major places worldwide for prediction of the air pollutant.
Keywords: Air Quality Index, Recurrent Neural Network, Long-Short Term Memory, Gated Recurrent Unit, Fuzzy Logic, Artificial Neural Network

1. INTRODUCTION

Some Asian Cities is so bad condition in air pollution, the cities are covered up by fog that slows visibility. According to WHO, the pollutant effect on human health are considered the critical limit, specifically in developing countries like India, China, Pakistan, and Bangladesh. In Asia small cities like Kathmandu, WHO suggested that the PM level be over moderate for some target. The Earliest few years ago, China has been covered by fog with smoggy pollution in their cities, India and Pakistan also include in it. PM is most severely in Delhi. The prediction gives the impurities awareness or the Air Quality Index (AQI). Air pollution predicting container done by join weather prediction with Biochemical transportation system and Environment distributed model. By using a machine-learning algorithm. The prediction takes local production sources (industry or traffic) and isolated sources. The prediction on a historical daily or hourly data and the longitudinal can modify from chunk determination. Forecasts of air quality cover 2 to 5 days Estimating meteorological conditions, there are representations to forecast stages of air quality and air pollution. There are different prediction methods that involve additional difficulty than climate prediction methods. These methods are measured the air impurities concentrate in the airborne. Air pollution arises when the surrounded air containing fumes, dirt, gases in risky to be uncertain to humans and wildlife, plants and resources.

— Benefits

Air pollution predicting is a valuable asset on several stages – global, national, community, and individual. Exact predicting services help people proposal ahead, reducing the effect on human health. If public are alert to dissimilarities in the air quality, the effect of impurities on health, a greater probability changes in individual behavior and public strategy, as public need air quality info. Such recognition has the possible to generate a clean atmosphere and also a better resident. Administrations too make usage of initial predicting to initiate procedures to decrease the seriousness of pollution levels.

— Accuracy in air quality forecasting

Air smog are powerfully connected with resident climate conditions and surrounded smog emissions. Forecasting air quality, so, not one of the contains the difficulties of climate predicting, it needs information on and data of:

- Resident impurity meditations and emissions.
- Impurity meditations and emissions from different places.
- Movements and probable revolutions of impurities.
- Prevailing air-streams.

The several issues on production in forecasting air quality effect in air pollution predicting existence both particular and objective.

— Air quality prediction techniques

There are many such prediction methods, and all need extra complication than climate prediction methods. These methods are measured simulations of how air impurities diffuse in the airborne. The first step to air quality prediction is an outstanding climate prediction. Atmospheric (climate) predicting can be considered into three types: climatology, statistical methods and 3-D models.

≡ Climatology

Climatology is based on the guess that the earlier is a decent pointer of the future. This technique is built on the relation among exact climate situations and smog levels, and so on actual one-dimensional.

This technique is frequently stretched to contain the identical of climate patterns to smog patterns. There are several limits to this technique and it is observed as a implement to quantity other predicting systems.

≡ **Statistical Methods**

The suggestion between climate forms and air quality can be measured using numerical approaches. Some are as follows:

» **Classification and Regression Tree (CART):**

Classification and regression tree (CART) are proposed to categorize information into different groups. Software classifies variables that associate by ambient effluence level. The information is used to prediction application built on climate situations also on connected impurity awareness.

» **Regression Analysis:**

Regression analysis evaluations relations among variables. By studying past datasets, organization is completed between smog levels and atmospheric statistical variables. The outcome is an equivalence used for prediction of upcoming effluence levels.

» **Artificial Neural Networks:**

Artificial neural networks usage adaptive knowledge & pattern recognition methods. Computer established systems are considered to simulate the human brain's capability for pattern recognition. This is uncertainly the maximum suitable technique for predicting smog outstanding toward its multi-dimensional method.

» **Three-dimensional (3-D) models**

Three-dimensional models exactly signify completely the significant developments that have an effect on outdoor air effluence phase. Three-dimensional method put on the production, transportation, and revolution of air pollution by production usage of some sub method, including:

Emission model:

The longitudinal supply of productions as usual human sources.

Meteorological model:

Produces a trajectory method to forecast the ambient points of effluence with the 3-D atmospheric method.

Chemical model:

Appearances at the revolution of initial pollution into secondary smog to determine the result of the impurity.

Pollution prediction methods are quickly developed and will remain growing in exactness. Exact and available air pollution predictions help increase community perception, allow designed for complex to plan fast, and make available administrations by material for public health warnings [13],[14].

— **Air Pollution Accidents**

Last few years ago we read or listen to the news about air pollution accidents in the media. We also listen to news about Bhopal Gas Tragedy it should happen cause of four-hour leakage of methyl isocyanate at chemical plant in1984, in this accident 2800 was died in Bhopal, Madhya Pradesh, India.

Table 1. Air Pollution Accidents

Days of fog	Year	Cities	Died People
-	1880	London	-
3	1930	Meuse valley, Belgium	60
9	1931	Manchester, England	592
4	1948	Donora, Penn	20
4	1952	London, England	4000
-	1953	New York	220-240
30	1963	New York	300-405
2	1966	New York	168
3	1991	London	160
12	2017	Punjab, Pakistan	20

LITERATURE REVIEW

Two methods for predicting air quality as namely, lazy learning (LL) and pruned neural network (PNN). PNNs establish a constraint ungenerous method, founded on the deletion of terminated constraints after completely linked ton neural networks; LL is a simple linear forecast system, which does a partial knowledge method each historical data estimate is essential. LL forecaster can be speedily established, then the easiness in the regressors permits equally to the overfitting problems [15].

Air quality estimating with machine learning methods to forecast the hourly of air impurities. Machine learning is capably training a model on large data by using extensive optimization method. They proposed distinguished models to forecast the hourly air smog absorption on the basis of atmospheric data of earlier times by preparing the calculation over 24 hours as a multi-task learning (MTL) [16].

The air quality is poorly affected various methods of smog produced by transport, electrical energy, gas usages etc. The harmful smokes are making a serious for the quality in towns. With growing air smog, effective air quality models collect material data of air impurities and make available valuation of air smog in every zone. From now, air quality estimation and forecast has turn out to be an important research topic. The multi-dimensional features with indeterminate variables, time, location. Authors published examination results air quality estimation with different methods of deep learning, decision trees, artificial intelligence [12].

Spatio-temporal deep learning (STDL) built forecast of the air quality that basically studies multi-dimensional and historical information is establish. A stacked auto encoder method is used to integrate air quality, and it is train on a grasping layer. Associated with time series estimate the models, model can forecast the air quality of places concurrently and demonstrations in all time periods. Support vector regression, auto regression moving average, and spatio-temporal artificial neural network models determines the method of performance air quality forecasts takings a more performance [17].

Air quality prediction is flattering. There are two tools for analysis and prediction, namely numerical and statistical tool. Mathematical and statistical techniques are used for air quality forecast, and other remaining parts used in the physical model. According to using algorithm data will be coded in mathematical form, sometimes they provide the limit for the accuracy so that's why get problem to take accurate accuracy at greatest point (such as taking the cut-off value in prediction) [2]. There are some techniques are used for air pollution prediction. Some areas following:

» Recurrent Neural Network (RNN)
» Long Short- Term Memory Unit (LSTM)
» Gated Recurrent Unit (GRU)
» Artificial Neural Network (ANN)
» Support Vector Machine (SVM)
» Fuzzy Logic (FL).
» Genetic Algorithm (GA).

— Recurrent Neural Network (RNN)

RNN is an open-source machine learning framework that implements Recurrent Neural Network architectures, such as LSTM and GRU. Fabio et al. (2019), proposed to predict the air quality index (AQI) pollution in the Apulia region. Authors have trained different RNN models by using GRU and LSTM neuron cell respectively and forecast the pollution level in some areas by using available data of that particular areas. Using these methods, the outlook on — air station and weather in the region, it is feasible to alert some days before on the pollution levels.

Estimate approaches based on multiple linear regression, neural network, and recurrent neural network used for the air quality in station are established and associated. The RNN model, forecast the air pollution at station by the prior historical data of the impurities on the model. The forecast models are useful to a actual indoor air quality data-set from tele-monitoring systems data, model shows that the certain variables consume though impact on the forecast presentations. It establishes the RNN that has the capability to model the dynamic system, nonlinear and the forecast outcome of the RNN method shows the good performance and developed interpretability than other forecasting models [18].

— Long Short-Term Memory (LSTM)

The prediction of PM2.5 concentrate using LSTM and RNN. They used TensorFlow tool for LSTM and RNN in python. Environmental Protection Administration of Taiwan data set is used for training (data from 2012 – 2016). Data for the year 2017 is used as test data. Prediction value of PM2.5 is evaluated, and concentrates for the next four hours at some number of stations. Prediction on PM2.5 outcome is poor when PM2.5 does not affect on air pollution [3].

Forecast PM 2.5 smog of air quality station taking the historical data, atmospheric data, climate prediction data. Analytical model be made upon two mechanisms are long short-term memory (LSTM) model the local distinction of PM2.5 pollution and a neural network based three-dimensional combinatory to detention longitudinal dependence between the PM 2.5 pollution of station areas and that of neighbor stations areas. Estimate model on a dataset records of air quality stations in Beijing and associate it with artificial neural network and LSTM on the similar dataset. The outcomes show that LSTM-FC neural network gives a best performance [19].

— Gated Recurrent Unit (GRU)

GRU is simple than LSTM. GRU contain two types of gates as Update Gate and Reset Gate. Three different GRU in RNN to retain the form and reduce the parameter in reset and update gate. The GRU model on IMDB and MNIST data set. Gates occur to the recurrent state al about the other signals. They use GRU1, GRU2, and GRU3 RNN. Test accuracy is similar to three sequence length of them [4]. Beijing weather data and cluster data used as input vector. The training data is divided into four sections according to the season of winter, autumn, summer, and spring. Four models effect on forecasting PM 2.5 analysis by test data sets. After taking demonstration and persistent adaption of parameter, the forecasting errors and accuracy of models are examined and compared, then its work ability and advantages are verified by this method. Forecasting accuracy is built on the high GRU model, this model is effective for timeseries prediction of air pollution [5].

— Artificial Neural Network (ANN)

One-year data used for training and two-week data separately used for testing. Their huge amount of data removed from the training data set, compare with time-lagged model [7].

ANN is a data analysis tool used for optimizing the air quality data. It takes the three sets of data as test, train, and validation of models. Data set divided randomly training data set takes 75%, Testing takes 15%, and Validation data set takes 15% automatically. The result of air pollution in the atmosphere using different forecasting [6].

— Support Vector Machine (SVM)

SVM is a supervised learning, it used for regression or classification challenges.

Supervised learning (labeled data) used as training data. Air quality is divided into two types using Support vector machine as namely good or harmful. Mathematical formula Cumulative Index (CI) basis on four pollution as namely SO2, PM 2.5, PM 10, NO2. Possibility of input for SVM classifier value tested on real data. Polynomial kernel used in SVM that gives great accuracy and good performance more than forecasting. In the tuning model, accuracy is used primary metric [8].

— Fuzzy Logic (FL)

To predict air quality in urban areas and other cities by integrate CEP (Complex Event Processing) technology and fuzzy logic. Pollution data derive d from weather prediction and CEP engine by territory specialist. New fuzzy rule and input vector easily include in the FIS model and also modified a plan to fewer air pollution [9]. Develop electrostatic filter form on fuzzy logic to trim air pollution of PM. Electrostatic filter is O3 generate consist of plate corona expel and high volt DC generator. In experimental result s, they get trim Particulate matter (PM) of PM 10 in ten minutes by 55%, 68%, and 75% respectively for one, two, and three ozone generators [10].

— Genetic Algorithm (GA)

GA for selecting the starting weight and also used to learning something. It estimates in nature and then search for the final solution. GA calculates the starting weight. By using GA optimize the ANN nature. GA and ANN give the best performance by using a hybrid method [11].

Weather Research and prediction using California PUFF model. GA is used for the design of the best examine network [12].

SYSTEM ARCHITECTURE

Recurrent neural networks are one of the simplest models using the task of forecasting the afterward is a categorization based on the previous ones. Feedback is memorized portions of the involvements and used to make accurate predictions. Training a typical neural network involves the following steps:

Input an air quality and weather from a dataset.
The network will take that air quality, and weather, and apply some complex computations to it using randomly initialized variables (called weights and biases).
A predicted result will be produced.
Comparing that result to the expected value will give us an error.
Propagating the error back through the same path will adjust the variables.
Steps 1–5 are repeated until we are confident to say that our variables are well-defined.
A predication is made by applying these variables to a new unseen input.

The figure 1 shows the workflow of implementation to train the RNN. RNN can be trained to estimate CAQI level using air and weather data from different stations. Data split into two parts as the RNN model is used for trained and second data is used as RNN test data. In the training process, it takes all available data from datasets, then consider as test arbitrary sequential days. In the second test request to RNN, to make "blind forecast". First, randomly choose an air station, and then train the RNN to use data in a specific range. Estimate the direction between the selected station and other, and analyze weather state, trained to forecast CAQI level. Information about weather state of before days, depends on wind direction, RNN tries to evaluate the value of every impurity and CAQI [1].

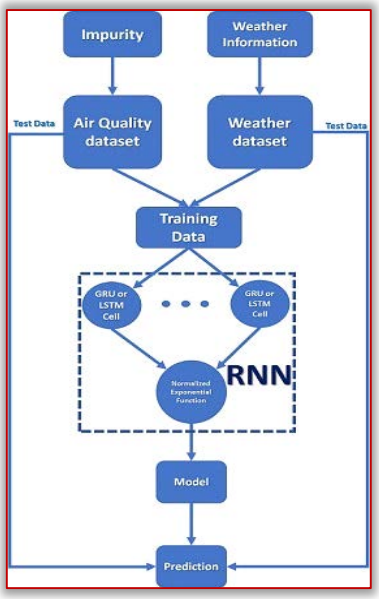

Figure 1. RNN model with Training and Test Data

CONCLUSION

In this paper, we study of air pollution and air quality forecasting using different algorithms. There is indisputable evidence of the unfavorable impacts of low air quality on the environment also on human health. Exact estimating benefits to public strategy gaining, reduce the belongings on fitness and the outlays are linked. If community are alert for differences in the value of the airborne, they blow, the result of impurities on fitness as well as meditations probable to basis opposing effects and activities to restrict smog. In forecasting of pollution, soft-computing methods are used. We also see that machine learning techniques and data mining techniques namely long short-term memory, recurrent neural network, gated recurrent unit, artificial neural network, support vector machine, fuzzy logic, genetic algorithm is used in major places worldwide for prediction of the air pollutant.

References

[1] Cassano. F., Casale, A., Regina, P., Spadafina, L., & Sekulic, P. (2019). A Recurrent Neural Network Approach to Improve the Air Quality Index Prediction. Ambient Intelligence- Software and Applications –,10th International Symposium on Ambient Intelligence, 36–44

[2] Niharika, Venkatadri M*, Padma S. Rao / (IJCSIT), A survey on Air Quality forecasting Techniques, International Journal of Computer Science and Information Technologies, Vol. 5 (1), 2014, 103-107.

[3] Tsai Y.-T., Zeng, Y.-R., & Chang, Y.-S., Air Pollution Forecasting Using RNN with LSTM. 2018 IEEE 16th Intl Conf on Dependable, Autonomic and Secure Computing, 16th Intl Conf on Pervasive Intelligence and Computing, 4th Intl Conf on Big Data Intelligence and Computing and Cyber Science and Technology Congress (DASC/PiCom/DataCom/CyberSciTech)
[4] R. Dey and F. M. Salemt, "Gate-variants of gated recurrent unit (GRU) neural networks," in Proc. IEEE 60th Int. Midwest Symp. Circuits Syst. (MWSCAS), Aug. 2017, pp. 1597–1600.
[5] Xinxing Zhou, Jianjun Xu, Ping Zeng, and Xiankai Meng, Air Pollutant Concentration Prediction Based on GRU Method, Laboratory of Software Engineering for Complex Systems, College of Computer, National University of Defense Technology, Changsha, China, IOP Conf. Series: Journal of Physics: Conf. Series1168 (2019) 032058
[6] M Venkatadri, A Novel Air Quality Prediction Model Using Artificial Neural Networks, International Journal of Engineering Research, 2014 - researchgate.net
[7] Madhavi Anushka Elangasinghe, Naresh Singhal, KimN. Dirks, Jennifer A. Salmond, Development of an ANN-based air pollution forecasting system with explicit knowledge through sensitivity analysis, Atmospheric Pollution Research (2014) 696-708.
[8] Saxena, A., and Shekhawat S. (2017). Ambient Air Quality Classification by Grey Wolf Optimizer Based Support Vector Machine. Journal of Environmental and Public Health, 2017, 1–12
[9] Macia. H., Díaz, G., Boubeta-Puig, J., Valero, E., & Valero, V. (2019). Combining Fuzzy Logic and CEP Technology to Improve Air Quality in Cities. Computational Science – ICCS 2019, 559–565
[10] Dewi Nurhaji Meivita, Muhammad Rivai, Astria Nur Irfansyah, Development of an Electrostatic Air Filtration System Using Fuzzy Logic Control, Vol.8 (2018) No.4ISSN: 2088-5334.
[11] Hao, Y., Xie, S., Optimal redistribution of an urban air quality monitoring network using atmospheric dispersion model and genetic algorithm, Atmospheric Environment (2018)
[12] Gaganjot Kaur Kang, Jerry Zeyu Gao, Sen Chiao, Shengqiang Lu, and Gang Xie, Air Quality Prediction: Big Data and Machine Learning Approaches, International Journal of Environmental Science and Development, Vol. 9, No. 1, 2018
[13] "National Air Quality Monitoring Program". CPCB. Archived from the original on 2 May 2013. Retrieved 31 May 2013.
[14] Climate change in Asia http://recap.asia/climate-asia/Air-Pollution-in-Asia.html
[15] Corani, G. (2005). Air quality prediction in Milan: feed-forward neural-networks, pruned neural networks and lazy learning. Ecological Modelling, 185(2-4), 513–529
[16] Zhu, D., Cai, C., Yang, T., & Zhou, X. (2018). A Machine Learning Approach for Air Quality Prediction: Model Regularization and Optimization. Big Data and Cognitive Computing, 2(1), 5
[17] Li, X., Peng, L., Hu, Y., Shao, J., & Chi, T. (2016). Deep learning architecture for air quality predictions. Environmental Science and Pollution Research, 23(22), 22408–22417
[18] Kim, M. H., Kim, Y. S., Lim, J., Kim, J. T., Sung, S. W., & Yoo, C. (2010). Data driven prediction model of indoor air quality in an underground space. Korean Journal of Chemical Engineering, 27(6), 1675–1680
[19] Zhao, J., Deng, F., Cai, Y., & Chen, J. (2019). Long short-term memory Fully connected (LSTM-FC) neural network for PM2.5 concentration prediction. Chemosphere, 220, 486–492

ACTA TECHNICA CORVINIENSIS – Bulletin of Engineering
ISSN: 2067-3809

Fascicule 2
[April – June]
tome XIII
[2020]

ACTA Technica CORVINIENSIS
BULLETIN OF ENGINEERING

ACTA TECHNICA CORVINIENSIS – Bulletin of Engineering
ISSN: 2067-3809

http://acta.fih.upt.ro

INDEXES & DATABASES

We are very pleased to inform that our international scientific journal **ACTA TECHNICA CORVINIENSIS – Bulletin of Engineering** completed its 12 years of publication successfully **[2008–2019, Tome I–XII]**.
In a very short period the **ACTA TECHNICA CORVINIENSIS – Bulletin of Engineering** has acquired global presence and scholars from all over the world have taken it with great enthusiasm.
We are extremely grateful and heartily acknowledge the kind of support and encouragement from all contributors and all collaborators!

ACTA TECHNICA CORVINIENSIS – Bulletin of Engineering is accredited and ranked in the **"B+" CATEGORY Journal** by **CNCSIS – The National University Research Council's Classification of Romanian Journals, position no. 940** (http://cncsis.gov.ro/).
ACTA TECHNICA CORVINIENSIS – Bulletin of Engineering is a part of the **ROAD, the Directory of Open Access scholarly Resources** (http://road.issn.org/).

ACTA TECHNICA CORVINIENSIS – Bulletin of Engineering is also indexed in the digital libraries of the following world's universities and research centers:

WorldCat – the world's largest library catalog
https://www.worldcat.org/
National Lybrary of Australia
http://trove.nla.gov.au/
University Library of Regensburg – GIGA German Institute of Global and Area Studies
http://opac.giga-hamburg.de/ezb/
Simon Fraser University – Electronic Journals Library
http://cufts2.lib.sfu.ca/
University of Wisconsin – Madison Libraries
http://library.wisc.edu/
University of Toronto Libraries
http://search.library.utoronto.ca/
The University of Queensland
https://www.library.uq.edu.au/
The New York Public Library
http://nypl.bibliocommons.com/
State Library of New South Wales
http://library.sl.nsw.gov.au/
University of Alberta Libraries – University of Alberta
http://www.library.ualberta.ca/
The University of Hong Kong Libraries
http://sunzi.lib.hku.hk/
The University Library – The University of California
http://harvest.lib.ucdavis.edu/

ACTA TECHNICA CORVINIENSIS – Bulletin of Engineering is indexed, abstracted and covered in the world–known bibliographical databases and directories including:

INDEX COPERNICUS – JOURNAL MASTER LIST
http://journals.indexcopernicus.com/
GENAMICSJOURNALSEEK Database
http://journalseek.net/
DOAJ – Directory of Open Access Journals
http://www.doaj.org/
EVISA Database
http://www.speciation.net/
CHEMICAL ABSTRACTS SERVICE (CAS)
http://www.cas.org/
EBSCO Publishing
http://www.ebscohost.com/
GOOGLE SCHOLAR
http://scholar.google.com
SCIRUS – Elsevier
http://www.scirus.com/
ULRICHSweb – Global serials directory
http://ulrichsweb.serialssolutions.com
getCITED
http://www.getcited.org
BASE – Bielefeld Academic Search Engine
http://www.base-search.net
Electronic Journals Library
http://rzblx1.uni-regensburg.de
Open J–Gate
http://www.openj-gate.com
ProQUEST Research Library
http://www.proquest.com
Directory of Research Journals Indexing
http://www.drji.org/
Directory Indexing of International Research Journals
http://www.citefactor.org/

ACTA TECHNICA CORVINIENSIS – Bulletin of Engineering
ISSN: 2067-3809